The bluest blues

Exploring the low photosynthetic efficiency of cyanobacteria in blue light

Luimstra, V.M.

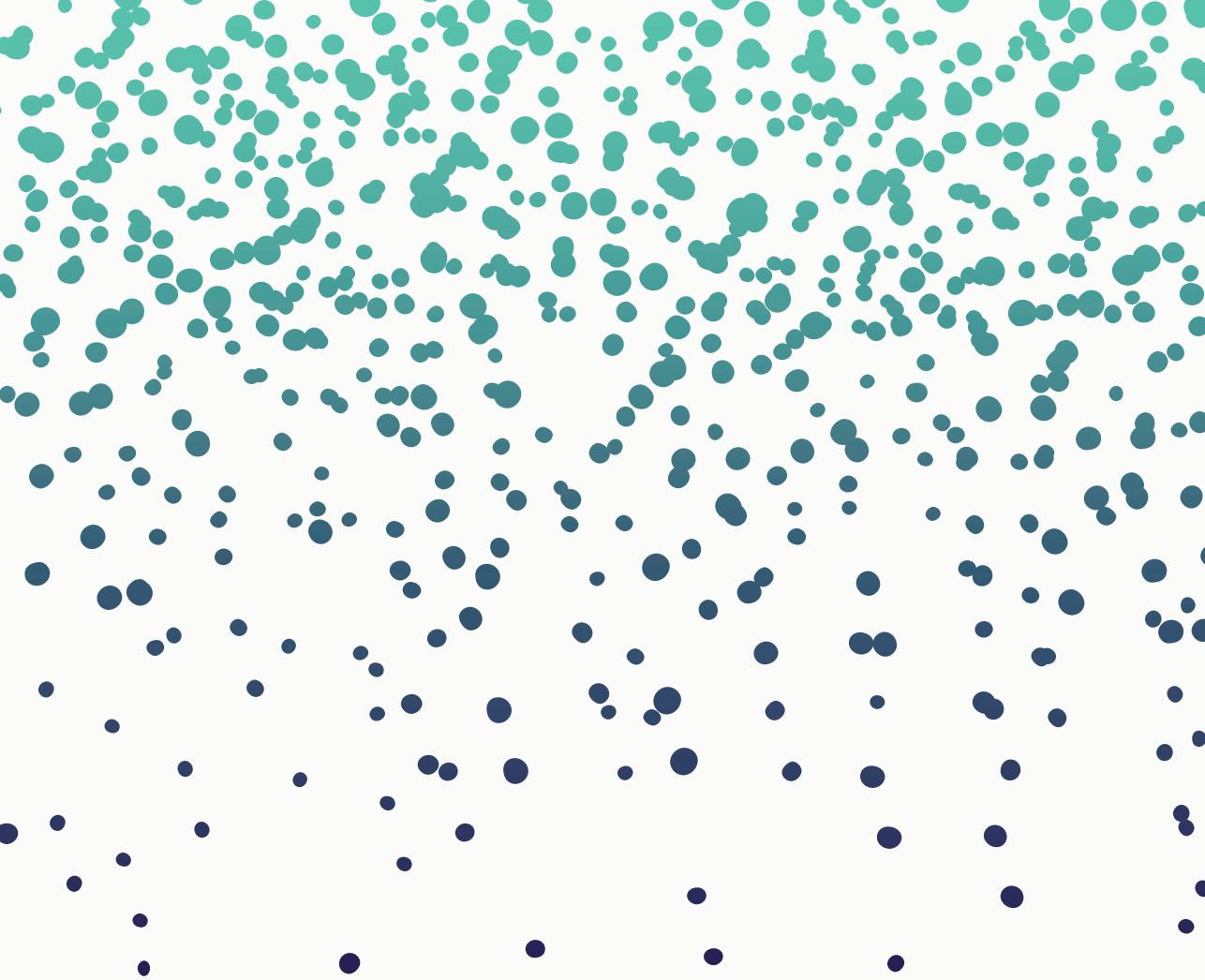

The Bluest Blues

Exploring the low photosynthetic efficiency of cyanobacteria in blue light

V.M. Luimstra

The Bluest Blues

Exploring the low photosynthetic efficiency of cyanobacteria in blue light

Veerle Minny Luimstra

This research was conducted at the Institute for Biodiversity and Ecosystem Dynamics (IBED), Department of Freshwater and Marine Ecology (FAME) of the Universiteit van Amsterdam, The Netherlands.
This work was performed in the cooperation framework of Wetsus, European Centre of Excellence for Sustainable Water Technology (*www.wetsus.eu*). Wetsus is co-funded by the Dutch Ministry of Economic Affairs and Ministry of Infrastructure and Environment, the Province of Fryslân and the Northern Netherlands Provinces.

ISBN: 978-94-91407-90-1
Title: The Bluest Blues (Alvin Lee ft George Harrison, 1994)
Cover: Specks, by Veerle Luimstra
Layout: Mike Valkenhoff and Jolien Luimstra
Support and catering: Robert van den Brink

Printed by: Gildeprint
Publisher: Universiteit van Amsterdam, The Netherlands

The Bluest Blues

Exploring the low photosynthetic efficiency of cyanobacteria in blue light

Academisch proefschrift

ter verkrijging van de graad van doctor
aan de Universiteit van Amsterdam
op gezag van de Rector Magnificus
prof. dr. ir. K.I.J. Maex,
ten overstaan van een door het College voor Promoties ingestelde commissie,
in het openbaar te verdedigen in de Aula der Universiteit
op vrijdag 13 november 2020, te 11:00 uur

door

Veerle Minny Luimstra

geboren te Amsterdam

Promotiecommissie

Promotores:	Prof. dr. J. Huisman	Universiteit van Amsterdam
	Prof. dr. K.J. Hellingwerf	Universiteit van Amsterdam
Co-promotor:	Dr. J.M. Schuurmans	Universiteit van Amsterdam
Overige leden:	Dr. D. Kirilovsky	CNRS, France
	Prof. dr. R. Croce	Vrije Universiteit Amsterdam
	Prof. dr. M.J. Barbosa	Wageningen University & Research
	Prof. dr. G. Muijzer	Universiteit van Amsterdam
	Dr. F. Branco dos Santos	Universiteit van Amsterdam
	Dr. S. Wilken	Universiteit van Amsterdam
	Dr. J.M.H. Verspagen	Universiteit van Amsterdam

Faculteit der Natuurwetenschappen, Wiskunde en Informatica

"Seaweed is cool, seaweed is fun,
it makes its food from the rays of the sun!"

- Mr. Ray
(Walt Disney & Pixar's Finding Nemo)

Dedicated to Hans, my 'Mr. Ray'

Table of contents

Chapter 1

Introduction

1

Introduction

Almost all living organisms rely on solar energy, either directly or indirectly. Organisms capable of photosynthesis (phototrophs) are able to capture the plentiful solar energy and convert this into chemical energy to produce biomass. In addition, all present-day atmospheric oxygen (O_2) is produced by oxygenic photosynthesis. The oxygenation of the early earth by ancestral cyanobacteria allowed the evolution of eukaryotes and multicellular organisms (Falkowski 2006; Schirrmeister et al. 2015). Therefore, oxygenic phototrophs support nearly all life on earth as most other organisms rely on the light energy harvested and stored by phototrophs, and on the oxygen produced as a by-product of photosynthesis. Even nowadays, half of the global primary production is still performed by freshwater and marine phytoplankton (Field et al. 1998).

In addition to their key role in aquatic ecosystems, phototrophic phytoplankton have received increasing interest in the search for sustainable production of food, renewable energy sources, and even biodegradable polymers. Many studies have been dedicated to opportunities for the use of algae and cyanobacteria as 'cell factories' that primarily use light and CO_2 (for reviews see, e.g., Gust et al. 2008; Rosenberg et al. 2008; Beer et al. 2009; Hellingwerf and Teixeira de Mattos 2009; Jones and Mayfield 2012; Wijffels et al. 2013; Branco dos Santos et al. 2014). Hence, an advanced understanding of photosynthesis and the process of light harvesting and conversion is of considerable importance for many fields of research. Conceptually, the process of oxygenic photosynthesis has remained virtually unchanged for billions of years and is very similar amongst all oxygenic phototrophs (Eberhard et al 2008; Blankenship 2014). Therefore, it is often studied in unicellular cyanobacteria and green algae.

All oxygenic phototrophs utilize the universal green pigment chlorophyll *a* (Chl *a*) (or its variant divinyl-Chl *a*), which predominantly captures light energy provided by blue and red light (Kirk et al. 2011). Therefore, one would assume that the efficiency of photosynthesis is similar in both light colors. However, cyanobacteria have often been shown to display lower rates of O_2 production and growth in blue light than in red light, in contrast to green algae and plants (e.g., Lemasson et al. 1973; Pulich and van Baalen 1974; Wilde et al. 1997; Tyystjärvi et al. 2002; Wang et al. 2007; Singh et al. 2009). The cause of this phenomenon is still unclear, yet has received surprisingly little attention.

Although the basic principles of photosynthesis are similar between oxygenic phototrophs, phytoplankton species can differ greatly in their photosynthetic pigments, light-harvesting antennae, photoacclimation and photoprotection mechanisms (Croce and van Amerongen 2014). It is possible that these differences play a role in the lower photosynthetic efficiency of cyanobacteria in blue light, compared to green algae and plants.

In this thesis we will investigate why most cyanobacteria display a low photosynthetic efficiency in blue light, and how this affects their physiology and growth. This knowledge will contribute to a further understanding of the mechanisms of photosynthesis, may have potential implications for successful application of cyanobacteria in biotechnology, and may help to clarify the growth and abundance of cyanobacteria in waters characterized by different underwater light spectra.

Photosynthesis

Basic principles of oxygenic photosynthesis

The processes of photosynthesis can be divided into two sets of reactions: the light reactions and the dark reactions (Blankenship 2014). While the light reactions are truly light-driven, the dark reactions, in which carbon dioxide (CO_2) is assimilated, are dependent on the products formed during the light reactions. Therefore, changes in light conditions influence the light reactions directly, but only indirectly affect the dark reactions of photosynthesis.

The light reactions involve light-harvesting antennae and two protein-pigment complexes, photosystem I (PSI) and photosystem II (PSII) (Nelson and Yocum 2006). The light-harvesting antennae absorb photons and transfer the absorbed light energy to PSI and PSII, and both photosystems can also absorb photons directly. Each photosystem contains a reaction center, consisting of Chl *a* and carotenoids, supplemented with several cofactors involved in electron transfer. The two photosystems are embedded in a thylakoid membrane and function in series to create a linear flow of electrons (Fig. 1). When a photon ($h\nu$) excites Chl *a* in the reaction center of PSII, Chl *a* is converted into the highly reactive singlet excited state, and will donate an electron to a plastoquinone (PQ) at its PQ-binding site (Eberhard et al 2008; Blankenship 2014). The excited Chl *a* in the PSII reaction center will acquire a new electron by splitting water molecules into electrons, O_2 and protons (H^+). After a second electron has been transferred, PQ is reduced to plastoquinol (PQH_2). From PQH_2, the electrons are transferred through the cytochrome b_6f complex (Cyt b_6f)

and plastocyanin to a photo-oxidized Chl *a* in PSI. Upon excitation, PSI will donate an electron to ferredoxin and ultimately to ferredoxin-NADP+ oxidoreductase that produces NADPH in a two-electron transfer process. During these light reactions, H^+ are produced by splitting of water at PSII and additional H^+ are transferred across the thylakoid membrane through photosynthetic reduction and oxidation of the PQ pool. This generates a H^+ gradient that drives ATP production (Fig. 1).

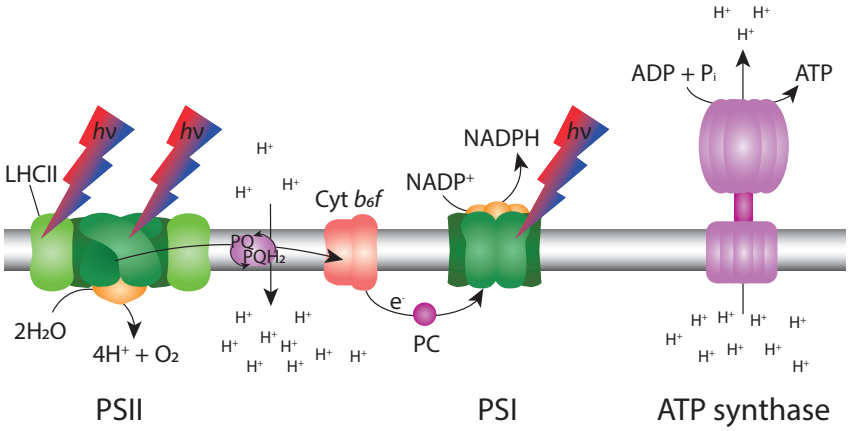

Fig. 1 | The light-dependent reactions of photosynthesis with the main components of the photosynthetic apparatus in green algae and plants. Apart from blue- and red light absorption by Chl *a* in the reaction centers of PSI and PSII, these phototrophs use the intrinsic light-harvesting antenna LHCII containing chlorophylls and carotenoids to absorb additional blue and red light. Arrows indicate electron (e^-) transfer. PSI: photosystem I; PSII: photosystem II; LCHII: light-harvesting complex II; PQ: plastoquinone; PQH_2: plastoquinol; Cyt b_6f: cytochrome b_6f; PC: plastocyanin; *hν*: photon. Cyanobacteria have an additional light-harvesting antenna of a very different nature; this will be discussed below.

The light reactions can be summarized as:

$$2\,H_2O + 8\,h\nu + 2\,NADP^+ + 3\,ADP + 3\,P_i \rightarrow O_2 + 2\,NADPH + 2\,H^+ + 3\,ATP$$

Most of the NADPH and ATP generated by the light reactions are used in carbon fixation, which requires 3 ATP and 2 NADPH molecules per fixed CO_2 molecule. In addition, carbon metabolism is tightly coupled to nitrogen metabolism, which requires ATP and NADPH as well, as does the assimilation of other nutrients such as phosphorus and sulfur (Singh et al. 2008). Therefore, a large variety of metabolic pathways are dependent on and intertwined with photosynthesis. Hence, an advanced regulation of energy production by photosynthesis and energy consumption by metabolic processes is essential. For example, if cellular ATP demand is higher than NADPH demand, the excited electrons at PSI can be transferred via ferredoxin (Fd) to the PQ pool and from there back to PSI

(Allen 2003; Munekage et al. 2004; Yeremenko et al. 2005). This cyclic electron flow contributes to the H^+ gradient needed to generate ATP, but does not lead to NADPH formation.

The light reactions of photosynthesis are conceptually similar in all oxygenic phototrophs, but experimental research is often easier in unicellular organisms than in plants (Blankenship 2014). Therefore, cyanobacteria and green algae are often used to study photosynthesis as they have high growth rates, are often relatively easy to transform, and they lack the additional metabolic complexity associated with the formation and functioning of stems, leaves, flowers, etc. However, although many aspects of oxygenic photosynthesis are similar between prokaryotic and eukaryotic phototrophs, some aspects are fundamentally different.

Cyanobacteria are often referred to as blue-green algae, a misleading term dating back to before the days that they were identified as prokaryotes. To this day, cyanobacteria are the only known oxygenic photosynthesizing prokaryotes. Some of the oldest fossils in the world show that cyanobacteria were already around 3.5 billion years ago and they are considered to be the drivers of the great oxygenation event 2.3 billion years ago (Planavsky et al 2014; Schirrmeister et al 2015; Nutman et al 2016). Their long existence on Earth has resulted in an impressive physiological versatility of cyanobacteria. They have diversified over a wide variety of habitats, ranging from hot springs to Antarctic soils, from oligotrophic oceans to hypereutrophic lakes, and nearly everywhere in between (Bryant 1994).

Eukaryotic algae emerged much later than cyanobacteria, around 1.5 billion years ago, when a primitive eukaryotic cell endocytosed a cyanobacterium (Margulis 1993). Eventually, this cyanobacterial cell was integrated into the host cell as a chloroplast, leading to primary endosymbiosis, which led to the emergence of red algae, green algae and glaucophytes. Secondary and tertiary endosymbiosis events have subsequently resulted in further development of algal groups such as euglenoids, cryptophytes and dinoflagellates (Keeling 2010). Green algae are acknowledged as the evolutionary precursors of plants, and can be found in many different marine and freshwater environments.

Light-harvesting strategies

Pigments

In nature the conversion efficiency of light energy into biomass ranges from far less than 1% up to 6.4% of the total solar radiation for plants, and up to 10% for microalgae (including cyanobacteria) (Melis 2009; Zhu et al. 2010). This efficiency is affected by several factors, including species traits, light intensity and light color. As early as 1882, the German scientist Theodor Engelmann discovered that photosynthesis displays a light-color dependence. He performed a simple experiment using a filamentous green alga of the genus *Cladophora*, which he placed on a microscopic slide (Engelmann 1882). He illuminated the filament, using a prism to divide sunlight into separate wavelengths, and then introduced aerotactic bacteria. These motile bacteria aggregated around the algal filament, but mostly in the blue and red parts of the light spectrum. Hence, the experiment of Engelmann showed that photosynthetic O_2 production by the green alga occurred at highest rates in blue and red light (Fig. 2).

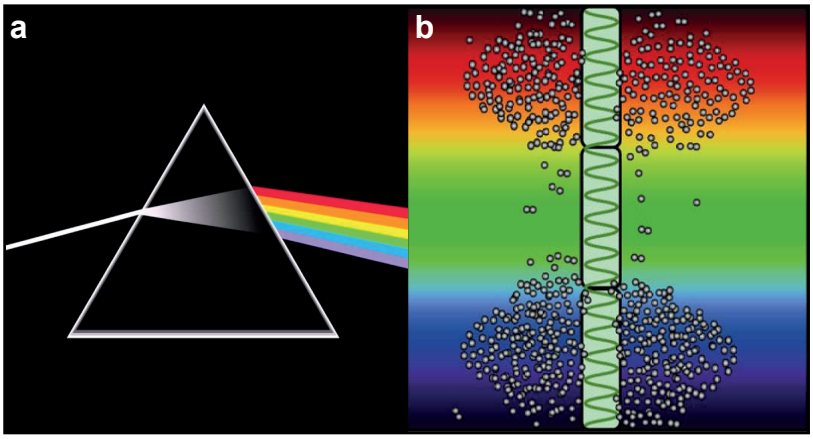

Fig. 2 | The first 'action spectrum' of chlorophyll. (a) Engelman (1883) used a prism to turn white light into a spectrum of light colors. (b) He used this rainbow to illuminate a microscopic slide containing a single filament of the green alga *Cladophora*. By using aerotactic motile bacteria he showed that photosynthetic oxygen production was highest in the blue and red parts of the light spectrum. Adapted from (a) Pink Floyd's *Dark Side of the Moon* and (b) Stomp (2008).

In later years, Engelmann demonstrated that in the cyanobacterium *Oscillatoria* oxygenic photosynthesis occurred not only in red and blue light, but also in orange light (Engelmann 1883; Engelmann 1884). These results were confirmed 60 years later, by Emerson and Lewis (1942), who showed that cyanobacteria and red algae can use phycobili-pigments to absorb orange light for photosynthesis. Since then, a wide variety of photosynthetic pigments has been identified in an even wider variety of species, including chlorophylls, phycobili-pigments and carotenoids (Blankenship 2014; Croce and van Amerongen 2014). Each pigment has a unique absorption spectrum which allows these pigments to absorb light of specific wavelengths. Although the basic principles of photosynthesis are similar between oxygenic phototrophs, pigment composition and light-harvesting strategies can vary greatly between species. Table 1 shows the distribution of pigments amongst some of the most abundant groups of phototrophs.

Table 1 | Distribution of photosynthetic pigments in some major groups of phototrophs. Wavelengths of absorption peaks are added. *Prochlorococcus* was separated from other cyanobacteria to illustrate its unique pigmentation. Chl: chlorophyll; PUB: phycourobilin; PEB: phycoerythrobilin; PCB: phycocyanobilin; APC: allophycocyanin.

	Chlorophylls			Phycobili-pigments				Carotenoids
	Chl *a* 440 & 680 nm	**Chl *b*** 450 & 650 nm	**Chl *c*** 460 & 640 nm	**PUB** 495 nm	**PEB** 545 nm	**PCB** 620 nm	**APC** 650 nm	400-500 nm
Plants	+	+						+
Green algae	+	+						+
Diatoms	+		+					+
Brown algae	+		+					+
Dinoflagellates	+		+					+
Cryptophytes	+		+		+	+		+
Red algae	+			+	+	+	+	+
Cyanobacteria[#]	+			+	+	+	+	+
Prochlorococcus[*]	+	+		(+)	(+)			+

[#]Some cyanobacteria also contain Chl *d* or Chl *f* (Miyashita et al. 1997; Chen et al. 2010)
[*]*Prochlorococcus* contains divinyl-chlorophyll *a* and *b* which absorb similar light colors as Chl *a* and Chl *b*, respectively. *Prochlorococcus* lacks functional PBS, but some strains have genes encoding PUB and PEB (Hess et al 1996; Steglich et al. 2003).

Reaction centers and light-harvesting antennae

The ubiquitous Chl *a* is present in the reaction centers of PSI and PSII of oxygenic phototrophs and absorbs in the blue and red regions of the light spectrum. While PSI contains around 100 molecules of Chl *a* (Jordan et al. 2001; Kennis et al. 2001), PSII contains only around 35 molecules of Chl *a* (Guskov et al. 2009; Umena et al. 2011). Hence, a PSI unit will absorb more light than a PSII unit, which is often compensated by light-harvesting antennae that absorb additional light energy for PSII.

In addition to Chl *a*, phytoplankton species utilize a variety of other pigment complexes, often fine-tuned to specific light colors (Croce and van Amerongen 2014). These accessory pigments can be incorporated in highly specialized antennae complexes, deployed to capture additional light which can be transferred to PSI or PSII to balance excitation energy between the photosystems. For example, the photosystems contain several carotenoids absorbing in the violet and blue-green regions (400-500 nm). Carotenoids can be involved in light-harvesting, but also often protect the cells by dissipating harmful excess excitation energy as heat (Ritz et al. 2000). Although both photosystems of cyanobacteria contain carotenoids, only the carotenoids in PSI appear to be involved in light harvesting (Stamatakis et al. 2014). In contrast, in green algae and plants, the carotenoids of both photosystems can play a role in photosynthetic light harvesting (Takaichi et al. 2011).

In the prokaryotic cyanobacteria, PSI and PSII are embedded in the thylakoid membrane, which stretches along the inside of the cell membrane and forms concentric shells (Nevo et al. 2007; Rast et al 2015). Cyanobacteria display large differences in the arrangement of their thylakoid membranes (Herrero and Flores 2008). Most cyanobacteria utilize phycobilisomes (PBS) as large extrinsic light-harvesting antennae (Fig. 3; for reviews see Tamary et al 2012; Watanabe and Ikeuchi 2013; Stadnichuk and Tropin 2017). PBS consist of an allophycocyanin core and stacked rods of phycobili-proteins with a variety of pigments (bilins), including phycocyanobilin absorbing orange light (620 nm), phycoerythrobilin absorbing green light (545 nm), and phycourobilin absorbing blue-green light (495 nm) (Grossman et al. 1993; Tandeau de Marsac 2003; Six et al. 2007). PBS typically transfer the absorbed light energy to PSII, although they can also associate with PSI and/or dissociate from the photosystems. Some eukaryotic phytoplankton groups - such as red algae, glaucophytes and cryptophytes - also utilize phycobili-pigments, although cryptophytes do not incorporate these into PBS (Cunningham et al. 2018; Greenwold et al. 2019).

Plants and green algae do not have PBS but utilize light-harvesting complex II (LHCII) as their light-harvesting antenna. LHCII generally associates with PSII but is much smaller than PBS (i.e., it has a much lower number of pigment molecules). LHCII is embedded in the thylakoid membrane, which in green algae and plants is located in the chloroplast (Fig. 1). This light-harvesting complex contains Chl *a*, Chl *b* and carotenoids (Kühlbrandt 1994; Takaichi 2011), and hence absorbs in both the blue and red part of the light spectrum. In contrast to most cyanobacteria, the cyanobacterium *Prochlorococcus* lacks PBS and instead uses divinyl-

Chl *a* and divinyl-Chl *b* in its light-harvesting antennae, thereby absorbing blue and red light in a quite similar way as plants and green algae (Chisholm et al. 1992; Ting et al. 2002).

The structural arrangement and pigment composition of the photosystems and their light-harvesting antennae implies that PBS-containing cyanobacteria distribute light energy of specific colors in a different way over their photosystems than the chlorophyll-based green algae and terrestrial plants. In PBS-containing cyanobacteria, the PBS transfer orange, green and blue-green light mainly to PSII, whereas blue light < 450 nm and red light > 660 nm are mainly harvested for photosynthesis by the pigments in PSI (Fig. 3). By contrast, in green algae and terrestrial plants, blue and red light are absorbed by the light-harvesting complexes and reaction centers of both PSI and PSII (Fig. 1).

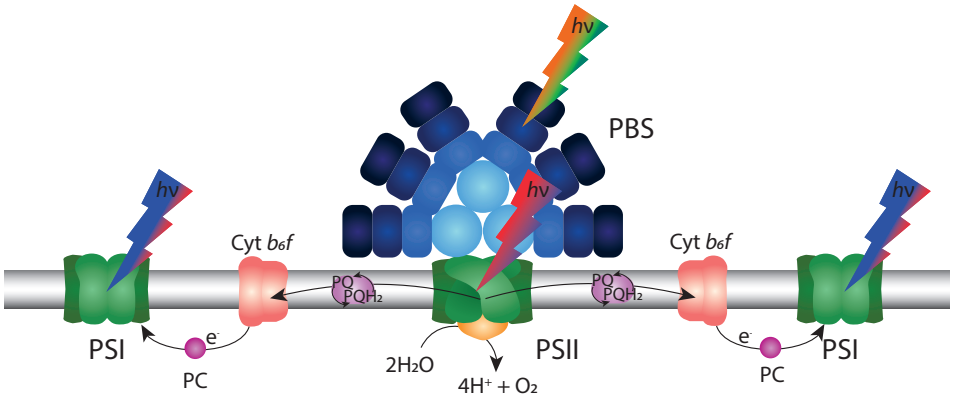

Fig. 3 | The major components of the photosynthetic apparatus of cyanobacteria. For illustration purposes, ATP-synthase and the proton gradient needed to propel this complex were omitted from this figure (but see Fig. 1 for an overview). Apart from blue- and red light absorption by Chl *a* in the reaction centers of PSI and PSII, these phototrophs use large peripheral PBS as light-harvesting antennae. PBS can contain (combinations of) phycobili-pigments that absorb blue-green, green or orange light (see Table 1). PSI: photosystem I; PSII: photosystem II; PBS: phycobilisome; PQ: plastoquinone; PQH_2: plastoquinol; Cyt b_6f: cytochrome b_6f; PC: plastocyanin; *hv*: photon.

Acclimation to changing light intensities

Because light conditions change continuously and often rapidly, phototrophs have to constantly acclimate to the available light color and intensity, in order to maximize rates of photosynthesis and minimize damage through over-excitation (Eberhard et al 2008). If light availability exceeds the rates of photon processing by PSI, the PQ pool becomes completely reduced. Continued excitation of Chl *a* in the PSII reaction center may then lead to the formation of reactive oxygen species, photodamage and ultimately photoinhibition, or even cell death.

Cyanobacteria and eukaryotic algae have developed a range of strategies that allow them to acclimate to different light conditions (Eberhard et al 2008). Within seconds to minutes, cyanobacteria can decouple their PBS from PSII to prevent overexcitation (Ranjbar Choubeh et al. 2018; Calzadilla et al. 2019). Several hypotheses have been proposed concerning state transitions in cyanobacteria, a process where the PBS move from PSII to PSI to redistribute excitation energy (Mullineaux and Emlyn-Jones 2005). The process is assumed to be initiated by an overreduction of the PQ pool, but thus far no consensus has been reached on the basic mechanisms, and it has recently been questioned whether relocation of PBS from PSII to PSI actually takes place (Ranjbar Choubeh et al. 2018; Calzadilla et al. 2019). Like cyanobacteria, green algae perform state transitions but the underlying processes are very different and well identified in green algae (Wientjes et al 2013). In green algae and plants, reduction of the PQ pool induces phosphorylation of LHCII which releases from PSII and can move to PSI (Allen 2003, Minagawa 2011).

In addition to state transitions, cyanobacteria can eliminate excess excitation energy through photoprotective proteins such as the orange carotenoid protein (OCP; see e.g., Rakhimberdieva et al. 2007; Gorbunov et al. 2011; Tian et al. 2012), the iron-stress inducible protein A (IsiA; see e.g., Wilson et al. 2007; Wahadoszamen et al. 2015) and dimers of the flavodiiron proteins Flv1/3 (see e.g., Allahverdiyeva et al 2013) and Flv2/4 (see e.g., Zhang et al. 2012; Bersanini et al. 2014). In green algae, excess light energy activates a photoprotective xanthophyll cycle, which dissipates the excess energy as heat (Demmig-Adams 1990). Photoprotective proteins are often constitutively expressed and can be rapidly activated. However, in case of long-term changes in light conditions, phototrophs can further up- or downregulate the expression of genes related to these photoprotective proteins as well as genes related to light-harvesting antennae or photosynthetic pigments. Furthermore, phototrophs can extensively vary the ratio of their photosystems. In cyanobacteria, PSI is around 2-5 times more abundant than PSII depending on light conditions, whereas green algae generally maintain a PSI:PSII ratio close to 1 (Shen et al. 1993; Fujita 1997; Olive et al. 1997; Singh et al. 2009; Allahverdiyeva et al. 2014).

Colorful diversity of light-harvesting strategies

The diversity of photosynthetic pigments and light-harvesting strategies allows different phytoplankton species to occupy specific niches within the water column. Photosynthetically active radiation (PAR) for oxygenic phototrophs ranges from 400 nm (violet-blue light) to about 700 nm (far-

red light), and even to 750 nm for those cyanobacteria containing Chl *f* (Miyashita et al 1997; Chen et al 2010). Water molecules strongly absorb in the red part and poorly in the blue part of the light spectrum, which is why blue light dominates in the clear waters of the open ocean whereas red light is only available near the surface (left column in Fig. 4; see also Stomp et al. 2007; Kirk 2011). Conversely, colored dissolved organic matter ('gilvin') and particulate organic matter ('tripton') strongly absorb in the blue part of the light spectrum, but poorly in the red part. Hence, in turbid waters with a high organic matter content, such as peat lakes, the underwater light color is often shifted towards red wavelengths (right column in Fig. 4; see also Stomp et al. 2007; Kirk 2011). In moderately turbid waters, such as in coastal areas, the underwater light spectrum is dominated by green light, as blue light is absorbed by the water molecules and red light by the dissolved organic matter (middle column in Fig. 4).

The phytoplankton species dominating these different aquatic ecosystems often have photosynthetic pigments tuned to the available underwater light spectrum (Fig. 4g-i). For example, the cyanobacterium *Prochlorococcus* effectively absorbs blue light by its pigments (divinyl-)Chl *a* and *b* and is highly abundant in the blue-light dominated layers of the open ocean (Fig. 4g). Red *Synechococcus* strains using phycoerythrobilin to absorb green light are widespread in more turbid coastal waters where green light prevails (Fig. 4h). Lastly, orange-red light dominated peat lakes are often dominated by green cyanobacteria that deploy light-harvesting antennae containing phycocyanobilin, which allows them to absorb orange-red light (Fig. 4i).

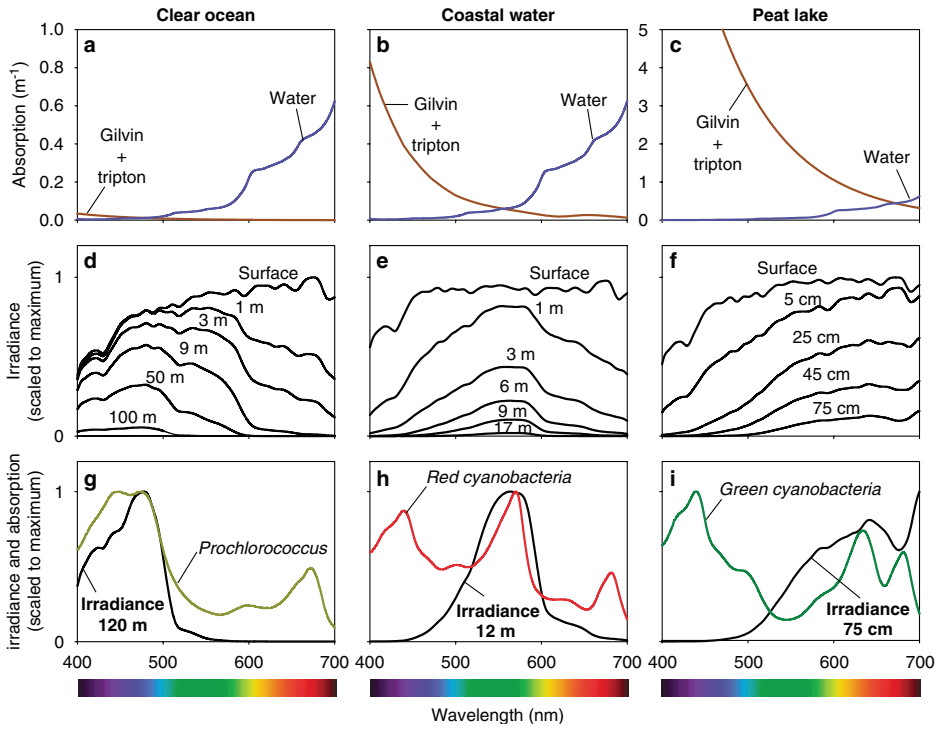

Fig. 4 | Underwater light spectra of (a) the open ocean near the ALOHA station, located just north of Hawaii in the Pacific Ocean, (b) coastal waters of the Baltic Sea, and (c) a peat lake (Grote Moost) in the Netherlands. Blue lines show light absorption by water molecules, and brown lines by dissolved organic matter (gilvin and tripton). (d-f) Light penetration was measured at several depths, showing that at the bottom of the euphotic zone blue light dominates in ocean waters, green light dominates in the Baltic Sea and red light dominates in peat lakes. (g-i) Phytoplankton was sampled at the bottom of the euphotic zone (defined as the depth at which the irradiance is reduced to 1% of the surface irradiance), and their absorption spectrum is compared to measurements of the underwater light spectrum at these depths. (g) At 120 m depth, blue light dominated the Pacific Ocean; in agreement with the available light color, *Prochlorococcus*, which contains blue-light absorbing divinyl Chl *a* and *b*, was the most abundant phytoplankton species. (h) At 12 m depth, green light dominated the Baltic Sea; in agreement with the available light color, red *Synechococcus* strains containing the green-light absorbing phycoerythrobilin were the most abundant phytoplankton species. (i) At 75 cm depth, orange and red light dominated the peat lake Groote Moost; in agreement with the available light color, green cyanobacteria containing the orange-light absorbing phycocyanobilin were the most abundant phytoplankton species. After Stomp et al. (2007a), reprinted with permission of Springer Nature.

This thesis

As outlined above, several studies have shown that phycobilisome-containing cyanobacteria use blue light much less efficiently than red light (e.g. Lemasson et al. 1973; Pulich and van Baalen 1974; Wilde et al. 1997; Tyystjärvi et al. 2002; Wang et al. 2007; Singh et al. 2009). This striking phenomenon is not observed in e.g., green algae and plants. The low photosynthetic efficiency of cyanobacteria in blue light may have major consequences for their ecological distributions in lakes and oceans, for our understanding of the evolution of photosynthetic organisms, and for many applications of cyanobacteria in biotechnology. Therefore, the aim of this thesis is threefold. We want to explore why most cyanobacteria use blue light less efficiently, how this affects their photophysiology and growth, and what the implications are for the competitive interactions between cyanobacteria and other species in phytoplankton communities.

In **chapter 2**, we set the stage by a comprehensive study of the physiological response of the model cyanobacterium *Synechocystis* sp. PCC 6803 to blue, orange and red light. The results confirm that this freshwater cyanobacterium indeed has much lower rates of photosynthesis and growth in blue light than in orange and red light. Furthermore, specific growth rates of two marine cyanobacteria utilizing phycocyanobilin and phycoerythrobilin, respectively, were also much lower in blue light than in orange and red light. In contrast, growth rates of the green alga *Chlorella sorokiniana* 211-8K, which uses chlorophyll-based light-harvesting antennae, were similar in blue and red light. We hypothesize that the lack of blue-light absorption by the PBS leads to an imbalance between the rates of excitation of PSI and PSII, which plays an important role in the low photosynthetic efficiency of cyanobacteria in blue light.

To investigate this hypothesis, we compare growth and photosynthesis of wildtype *Synechocystis* and a mutant strain lacking PBS (known as the PAL mutant) in **chapter 3**. Due to its lack of PBS, the PAL mutant will be unable to transfer light energy from PBS to PSII, while the higher chlorophyll content of PSI may still enable sufficient photosynthetic activity at PSI. The question is whether this mutant will have low rates of oxygen production and growth in both blue and red light, comparable to the wildtype in blue light. If so, the PAL mutant displays a similar photophysiology in both light colors as PBS-containing cyanobacteria grown in blue light. This observation would support our hypothesis that, in blue light, insufficient light energy arrives at PSII to sustain high rates of linear photosynthetic electron flow.

In **chapter 4**, we compare the transcriptome response of *Synechocystis* after a switch from artificial white light to either blue, orange or red light. Our expectation is that the switch to blue light will have a much stronger effect on the transcriptome than the switch to orange and red light. Moreover, if our hypothesis that blue light results in an energy shortage at PSII is correct, we expect up-regulation of PSII-related genes and down-regulation of PSI-related genes. In line with expectation, the results show that blue light induced major changes in the expression of 145 genes, whereas only a handful of genes responded to orange and red light. The transcriptome data provide a highly detailed view of how cyanobacteria acclimate to the adverse conditions imposed by blue light

In **chapter 5**, we aim to predict how differences in photosynthetic efficiency in blue light affect competition between phytoplankton species with PBS-based versus chlorophyll-based light-harvesting antennae. Aquatic environments are dominated by different underwater light colors, and hence we speculate that the observed differences in light-use efficiency may explain the outcome of phytoplankton competition. Therefore, we extend existing resource competition models and test the model predictions using competition experiments between the cyanobacterium *Synechocystis* and the green algae *Chlorella*, which use PBS-based and chlorophyll-based light-harvesting antennae, respectively. Our findings show that the biogeographical distributions of different phytoplankton species can indeed be explained by their light-harvesting strategies.

Finally, in **chapter 6** the results of all chapters are integrated and placed in the context of the general scientific literature. The implications of our findings for other research fields will be discussed, and recommendations will be presented for future research.

Chapter 2

Blue light reduces photosynthetic efficiency of cyanobacteria through an imbalance between photosystems I and II

Veerle M. Luimstra[1,2], J. Merijn Schuurmans[1], Antonie M. Verschoor[2,4], Klaas J. Hellingwerf[3], Jef Huisman[1], Hans C. P. Matthijs[1†]

[1]Department of Freshwater and Marine Ecology, Institute for Biodiversity and Ecosystem Dynamics, University of Amsterdam, Amsterdam, The Netherlands
[2]Wetsus, European Centre of Excellence for Sustainable Water Technology, Leeuwarden, The Netherlands
[3]Swammerdam Institute for Life Sciences, University of Amsterdam, Amsterdam, The Netherlands
[4]Present Address: KWR Watercycle Research Institute, Nieuwegein, The Netherlands
†Deceased, April 17, 2016

This chapter is published in:
Photosynthesis Research 138:177–189 (2018)

Abstract

Several studies have described that cyanobacteria use blue light less efficiently for photosynthesis than most eukaryotic phototrophs, but comprehensive studies of this phenomenon are lacking. Here, we study the effect of blue (450 nm), orange (625 nm), and red (660 nm) light on growth of the model cyanobacterium *Synechocystis* sp. PCC 6803, the green alga *Chlorella sorokiniana* and other cyanobacteria containing phycocyanin or phycoerythrin. Our results demonstrate that specific growth rates of the cyanobacteria were similar in orange and red light, but much lower in blue light. Conversely, specific growth rates of the green alga *C. sorokiniana* were similar in blue and red light, but lower in orange light. Oxygen production rates of *Synechocystis* sp. PCC 6803 were five-fold lower in blue than in orange and red light at low light intensities but approached the same saturation level in all three colors at high light intensities. Measurements of 77 K fluorescence emission demonstrated a lower ratio of photosystem I to photosystem II (PSI:PSII ratio) and relatively more phycobilisomes associated with PSII (state 1) in blue light than in orange and red light. These results support the hypothesis that blue light, which is not absorbed by phycobilisomes, creates an imbalance between the two photosystems of cyanobacteria with an energy excess at PSI and a deficiency at the PSII-side of the photosynthetic electron transfer chain. Our results help to explain why phycobilisome-containing cyanobacteria use blue light less efficiently than species with chlorophyll-based light-harvesting antennae such as *Prochlorococcus,* green algae and terrestrial plants

Introduction

Almost 140 years ago, professor Theodor Engelmann showed that light color plays an important role in photosynthesis (Engelmann 1882). In his classic experiment, Engelmann placed a filamentous green alga from the genus Cladophora on a microscopic slide, which he illuminated through a prism glass, thus dividing sunlight into separate wavelengths across the filament. By introducing aerotactic bacteria and observing in which regions of visible light these bacteria aggregated, he established that photosynthetic oxygen (O_2) production occurred in red and blue light, thereby creating the first "living" action spectrum of chlorophyll.

In the following years, Engelmann continued his studies with cyanobacteria from the genus Oscillatoria, demonstrating that in these cyanobacteria, not only red and blue light but also orange light resulted in high O_2 production rates (Engelmann 1883; 1884). Engelmann's findings were criticized for many years, but 60 years later, his results were confirmed by Emerson and Lewis, who showed that the phycobiliproteins of cyanobacteria and red algae play a key role in light-harvesting for photosynthesis (Emerson and Lewis 1942). We now know that these phycobiliproteins make up specialized light-harvesting antennae, called phycobilisomes (PBSs), consisting of an allophycocyanin core and stacked rods of phycocyanin often in combination with phycoerythrin. These phycobiliproteins consist of an apo-protein and one or more chromophores, also known as bilins, including phycocyanobilin absorbing orange light (620 nm), phycoerythrobilin absorbing green light (545 nm), and phycourobilin absorbing blue-green light (495 nm) (Grossman et al. 1993; Tandeau de Marsac 2003; Six et al. 2007). Recent reviews on the structure and function of PBSs are provided by Tamary et al. (2012), Watanabe and Ikeuchi (2013), and Stadnichuk and Tropin (2017).

Light energy absorbed by PBSs is effectively transferred via allophycocyanin to the chlorophyll *a* (Chl *a*) pigments in the photosystems (Arnold and Oppenheimer 1950; Duysens 1951; Lemasson et al. 1973). It has long been assumed that most PBSs transfer their energy to photosystem II (PSII). It is now well established, however, that cyanobacteria are able to re-balance excitation energy by moving PBSs between photosystem I (PSI) and PSII in a process called state transitions (van Thor et al. 1998; Mullineaux 2008). As a consequence of these state transitions, which occur at time scales of seconds to minutes, the PBSs associate with PSII (state 1) or PSI (state 2) and transfer the absorbed light energy to the reaction center of the photosystem they are associated with (Kirilovsky 2015). At longer time scales, cyanobacteria an also adjust their PSI:PSII ratio to optimize their photosynthetic activity under different environmental conditions (Fujita 1997). In cyanobacteria, the PSI:PSII ratio generally ranges between 5:1 and 2:1 depending on light quality and intensity, which is higher than the approximately 1:1 ratio often found in eukaryotic phototrophs (Shen et al. 1993; Murakami et al. 1997; Singh et al. 2009; Allahverdiyeva et al. 2014; Kirilovsky 2015).

Since blue and red light are both strongly absorbed by Chl *a*, and the intermediate wavelengths by the different phycobiliproteins, one would expect that these light colors are all used for photochemistry at approximately equal efficiency. However, several studies have described that blue light yields lower O_2 production rates than red light

in cyanobacteria (Lemasson et al. 1973; Pulich and van Baalen 1974; Jørgensen et al. 1987; Tyystjärvi et al. 2002), in cyanolichens (Solhaug et al. 2014), and also in PBS-containing red algae (Ley and Butler 1980; Figueroa et al. 1995). Furthermore, other studies noted that blue light resulted in lower growth rates in a variety of cyanobacteria (Wyman and Fay 1986), including *Synechocystis* sp. PCC 6803 (Wilde et al. 1997; Singh et al. 2009; Bland and Angenent 2016), *Synechococcus* sp. (Choi et al. 2013), and *Spirulina platensis* (Wang et al. 2007; Chen et al. 2010).

A possible explanation for their poor performance in blue light might be that most chlorophyll of cyanobacteria is located in PSI (Myers et al. 1980; Fujita 1997; Solhaug et al. 2014; Kirilovsky 2015), and hence, blue light induces high PSI but low PSII activity. This phenomenon is also known from fluorescence studies, where the use of blue measuring light complicates interpretation of the fluorescence signal of cyanobacteria (Campbell et al. 1998; Ogawa et al. 2017). However, although several of the above-cited studies measured growth rates and/or pigment composition in different light colors, they did not report on, e.g., O_2 production, PSI:PSII ratios, or state transitions. Conversely, other studies measured O_2 production rates or PSI:PSII ratios but did not measure growth rates or other relevant parameters. To our knowledge, more comprehensive studies of the photophysiological response of cyanobacteria to blue light are largely lacking, and no clear consensus has yet been reached on the question why their photosynthetic activity might be hampered by blue light.

In this study, we compare the effect of blue light with that of orange and red light on the model cyanobacterium *Synechocystis* sp. PCC 6803. This cyanobacterium uses Chl *a* in its photosystems and phycocyanin but not phycoerythrin in its phycobilisomes, and hence effectively absorbs blue, orange, and red light. We investigate its photosynthetic performance, the composition of its photosynthetic machinery, and its growth rate at different light intensities for all three colors, and compare these results with growth of the green alga *Chlorella sorokiniana* and of other cyanobacteria containing phycocyanin and phycoerythrin. The experiments will make use of blue, orange, and red LED light with narrow-band wavelengths, which allows more precise investigation of the photosynthetic response to different light colors than the broad-band light filters used in the older literature. Our results demonstrate that blue light has a major impact on the photophysiology of cyanobacteria.

Materials and Methods

Strains and culture conditions

The freshwater cyanobacterium *Synechocystis* sp. strain PCC 6803 and green alga *Chlorella sorokiniana* 211-8K were pre-grown in light-limited continuous cultures (1.8 L) as described by Huisman et al. (2002). The continuous cultures were provided with BG-11 medium supplemented with 5 mM Na_2CO_3 and maintained at 30°C at a dilution rate of D = 0.015 h^{-1} (0.36 d^{-1}). Steady-state culture densities were 7.8 x 10^7 cells mL^{-1} for *Synechocystis* and 2.4 x 10^7 cells mL^{-1} for *C. sorokiniana.* The cultures were mixed by bubbling with CO_2-enriched air (2% v/v) flowing at a rate of 30 L h^{-1}. Lighting was provided by white fluorescent tubes (Philips Master TL-D 90 De Luxe 18 W/965, Philips Lighting B.V., Eindhoven, The Netherlands) at an incident light intensity of 35 µmol photons m^{-2} s^{-1}. Light intensities (PAR) were measured with an LI-250 light meter (LI-COR Biosciences, Lincoln, NE, USA). The CO_2 concentration of the gas mixture was regularly monitored using an Environmental Gas Monitor for CO_2 (EGM-4; PP Systems, Amesbury, MA, USA).

The marine cyanobacteria *Synechococcus* sp. strain CCY 9201 (formerly known as BS4) and *Synechococcus* sp. strain CCY 9202 (formerly known as BS5) were pre-grown in Erlenmeyer flasks at 21°C with incident white light of 15 µmol photons m^{-2} s^{-1}. Both *Synechococcus* strains were grown in brackish medium as described by Stomp et al. (2004).

For batch experiments using *Synechocystis* and *C. sorokiniana,* samples from each starter culture were diluted in fresh BG-11 medium supplemented with 20 mM $NaHCO_3$. For batch experiments using *Synechococcus* sp. CCY 9201 and CCY 9202, samples from each pre-culture were diluted in fresh brackish medium. Each culture was diluted to an OD_{750} of 0.04 to allow light acclimation already in early cell generations, before density increases could be detected.

Batch experiments using an incubation shaker

To allow semi-high throughput screening of growth rates, an incubation shaker (Multitron Pro, Infors-HT, Velp, The Netherlands) was adapted at the University of Amsterdam Technology Centre for use with LED lighting (Fig. 1). The incubator was divided into three color zones separated by black curtains, with LED lamps (custom made by Philips Lighting B.V., Eindhoven, The Netherlands) positioned above each zone (Fig. 1a,b). The three color zones were illuminated by blue (450 nm), orange (625 nm) or red (660 nm) LED light, each with a full width at half maximum of ~20 nm. Emission spectra of the three LED light sources are shown in Fig. 2.

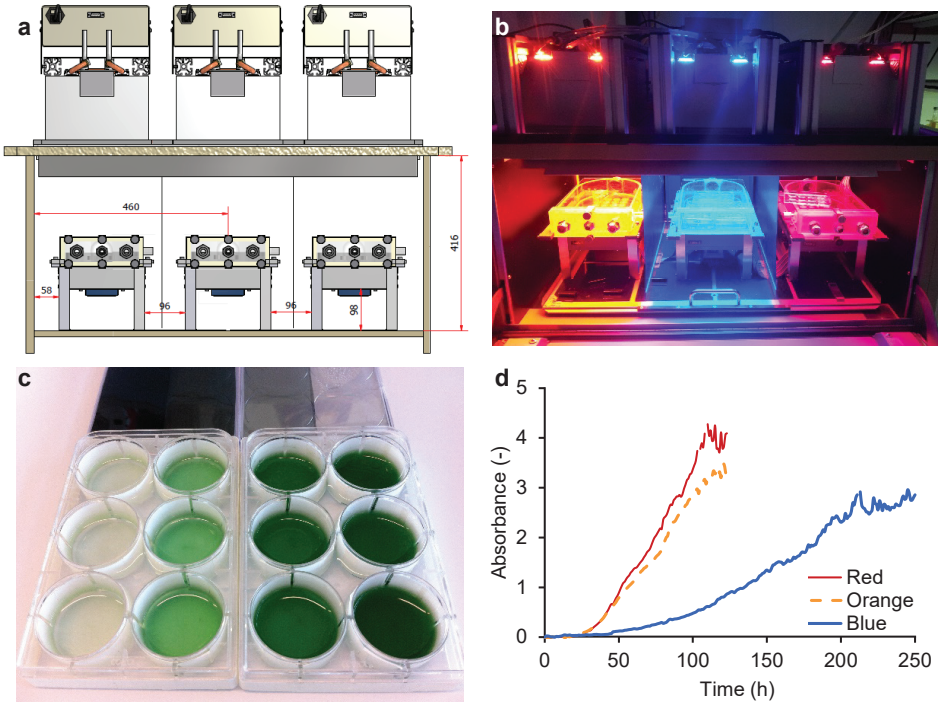

Fig. 1 | Experimental setup for the batch-culture experiments. (a) Schematic overview of the incubation shaker adapted for controlled experiments with phototrophic microorganisms. LED lights are placed above the incubator, which is partitioned into three color zones each containing a glass vessel mounted on a platform. (b) The incubation shaker in use with orange, blue and red LED light. (c) Each glass vessel contains two six-well plates with a lid on which neutral density (ND) filters are attached to create different light intensities. Here we show an example of *Synechocystis* sp. PCC 6803 batch cultures in blue light using 1.2, 0.6, 0.3 and 0.15 ND filters resulting in light intensities of 6, 22, 44 and 70 µmol photons m^{-2} s^{-1}, respectively; each light intensity is applied in triplicate. (d) Photodiodes below each well provide automated recording of the light attenuation by each batch culture, from which high-resolution growth curves were calculated (Supplementary Fig. S2). The growth curves shown here were calculated from the batch cultures in 70 µmol photons m^{-2} s^{-1} of red, orange and blue light. Each growth curve is the average of three biological replicates.

Each color zone contained a glass vessel mounted on a rotating platform. Each glass vessel contained two six-well plates (Corning Costar, Sigma) for batch experiments, with lids on which neutral density (ND) filters (Controllux Lichttechniek BV, Alphen aan den Rijn, The Netherlands) were attached to create different light intensities. The six-well plates were sterilized prior to the experiments using 70% ethanol and air-dried in a laminar flow hood. We applied four light intensities (6, 22, 44, 70 µmol photons m^{-2} s^{-1}) per color zone using 1.2, 0.6, 0.3 and 0.15 ND filters, respectively (Fig. 1c). Each light intensity was applied in

triplicate. In addition, each glass vessel held a twelve-well plate, without lid, containing sterilized milli-Q water to maintain a high humidity within the vessel. CO_2-enriched air (2,000 ppm) was provided to the incubation shaker through a sterile 0.20 µm Midisart 2000 filter (Sartorius Stedim Biotech GmbH, Göttingen, Germany) to minimize the risk of infection. Temperature in the incubation shaker was maintained at 30°C and rotation speed of the platform was 100 RPM.

Silicon photodiodes (OSI Optoelectronics, Hawthorne, CA, USA) fixed under each well measured light transmission at hourly intervals, thereby providing automated monitoring of the culture density in the wells. For each photodiode measurement, the applied treatment light was switched off while LED measurement light of 660 nm was switched on at the highest intensity of 185 ± 10 µmol photons m^{-2} s^{-1} for 2-4 seconds to allow a standardized comparison of the culture density between wells exposed to different treatments.

At the start of the experiments, samples taken from the pre-cultures were diluted in fresh mineral medium to an OD_{750} of 0.04. Subsequently, 5 mL culture of OD_{750} = 0.04 was transferred to each well in the six-well plates to initiate the batch experiments.

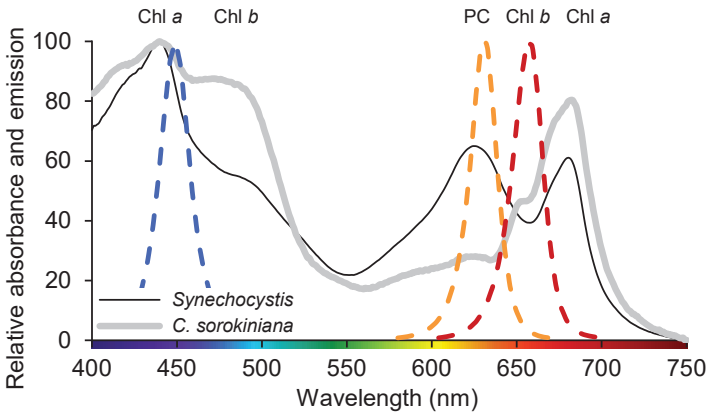

Fig. 2 | Light absorption spectra of the cyanobacterium *Synechocystis* sp. PCC 6803 (black line) and the green alga *C. sorokiniana* 211-8K (grey line) acclimated to 35 µmol photons m^{-2} s^{-1} white light. Light absorption peaks of Chl *a*, Chl *b* and phycocyanin (PC) are indicated. Light absorption is normalized to minimum absorbance at 750 nm and maximum absorbance. Dashed lines show emission spectra of the blue (450 nm), orange (625 nm) and red (660 nm) LED light sources used in the experiments, each with a full width at half maximum of ~20 nm.

Growth curves

Photodiodes converted the light intensity transmitted through the wells into a voltage signal. To calculate the specific growth rate, first the minimum recording was subtracted to remove the background signal of the photodiodes. The remaining signal can be interpreted as the light intensity $I(t)$ measured at time t, transmitted through a well containing a cell density $X(t)$ at time t. According to Lambert-Beer's law, this light intensity can be written as:

$$I(t) = I_{\max} \exp(-kX(t)z)$$

where I_{max} is the light intensity transmitted through the well when filled with mineral medium without cells, k is the specific light attenuation coefficient of the cells, and z is path length. Photodiode reads were normalized by dividing the signal $I(t)$ by I_{max}, and then ln-transformed and multiplied by -1. This gives

$$\ln\left(I_{\max}/I(t)\right) = kX(t)z$$

Hence, in case of exponential cell growth, we obtain

$$\ln\left(I_{\max}/I(t)\right) = kzX_0 e^{\mu t}$$

where X_0 is the cell density at time 0 and μ is the specific growth rate. Accordingly, the transformed signal $\ln(I_{max}/I(t))$ was fitted to an exponential trend line, and the specific growth rate, μ, was estimated from the coefficient in the exponent. More specifically, we established the exponential growth phase by plotting the transformed signal $\ln(I_{max}/I(t))$ on a logarithmic scale and used the data in the exponential growth phase to calculate the specific growth rate. Some illustrations of these calculations for batch experiments at 70 µmol photons m^{-2} s^{-1} of blue and red light are provided in Supplementary Fig. S2.

Sampling procedures

To assess differences in photophysiology of *Synechocystis* cells exposed to blue, orange and red light, samples were taken in the exponential growth phase. Each experiment was run two times, using three wells per treatment to obtain triplicate measurements. The first run was used to calculate the specific growth rate and determine the timing of the exponential growth phase based on visual inspection of the transformed signal $\ln(I_{max}/I(t))$ plotted on a logarithmic scale. The next run was used to sample the wells during the exponential growth phase.

Samples were taken by opening the culture vessel within the incubator. First, 500 µL was transferred from each well to a fluorescence cuvette

prefilled with 2.5 mL 30% glycerol. After mixing by pipetting up and down three times the cuvettes were immediately frozen in liquid nitrogen. This procedure was performed within 20 seconds to minimize disturbance, ensuring 77 K fluorescence measurements reflected the actual cell status at the moment of sampling. The cuvettes were kept submerged in liquid nitrogen until 77 K fluorescence analysis. Thereafter, an additional 1 mL sample was taken from each well and transferred to a separate cuvette for measurements of absorbance and cell counts.

Oxygen production rates

O_2 production by *Synechocystis* cells was measured with samples taken directly from the steady-state continuous culture acclimated to white light. Fresh samples were taken every 30 minutes and cell densities were determined after each measurement. Chl *a* content was measured spectrophotometrically after extraction in 80% (v/v) acetone/5% (v/v) DMSO (Porra et al. 1989).

Three samples of 3 mL each were transferred simultaneously to three double-walled 3.2 mL glass chambers (UvA TC, Amsterdam) equipped with Firesting Optodes (Pyroscience, Aachen, Germany). Temperature was controlled by continuously pumping 30ºC water through the double wall. LED lamps were positioned on both sides of the three glass chambers to minimize shading. The LED lamps and O_2-optodes were computer-controlled and the percentage of dissolved O_2 was converted to µmol O_2. The value for 0% O_2 was set by flushing a water sample with pure nitrogen gas for at least 15 minutes and the 100% saturation value was set by flushing with compressed air (containing 20.9 vol% O_2) for at least 15 minutes. O_2-saturated BG-11 medium of 30ºC contains 234 µM O_2 at one atmosphere.

Starting with 3 minutes darkness, samples were exposed to increasing light intensities from 0 to 450 µmol photons m^{-2} s^{-1} while O_2 concentrations in the chamber were measured. The light intensity was increased every 3 minutes. The change in O_2 concentration was calculated 20 seconds after the light intensity was set until 20 seconds before the next change in light intensity. O_2 production rates (P) are presented as µmol O_2 per mg Chl *a* per minute versus light intensity (I). The maximum rate of oxygen production (P_{max}), photosynthetic efficiency (α, the initial slope of the curve at low light intensity) and oxygen consumption rate in darkness (R_d) were estimated by fitting a hyperbolic tangent function to the data (Platt and Jassby 1976):

$$P = P_{\max} \tanh\left(\frac{\alpha I}{P_{\max}}\right) - R_{\mathrm{d}}$$

The fits were based on a nonlinear least-squares regression using R version 3.3.3 (R Development Core Team 2017).

Cell counts

Cells were counted and their biovolume measured using a CASY 1 TTC cell counter with a 60 µm capillary (Schärfe Systems GmbH, Reutlingen, Germany), after diluting the samples to ~5 10^4 cells mL^{-1} in Casyton solution.

Absorption and 77 K fluorescence spectra

Light absorption spectra from 400-750 nm were measured with an updated Aminco DW2000 photospectrometer (OLIS, Bogart, GA, USA).

Samples for 77 K fluorescence measurements were analyzed using an OLIS DM45 spectrofluorimeter (OLIS, Bogart, GA, USA) equipped with a dewar cell. Cuvettes were kept submerged in liquid nitrogen and transferred to the measuring cell of the fluorimeter one at a time. We used 440 nm light to excite Chl *a* in the photosystems and 590 nm light to excite PBSs. Fluorescence emission was measured from 630 to 750 nm, yielding emission peaks at 695 and 725 nm for PSII and PSI, respectively, and two merged peaks around 650 to 665 nm for uncoupled PBSs and (allo)phycocyanin not involved in light harvesting. The ratios of the surface areas of these emission peaks are known to reflect the actual protein ratios quite accurately (Murakami 1997; Schuurmans et al. 2017).

Results

Light-harvesting pigments

Figure 2 shows light absorption spectra of the cyanobacterium *Synechocystis* sp. PCC 6803 and the green alga *Chlorella sorokiniana* 211-8K, when acclimated to 35 µmol photons m^{-2} s^{-1} of white light. The cyanobacterium has absorption peaks in the blue and red part of the spectrum (440 and 680 nm) due to chlorophyll *a* (Chl *a*), and in the orange part (620 nm) due to phycocyanin. Similar to the cyanobacterium, the green alga also has absorption peaks in the blue and red part of the spectrum (440 and 680 nm) due to Chl *a*. Adjacent to its Chl *a* peaks it has shoulders at 450-500 nm and 650-670 nm due to Chl *b*, while it lacks pigments specifically absorbing in the orange part of the spectrum. Both species also contain carotenoids, which absorb in the blue-green part (400-525 nm) of the spectrum but are not recognizable as separate peaks.

Growth rates in blue, orange and red light

To assess the growth rates of *Synechocystis* and *C. sorokiniana* in relation to light absorption by their major light-harvesting pigments, both species were grown in triplicate in batch cultures exposed to four different intensities of either blue (450 nm), orange (625 nm) or red light (660 nm) (Fig. 1).

Specific growth rates of the cyanobacterium *Synechocystis* sp. PCC 6803 were similar in orange and red light, but much lower in blue light at all four intensities (Fig. 3a). Specific growth rates of the green alga *C. sorokiniana* were similar in blue and red light, but lower in orange light (Fig. 3b).

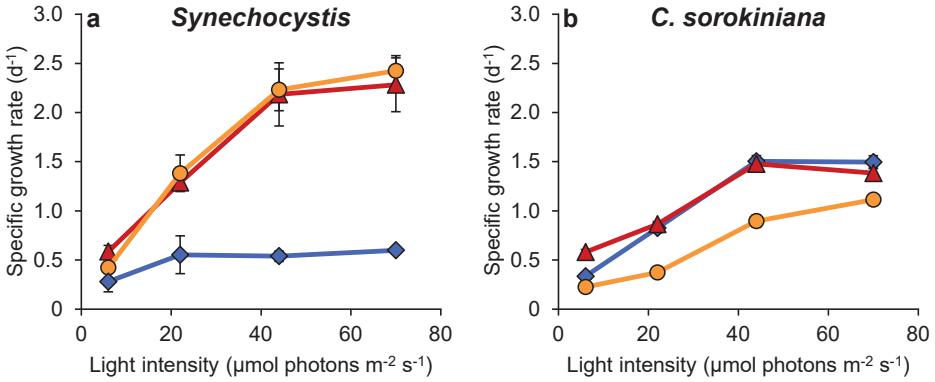

Fig. 3 | Specific growth rates of *Synechocystis* sp. PCC 6803 (a) and *C. sorokiniana* 211-8K (b) in batch cultures exposed to blue (blue diamonds), orange (orange circles) and red light (red triangles) at four different light intensities. Results are averages of three biological replicates ± SD; error bars are not visible when SD is smaller than symbol size.

Could addition of a minor amount of red light alleviate the inefficiency of blue light in *Synechocystis*? To address this question, we performed additional batch experiments, in which *Synechocystis* and *C. sorokiniana* were exposed to mixtures of blue light (450 nm) and red light (660 nm) with a total intensity of 70 µmol photons m^{-2} s^{-1} (Fig. 4). The specific growth rate of *C. sorokiniana* did not change with the percentage red light. In contrast, the specific growth rate of *Synechocystis* strongly increased with the percentage red light, up to 65% red light, and then gradually saturated (Fig. 4). We conjecture that growth rate saturated above 65% red light (i.e., ~45 µmol photons m^{-2} s^{-1}), because this percentage provided sufficient red light to saturate the photosynthetic rate (see Fig. 5). Hence, we did not observe a distinct enhancement effect in *Synechocystis* when blue and red light were combined, but rather a saturating increase of the growth rate in response to the relative availability of red to blue light.

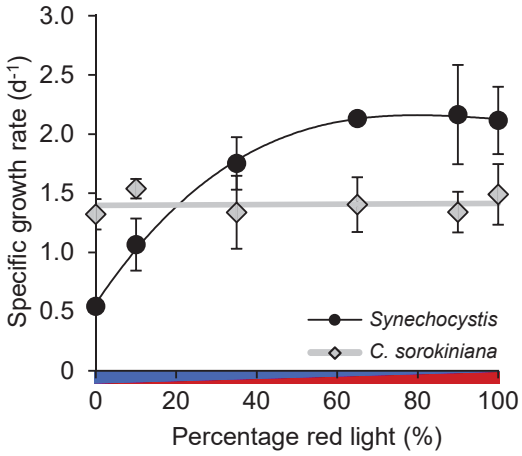

Fig. 4 | Specific growth rates of the cyanobacterium *Synechocystis* sp. PCC 6803 (black circles) and the green alga *C. sorokiniana* (grey diamonds) in batch cultures exposed to different combinations of red and blue light with a total light intensity of 70 µmol photons m^{-2} s^{-1}. Results are averages of three biological replicates ± SD; error bars are not visible when SD is smaller than the symbol size. The data were fitted to a polynomial trendline (using a third-order polynomial for Synechocystis and a constant for *C. sorokiniana*).

Oxygen production is lower in blue light

To investigate the effects of blue light in further detail, O_2 production rates of *Synechocystis* were measured at increasing intensities of blue (450 nm), orange (625 nm) and red light (660 nm). For this purpose, samples pre-acclimated to white light were transferred to temperature-controlled and airtight flasks, where they were exposed to blue, orange and red light while monitoring O_2 concentrations.

The O_2 production rates of *Synechocystis* responded in the same way to light color as the specific growth rates. The increase in O_2 production with irradiance (i.e., the slope *a* of the *p-I* curve) was similar in orange and red light, but much lower in blue light (Fig. 5, Table 1). Photosynthetic O_2 production saturated at ~50 µmol photons m^{-2} s^{-1} in orange and red light but continued to increase with intensity up to ~300 µmol photons m^{-2} s^{-1} in blue light. Interestingly, at these high intensities, photosynthetic activity in blue light approached an almost similar maximum O_2 production rate (i.e., similar P_{max}) as in orange and red light (Fig. 5, Table 1).

Table 1 | Photosynthetic parameters estimated by fitting a hyperbolic tangent to the O_2 production rates (in µmol O_2 mg Chl a^{-1} min^{-1}).

	85.9	3.38	5.1
	86.4	2.38	2.9

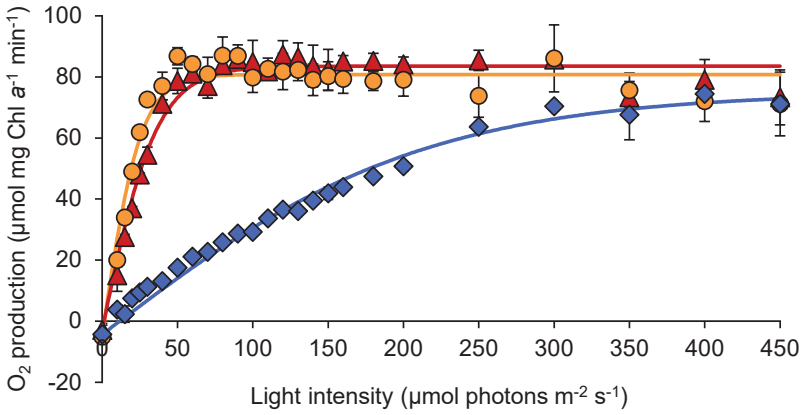

Fig. 5 | Net O_2 production by *Synechocystis* sp. PCC 6803 exposed to blue (blue diamonds), orange (orange circles) and red light (red triangles) at different light intensities. *Synechocystis* cells were sampled from a steady-state continuous culture acclimated to white light, and subsequently exposed to the different light colors in an airtight glass chamber to measure O_2 production using optodes. Data show the averages of three biological replicates ± SD; error bars are not visible when SD is smaller than the symbol size. Solid lines represent fitted *p-I* curves using the hyperbolic tangent function; see Table 1 for parameter estimates.

2

Absorption spectra and PSI:PSII stoichiometry

Absorption spectra and 77 K fluorescence emission spectra were measured in batch cultures of *Synechocystis* exposed to either blue, orange or red light at four different light intensities (Figs. 6 and 7). The absorption spectra show that the ratio between the phycocyanin peak at 620 nm and Chl *a* peak at 680 nm was higher in blue than in orange and red light, indicating that the phycocyanin content increased relative to Chl *a* when cells were grown in blue light. Furthermore, the absorption shoulder at 470-500 nm, indicative of carotenoids, increased with light intensity in red light and to a lesser extent also in orange light, but not in blue light (Fig. 6).

PSI:PSII ratios of *Synechocystis* were studied by means of low-temperature (77 K) fluorescence spectroscopy (Fig. 7a-c). By freezing cells at 77 K immediately after sampling, the positions of the photosynthetic components are fixed. However, excitation energy can still be transferred to the reaction centers. The subsequent fluorescence emission by the reactions centers of PSI and PSII provides insight into the relative amounts of the two photosystems.

Figure 7a-c show fluorescence emission spectra upon excitation of Chl *a* at 440 nm, which yields fluorescence emission peaks at 695 nm for PSII and at 725 nm for PSI. *Synechocystis* cells acclimated to orange and red light showed very similar results (Fig. 7b and 7c), with a PSI:PSII

fluorescence emission ratio of ~4:1 at all four light intensities. In contrast, *Synechocystis* cells acclimated to blue light showed a less characteristic photosystem stoichiometry, with a PSI:PSII fluorescence emission ratio of ~1.2:1 at 6, 22 and 44 µmol photons m^{-2} s^{-1} and of ~1.4:1 at 70 µmol photons m^{-2} s^{-1} (Fig. 7a). Hence, blue light reduced the PSI:PSII ratio of *Synechocystis*.

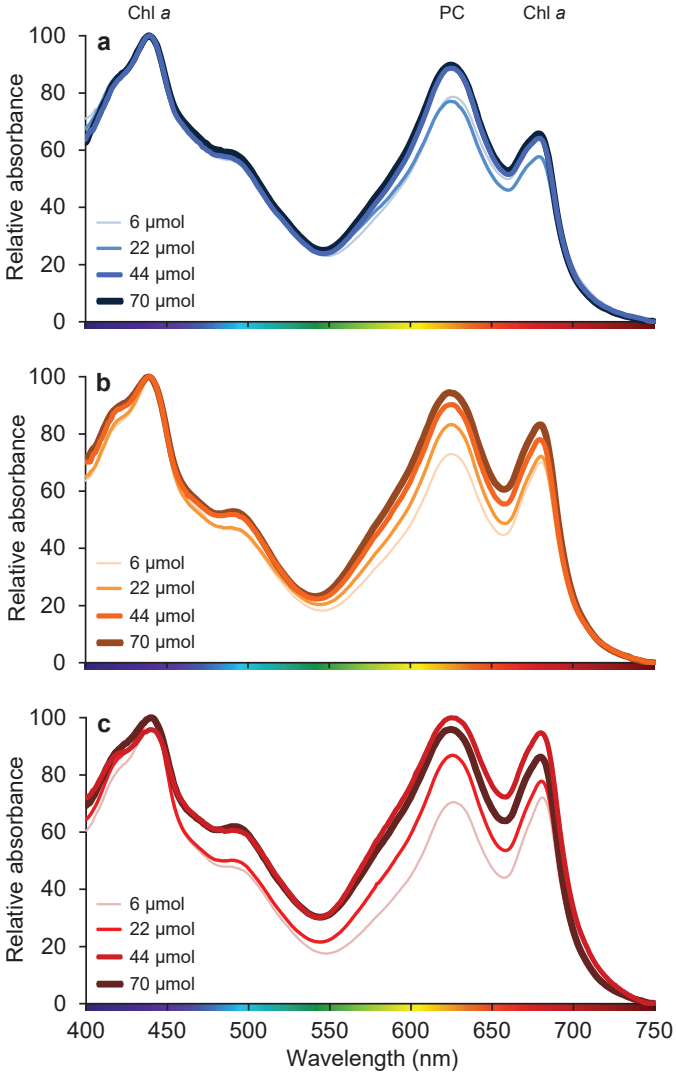

Fig. 6 | Absorption spectra of *Synechocystis* sp. PCC 6803 in batch cultures exposed to (a) blue light, (b) orange light, and (c) red light at four different light intensities (6, 22, 44 and 70 µmol photons m^{-2} s^{-1}). Light absorption peaks by Chl *a* and phycocyanin (PC) are indicated. Spectra show the averages of three biological replicates, and are normalized to minimum absorbance at 750 nm and maximum absorbance at 440 nm.

Changes in state transitions

Low-temperature (77 K) fluorescence also provides insight into the coupling of phycobilisomes (PBSs) to the reaction centers of PSI and PSII, and hence into state transitions. Figure 7d-f show fluorescence emission spectra upon excitation at 590 nm of phycocyanin, which is the major phycobiliprotein in PBSs of *Synechocystis* sp. PCC 6803. If PBSs are decoupled from the reaction centers, or phycocyanin is not incorporated into PBSs, excitation of phycocyanin results in fluorescence emission at 650-665 nm. If PBSs are coupled to the reaction centers, the excitation energy is transferred from the PBSs to the reaction centers, resulting in fluorescence emission peaks at 695 nm when coupled to PSII (state 1) or at 725 nm when coupled to PSI (state 2).

In *Synechocystis* cells acclimated to blue light, fluorescence emission by PSII at 695 nm was much higher than fluorescence emission by PSI at 725 nm (Fig. 7d). This indicates that, in blue light, most PBSs transferred their harvested light energy to PSII. By contrast, the difference in fluorescence emission by PSII and PSI was much less pronounced in cells exposed to orange and red light (Fig. 7e,f), indicating that in orange and red light the excitation energy harvested by the PBSs was distributed more or less evenly over both photosystems. We further note that in orange and red light a relatively large fraction of the PBSs seemed not functional in light-harvesting, as fluorescence emission at 650-665 nm was quite prominent (Fig. 7e,f).

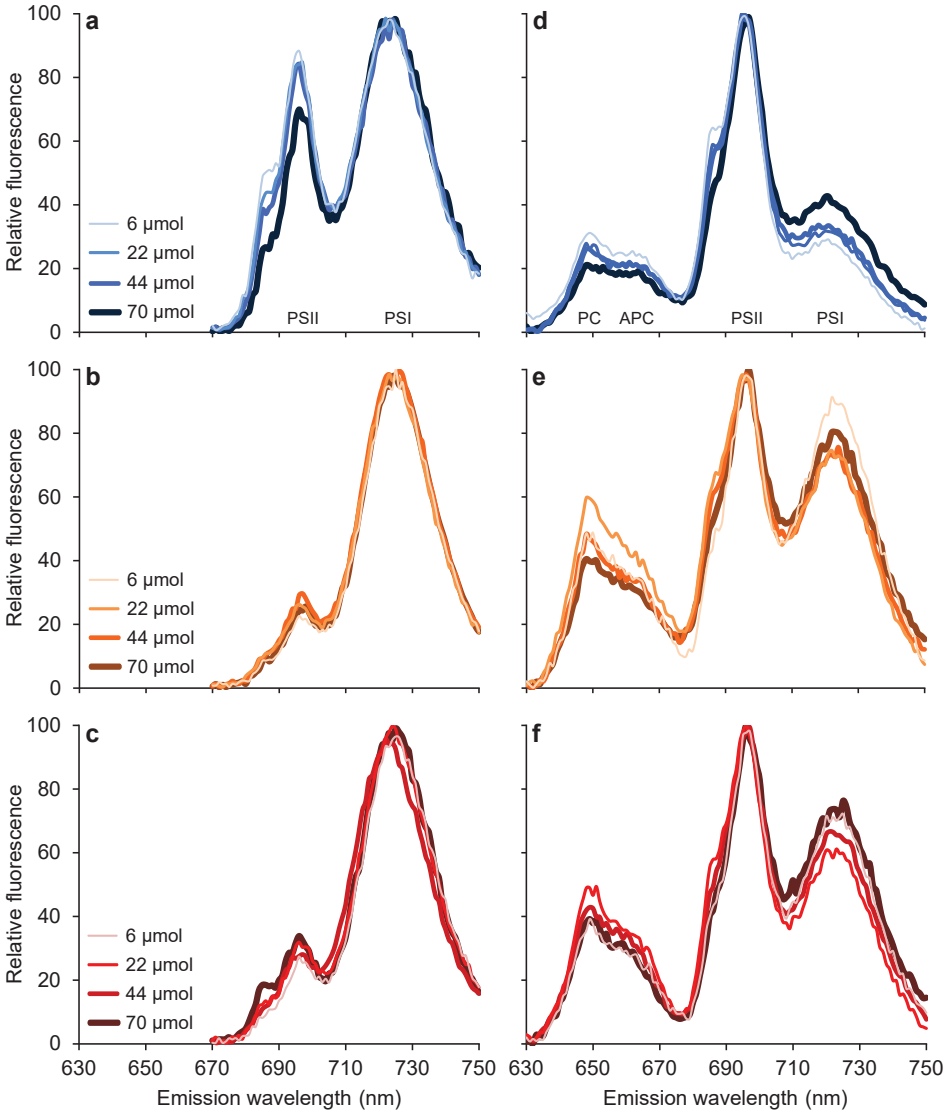

Fig. 7 | Low-temperature (77 K) fluorescence emission spectra of *Synechocystis* sp. PCC 6803 in batch cultures exposed to (a,d) blue light, (b,e) orange light, and (c,f) red light at four different light intensities (6, 22, 44 and 70 µmol photons m^{-2} s^{-1}). (a-c) Excitation of Chl *a* at 440 nm yields fluorescence emission peaks at 695 nm for PSII and at 720 nm for PSI. (d-f) Excitation of phycocyanin at 590 nm yields fluorescence emission peaks at 695 nm when PBSs are coupled to PSII (state 1) and at 720 nm when coupled to PSI (state 2). PBSs that are decoupled from the photosystems, or phycocyanin that is not incorporated into PBSs, result in fluorescence emission from phycocyanin and allophycocyanin at 650-665 nm. Spectra show the averages of three biological replicates, and are normalized to the minimum and maximum emission of each spectrum.

Comparison with other picocyanobacteria

To assess whether the low growth efficiency in blue light is a common phenomenon in cyanobacteria, growth rates were also determined for two marine *Synechococcus* strains, CCY 9201 (formerly known as BS4) and CCY 9202 (formerly BS5). These two picocyanobacteria are of considerable interest, because of their very close genetic relatedness based on the 16S rRNA-ITS operon, while they absorb different parts of the light spectrum because of their different phycobiliproteins (Stomp et al. 2004; Haverkamp et al. 2009). *Synechococcus* sp. CCY 9201 has a similar pigmentation as *Synechocystis* sp. PCC 6803: both utilize the orange-light absorbing phycocyanin in their light-harvesting antennae. In contrast, *Synechococcus* sp. CCY 9202 contains high amounts of phycoerythrin, with which it strongly absorbs in the green part (525-575 nm) of the spectrum (Supplementary Fig. S1).

Synechococcus sp. CCY 9201 had its lowest growth rate in blue light, and an eight-fold higher specific growth rate in orange and red light (Fig. 8). The specific growth rate of the phycoerythrin-rich strain CCY 9202 was also lowest in blue light, and it had a three- to four-fold higher specific growth rate in orange and red light, respectively. Hence, both *Synechococcus* strains displayed a qualitatively similar growth response as *Synechocystis* sp. PCC 6803. These results show that the diminished growth rate in blue light is not unique to phycocyanin-rich cyanobacteria, but can also be found in phycoerythrin-rich cyanobacteria.

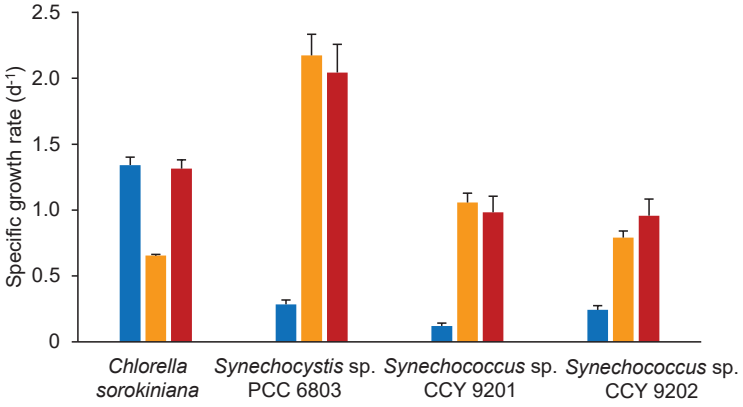

Fig. 8 | Specific growth rates of the green alga *C. sorokiniana* 211-8K and the cyanobacteria *Synechocystis* sp. PCC 6803, *Synechococcus* sp. CCY 9201 and *Synechococcus* sp. CCY 9202 in batch cultures exposed to blue, orange and red light at an intensity of 44 µmol photons·m^{-2}·s^{-1}. Light absorption spectra of these four species are provided in Supplemental Figure S1. Results show the averages of three biological replicates ± SD.

Discussion

Our results show that the cyanobacterium *Synechocystis* sp. PCC 6803 absorbs blue light to at least a similar extent as orange and red light (Figs. 2 and 6), but uses the absorbed blue light much less effectively for oxygenic photosynthesis and growth (Figs. 3-5). The poor photosynthetic performance of cyanobacteria in blue light has also been reported by several earlier studies (e.g., Lemasson et al. 1973; Wyman and Fay 1986; Wilde et al. 1997; Tyystjärvi et al. 2002; Wang et al. 2007; Singh et al. 2009; Chen et al. 2010; Choi et al. 2013; Solhaug et al. 2014; Bland and Angenent 2016), but in-depth investigations were still lacking. Our results support the hypothesis that blue light creates an imbalance between the two photosystems, with an excess of energy at the PSI-side and a deficiency at the PSII-side of the photosynthetic electron transport chain of cyanobacteria (e.g., Solhaug et al. 2014; Kirilovsky 2015). This hypothesis is explained below.

In orange and red light, cyanobacteria usually have 2 to 5 times more PSI than PSII (Fig. 7a-c; see also Singh et al. 2009; Allahverdiyeva et al. 2014; Kirilovsky 2015). Furthermore, cyanobacterial PSI contains around 100 molecules of Chl *a* (Jordan et al. 2001; Kennis et al. 2001), while a single PSII contains only about 35 Chl *a* molecules (Guskov et al. 2009; Umena et al. 2011). Hence, cyanobacteria invest much more of their chlorophyll in PSI than in PSII, and therefore PSI will absorb more photons than PSII (e.g., Myers et al. 1980; Fujita 1997). This dissimilarity between the two photosystems is compensated for by the light-harvesting PBSs, which tend to be associated mostly with PSII and hence transfer most of their absorbed photons to PSII (van Thor et al. 1998; Joshua et al. 2005; Mullineaux 2008). In this way, cyanobacteria can maintain linear electron flow by balancing excitation energy between the two photosystems, which will enable the production of both ATP and NADPH required for growth (Allen 2003; Nogales et al. 2012; Mullineaux 2014).

In blue light, the PBSs do not absorb photons very effectively, because the short wavelength of 450 nm does not match the absorption spectrum of phycocyanin (Fig. 2; see also, e.g., Tandeau de Marsac 2003; Six et al. 2007). Hence, in blue light, the PBSs hardly transfer any light energy to PSII. In contrast, the chlorophylls of the more abundant PSI still absorb blue light effectively. Moreover, in cyanobacteria, β-carotenes absorbing blue and green wavelengths are also more abundant in PSI than PSII and further contribute to photosynthetic light harvesting by PSI (Ritz et al. 2000; Takaichi 2011; Stamatakis et al. 2014). Hence, most blue photons are absorbed at PSI, while in comparison PSII has a severe

shortage of photons, which will suppress linear electron transport. This is supported by the low O_2 production rates that we measured when the cyanobacteria were exposed to limiting levels of blue light. Interestingly, once the intensity of blue light was high enough to saturate PSII, the O_2 production rate in blue light approached the rate found in orange and red light (Fig. 5).

The important role of PBS in the distribution of excitation energy over the two photosystems is illustrated by a study of Campbell (1996) on complementary chromatic adaptation of the cyanobacterium *Calothrix* sp. strain PCC 7601. When acclimated to green light the PBSs of this species contain mostly phycoerythrin, while they contain mostly phycocyanin when adapted to red light. Rates of photosynthesis were similar in both light colors, but 77 K fluorescence emission revealed major differences in the distribution of light by the PBSs. Similar to our experimental results, red light (600-750 nm) applied by Campbell (1996) was absorbed by both Chl *a* and (allo)phycocyanin, and the PBSs of red-light acclimated cells were mostly associated with PSII while Chl *a* harvested light for PSI. In contrast, green light (500-575 nm) was only absorbed by phycoerythrin, and the phycoerythrin-containing PBSs of green-light acclimated cells transferred light energy to both PSI and PSII to maintain the balance between these two photosystems.

Our results indicate that blue-light acclimated cells attempt to restore the balance between the two photosystems in a similar way. Fluorescence emission by the two photosystems after excitation of Chl *a* at 440 nm showed that blue-light acclimated cells decrease their PSI:PSII ratio (Fig. 7a-c), which will increase light absorption by PSII relative to PSI. Furthermore, fluorescence emission after excitation of phycocyanin at 590 nm revealed that blue-light acclimated cells associate even more of their PBSs with PSII than cells acclimated to orange and red light (Fig.7d-f). All these results indicate that cells exposed to blue light try to increase the transfer of light energy to PSII, to restore the balance. Yet, the low O_2 production rates indicate that cells in blue light are still unable to sustain a high rate of linear electron flow in comparison to those in orange and red light, unless saturating amounts of blue light are provided.

Previous research has shown that in high CO_2 conditions, cyanobacteria decrease their PSI:PSII ratio and increase phycocyanin relative to Chl *a* (MacKenzie et al. 2004; Eisenhut et al. 2007). These changes are similar to the changes we observed in blue-light acclimated cultures, indicative of an increased transfer of light energy to PSII at high CO_2 conditions. Since our experiments were also performed at high CO_2 conditions, the results of MacKenzie et al. (2004) and Eisenhut et al. (2007) suggest that

the photosynthetic efficiency of cyanobacteria in blue light might be even lower under carbon-limiting conditions.

Since red light is also absorbed by Chl *a*, why did red light not give the same results as blue light? The answer is probably related to the wavelength of 660 nm that we used as the red-light source in our experiments. This wavelength is already longer than the 620-650 nm-red light used in many previous studies (Wyman and Fay 1986; Figueroa et al. 1995; Wang et al. 2007; Singh et al. 2009; Chen et al. 2010; Choi et al. 2013; Solhaug et al. 2014; Zavřel et al. 2017). This range of wavelengths around 660 nm is absorbed not only by chlorophyll, but also very effectively by allophycocyanin in the core of the PBS (Lemasson et al. 1973; Glazer and Bryant 1975; MacColl 2004). Hence, the PBSs can still redistribute photons of 660 nm over both photosystems, as indicated by the 77 K fluorescence data of the red-light acclimated cells after excitation of the PBSs (Fig. 7f). One would expect that cells grown with red light at a longer wavelength of 680 nm, which is much less absorbed by allophycocyanin and hence specifically targets Chl *a*, would display similar results as our blue-light exposed cells. Indeed, other studies provide support for this hypothesis. For instance, Murakami (1997) showed that *Synechocystis* sp. PCC 6714 had a substantially lower PSI:PSII ratio when grown at 680-nm red light than at 650-nm red light, resembling the low PSI:PSII ratio that we found for *Synechocystis* sp. PCC 6803 in blue light. Bland and Angenent (2016) found that *Synechocystis* sp. PCC 6803 had a lower specific growth rate at 680 nm than at 660 nm, although the growth rate was even lower in blue light (440 and 460 nm). Blue-light absorbing β-carotenes are more abundant in PSI than in PSII, and in cyanobacteria they contribute to light harvesting only for PSI (Stamatakis et al. 2014). Hence, we speculate that blue light causes an even stronger imbalance between PSI and PSII than red light of 680 nm, which may explain their observation (Bland and Angenent 2016) that the growth rate was even lower in blue light than in red light of 680 nm.

Our findings show that the poor performance in blue light is not specific for the freshwater cyanobacterium *Synechocystis* sp. PCC 6803, but also applies to marine cyanobacteria including both phycocyanin-rich strains such as *Synechococcus* sp. CCY 9201 and phycoerythrin-rich strains such as *Synechococcus* sp. CCY 9202 (Fig. 8). The low rates of growth and photosynthesis in blue light even extend to red algae which also possess PBSs composed of phycocyanin and phycoerythrin (Ley and Butler 1980; Figueroa et al. 1995). Hence, although the chromophores phycoerythrobilin and phycourobilin absorb green light (absorption peak at 545 nm) and blue-green light (495 nm), respectively, these organisms

are not able to absorb and redistribute deep blue light (< 450 nm) very effectively between the two photosystems.

In green algae, growth rates in blue and red light are comparable (Fig. 3b; see also Teo et al. 2014; Yan and Zheng 2014; Zhao et al. 2015; de Mooij et al. 2016), thus blue light does not seem to result in an excitation imbalance between their PSII and PSI. Green algae maintain a lower PSI:PSII ratio than cyanobacteria (Murakami et al. 1997; Kirilovsky 2015) and utilize light-harvesting antennae composed of Chl *a* and *b* (Kühlbrandt et al. 1994). Additionally, green algae are able to use blue light more efficiently due to a wider variety of light-harvesting carotenoids, in their photosystems and light-harvesting antennae, which also absorb photons in the blue-green part of the visible light spectrum (Takaichi 2011). Contrary to cyanobacteria, these carotenoids harvest light energy not only for PSI, but also for PSII (Goedheer 1969). Hence, in contrast to the cyanobacterial PBSs, the light-harvesting antennae of green algae absorb both blue and red light, and transfer the absorbed light energy to both PSI and PSII in a balanced way.

Our results help to explain why *Prochlorococcus* species dominate over *Synechococcus* species in the oligotrophic oceans (Partensky et al. 1999; Biller et al. 2015). Because red light is strongly absorbed by water molecules, blue light (400-500 nm) prevails in the deeper water layers of the open ocean (Stomp et al. 2007a). Instead of PBSs, *Prochlorococcus* utilizes light-harvesting antennae composed of divinyl Chl *a* and *b* (Chisholm et al. 1992; Ting et al. 2002). Consequently, like green algae, they can balance the amply available blue light between both photosystems. In contrast, *Synechococcus* species utilize blue light much less effectively. The PBSs of marine *Synechococcus* strains of the oligotrophic ocean often contain high contents of phycourobilin (Palenik 2001; Everroad et al. 2006; Six et al. 2007; Grébert et al. 2018), with which they do absorb blue-green light (495 nm). However, none of the phycobiliproteins described so far extends its absorption to the deep-blue wavelengths (< 450 nm) that form a major part of the underwater light spectrum characteristic of the oligotrophic ocean. Hence, not only does blue light offer a suitable habitat for the chlorophyll-based light-harvesting antennae of *Prochlorococcus*, as has been described by many previous studies (Scanlan and West 2002; Ting et al. 2002; Rocap et al. 2003; Stomp et al. 2007a), but blue light (< 450 nm) is also less suitable for phycobilisome-containing cyanobacteria such as *Synechococcus*.

Acknowledgments

This manuscript is dedicated to the memory of our dear colleague and co-author dr. Hans C.P. Matthijs, who initiated and encouraged the research reported here. We are most grateful to Tania S. Darphorn and Joris Solleveld for their help with the experiments and to Theo van Lieshout, Gerrit Hardeman, Mattijs Bakker and Johan Mozes of the Technology Centre of the University of Amsterdam for their help in designing and manufacturing the experimental incubator. We thank Douglas Campbell and an anonymous reviewer for constructive comments on the manuscript, and participants of the Wetsus research theme "Algae" and the FAME department of the University of Amsterdam for fruitful discussions. This work has been performed in the cooperation framework of Wetsus, European Centre of Excellence for Sustainable Water Technology (www.wetsus.eu). Wetsus is co-funded by the Dutch Ministry of Economic Affairs and Ministry of Infrastructure and Environment, the Province of Fryslân and the Northern Netherlands Provinces.

Supplementary information

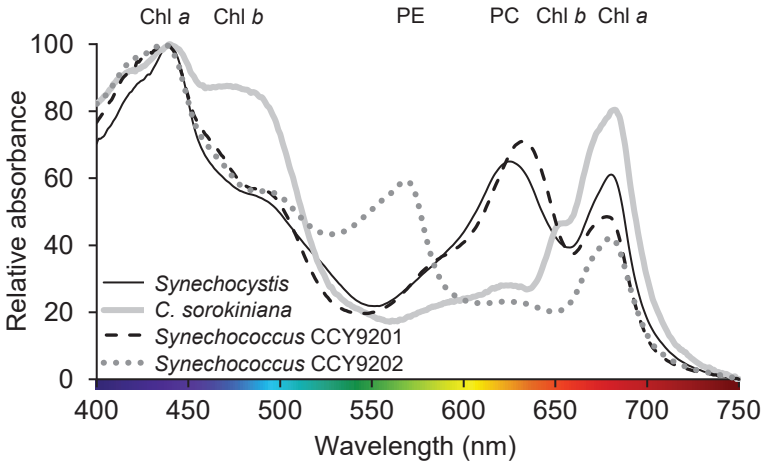

Supplementary Fig. S1 | Light absorption spectra of three cyanobacteria and a green alga. All four species have absorption peaks for Chl *a* (440 and 680 nm) and carotenoids (400-525 nm). The cyanobacteria *Synechocystis* sp. PCC 6803 (black solid line) and *Synechococcus* sp. CCY 9201 (black dashed line) have an additional absorption peak for phycocyanin (PC) at 620 nm. The cyanobacterium *Synechococcus* sp. CCY 9202 (grey dotted line) has an additional absorption peak for phycoerythrin (PE) at 565 nm. The green alga *C. sorokiniana* (grey solid line) has additional absorption shoulders for Chl *b* at 450-500 nm and 650-670 nm. The species were all grown at 35 µmol photons m^{-2} s^{-1} of white light.

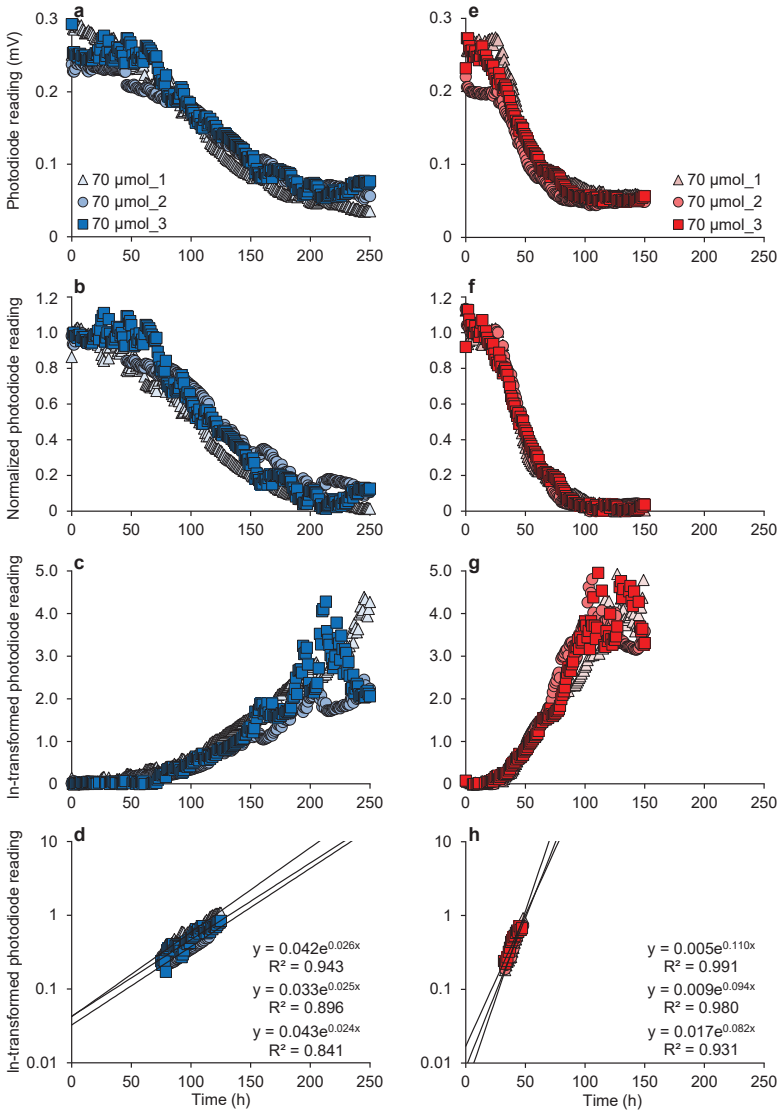

Supplementary Fig. S2 | Calculation of the specific growth rate from photodiode reads of batch cultures in the incubation shaker. Here we show examples for three replicate batch cultures of *Synechocystis* sp. PCC 6803 grown in blue (a-d) and red light (e-h) at 70 µmol photons m^{-2} s^{-1}. (a,e) The photodiodes record voltage as a measure of light intensity. (b,f) First, the minimum recording was subtracted to remove the background signal of the photodiodes and, subsequently, the photodiode reads were normalized by dividing the data by the recording of mineral medium without cells. (c,g) Next, data were ln-transformed and multiplied by -1. (d,h) Finally, the ln-transformed data were presented on a logarithmic scale and we used the linear part of these growth curves to calculate the specific growth rate by fitting an exponential trendline to the data. The three replicates resulted in three specific growth rates for each experimental condition.

Chapter 3

Exploring the low photosynthetic efficiency of cyanobacteria in blue light using a mutant lacking phycobilisomes

Veerle M. Luimstra[1,2], J. Merijn Schuurmans[1], Carolina F. M. de Carvalho[1], Hans C. P. Matthijs[1†], Klaas J. Hellingwerf[3], Jef Huisman[1]

[1]Department of Freshwater and Marine Ecology, Institute for Biodiversity and Ecosystem Dynamics, University of Amsterdam, Amsterdam, The Netherlands
[2]Wetsus, European Centre of Excellence for Sustainable Water Technology, Leeuwarden, The Netherlands
[3]Swammerdam Institute for Life Sciences, University of Amsterdam, Amsterdam, The Netherlands
†Deceased, April 17, 2016

This chapter is published in:
Photosynthesis Research 141:291-301 (2019)

Abstract

The ubiquitous chlorophyll *a* (Chl *a*) pigment absorbs both blue and red light. Yet, in contrast to green algae and higher plants, most cyanobacteria have much lower photosynthetic rates in blue than in red light. A plausible but not yet well-supported hypothesis is that blue light results in limited energy transfer to photosystem II (PSII), because cyanobacteria invest most Chl *a* in photosystem I (PSI), whereas their phycobilisomes (PBS) are mostly associated with PSII but do not absorb blue photons. In this paper, we compare the photosynthetic performance in blue and orange-red light of wildtype *Synechocystis* sp. PCC 6803 and a PBS-deficient mutant. Our results show that the wildtype had much lower biomass, Chl *a* content, PSI:PSII ratio and O_2 production rate per PSII in blue light than in orange-red light, whereas the PBS-deficient mutant had a low biomass, Chl *a* content, PSI:PSII ratio, and O_2 production rate per PSII in both light colors. More specifically, the wildtype displayed a similar low photosynthetic efficiency in blue light as the PBS-deficient mutant in both light colors. Our results demonstrate that the absorption of light energy by PBS and subsequent transfer to PSII are crucial for efficient photosynthesis in cyanobacteria, which may explain both the low photosynthetic efficiency of PBS-containing cyanobacteria and the evolutionary success of chlorophyll-based light-harvesting antennae in environments dominated by blue light.

Introduction

Cyanobacteria are the oldest known oxygen-producing photosynthetic organisms on our planet and their photosynthetic activity is widely held responsible for oxygenation of the Earth's atmosphere about 2.3 billion years ago (Holland 2002; Schirrmeister et al. 2015). The ubiquitous chlorophyll *a* (Chl *a*) pigment in the photosystems of oxygenic phototrophs absorbs both blue (440 nm) and red light (678 nm), and hence one would expect that these two colors of light are used at approximately equal efficiency. Yet, in contrast to green algae and higher plants, cyanobacteria appear to have much lower oxygen (O_2) production and growth rates in blue light than in red light (e.g. Lemasson et al. 1973; Pulich and van Baalen 1974; Wilde et al. 1997; Tyystjärvi et al. 2002; Wang et al. 2007; Singh et al. 2009; Luimstra et al. 2018).

Why cyanobacteria perform less well in blue light is not yet fully resolved. It is often hypothesized that the distribution of absorbed light energy between photosystem I (PSI) and photosystem II (PSII) plays a key role (Fujita 1997; El Bissati and Kirilovsky 2001; Wang et al. 2007; Singh

et al. 2009; Solhaug et al. 2014; Kirilovsky 2015; Luimstra et al. 2018). To optimize absorption of light energy, cyanobacteria use phycobilisomes (PBS) as light-harvesting antennae, which transfer absorbed light energy to the photosystems (Grossman et al. 1993; Tandeau de Marsac 2003). Most of the PBS are typically associated with PSII (state 1), but PBS can be relocated to PSI (state 2) at time scales of seconds to minutes, or they can be detached from the photosystems in which case they do not contribute to the photosynthetic activity of the cells (Joshua et al. 2005; Mullineaux 2014; Kirilovsky 2015). Blue light ≤ 450 nm is very poorly absorbed by PBS (Tandeau de Marsac 2003; Six et al. 2007), however, and hence PBS cannot distribute the absorbed light energy over the two photosystems.

Instead, blue light is directly absorbed by chlorophyll and carotenoids associated with the two photosystems. Cyanobacteria contain ~100 molecules of Chl *a* per PSI (Jordan et al. 2001) but only ~35 molecules of Chl *a* per PSII (Umena et al. 2011). Moreover, the PSI:PSII ratio of cyanobacteria usually ranges between 5:1 and 2:1, depending on the growth conditions, which is higher than the approximately 1:1 ratio often found in eukaryotic phototrophs (Shen et al. 1993; Fujita 1997; Olive et al. 1997; Singh et al. 2009; Allahverdiyeva et al. 2014). Since cyanobacteria usually invest most of their Chl *a* in PSI (e.g. Myers et al. 1980; Fujita 1997; Luimstra et al. 2018) and, in cyanobacteria, only the carotenoids in PSI are involved in light harvesting (Stamatakis et al. 2014), PSI will absorb more blue photons than PSII. This implies that blue light is likely to cause an excitation imbalance between both photosystems, with low O_2 production by PSII and limited linear electron transport (Fujita 1997; Solhaug et al. 2014; Kirilovsky 2015), which then explains the low photosynthetic efficiency and growth rate of cyanobacteria in blue light (Luimstra et al. 2018). However, although many observations support this hypothesis, conclusive evidence is still limited.

In this paper, we aim to contribute to a further understanding of why cyanobacteria display a low photosynthetic efficiency in blue light. Therefore, we compare the photosynthetic efficiency in blue and orange-red light of *Synechocystis* sp. PCC 6803 and a mutant strain lacking PBS known as the PAL mutant (Ajlani and Vernotte 1998). The PAL mutant does not have light-harvesting antennae that are able to redistribute light energy over both photosystems. Consequently, our expectation is that the PAL mutant will have limited energy transfer to PSII irrespective of the light color and hence will display a similarly low photosynthetic efficiency in both orange-red and blue light as the wildtype in blue light. An advanced understanding of the light-color dependence of cyanobacterial

photosynthesis may contribute to an improved design of successful culture conditions in biotechnological applications, and to further clarification of the ecological distributions of cyanobacteria in waters dominated by different wavelengths.

Materials and Methods

Strains and culture conditions

We investigated a wildtype and a mutant strain of *Synechocystis* sp. PCC 6803, which uses the phycobilin-pigment C-phycocyanin in its PBS. The wildtype strain was provided by professor D. Bhaya (University of Stanford, USA) and the phycobilisome-deficient PAL mutant strain was provided by Dr. G. Ajlani (Université Paris-Sud, France).

The experimental set-up is illustrated in Fig. 1a,b. The strains were grown at 30°C in 1.8 L light-limited chemostats with flat culture vessels illuminated from one side (Huisman et al. 2002). Blue light (450 nm) or orange-red light (660 nm) with a full width at half maximum of ~20 nm was provided by narrow-band LED panels (Philips Lighting B.V., Eindhoven, The Netherlands) at an incident light intensity of 45 µmol photons $m^{-2}\,s^{-1}$. Light intensities were measured with an LI-250 light meter (LI-COR Biosciences, Lincoln, NE, USA). The chemostats had an optical path length of 5 cm. Cultures were provided with BG-11 medium (Merck, Darmstadt, Germany) supplemented with 5 mM Na_2CO_3, at a constant dilution rate of D = 0.015 h^{-1} (0.36 d^{-1}). Chloramphenicol (20 µg mL^{-1}) was added to the first 6 L of medium for the PAL mutant to prevent growth of the wildtype (Ajlani and Vernotte 1998). The cultures were mixed by bubbling with CO_2-enriched air (2% v/v) flowing at a rate of 30 L h^{-1}. The CO_2 concentration of the gas mixture was regularly monitored using an Environmental Gas Monitor for CO_2 (EGM-4; PP Systems, Amesbury, MA, USA).

Cell counts and chlorophyll analysis

A CASY 1 TTC cell counter with a 60 µm capillary (Schärfe Systems GmbH, Reutlingen, Germany), was used to count cells and measure their biovolume. Samples were diluted to ~5 × 10^4 cells mL^{-1} in Casyton solution prior to measuring. Chl *a* content of the cells was measured spectrophotometrically using a Novaspec III Visible Spectrophotometer after extraction in 80% (v/v) acetone/5% (v/v) DMSO (Porra et al. 1989).

Absorption and 77 K fluorescence spectra

After the chemostats reached steady-state, 1 mL and 1.5 mL samples were taken for the measurement of light absorption spectra and 77 K fluorescence spectra, respectively. Immediately after sampling, light absorption spectra were measured from 400-750 nm using an updated Aminco DW2000 spectrophotometer (OLIS, Bogart, GA, USA). The spectra were normalized to Chl *a* absorbance at 678 nm, after baseline correction for minimum absorbance at 750 nm. Molar phycocyanin-to-Chl *a* (PC:Chl) ratios were estimated from the absorption spectra according to Rakhimberdieva et al. (2001):

$$\mathrm{PC{:}\,Chl} = \frac{4.9A_{625} - 2.1A_{652} - 0.8A_{678}}{0.1A_{625} - 0.7A_{652} + 15.8A_{678}}$$

where A_{625}, A_{652} and A_{678} are the absorption peaks of PC, allophycocyanin and Chl *a*, respectively. Cellular PC contents (quantified as monomers) were calculated from the measured Chl *a* content and estimated PC:Chl ratio.

For the 77 K fluorescence spectra, the 1.5 mL samples were transferred to 3 mL-cuvettes prefilled with 1.5 mL 60% glycerol. The final glycerol concentration in the cuvettes was 30% to minimize dissociation of PBS, and cell concentrations were below 410^7 cells mL^{-1} to minimize re-absorption of the fluorescence signal (Mao et al. 2003). Samples were mixed by pipetting up and down three times and the cuvettes were frozen in liquid nitrogen. To guarantee that the fluorescence spectra reflected the quantities of photosynthetic components at the time of sampling, this procedure was performed within 20 seconds. Cuvettes were stored at -80°C, for maximally one week, until 77 K fluorescence analysis with an OLIS DM45 spectrofluorimeter (OLIS, Bogart, GA, USA) equipped with a Dewar cell. Fluorescence emission was measured from 630-750 nm with excitation at 440 nm (mainly Chl *a*). The peak areas of PSI (emission at 725 nm) and PSII (emission at 695 nm) were calculated by deconvolution of the spectra according to Du et al. (2016) using R version 3.3.3 (R Development Core Team 2017).

Earlier studies have shown that the ratio of the surface areas of the PSI and PSII peaks in the 77 K fluorescence emission spectra corresponds quite well to the molar PSI:PSII ratio of the actual protein complexes (Murakami 1997; Schuurmans et al. 2017). Therefore, cellular PSI and PSII contents (in mol $cell^{-1}$) were calculated using the PSI:PSII ratio obtained from the deconvoluted 77 K spectra and the cellular Chl *a* content (mol $cell^{-1}$, where Chl *a* has a molecular weight of 893.5 g mol^{-1}).

The calculation assumes that PSI and PSII contain 100 and 35 Chl *a* molecules, respectively (Jordan et al. 2001; Umena et al. 2011):

$$\mathrm{PSI_{cell}} = \frac{[\mathrm{Chl}\ a]}{100 + 35/(\mathrm{PSI{:}\ PSII})}$$

$$\mathrm{PSII_{cell}} = \frac{[\mathrm{Chl}\ a]}{100\times(\mathrm{PSI{:}\ PSII}) + 35}$$

We note that these calculations should be interpreted with care, and provide only a rough estimate of relative changes in PSI and PSII content.

Oxygen production and consumption rates analyzed using MIMS

O_2 production and consumption were measured using membrane-inlet mass spectrometry (MIMS), via high-vacuum-supported diffusive equilibration of the dissolved O_2 through a gas permeable membrane coupled to a mass spectrometer (Kana et al. 1994). Small amounts of gasses can flow out of the liquid culture into the sensor of the mass spectrometer through a thin Teflon membrane. Addition of $^{18}O_2$ and subsequent quantification of both stable oxygen isotopes ($^{16}O_2$ and $^{18}O_2$) allows for distinction between O_2 production (evolution of $^{16}O_2$ from water-splitting at PSII) and O_2 consumption (uptake of the added $^{18}O_2$) in a single sample. Samples were taken from the steady-state continuous cultures of *Synechocystis* sp. PCC 6803 wildtype and the PAL mutant acclimated to orange-red and blue light. To facilitate comparison, all samples were diluted to the same OD_{750} of 0.04 prior to the MIMS analysis.

A fresh sample was taken for each measurement and transferred to a double-walled, airtight 10 mL glass chamber (a DW3 cuvette from Hansatech Instruments, modified by the Technology Centre of the University of Amsterdam) equipped with a magnetic stirrer. The inlet sensor of the mass spectrometer was placed directly in the culture. Prior to measurements, $NaHCO_3$ was added at a final concentration of 15 mM to prevent carbon limitation during the experiment. The samples were flushed with N_2 gas to reduce the $^{16}O_2$ concentration to ~5% of the value in air-equilibrated medium to prevent O_2 saturation during the experiment, after which $^{18}O_2$ (95%–98% pure; Cambridge Isotope Laboratories) was added in the headspace. The magnetic stirrer allowed for diffusion into the liquid culture. When the $^{18}O_2$ concentration reached ~20% of the value in air-equilibrated medium the headspace was aspirated and the glass chamber closed.

Temperature in the glass chamber was maintained at 30ºC by water pumped through its double wall. Two LED lamps, identical to those used for the chemostats, illuminated the glass chamber from both sides to minimize shading effects. The samples were exposed to orange-red or blue light at increasing light intensities (summed over both lamps) from 0-400 µmol photons m^{-2} s^{-1}. After 10 min dark adaptation, light intensity was increased every 3 min while O_2 concentrations were measured continuously by the MIMS. The MIMS signals were normalized to argon according to Kana et al. (1994), and O_2 production and consumption rates were calculated according to Bañares-España et al. (2013).

O_2 production and consumption rates were expressed as fmol O_2 per cell per minute and as mol O_2 per mol PSII per second. Cell densities were determined directly after each MIMS experiment. Gross O_2 production (P) rates were plotted versus light intensity (I) and fitted to *p-I* curves using a hyperbolic tangent function (Platt and Jassby 1976):

$$P = P_{\max} \tanh\left(\frac{\alpha I}{P_{\max}}\right)$$

where P_{max} is the maximal rate of O_2 production and α is the affinity for light (i.e., the initial slope of the *p-I* curve). The fits were based on a nonlinear least-squares regression using R version 3.3.3 (R Development Core Team 2017).

Results

The PAL mutant produced less biomass in both orange-red and blue light

Photos of the steady-state chemostats illustrate the conspicuous difference in growth performance between *Synechocystis* sp. PCC 6803 wildtype grown in orange-red (Fig. 1a) and in blue light (Fig. 1b). Both strains grew sufficiently well to sustain a steady state, which implies that their maximum specific growth rates exceeded the dilution rate of 0.015 h^{-1} in both light colors. However, the wildtype produced much higher steady-state biomass and cell numbers in orange-red light than in blue light (Fig. 1c,d).

By contrast, the steady-state biomass and cell numbers of the PAL mutant were low in both orange-red and blue light, and comparable to those of the wildtype in blue light (Fig. 1c,d). Furthermore, the wildtype had a higher Chl *a* content per cell in orange-red light than in blue light, whereas the PAL mutant had a low Chl *a* content in both orange-red and blue light (Fig. 1e). The wildtype had a lower cell volume in orange-red

light (5.41 ± 0.03 μm³) than in blue light (7.4 ± 0.03 μm³), whereas the PAL mutant produced smaller cells in both light colors (3.6 ± 0.1 μm³).

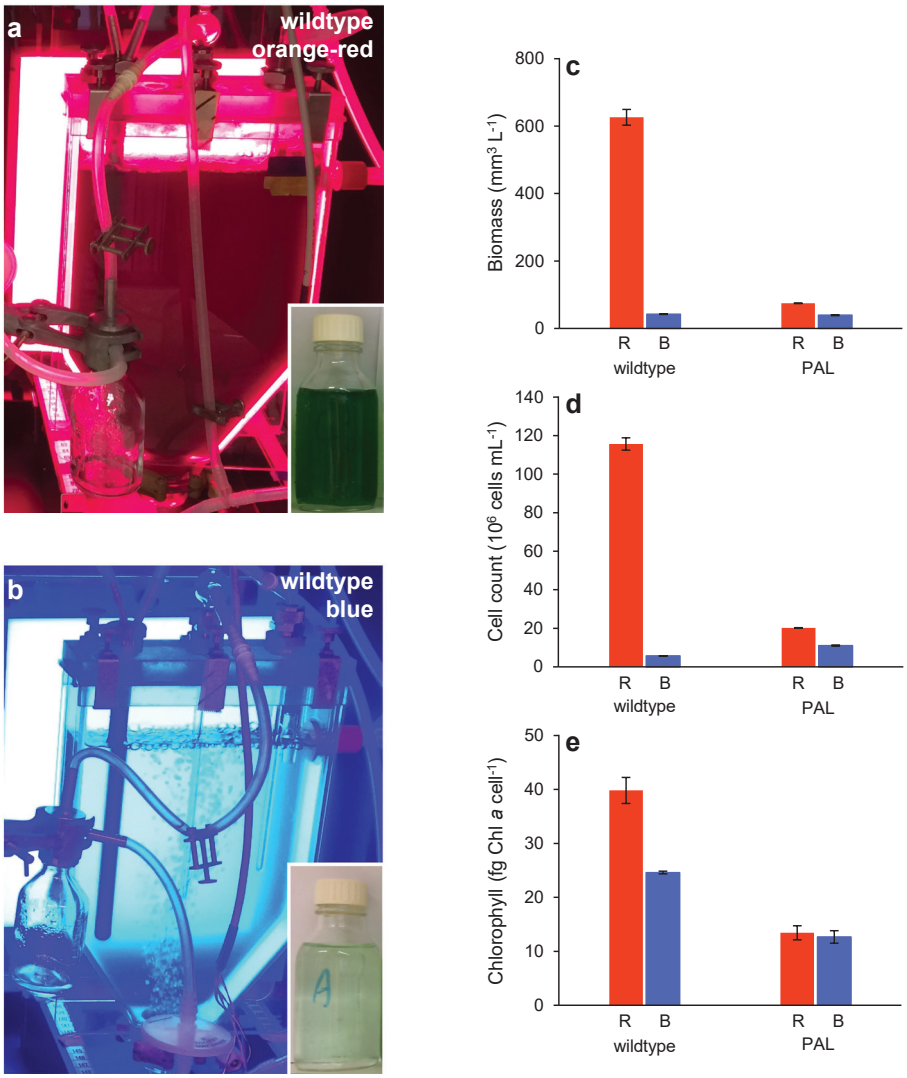

Fig. 1 | *Synechocystis* sp. PCC 6803 wildtype and the PAL mutant were grown in light-limited chemostats and provided with either (a) orange-red (660 nm) or (b) blue (450 nm) LED light. Insets show samples taken from steady-state chemostats of the wildtype, which illustrate that the wildtype produced much higher biomass in orange-red than in blue light. Bar graphs show biomass (c), cell counts (d) and Chl *a* content (e) of each strain at steady state in orange-red (R) and blue (B) light. Biomass production is expressed as total biovolume of the cells per mL. Data show the averages of three (biomass production) or two (Chl *a* content) technical replicates ± SD.

The PAL mutant showed identical absorption spectra in both orange-red and blue light

Absorption spectra normalized to Chl *a* revealed that *Synechocystis* sp. PCC 6803 wildtype had lower PC:Chl ratios in orange-red light than in blue light (Fig. 2a; Table 1). By contrast, the PAL mutant lacks absorption by PC (at 625 nm) and its absorption spectra were completely identical when grown in orange-red and blue light (Fig. 2b). Furthermore, the PAL mutant had a bleached appearance with a low Chl *a* content per cell and showed higher absorption in the blue part of the spectrum, both when acclimated to blue and when acclimated to orange-red light (Fig. 2b).

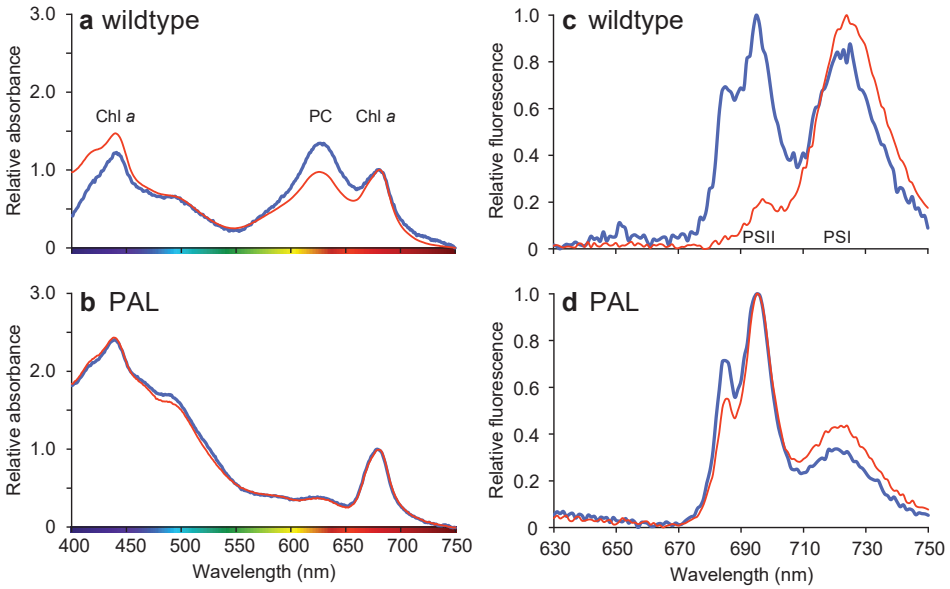

Fig. 2 | (a,b) Light absorption spectra of *Synechocystis* sp. PCC 6803 wildtype (a) and PAL mutant (b), sampled from steady-state chemostats acclimated to either orange-red (red line) or blue (blue line) light. Main absorption peaks of chlorophyll *a* (Chl *a*) and phycocyanin (PC) are indicated in panel a. Light absorption was normalized to Chl *a* absorbance at 678 nm, after baseline correction for minimum absorbance at 750 nm. (c,d) Low-temperature (77 K) fluorescence emission spectra of *Synechocystis* sp. PCC 6803 wildtype (c) and PAL mutant (d). Excitation of the cells at 440 nm (mainly Chl *a*) yields fluorescence emission peaks around 695 nm for PSII and around 720 nm for PSI, as indicated in panel c. The 77 K fluorescence emission spectra were normalized to the minimum and maximum emission of each spectrum. All spectra show the averages of three technical replicates.

Table 1 | Cellular contents of Chl *a*, PC, PSI and PSII of the wildtype and PAL mutant, in steady-state chemostats acclimated to either orange-red or blue light.

	Wildtype		PAL mutant		
	Orange-red	Blue	Orange-red	Blue	Units
Chl *a* content[1]	45	28	15	14	10^{-18} mol cell^{-1}
PSI content[2]	0.43	0.22	0.11	0.09	10^{-18} mol cell^{-1}
PSII content[2]	0.04	0.15	0.12	0.14	10^{-18} mol cell^{-1}
PSI:PSII ratio[3]	11.7	1.5	0.9	0.7	-
PC content[4]	8.0	7.4	n.a.	n.a.	10^{-18} mol cell^{-1}
PC:Chl ratio[5]	0.18	0.26	n.a.	n.a.	-
PC:PSII ratio[6]	217	50	n.a.	n.a.	-

[1]Chl *a* content was measured spectrophotometrically
[2]PSI and PSII content were calculated from the Chl *a* content and PSI:PSII ratio
[3]PSI:PSII ratio was estimated from deconvolution of the 77 K fluorescence spectra
[4]PC content was calculated from the Chl *a* content and PC:Chl ratio
[5]PC:Chl ratio was estimated from the absorption spectra
[6]PC:PSII ratio was calculated from the PC and PSII content

The PAL mutant had a low PSI:PSII ratio in both orange-red and blue light

Fluorescence peaks of PSI and PSII at 725 nm and 695 nm, respectively, were very prominent in the 77 K fluorescence spectra (Fig. 2c,d). The wildtype allocated most of its Chl *a* to PSI when grown in orange-red light, whereas it decreased its allocation to PSI and increased its allocation to PSII when grown in blue light (Fig. 2c). Hence, the wildtype had much lower PSI:PSII ratios and PC:PSII ratios in blue light than in orange-red light (Table 1). By contrast, the PAL mutant had a relatively low PSI content and high PSII content in both light colors, resulting in a low PSI:PSII ratio in both orange-red and blue light (Fig. 2d; Table 1). The blue-light acclimated wildtype showed an additional fluorescence peak at 685 nm (Fig. 2c), which is commonly attributed to the chlorophyll antenna CP43 in PSII (Andrizhiyevskaya et al. 2005; Wilson et al. 2007; Brecht et al. 2014). In the PAL mutant, this peak was present in both orange-red and blue light (Fig. 2d).

The PAL mutant had a low oxygen production in both orange-red and blue light

Membrane-inlet mass spectrometry (MIMS) was used to separately measure photosynthetic O_2 production and O_2 consumption at different light intensities. O_2 production and consumption rates were expressed in two different ways: per mol PSII (Fig. 3) and per cell (Fig. 4). We note that our estimates of the O_2 production rate per PSII are consistent with turnover rates of the PSII-water oxidizing complex measured in microalgae (Ananyev and Dismukes 2005).

In the wildtype, net and gross O_2 production per PSII increased much more steeply with light intensity (had higher α) and maximum O_2 production rates per PSII (higher P_{max}) were higher in orange-red than in blue light (Fig. 3a,b; Table 2). By contrast, the PAL mutant had low α and low P_{max} in both orange-red and blue light (Fig. 3c,d), very similar to the low α and low P_{max} of the wildtype in blue light (Fig. 3b).

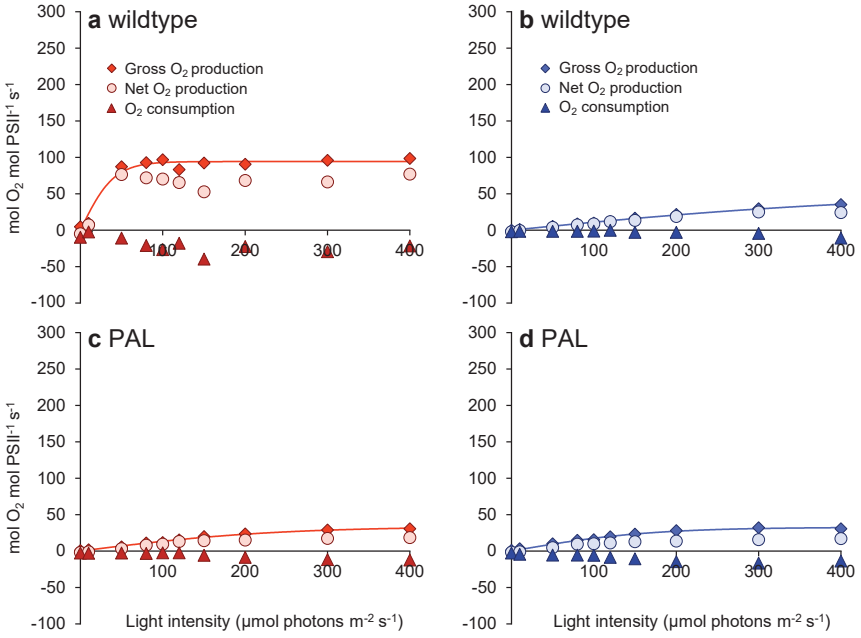

Fig. 3 | O_2 production and consumption rates per PSII of *Synechocystis* sp. PCC 6803 wildtype (a,b) and the PAL mutant (c,d). Cells were acclimated to orange-red (a,c) or blue (b,d) light and subsequently exposed to increasing intensities of the same light color. The data show averages of gross photosynthetic O_2 production (diamonds), net O_2 production (circles) and O_2 consumption (triangles), measured in duplicate samples using membrane-inlet mass spectrometry (MIMS). Lines represent *p-I* curves fitted to the gross O_2 production using the hyperbolic tangent function; parameter estimates are given in Table 2.

When O_2 production and consumption rates were expressed per cell rather than per PSII, we obtained similar results (Fig. 4). The wildtype again had higher α in orange-red light than in blue light (Fig. 4a,b; Table 2), whereas the PAL mutant had a low α in both orange-red and blue light comparable to the low α of the other strains in blue light (Fig. 4c,d). However, in contrast to P_{max} per PSII, P_{max} per cell was of similar magnitude in blue and orange-red light for both strains (Fig. 4).

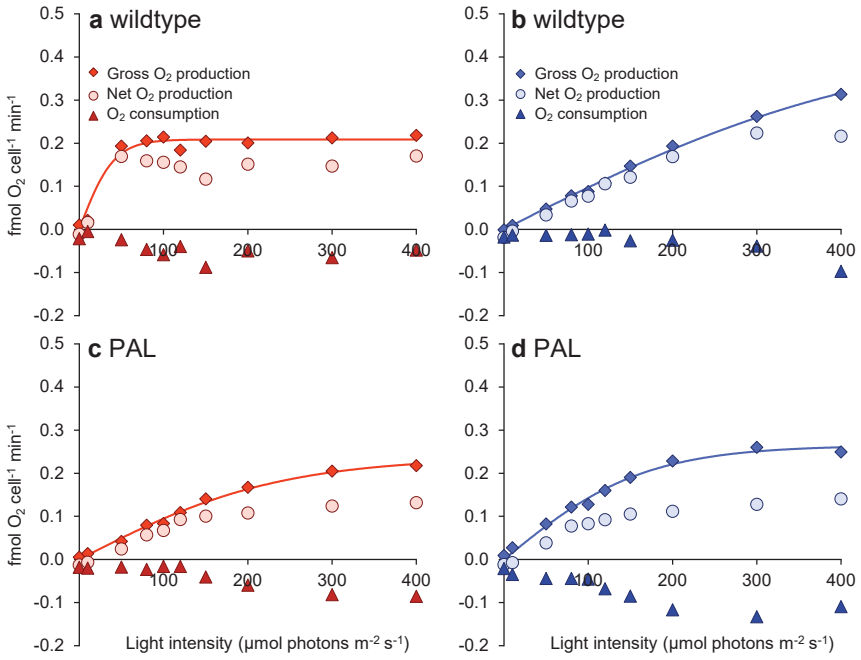

Fig. 4 | O_2 production and consumption rates per cell of *Synechocystis* sp. PCC 6803 wildtype (a,b) and the PAL mutant (c,d). See Figure 3 for further details.

Table 2 | Photosynthetic parameters estimated by fitting a hyperbolic tangent to the gross O_2 production rate per PSII and the gross O_2 production rate per cell. Standard errors are indicated by bracketed values.

Parameter	Wildtype		PAL mutant	
	Orange-red	Blue	Orange-red	Blue
O_2 production per PSII (mol O_2 mol $PSII^{-1}$ s^{-1})				
α	2.32 (0.43)	0.11 (0.00)	0.14 (0.01)	0.20 (0.01)
P_{max}	94.2 (3.1)	50.1 (3.5)	33.6 (1.3)	32.6 (1.0)
O_2 production per cell (fmol O_2 $cell^{-1}$ min^{-1})				
α	5.1×10^{-3} (9.6×10^{-4})	1.0×10^{-3} (0.3×10^{-4})	1.0×10^{-3} (0.4×10^{-4})	1.6×10^{-3} (0.7×10^{-4})
P_{max}	0.209 (0.007)	0.446 (0.032)	0.237 (0.009)	0.265 (0.008)

Discussion

What happens if phycobilisomes cannot be used?

Our results show that *Synechocystis* sp. PCC 6803 wildtype displays much lower O_2 and biomass production rates in blue light than in orange-red light, in agreement with previous studies (e.g. Wilde et al. 1997; El Bissati and Kirilovsky 2001; Tyystjärvi et al. 2002; Singh et al. 2009; Bland and Angenent 2016; Luimstra et al. 2018). We tested the hypothesis that cyanobacteria have a low photosynthetic efficiency in blue light because PBS do not absorb wavelengths ≤ 450 nm, and hence blue light mainly excites PSI while fewer photons excite the PSII reaction center (Myers et al. 1980; Fujita 1997; Solhaug et al. 2014; Kirilovsky 2015). This results in an excitation imbalance between the two photosystems in blue light (Luimstra et al. 2018). The PAL mutant lacks PBS. Therefore, if our hypothesis is correct, then the PAL mutant should have (i) a similar low biomass and O_2 production rate and (ii) a similar low PSI:PSII ratio in both orange-red and blue light as the wildtype in blue light. This reasoning is confirmed by our experiments, in which the PAL mutant indeed displayed a similar low biomass (Fig. 1c), cell production (Fig. 1d), Chl *a* content (Fig. 1e), PSI:PSII ratio (Fig. 2c,d; Table 1) and O_2 production rate per PSII (Fig. 3) in both orange-red and blue light as the wildtype in blue light. In other words, the poor photosynthetic performance of PBS-containing cyanobacteria in blue light was similar to the performance of a PBS-deficient mutant in both light colors.

We note that our results also show some differences between the wildtype in blue light and the PAL mutant. In particular, the photophysiology of the PAL mutant shows enhanced absorption in the 400-500 nm range (Fig. 2b), indicative of enhanced carotenoid production (see also Ajlani and Vernotte 1998; Kwon et al. 2013) and an even lower PSI:PSII ratio than the wildtype in blue light (Fig. 2d). Hence, in a sense, the PAL mutant lacking PBS might be interpreted as a more extreme phenotype in comparison to the wildtype that contains PBS but cannot use them in blue light.

The low growth rate and low PSI:PSII ratio of the PAL mutant have also been described by many other studies (Ajlani and Vernotte 1998; El Bissati and Kirilovsky 2001; Bernát et al. 2009; Stadnichuk et al. 2009; Collins et al. 2012; Kwon et al. 2013; Liberton et al. 2017). Comparison of different antenna mutants revealed that the PSI:PSII ratio decreases with a decrease in antenna size of the PBS, as a response to the diminished energy transfer from PBS to PSII when the antenna size is gradually reduced (Ajlani et al. 1995; Olive et al. 1997; Bernát et al. 2009;

Stadnichuk et al. 2009; Collins et al. 2012; Kwon et al. 2013; Liberton et al. 2017). Likewise, Page et al. (2012) reported that growth rates were highest in the *Synechocystis* PCC 6803 wildtype, and decreased progressively with a decrease in antenna size of a series of antenna mutants. We also note the presence of the fluorescence peak at 685 nm in the 77 K fluorescence spectra of the PAL mutant (Fig. 2d), which has also been found in previously published 77 K spectra of the PAL mutant (Ajlani and Vernotte 1998; Bernát et al. 2009; Stadnichuk et al. 2009; Collins et al. 2012; Kwon et al. 2013). This peak, which is commonly attributed to the chlorophyll-binding protein CP43 in PSII (Andrizhiyevskaya et al. 2005; Wilson et al. 2007; Brecht et al. 2014), is also present in the wildtype in blue light (Fig. 2c). Hence, our findings with the PAL mutant are well in line with many previous studies. The novelty of our results is the recognition that, in many respects, the phenotype of the PAL mutant resembles the phenotype of the wildtype strain in blue light. This is further confirmed by our analysis of the oxygen production rates of the wildtype and PAL mutant, as measured by MIMS (Fig. 3 and Fig. 4).

It has been shown that deletion of PBS in the PAL mutant is accompanied by profound changes in the proteome in comparison to the wildtype (Kwon et al. 2013; Liberton et al. 2017). Kwon and colleagues report a major increase of PSII proteins accompanied by a slight decrease of PSI proteins in the PAL mutant. Furthermore, they found that the PAL mutant has increased abundances of proteins involved in stress responses to high light and in carbohydrate metabolism (mostly gluconeogenesis). More recent proteome analyses by Liberton et al. (2017) support these findings, and in addition these authors found a decrease in bicarbonate transport proteins and an increase in transport proteins involved in nitrate uptake in the PAL mutant. Interestingly, the physiology of the wildtype is also completely changed when transferred from white to blue light (Singh et al. 2009). Transcriptome analysis by Singh and colleagues revealed that *Synechocystis* sp. PCC 6803 wildtype cells grown in blue light showed, among others, an increased expression of genes encoding PSII subunits and proteins involved in stress responses to high light, carbohydrate metabolism and nitrate uptake, which resembles several of the proteome results in the PAL mutant (Kwon et al. 2013; Liberton et al. 2017). This indicates again that the PAL mutant and wildtype in blue light share many similarities, not only in their photophysiological traits but also in terms of their cellular metabolism.

Implications for biotechnology

Several studies have argued that truncation of light-harvesting antennae may be an advantage in crop and algal biomass production for e.g. biotechnological applications (see e.g. Ort and Melis 2011; Work et al. 2012; de Mooij et al. 2015; Kirst et al. 2017). In dense algal cultures or plant canopies, cells near the surface absorb excessive amounts of light energy that they largely dissipate as heat, while cells deeper down in the culture receive insufficient light for photosynthesis (Melis 2009; Blankenship and Chen 2013). As a consequence, much of the absorbed light energy is wasted rather than invested in biomass production. Truncation of the light-harvesting antennae reduces absorption per individual cell and thereby distributes light more evenly among the cells in dense algal cultures. It has indeed been demonstrated that antenna truncation can increase the biomass production of green algae (e.g. Polle et al. 2002; Perrine et al. 2012; de Mooij et al. 2015; Shin et al. 2016).

Our results indicate that truncation of the PBS of cyanobacteria has other effects than the truncation of the chlorophyll-based light-harvesting complexes of green algae. Green algae generally maintain a PSI:PSII ratio of around 1:1, in contrast to cyanobacteria which usually have a much higher PSI:PSII ratio (Shen et al. 1993; Singh et al. 2009; Kirilovsky 2015) and mainly use their PBS to direct sufficient light energy to PSII. Therefore, truncation of PBS in cyanobacteria will have a stronger effect on light redistribution between the two photosystems than truncation of the light-harvesting complex in green algae. In particular, our findings show that complete deletion of the PBS of cyanobacteria, in the PAL mutant, yields an excitation imbalance between the two photosystems, which results in a low PSII activity (Fig. 3) and low biomass production (Fig. 1) in both blue and orange-red light. This matches earlier results of e.g. Ajlani and Vernotte (1998), Bernát et al. (2009), Page et al. (2012) and Kwon et al. (2013), who also found that the PAL mutant has a lower biomass production than the wildtype.

Possibly, partial truncation of the antennae by shortening or removing the rods of the PBS might improve the biomass production of cyanobacteria, as the PBS can then still distribute the absorbed light energy over the two photosystems while overall absorbance per cell is lower (Lea-Smith et al. 2014). Partial truncation of the PBS likely implies that less light will be transferred to PSII, which must be compensated by a decreased PSI:PSII ratio, to maintain the balance between the two photosystems. Several cyanobacterial studies show that partial truncation mutants indeed decreased their PSI:PSII ratio progressively and proportionally to a decrease in antenna size (Ajlani et al. 1995; Olive et al. 1997; Bernát

et al. 2009; Stadnichuk et al. 2009; Collins et al. 2012; Kwon et al. 2013; Liberton et al. 2017). Although most of these mutants did not show a higher productivity than the wildtype, removal of the phycocyanin rods but not the allophycocyanin core in the Olive mutant (Rögner et al. 1990) resulted in an enhanced cyanobacterial productivity at high light intensities (Kwon et al. 2013) and low carbon conditions (Lea-Smith et al. 2014).

Implications for cyanobacterial photosynthesis in the blue ocean

Marine cyanobacteria of the *Synechococcus* genus often use the phycobilin pigments phycoerythrobilin (PEB) and phycourobilin (PUB) to absorb wavelengths in the green part (525-575 nm) and blue-green part (475-515 nm) of the light spectrum (Six et al. 2007; Grébert et al. 2018). These phycobilin pigments do not absorb photons in the violet-blue part of the spectrum (< 450 nm), and hence, similar to *Synechocystis* PCC 6803, marine *Synechococcus* will be unable to use their PBS to harvest blue photons < 450 nm for PSII (Luimstra et al. 2018). Consequently, *Synechococcus* usually thrives in the near-surface layers of the oceans and in coastal waters, where green and blue-green light is available (Partensky et al. 1999; Scanlan and West 2002; Stomp et al. 2007b).

Cyanobacteria of the genus *Prochlorococcus* abound in the subtropical ocean gyres and usually their populations extend deeper down in the water column than *Synechococcus* (Partensky et al. 1999; Scanlan and West 2002). They use a different light-harvesting strategy. *Prochlorococcus* does not deploy PBS, but has evolved light-harvesting antennae that effectively absorb blue light using divinyl-Chl *a* and *b* (Chisholm et al. 1992; Ting et al. 2002; Stomp et al. 2007a). *Prochlorococcus* likely evolved from a PBS-containing cyanobacterium (Kettler et al. 2007; Scanlan et al. 2009), and some *Prochlorococcus* strains still have genes for the synthesis of phycoerythrin (Hess et al. 1996). Interestingly, our results show that the loss of PBS does not have major negative fitness consequences in habitats dominated by blue light, as the PAL mutant had a similarly low biomass and cell production in blue light as the wildtype. Furthermore, we note that the 685-nm peak in our 77 K fluorescence spectra, indicative of the chlorophyll-binding protein CP43, was strongly induced by blue light (Fig. 2c) and in the PBS-deficient mutant (Fig. 2d; see also Ajlani and Vernotte 1998; Kwon et al. 2013). The chlorophyll-binding proteins (Pcb) in the light-harvesting antennae of *Prochlorococcus* are closely related to CP43 (Chen and Bibby 2005). Our results therefore suggest that the loss of PBS and transformation from an ancestral chlorophyll-binding protein of the CP43 family to Pcb caused a major evolutionary transition, from the poor

photosynthetic performance in blue light by PBS-based cyanobacteria to efficient utilization of blue light by the chlorophyll-based light-harvesting antennae of *Prochlorococcus*. Harnessing of blue light will have provided a major selective advantage for *Prochlorococcus* over PBS-containing cyanobacteria in the deep blue waters of the open ocean.

Acknowledgments

We are most grateful to our late colleague dr. Hans Matthijs for initiating this research. *Synechocystis* sp. PCC 6803 strains were kindly provided by Devaki Bhaya (wildtype) and Ghada Ajlani (PAL mutant). We thank Hugo Pineda Hernández for help with R, participants of the Wetsus research theme *Algae* and the FAME department of the University of Amsterdam for fruitful discussions, and two anonymous reviewers for useful comments on the manuscript. This work has been performed in the cooperation framework of Wetsus, European Centre of Excellence for Sustainable Water Technology (www.wetsus.eu). Wetsus is co-funded by the Dutch Ministry of Economic Affairs and Ministry of Infrastructure and Environment, the Province of Fryslân and the Northern Netherlands Provinces.

Chapter 4

Blue light induces major changes in the gene expression profile of the cyanobacterium *Synechocystis* sp. PCC 6803

Veerle M. Luimstra[1,2], J. Merijn Schuurmans[1], Klaas J. Hellingwerf[3], Hans C. P. Matthijs[1,†], Jef Huisman[1*]

[1]Department of Freshwater and Marine Ecology, Institute for Biodiversity and Ecosystem Dynamics, University of Amsterdam, Amsterdam, The Netherlands
[2]Wetsus, European Centre of Excellence for Sustainable Water Technology, Leeuwarden, The Netherlands
[3]Swammerdam Institute for Life Sciences, University of Amsterdam, Amsterdam, The Netherlands
†Deceased, April 17, 2016

This chapter is published in:
Physiologia Plantarum 170:10-26 (2020)

and featured In the spotlight:
More than just a pair of blue genes: how cyanobacteria adapt to changes in their light environment
Robert H. Calderon *Physiologia Plantarum* 170:7-9 (2020)

Abstract

Although cyanobacteria absorb blue light, they use it less efficiently for photosynthesis than other colors absorbed by their photosynthetic pigments. A plausible explanation for this enigmatic phenomenon is that blue light is not absorbed by phycobilisomes and, hence, causes an excitation shortage at photosystem II (PSII). This hypothesis is supported by recent physiological studies, but a comprehensive understanding of the underlying changes in gene expression is still lacking. In this study, we investigate how a switch from artificial white light to blue, orange or red light affects the transcriptome of the cyanobacterium *Synechocystis* sp. PCC 6803. In total, 145 genes were significantly regulated in response to blue light, whereas only a few genes responded to orange and red light. In particular, genes encoding the D1 and D2 proteins of PSII, the PSII chlorophyll-binding protein CP47 and genes involved in PSII repair were upregulated in blue light, whereas none of the photosystem I (PSI) genes responded to blue light. These changes were accompanied by a decreasing PSI:PSII ratio. Furthermore, many genes involved in gene transcription and translation and several ATP synthase genes were transiently downregulated, concurrent with a temporarily decreased growth rate in blue light. After 6-7 days, when cell densities had strongly declined, the growth rate recovered, and the expression of these growth-related genes returned to initial levels. Hence, blue light induces major changes in the transcriptome of cyanobacteria, in an attempt to increase the photosynthetic activity of PSII and cope with the adverse growth conditions imposed by blue light.

Introduction

Cyanobacteria play a key role in aquatic ecosystems, are widely hailed as the evolutionary ancestors of chloroplasts, and are often used as model organisms to study oxygenic photosynthesis. Similar to eukaryotic photosynthetic organisms, cyanobacteria use the ubiquitous pigment chlorophyll *a* (Chl *a*) in photosystem I (PSI) and photosystem II (PSII). Chl *a* absorbs in the blue part (peak wavelength at ~440 nm) and red part (680 nm) of the light spectrum (Engelmann 1882; Kirk 2011). In addition, cyanobacteria deploy a diversity of phycobili-pigments in large light-harvesting antennae, known as phycobilisomes (PBS). These phycobili-pigments include phycourobilin, phycoerythrobilin and phycocyanobilin, which have absorption maxima in cyan (495 nm), green (545 nm) and orange light (625 nm), respectively (Tandeau de Marsac 2003; Six et al. 2007).

Hence, cyanobacteria absorb blue light ≤ 450 nm. Yet, contrary to green algae and plants, PBS-containing cyanobacteria have much lower rates of photosynthesis and growth in blue light than in the other light colors absorbed by their photosynthetic pigments (Lemasson et al. 1973; Pulich and van Baalen 1974; Wyman and Fay 1986; Jørgensen et al. 1987; Wilde et al. 1997; Tyystjärvi et al. 2002; Wang et al. 2007; Singh et al. 2009; Chen et al. 2010; Choi et al. 2013; Bland and Angenent 2016; Luimstra et al. 2018). As a consequence, PBS-containing cyanobacteria can be strong competitors in cyan, green or orange light absorbed by their PBS, but they are very poor competitors in blue light ≤ 450 nm in comparison to photosynthetic organisms with chlorophyll-based light-harvesting complexes (Luimstra et al. 2020). The cyanobacterium *Prochlorococcus* is an interesting exception. *Prochlorococcus* lacks PBS but instead uses divinyl-chlorophyll-based light-harvesting complexes quite similar to green algae and terrestrial plants, and it performs very well in blue light as it is the most abundant cyanobacterium in the blue waters of the open ocean (Chisholm et al. 1988; Flombaum et al. 2013).

Why PBS-containing cyanobacteria have a low photosynthetic efficiency in blue light is not yet fully resolved, but most likely it can be attributed to an imbalance of the light energy captured by PSI and PSII. In contrast to green algae and plants, PBS-containing cyanobacteria invest much more of their Chl *a* in PSI than in PSII (e.g., Myers et al. 1980; Fujita 1997; Luimstra et al. 2018). As a consequence, PSI will absorb more blue light than PSII. Conversely, the PBS of cyanobacteria transfer most of their absorbed light energy to PSII (Joshua et al. 2005; Mullineaux 2014; Kirilovsky 2015). However, the phycobili-pigments of PBS do not absorb blue light ≤ 450 nm (Grossman et al. 1993; Tandeau de Marsac 2003; Six et al. 2007). Hence, especially under light-limited conditions, blue light provides sufficient excitation energy at PSI but insufficient excitation energy at PSII to sustain high rates of linear electron flow (Fujita 1997; Solhaug et al. 2014; Kirilovsky 2015; Luimstra et al. 2018, 2019).

Several recent observations support the above-mentioned explanation for the low photosynthetic efficiency of PBS-containing cyanobacteria in blue light. At low light intensities, oxygen production rates of *Synechocystis* sp. PCC 6803 were much lower in blue than in orange and red light, whereas at high light intensities the maximum oxygen production rates were similar in all three light colors (Luimstra et al. 2018). Furthermore, several studies have shown that the PSI:PSII ratio of PBS-containing cyanobacteria strongly decreases in blue light (Wilde et al. 1997; El Bissati and Kirilovsky 2001; Singh et al. 2009; Luimstra et al. 2018, 2019).

Finally, a PBS-deficient mutant of *Synechocystis* sp. PCC 6803 showed a similar low photosynthetic efficiency in both blue and orange-red light, comparable to the PBS-containing wildtype in blue light (Luimstra et al. 2019). These observations are all consistent with the hypothesis that the low absorption of blue light by the light-harvesting PBS, and hence the limited transfer of excitation energy to PSII, is the rate-limiting factor for photosynthesis in blue light.

In view of these strong photo-physiological responses, we hypothesize that PBS-containing cyanobacteria will display major changes in their gene expression profile when exposed to blue light. In particular, if blue light causes an imbalance between PSI and PSII, one may expect upregulation of PSII genes and downregulation of PSI genes. Furthermore, preferential excitation of PSI may lead to enhanced ATP production through cyclic electron flow without NADPH production (Allen 2003; Munekage et al. 2004; Yeremenko et al. 2005), which is likely to induce major shifts in the expression of many genes involved in the metabolic pathways that are dependent on the photosynthetic activity of the cells. Yet, although several studies have investigated how changing light conditions affect cyanobacterial gene expression (e.g., Hihara et al. 2001; Gill et al. 2002; Huang et al. 2002; Billis et al. 2014; Xiong et al. 2015), the transcriptome response of cyanobacteria to different colors of light has received much less attention (but see Singh et al. 2009 and Hübschmann et al. 2005).

In this study, we therefore investigate how blue, orange and red light affect the gene expression profile of *Synechocystis* sp. PCC 6803. This PBS-containing model cyanobacterium was grown in light-limited chemostats and acclimated to 'artificial white' light (or more precisely, polychromatic light with an equal mix of blue, orange and red photons). When the chemostats reached steady-state, the incident light was switched to monochromatic blue, orange or red light. The transcriptomes were analyzed just before and at several time points after this switch in light color, until a new steady-state was reached. Hence, our transcriptome analysis allowed investigation of changes in gene expression associated with transient cellular processes as well as with long-term acclimation to the three different light colors. In line with our hypothesis, the switch to blue light had a much stronger effect on the transcriptome than the switch to red and orange light, consistent with a cellular effort to restore the excitation balance between PSI and PSII. This striking difference in regulatory responses to different light colors adds further insight into the photosynthetic traits of cyanobacteria, which is of relevance for both biotechnological and ecological applications.

Materials and Methods

Strains and culture conditions

All experiments were performed using the cyanobacterium *Synechocystis* sp. PCC 6803, which was kindly provided by D. Bhaya (University of Stanford, USA). *Synechocystis* sp. PCC 6803 was cultured in flat-walled 1.8 L chemostats as described by Huisman et al. (2002). These chemostats allow full control of light conditions, CO_2 and nutrient inflow, and temperature. Light was provided by narrow-band LED panels with a full width at half maximum of ~20 nm (Philips Lighting B.V., The Netherlands) at a total incident light intensity (I_{in}) of 60 µmol photons m^{-2} s^{-1}. Light passing through the chemostats (I_{out}) was measured using a LI-250 light meter (LI-COR Biosciences, USA). The cultures were provided with a nutrient-rich mineral medium (BG-11 medium; Merck, Germany) supplemented with 5 mM Na_2CO_3 and were maintained at a dilution rate of D = 0.03 h^{-1}. Temperature was kept constant at 30°C. CO_2-enriched air (2% v/v) flowing at a rate of 30 L h^{-1} was used to provide CO_2 and to keep the culture mixed. The CO_2 concentration of the gas influx was regularly monitored using an Environmental Gas Monitor for CO_2 (EGM-4; PP Systems, USA).

Chemostat experiments

Nine chemostats were illuminated with 'artificial white' light, consisting of an even mixture of LEDs emitting blue (450 nm), orange (625 nm) and red light (660 nm). Each of these light colors was provided at 20 µmol photons m^{-2} s^{-1}, reaching a total I_{in} of 60 µmol photons m^{-2} s^{-1} until steady-state was reached after 5-6 volume changes. After steady-state was reached, the light color was switched to 60 µmol photons m^{-2} s^{-1} of either monochromatic blue, orange or red light. Each light color was applied to three chemostats, providing three independent biological replicates per color for cell counts, absorbance, fluorescence and transcriptome analyses.

Cell counts in the chemostats that were switched to blue light declined strongly, and became much lower than those in orange and red light. The lower cell numbers imply that cells in blue light were exposed to a higher average photon dosage per cell than cells in red and orange light, which may affect their physiology and gene expression. To distinguish between effects of light color and light intensity, we therefore also ran a series of chemostats (n = 3) in red light with a higher dilution rate (0.06 h^{-1}), to obtain a similar dilute cell culture as in the chemostats exposed to blue light. These will be referred to as the 'dilute chemostats in red light'.

Sampling and measurements

Sampling occurred directly before (t = 0 h) and at 1, 2, 4, 8, 24, 48, 72, 96, 168, 192 and 216 h after the light switch. Cell counts and biovolume were measured on the day of sampling using a CASY 1 TTC cell counter with a 60 µm capillary (Schärfe Systems GmbH, Germany). Samples were measured in triplicate and diluted to ~5 × 10^4 cells mL^{-1} in Casyton solution.

UV/visible absorbance spectra were measured directly after sampling using an updated Aminco DW2000 photospectrometer (OLIS, USA). Absorbance was measured from 400-750 nm and normalized to maximum absorbance at 440 nm, after baseline correction for minimum absorbance at 750 nm.

To measure low-temperature (77 K) fluorescence spectra, 1.5 mL of each sample was transferred to 3 ml-cuvettes prefilled with 1.5 mL 60% glycerol and mixed by pipetting up and down three times. Cuvettes were flash-frozen in liquid nitrogen and stored at -80°C. Fluorescence at 77 K was measured within a week from sampling with an OLIS DM45 spectrofluorometer (OLIS, Bogart, GA, USA) equipped with a Dewar cell. Fluorescence emission was measured from 630-750 nm with excitation at 440 nm (mainly Chl *a*) and 590 nm (mainly PBS). The final glycerol concentration in the cuvettes did not exceed 30% to minimize dissociation of PBS from the thylakoid membranes, and cell concentrations were below 4 × 10^7 cells mL^{-1} to minimize re-absorption of the fluorescence signal (Mao et al. 2003).

To guarantee that the fluorescence spectra reflected the photophysiology of the cells at the time of sampling, samples for the 77 K fluorescence analyses were processed and frozen within 20 seconds from the moment of sampling. Consequently, the photosynthetic proteins were fixed in the position they were in at the moment of sampling. As absorbed excitation energy can still be transferred between associated pigments, the heights of the fluorescence emission peaks can be used to estimate the relative contents and interactions of PSI and PSII and their associated PBS (e.g., Murakami 1997; Schuurmans et al. 2017). Our transcriptome results indicate that the expression of PSI genes remained rather stable while expression of PSII genes was regulated. Therefore, fluorescence emission by PBS (at 650 nm) and PSII (at 695 nm) was quantified relative to the fluorescence emission by PSI (at 725 nm).

Microarray analysis

To investigate light-color dependent differences in gene expression, total RNA was sampled from each chemostat (n = 3 per light color). Because large changes in physiology were observed within the first hours after the switch to blue light, RNA samples were collected from the blue-light chemostats at t = 0, 1, 4, 24, 48 and 192 h and from the red- and orange-light chemostats at t = 0 h (just before the switch), t = 4 h (during acclimation) and t = 192 h (in steady-state). Additionally, an RNA sample was collected from the dilute chemostat in red light at t = 192 h. The 50 mL samples were centrifuged at 3000 × *g* at 4°C for 10 min. Cell pellets were immediately frozen in liquid nitrogen after resuspension in 1 mL TRIzol (Life Technologies, Grand Island, NY, USA) and stored at −80°C. RNA extraction was performed using the Direct-Zol™ RNA MiniPrep kit (Zymo Research, USA), including the in-column DNAse I treatment. All samples had A_{260}/A_{280} and A_{260}/A_{230} values above 1.8 as quantified using a Nanodrop ND-1000 spectrophotometer (Thermo Scientific, USA). RNA integrity was verified using an Agilent 2100 Bioanalyzer (Agilent Technologies, The Netherlands).

Custom-made 45–65-mer oligonucleotide microarrays were designed as described by Aguirre von Wobeser et al. (2011; see also Eisenhut et al. 2007; Krasikov et al. 2012) and printed on a 1 × 3 inch glass slide in a standard 2 × 11K format by Agilent. All 3 264 genes of *Synechocystis* PCC 6803 described in CyanoBase (http://genome.microbedb.jp/CyanoBase) were represented in the array design. We used 1-4 different probes per gene. Cy3- and Cy5-labeled cDNA was generated from the total RNA with the Superscript III Reverse Transcriptase kit (Invitrogen Life Science, the Netherlands) and hybridized to the arrays as described by Eisenhut et al. (2007) using a loop design (Supplementary Table S1).

The microarray data were analyzed with the *limma* package (version 3.24.14; www.bioconductor.org; Ritchie et al. 2015) using R version 3.2.1. (www.R-project.org), following the same approach as Schuurmans et al. (2018). First, background correction was applied to the raw array intensity data according to the *normexp* + *offset* = 20 method (Ritchie et al. 2007). Subsequently, within-array normalization was applied using the *global loess* method and between-array normalization was applied

using the *A-quantile* method (Smyth and Speed 2003). The *avedups* function was used to average replicate spot intensities (Smyth et al. 2005). All gene expression data were compared to expression in the chemostat cultures acclimated to artificial white light at t = 0 h using the linear modeling approach function *lmfit* (Smyth 2004). The empirical Bayes method incorporated in the *eBayes* function was used to evaluate the significance of changes in gene expression. For this purpose, we averaged the $\log_2$ ratios of different probes for the same gene and we used Fisher's method in the *metap* package (version 0.6) of R to combine the adjusted *P*-values of these probes. Genes expressed with a $\log_2$ fold change of <-1.4 or >1.4 and adjusted *P*-values < 0.05 were considered differentially expressed. Heatmaps of the differentially expressed genes were made with the *Heatmap.2* function from the *gplot* package (version 2.17.0), and the *hclust* function was applied for hierarchical clustering of the genes based on Euclidean distances.

Results

Growth of *Synechocystis* in blue, orange and red light

The experiments were started by switching the wavelength of the light provided to steady-state chemostats with *Synechocystis* sp. PCC 6803 from artificial white light to either blue, orange or red light. In orange and red light, cell counts and biomass were not strongly affected by this switch in light color (Fig. 1a,b). In blue light, however, cell counts and biomass decreased by ~85% and a new steady-state was reached after ~168 h, with 5.2 ± 1.5 million cells mL^{-1} (Fig. 1a) and a total biomass (expressed as biovolume) of 33.5 ± 8.0 mm^3 L^{-1} (Fig. 1b).

To distinguish between effects of light color and light intensity, we also ran a series of chemostats in red light with a higher dilution rate (0.06 h^{-1}). These dilute chemostats in red light obtained a steady-state cell density of 5.1 ± 0.6 million cells mL^{-1} (red-dotted square in Fig. 1b), which is comparable to that of the blue-light chemostats.

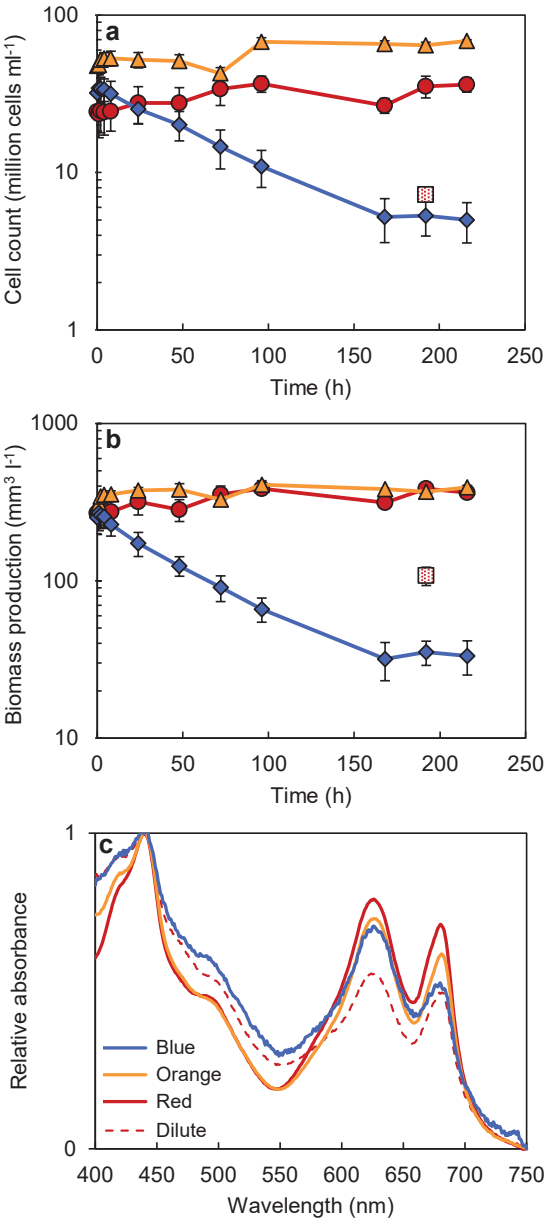

Fig. 1 | Cell and biomass production in light-limited chemostats of *Synechocystis* sp. PCC 6803, after a switch from artificial white light to monochromatic blue, orange and red light. Cell counts (a) and biomass (b) obtained during growth in blue (diamonds), orange (triangles) and red light (circles). The red-dotted square indicates the steady-state cell count and biomass of the dilute chemostat in red light. Data are averages of three biological replicates ± SD (n = 3). Light absorption spectra of the cells after acclimation to blue (blue line), orange (orange line) and red light (red line) (c). The dashed red line indicates absorption by the dilute chemostat in red light. Samples were taken after 192 h, when chemostats were in steady-state. The spectra were normalized to maximum absorbance at 440 nm, after baseline correction for minimum absorbance at 750 nm. Spectra are averages of three biological replicates (n = 3); SD averaged over the range from 400-750 nm was 0.036 in blue light, 0.007 in orange light, 0.033 in red light, and 0.013 in the red dilute chemostat.

Blue light induces changes in pigmentation and photosystem ratios

Absorption spectra measured at steady state of the chemostats revealed subtle differences in pigmentation of the cells (Fig. 1c). The phycocyanin (PC):Chl *a* ratio (relative absorption by PC at 625 nm versus Chl *a* at 680 nm) was highest in cells grown in blue light, indicating that *Synechocystis* sp. PCC 6803 produced more PC relative to Chl *a* in blue light than in orange and red light. Furthermore, the ratio of absorption at 440 nm (absorption by both Chl *a* and carotenoids) versus 680 nm (absorption by Chl *a*) indicates that it produced more carotenoids relative to Chl *a* in blue light and in the dilute chemostat in red light than in the other chemostats (Fig. 1c).

Low-temperature fluorescence spectra of cells flash-frozen at 77 K offer an estimate of the relative abundances of the two photosystems and their association with PBS. The PBS and photosystems in these frozen cells have a fixed position, but still absorb photons and transfer the excitation energy to the reaction centers. Upon excitation of Chl *a* at 440 nm, fluorescence is emitted by PSII at 695 nm (F_{695}) and by PSI at 725 nm (F_{725}) (Supplementary Fig. S1). After the switch to orange and red light, the PSI:PSII fluorescence emission ratio remained rather constant around 2.55 ± 0.34 (Fig. 2a), which is within the typical range for *Synechocystis* sp. PCC 6803 and other cyanobacteria (Shen et al. 1993; Murakami et al. 1997; Kirilovsky 2015). In contrast, in blue light the PSI:PSII fluorescence emission ratio decreased drastically to 0.90 ± 0.01 in steady-state. Cells in the dilute chemostat in red light showed a similar PSI:PSII fluorescence emission ratio as those in the orange and red light chemostats, indicating that the low PSI:PSII ratio in blue light is a response to light color rather than to light intensity (Fig. 2a).

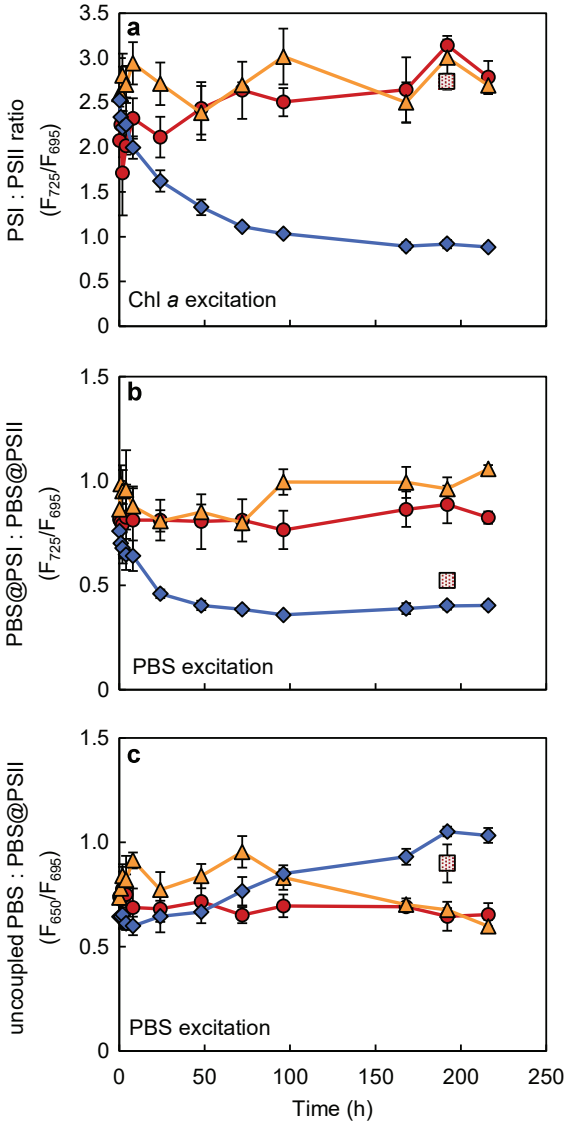

Fig. 2 | Ratios of PSI, PSII and PBS fluorescence emission peaks measured at 77 K of *Synechocystis* sp. PCC 6803, after a switch from artificial white light to monochromatic blue, orange and red light. (a) Changes in PSI:PSII fluorescence emission ratio during acclimation to blue (diamonds), orange (triangles) and red light (circles). The PSI:PSII ratio was estimated from 77 K fluorescence emitted by PSI (725 nm; F_{725}) relative to PSII (695 nm; F_{695}) after excitation of chlorophyll a at 440 nm. (b) Changes in the ratio of PBS excitonically coupled to PSI versus PBS coupled to PSII, estimated from 77 K fluorescence emitted by PSI relative to PSII after excitation of phycocyanin at 590 nm. (c) Changes in the ratio of uncoupled phycocyanin versus PBS coupled to PSII, estimated from 77 K fluorescence emitted by phycocyanin (650 nm; F_{650}) relative to PSII after excitation of phycocyanin at 590 nm. Red-dotted squares in (a-c) indicate steady-state fluorescence ratios of the dilute chemostat in red light. Data are averages of three biological replicates ± SD (n = 3). The 77 K fluorescence emission spectra are shown in Supplementary Fig. S1.

Upon excitation of PBS at 590 nm, fluorescence is emitted by PSII coupled to PBS (F_{695}), by PSI coupled to PBS (F_{725}), and by PBS not involved in light transfer to any of the two photosystems (uncoupled PBS at 650 nm; F_{650}) (Supplementary Fig. S1). The fluorescence emission peaks indicate that the distribution of PBS over the two photosystems was not affected by the switch from artificial white light to monochromatic orange and red light (Fig. 2b). In contrast, the switch to blue light strongly decreased the coupling of PBS to PSI relative to PSII (Fig. 2b) and increased the amount of uncoupled PBS (Fig. 2c). The distribution of PBS in the dilute chemostat in red light showed a qualitatively similar but less pronounced response as in blue light (Fig. 2b,c).

Blue light has more effect on the transcriptome than orange and red light

Microarrays were used to study changes in gene expression of *Synechocystis* sp. PCC 6803 after the switch from artificial white light to monochromatic blue, orange and red light. We calculated $\log_2$ fold changes in gene expression, by comparing the transcriptome at time points after the light switch with the transcriptome before the light switch (i.e., at t = 0 h). The complete transcriptome data are presented in Supplementary Table S2, and the regulated genes are detailed in Supplementary Table S3. In total, 145 of the 3 264 investigated genes were significantly up- or downregulated at one or more time points in blue light. In contrast, only five genes were differentially expressed in orange light, four genes in red light, and two genes in the dilute chemostat in red light. Hence, the switch to blue light induced a much larger transcriptome response than the switch to orange and red light.

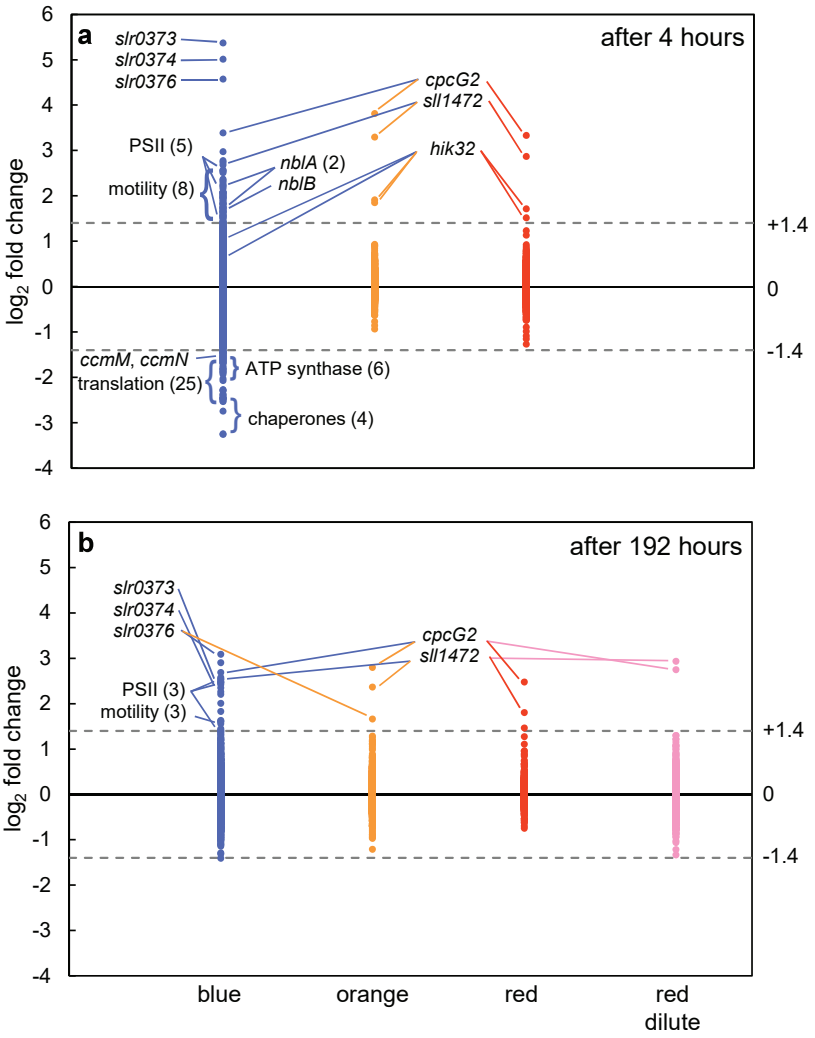

Fig. 3 | Overview of changes in gene expression of *Synechocystis* sp. PCC 6803, after a switch from artificial white light to monochromatic blue, orange and red light. (a) Gene expression levels of all analyzed genes, 4 h after the switch to blue (left), orange (middle) and red light (right). (b) Gene expression levels during steady state of the chemostats, 192 h after the switch to blue (left), orange (middle) and red light (right). Pink data points on the far right indicate gene expression by cells in the dilute chemostat in red light. Gene expression was compared to the expression levels in steady-state cells acclimated to artificial white light at t = 0 h. Dashed horizontal lines indicate the threshold $\log_2$ fold changes for significantly upregulated (>+1.4) and downregulated (<−1.4) genes. Names or functional descriptions of the strongly regulated (groups of) genes are indicated. Bracketed values indicate the number of regulated genes in a functional group. The data points cover all 3264 genes investigated in this study, and are based on three biological replicates (n = 3) for each light color. A complete list of all differentially expressed genes can be found in Supplementary Table S3.

Many of the observed changes in gene expression already occurred within the first 4 h after the light switch (Fig. 3a). After 4 h in orange and red light only four genes, which all belong to the light-sensing *ccaS* gene cluster, were significantly upregulated (i.e., with a $\log_2$ fold change > 1.4), while none of the investigated genes were downregulated. In contrast, after 4 h in blue light, 115 genes were differentially expressed, of which 61 genes were upregulated and 55 were downregulated (Fig. 3a).

After 192 h, when the chemostats had reached a new steady-state, only three genes were still upregulated in orange and red light, whereas 21 genes were upregulated and one was downregulated in blue light (Fig. 3b). Moreover, only two genes were upregulated in the dilute chemostat in red light. These results imply that most observed changes in gene expression are a response to blue light specifically rather than to light intensity, and that many of these responses turn out to be transient.

Response of genes related to photosynthesis and respiration

We used Cyanobase (http://genome.kazusa.or.jp/cyanobase) as a guideline to distinguish between genes of different functional categories. Furthermore, we have added the annotation of several genes that are listed as unknown or hypothetical in CyanoBase, but are annotated in the Kyoto Encyclopedia of Genes and Genomes (KEGG) (https://www.kegg.jp/), or in recent literature. Annotations of all differentially expressed genes can be found in Supplementary Table S3. Several of the significantly regulated genes were in the category photosynthesis and respiration (Fig. 4). In blue light, five genes related to PSII (*psbA2*, *psbA3*, *psbD*, *psbD2*, *psbB*), encoding two D1 proteins, two D2 proteins and a CP47 protein, respectively, were strongly upregulated (Fig. 4a). Furthermore, four genes related to PBS, encoding the PBS degradation proteins NblA1, NblA2 and NblB2 and the rod-core linker protein CpcG2, were also upregulated. Conversely, seven genes (*atpA*, *atpC-atpH*) encoding structural proteins of the ATP synthase complex, and two genes (*ccmM*, *ccmN*) encoding carboxysome proteins, were significantly downregulated in blue light (Fig. 4b).

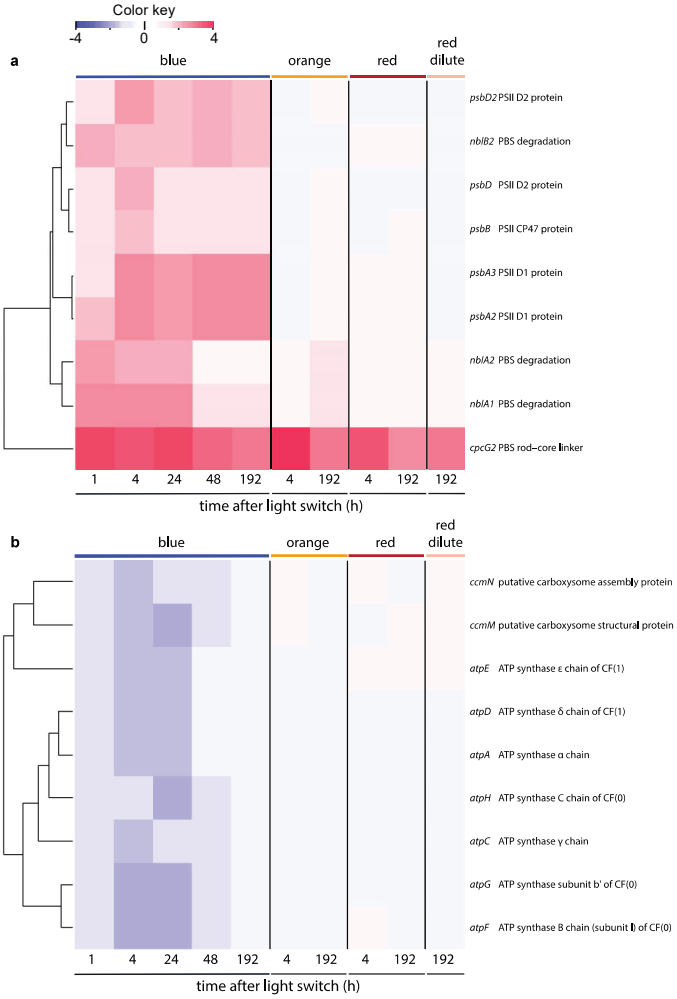

Fig. 4 | Expression of genes related to photosynthesis and respiration of *Synechocystis* sp. PCC 6803, after a switch from artificial white light to monochromatic blue, orange and red light. Changes in expression of genes related to (a) PSII and PBS, and (b) carboxysome production and ATP synthase, at several time points after the switch to monochromatic blue, orange and red light. Genes related to PSI, cytochrome b_6f, NADH turnover, respiratory terminal oxidases and soluble electron carriers were not differentially expressed in any of the experimental light conditions. Gene expression after the switch was compared to expression of cells acclimated to white light prior to the switch (i.e., at t = 0 h). Changes in gene expression in the dilute chemostat in red light are also indicated. Expression is shown only for genes that were significantly regulated ($P < 0.05$) and displayed a $\log_2$ fold change <-1.4 or $>+1.4$ for at least one of the time points. A complete list of all differentially expressed genes can be found in Supplementary Table S3. The heatmaps are ordered based on hierarchical clustering of the gene expression patterns. The data are based on three biological replicates (n = 3) for each light color.

In orange and red light and in the dilute chemostat in red light, the only gene within the category of photosynthesis and respiration that displayed a significant change in expression level was *sll1471* encoding the PBS rod-core linker protein CpcG2 (Fig. 4a). This gene was also upregulated in blue light, and belongs to the *ccaS* gene cluster (Hirose et al. 2008).

Genes related to PSI, cytochrome b_6f, NADH turnover, respiratory terminal oxidases and soluble electron carriers were not differentially expressed in any of the tested conditions; in addition, neither were any of the genes encoding photoprotective proteins, such as the orange carotenoid protein (OCP), iron-stress inducible protein A (IsiA) or flavodiiron proteins (Flv1-4).

Genes related to other functional categories

In the other functional categories, again many more genes were differentially expressed in blue light than in orange and red light (Fig. 5). Specifically, 29 genes belonging to other known functional categories were significantly upregulated in blue light, including genes encoding proteins involved in cellular motility (7 genes), PSII repair and turnover (6 genes), transposases (5 genes), histidine kinases (*hik32* and *hik35*) and the glutamine synthetase inactivating factors *gifA* and *gifB*. Conversely, 47 genes of the other functional categories were significantly downregulated in blue light, including genes encoding ribosomal proteins (24 genes), other proteins involved in transcription and translation (6 genes), chaperones (4 genes) and proteins involved in amino acid biosynthesis (2 genes).

The only two genes in the other functional categories that were differentially expressed in orange and red light and in the dilute chemostat in red light encode the histidine kinase Hik32, interrupted by an insertion sequence (Okamoto et al. 1999) (Fig. 5; Supplementary Table S3). *Hik32* also belongs to the previously mentioned *ccaS* gene cluster (Hirose et al. 2008).

In the categories of hypothetical genes and genes with unknown function, 40 genes were upregulated and 10 genes were downregulated in blue light (Supplementary Fig. S2). The three most strongly upregulated genes in blue light (*slr0373*, *slr0374* and *slr0376*; see also Fig. 3a) are hypothetical genes that are located in a single stress-related gene operon (Singh and Sherman 2002). The gene *sll1472* was upregulated in all three light colors, and is again part of the *ccaS* gene cluster (Hirose et al. 2008).

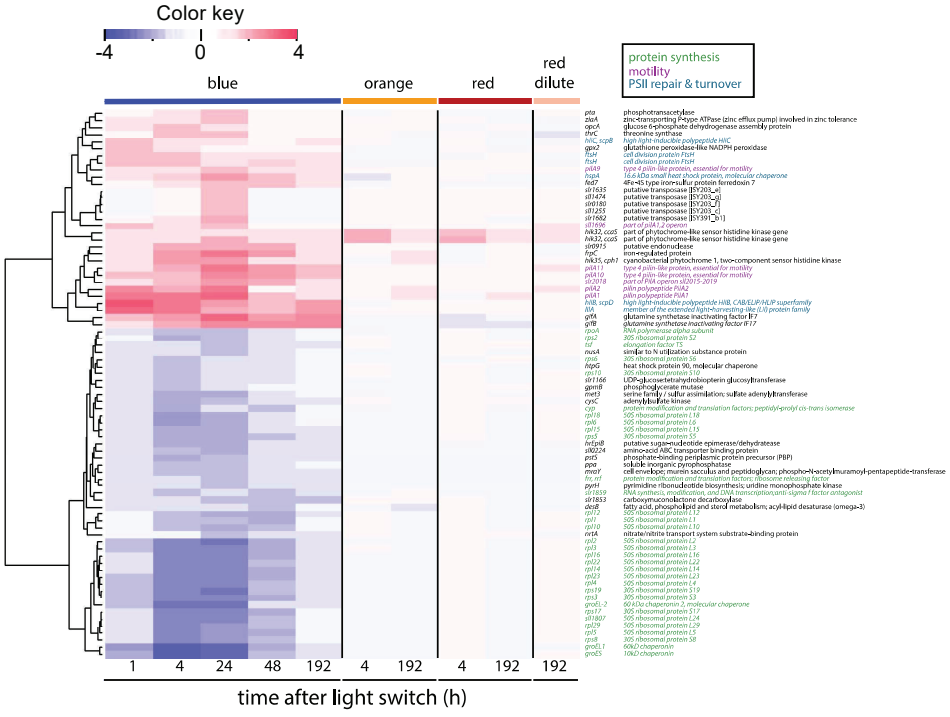

Fig. 5 | Expression of genes from several functional categories of *Synechocystis* sp. PCC 6803, after a switch from artificial white light to monochromatic blue, orange and red light. The heatmap shows changes in expression for all known genes that were regulated in response to the light switch, except those related to photosynthesis and respiration (which are shown in Fig. 4). Genes encoding proteins involved in protein synthesis and stability (green), motility (magenta), PSII repair and turnover (light blue) as annotated in CyanoBase, KEGG, or recent literature, are highlighted in color. Genes classified as hypothetical or unknown genes are shown in Supplementary Fig. S2. The layout and analyses are as in Fig. 4.

Discussion

Blue light alters photophysiology

Our results show that *Synechocystis* sp. PCC 6803 produces much less biomass in blue light than in orange, red, and artificial white light (Fig. 1). The low biomass production of PBS-containing cyanobacteria in blue light is consistent with many previous findings (Wyman and Fay 1986; Wilde et al. 1997; Wang et al. 2007; Singh et al. 2009; Chen et al. 2010; Choi et al. 2013; Bland and Angenent 2016; Luimstra et al. 2018). Blue light at wavelengths ≤ 450 nm is not absorbed by the PBS (Tandeau de Marsac 2003; Six et al. 2007), which usually transfer most of their absorbed light energy to PSII. Blue light is absorbed by Chl *a* and carotenoids. Cyanobacteria tend to invest much more of their Chl *a* in PSI than in PSII (Myers et al. 1980; Fujita 1997). Moreover, in cyanobacteria, only carotenoids of PSI appear to be involved in light harvesting, whereas carotenoids of PSII are involved in heat dissipation (Stamatakis et al. 2014). Hence, the low photosynthetic efficiency of cyanobacteria in blue light is commonly explained by the hypothesis that blue light causes an excitation imbalance between the two photosystems, with more light absorption by PSI than by PSII (Fujita 1997; Solhaug et al. 2014; Kirilovsky 2015; Luimstra et al. 2019). This hypothesis also provides a rationale for the strong decrease of the PSI:PSII fluorescence emission ratio (Fig. 2a and Supplementary Fig. S1a) and the decreased coupling of PBS to PSI, relative to PSII, after the switch from white to blue light (Fig. 2b and Supplementary Fig. S1d). Similar physiological changes in response to blue light have been observed in previous studies (Tsinoremas et al. 1994; Wilde et al. 1997; El Bissati and Kirilovsky 2001; Singh et al. 2009; Luimstra et al. 2018), and reflect increased investments in PSII and/or decreased investments in PSI to compensate for the excitation imbalance between the two photosystems.

The strong physiological response to blue light is also reflected in the transcriptome data, which showed that 145 genes responded to a switch from white to blue light whereas only a handful of genes responded to orange or red light (Fig. 3). In blue light several genes encoding structural PSII proteins were upregulated (Fig. 4a), indicative of an effort to overcome the low amount of excitons reaching PSII relative to PSI. This response included an increased expression of the D1 and D2 proteins that form the core of the PSII reaction center, and the PSII core antenna protein CP47. Furthermore, we observed an increase in several genes related to PSII turnover, including 2 *ftsH* genes, *hliB*, *hliC* and *lilA* (Fig. 5). The *ftsH* genes encode proteins that are involved in the degradation of

damaged D1 (Cheregi et al. 2007) and quality control of newly synthesized D1 (Komenda et al. 2006). The *hliB* and *hliC* genes encode high-light inducible proteins that are suggested to stabilize PSII subunits during PSII repair (Promnares et al. 2006; Yao et al. 2007). The *lilA* gene encodes a protein of the light-harvesting protein family that associates with HliB and HliC (Kufryk et al. 2008). In contrast to this strong response of several genes related to PSII synthesis, none of the genes encoding PSI subunits were differentially expressed in blue light. Hence, the observed decrease in the PSI:PSII fluorescence emission ratio in blue light (Fig. 2a and Supplementary Fig. S1a) seems to originate from an increased expression of PSII rather than a decreased expression of PSI. This is consistent with previous research using *Synechocystis* sp. PCC 6803, where blue light resulted in an upregulation of *psbA* encoding the PSII D1 protein, while expression levels of *psaE* encoding the Psa-E subunit of PSI remained similar (El Bissati and Kirilovsky 2001).

Furthermore, in blue light we observed an increase in the expression of *nblA1* and *nblA2*, encoding two PBS degradation proteins (Fig. 4a). The gene *slr1687* is presumed to encode another PBS degradation protein, NblB2 (Li and Sherman 2002), and was also upregulated in blue light (Fig. 4a). Moreover, the expression of a molecular chaperone that is involved in stabilization of PBS (HtpG, see Sato et al. 2010) was downregulated (Fig. 5). Degradation of PBS might be induced because these antennae are not functional in blue light. Nitrogen-rich PBS can constitute up to 50% of the total cellular protein content in cyanobacteria (Grossman et al. 1993), and their degradation provides building blocks for the production of other proteins. Indeed, the 77 K fluorescence spectra showed an increased decoupling of PBS from the photosystems in blue light (Fig. 2c; Supplementary S1d). However, whole-cell absorption spectra still showed considerable light absorption by phycocyanin at 625 nm relative to Chl *a* (Fig. 1c), while previous research has shown that PBS degradation induced by NblA1 and NblA2 is accompanied by a decreased absorption by phycocyanin (Baier et al. 2001). Hence, although changes in gene expression appear to prepare the degradation of PBS and disassembly of the PBS may have been initiated, the degradation process is not yet fully activated in nutrient-replete cells exposed to blue light.

Blue light induces flocculation and pili formation

Another interesting observation is the blue-light induced upregulation of genes that play a role in phototactic motility (Fig. 5). In particular, our results show that the switch to blue light resulted in initial upregulation of *pilA1*, known to be essential for the formation of Type-IV pili and hence for

twitching motility (Bhaya et al. 2000), and of *pilA2* and *sll1696*, which are part of the same operon. Type IV-based motility facilitates gliding of the cells over short distances on moist surfaces (Bhaya et al. 2001). Previous studies have indeed shown that blue light increases motility and negative phototaxis of *Synechocystis* sp. PCC 6803 (Ng et al. 2003; Terauchi and Ohmori 2004; Fiedler et al. 2005).

After initial upregulation of the *pilA1-pilA2* operon, the *pilA9*, *pilA10*, and *pilA11*-containing operon *slr2015-slr2019* (encoding minor pili subunits) was also upregulated in blue light (Fig. 5). PilA9-PilA11 have recently been shown to modulate the adhesive properties of Type-IV pili and to enhance flocculation of the cells (Yoshihara and Ikeuchi 2004; Panichkin et al. 2006; Conradi et al. 2019). This was consistent with our observations, which showed increased flocculation and wall growth in the blue-light chemostats (V.M. Luimstra, personal observation), a phenomenon that has also been described in previous studies (Enomoto et al. 2015; Agostoni et al. 2016). Flocculation and negative phototaxis may be interpreted as a stress response, protecting *Synechocystis* cells from adverse light conditions imposed by blue light. Moreover, in *Synechocystis* sp. PCC 6803, type-IV pili are essential for the uptake of extracellular DNA (Yoshihara et al. 2001) and flocculation of the cells might therefore also contribute to horizontal gene transfer (Conradi et al. 2019).

Transient changes in gene expression related to reduced growth

Remarkably, although genes associated with PSII and motility were upregulated in response to blue light for the entire duration of the experiment, many other genes were differentially expressed only temporarily after the switch to blue light and thereafter returned to their initial expression levels (Figs 4b, 5 and Supplementary Fig. S2). These transient changes in gene expression can be attributed to a temporary reduction of the growth rate after the switch to blue light, as illustrated by the declining cell numbers and biomass (Fig. 1a,b). At steady state, the growth rate equals the dilution rate of the chemostat. Hence, after ~150 h, the cell numbers stabilized at a new steady state and the growth rate recovered to the same value as before the light switch.

Low growth rates are usually associated with low ribosomal abundances (Scott et al. 2014; Zavřel et al. 2019). The transient period of low growth rate in blue light was indeed accompanied by a temporary down-regulation of 24 genes encoding ribosomal proteins and several other genes involved in transcription and translation (Fig. 5). Cellular metabolism is strongly ATP-dependent, which explains why genes encoding ATP-synthase were

also temporarily downregulated during the transient period of reduced growth (Fig. 4b). Furthermore, several genes encoding chaperones (*groES*, *groEL1*, *groEL2* and *htpG*), which commonly play an important role in the folding and stabilization of proteins, were also temporarily downregulated in blue light (Fig. 5). Interestingly, the only chaperone that was temporarily upregulated in blue light was the small heat-shock protein HspA (Fig. 5), which plays a role in the stabilization of PSII and the thylakoid membrane (Nitta et al. 2005; Sakthivel et al. 2009).

Light sensing in cyanobacteria

To allow acclimation to changes in their environment, microorganisms have developed highly efficient mechanisms to sense, transduce and respond to external signals. Cyanobacteria often use two-component systems composed of a histidine kinase (Hik) and a cognate response regulator (Rre) (Appleby et al. 1996; Mizuno et al. 1996; Capra and Laub 2012). In total, *Synechocystis* contains 49 Hiks, of which six Hiks that have phytochrome-like features are suggested to function as light sensors (hik1, hik3, hik24, hik32, hik35, and hik44; see Xu and Wang 2019). Of these six Hiks, only *hik35* and *hik32* were differentially expressed in our experiments.

Hik35 (*slr0473*) encodes the cyanobacterial phytochrome-like protein Cph1 (Hughes et al. 1997) and appears to be involved in the regulation of at least ten genes (Hübschmann et al. 2005). *Hik35* and five Hik35-regulated genes (*gifA*, *thrC*, *lilA*, *slr0373*, *slr0376*) were upregulated in our experiments after the switch to blue light, whereas one of the Hik35-regulated genes (*tsf*) was downregulated. *tsf* encodes the elongation factor TS which is involved in translation. The Hik35-regulated genes *slr0373* and *slr0376* form an operon with *slr0374*, and together these three genes represent the most strongly regulated genes in blue light (Fig. 3). The function of this operon is yet unknown, but it is known to respond to different stress conditions, such as iron deficiency, sulfur deficiency, nitrogen deficiency, high salinity, high light and oxidative stress (Singh and Sherman 2002; Singh et al. 2004). The *slr0374* gene encodes the highly conserved protein Ycf46. Inactivation of this gene reduces activity of the extracellular carbonic anhydrase EcaB, which indicates that it plays a role in the regulation of photosynthetic carbon fixation (Jiang et al. 2015).

Hik32, also known as CcaS, is encoded by two *hik32* genes (*sll1473* and *sll1475*; see Kondo et al. 2007), which were among the few genes that were significantly upregulated in orange and red light (Fig. 3). These two *hik32* genes are interrupted by a transposase (*sll1474*) in the *Synechocystis* strain ("Kazusa") sequenced in Cyanobase, but have been

shown to form one gene in the original PCC 6803 strain that was used here (Okamoto et al. 1999). The two-component system histidine kinase Hik32 and the cognate upstream response regulator CcaR (*slr1584*) regulate the expression of *cpcG2* (*sll1471*) and the hypothetical gene *sll1472* (Hirose et al. 2008), which were the two most strongly upregulated genes in orange and red light (Fig. 3). *CpcG2* encodes a rod-core linker protein that leads to the formation of atypical PBS that lack the allophycocyanin core and preferentially transfer energy to PSI, in contrast to the conventional PBS (containing CpcG1) that mainly transfer light energy to PSII (Kondo et al. 2005, 2007). The phycocyanin-containing PBS of *Synechocystis* sp. PCC 6803 absorb orange and red light very effectively (Tandeau de Marsac 2003), and usually transfer most of the absorbed light energy to PSII. Hence, the strong upregulation of *cpcG2* in orange and red light might be interpreted as a functional adaptation to redistribute part of the light energy absorbed by PBS to PSI, presumably to maintain the excitation balance between PSI and PSII in orange and red light. It remains to be elucidated why *cpcG2* and the hypothetical gene *sll1472* were also upregulated after the transfer from white to blue light (Fig. 4 and Supplementary Fig. S2). Possibly, they might play a role in the observed uncoupling of PBS from the photosystems in blue light (Fig. 2c and Supplementary Fig. S1d).

None of the additional (blue light) photoreceptors (Fiedler et al. 2005; Moon et al. 2010) showed a measurable transcriptional response to the imposed changes in light conditions.

Comparison with other studies

To the best of our knowledge, only one study has thus far focused on changes in the transcriptome of cyanobacteria in response to blue light (Singh et al. 2009). In their experiments, cells from a relatively dense *Synechocystis* culture acclimated to white light were inoculated in dilute batch cultures that were exposed to either blue or red light. Gene expression levels were measured only during the first six hours of their experiments. Singh et al. (2009) observed a similar physiological response of *Synechocystis* sp. PCC 6803 as in our study, with a lower PSI:PSII ratio in blue light compared to red or white light. Some cautionary notes should be made before comparing their gene expression data with our results, however. In particular, Singh et al. (2009) quantified gene expression as the $\log_2$ ratio of gene expression levels in red light relative to expression levels in blue light. Therefore, if gene expression was designated as, e.g., higher in red light it is uncertain whether this response actually reflected upregulation in red light, downregulation in blue light, or both. Furthermore, their batch cultures in red light showed a strong increase in

cell numbers, while cell numbers in blue light barely increased during the first ~24 h. Hence, it is likely that differences in gene expression between red and blue light observed in their experiments reflect differences in light color, average light intensity perceived by the cells, and growth rate. This contrasts with our experiments, where we have used chemostats to separate transient effects caused by temporary changes in growth rate from persistent effects caused by differences in light color. Furthermore, we have used a dilute chemostat to separate effects of light color and light intensity.

Despite these differences in experimental design, Singh et al. (2009) also report major changes in the expression of photosynthesis genes, with a higher expression of genes associated with PSII (and its synthesis) in blue light than in red light, including *hliB*, *hliC*, *lilA*, and *hspA*, which are involved in PSII turnover and protection. Their Table S2 indicates that they also observed that the putative pilin genes *pilA9-pilA11* (related to motility) and the stress-response operon containing *slr0373*, *slr0374* and *slr0376* had higher expression levels in blue light than in red light. Furthermore, in accordance with the lower growth rate in blue light, they also observed lower transcript levels of genes encoding many ribosomal proteins, ATP synthase subunits and the chaperones GroES, GroEL1, GroEL2 after 3-6 h in blue light.

In contrast to our findings, however, Singh et al. (2009) also observed a lower expression of several PSI genes in blue light than in red light. Furthermore, they report that expression of the motility genes *pilA1* and *pilA2*, and the PBS degradation genes *nblaA1* and *nblA2* was higher in red light than in blue light. This might be related to the lower light intensities used in their experiments, in line with results of Ogawa et al. (2018). Also, an increased expression of the *cpcG1* gene encoding the conventional rod-core linker protein of the PBS was observed in blue light while no data for the alternative *cpcG2* gene were available from their experiments. In addition, contrary to our results, Singh et al. (2009) found large differences in cellular carbon and nitrogen metabolism between red and blue light. This might be related to differences in growth conditions between red and blue light in the experiments of Singh et al. (2009), where cells in blue light were still in initial lag phase and had not yet resumed growth.

Hübschmann et al. (2005) investigated differences in gene expression between batch cultures of *Synechocystis* sp. PCC 6803 exposed to red light (652 nm) and far-red light (734 nm). Red light of 652 nm is absorbed by Chl *a* and can also be absorbed by allophycocyanin in the core of the PBS, whereas far-red light is absorbed only by Chl *a* and not by PBS (Lemasson

et al. 1973; Glazer and Bryant 1975; MacColl 2004). Hence, we have theorized previously (Luimstra et al. 2018) that, similar to blue light, growth in far-red light may also lead to an excitation imbalance between PSI and PSII. In line with this prediction, Murakami (1997) showed that red light of 680 nm (which is not absorbed by PBS) resulted in a substantially lower PSI:PSII ratio than red light of 650 nm. Hübschmann et al. (2005) found that far-red light of 734 nm indeed resulted in lower growth rates than red light of 652 nm. Moreover, many genes that were up-regulated in blue light in our experiments were similarly up-regulated in far-red light in their experiments, including several genes related to PSII synthesis (*psbA2*, *psbA3*, *psbD2*, *psbB*) and to PSII stabilization and turnover (*hliB*, *hliC*, *lilA*, *hspA*). Similarly, their supplementary Table S2 shows that the PBS degradation genes *nblA2* and *nlbB2*, and the genes *slr0374* and *slr0376* from the stress-responsive operon described by Singh and Sherman (2002) were also upregulated in far-red light. Furthermore, Hübschmann et al. (2005) found that the expression of more than 20 genes related to ribosomal proteins and several genes related to ATP synthase was lower in far-red light than in red light, in line with the transient changes in gene expression when blue light temporarily reduced the growth rate in our experiments. This comparison indicates that many genes involved in photosynthesis and growth are similarly regulated in blue and in far-red light, suggesting that these genes are indeed affected by the excitation imbalance between the two photosystems.

However, some genes that were strongly upregulated or downregulated in blue light were not differentially expressed in far-red light, indicating that these genes responded to blue light specifically. For example, *hik35* encoding the cyanobacterial phytochrome Cph1 was upregulated in blue light in our study, but was not differentially expressed in red or far-red light in the experiments of Hübschmann et al. (2005). And while blue light downregulated the expression of genes encoding the chaperones GroES, GroEL2 and HtpG in our experiments, these genes were upregulated in far-red light in their experiments. Hübschmann et al. (2005) also found that most pilin genes were not regulated or even downregulated in far-red light. By contrast, in our experiments blue light induced upregulation of several pilin-genes involved in motility and flocculation of cells (Fig. 5), in line with other research showing that blue light has distinct effects on cellular motility and flocculation (Ng et al. 2003; Terauchi and Ohmori 2004; Fiedler et al. 2005; Savakis et al; 2012, Enomoto et al. 2015; Agostoni et al. 2016).

Conclusions

Our results show that the switch from artificial white to blue light had a much stronger effect on the gene expression profile, photophysiology and growth of *Synechocystis* sp. PCC 6803 than the switch to orange and to red light. In particular, PSII genes were upregulated in blue light, in agreement with the decreased PSI:PSII ratio of the cells. This photophysiological acclimation will improve the distribution of excitation energy between PSII and PSI, even though the low growth rate in blue light indicates that upregulation of PSII was insufficient to fully restore linear photosynthetic electron flow. Conversely, many ribosomal genes and other genes involved in protein synthesis were temporarily downregulated in blue light, concomitant with the transient decline of the growth rate. Hence, blue light not only results in a limited transfer of excitation energy to PSII and a low photosynthetic efficiency of PBS-containing cyanobacteria, but also induces marked changes in their transcriptome to counter these adverse light conditions.

Acknowledgments

We are most grateful to Selina van Leeuwen (Microarray Department, University of Amsterdam) for her advice and technical support of the microarray analysis, and we thank the two reviewers for their helpful comments. This work has been performed in the cooperation framework of Wetsus, European Centre of Excellence for Sustainable Water Technology (www.wetsus.eu). Wetsus is co-funded by the Dutch Ministry of Economic Affairs and Ministry of Infrastructure and Environment, the Province of Fryslân and the Northern Netherlands Provinces.

Supplementary information

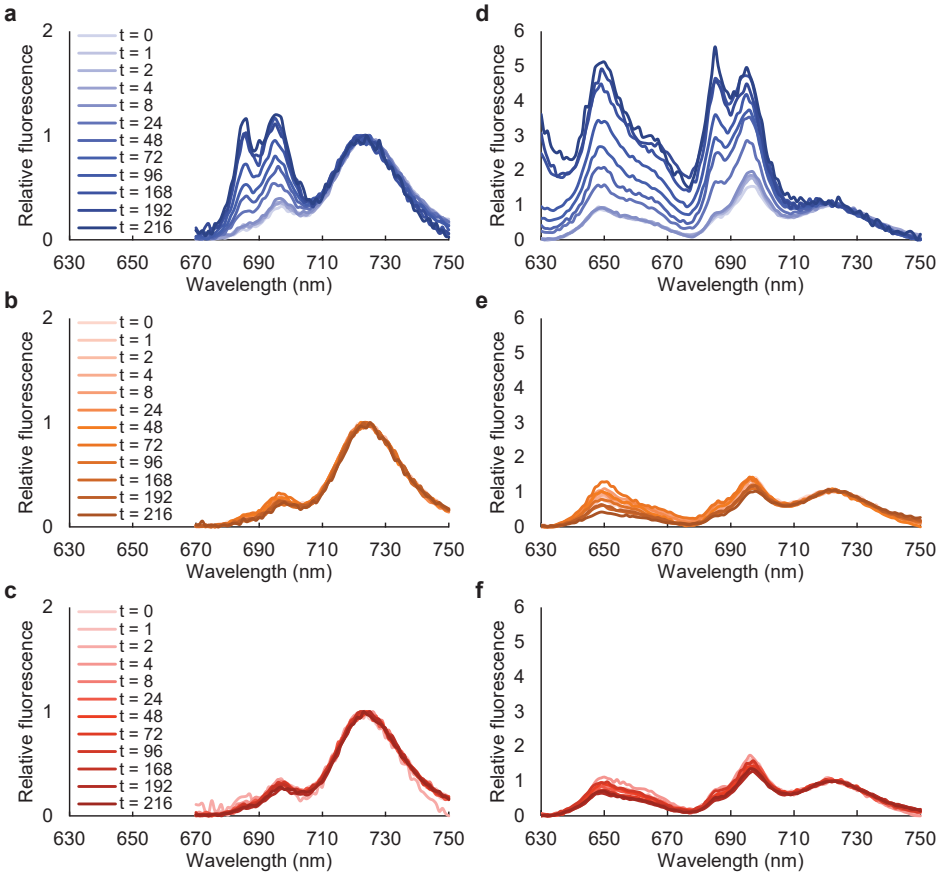

Supplementary Fig. S1 | Low-temperature (77 K) fluorescence emission spectra of *Synechocystis* sp. PCC 6803, before and after a switch from artificial white light to monochromatic blue, orange and red light. 77 K spectra were measured before (t = 0 h) and at several time points after the switch to blue light (a,d), orange light (b,e), and red light (c,f). (a-c) Excitation of Chl *a* at 440 nm yields fluorescence emission peaks at 695 nm for PSII and at 725 nm for PSI. (d-f) Excitation of phycocyanin at 590 nm yields fluorescence emission peaks at 695 nm when PBSs are excitonically coupled to PSII and at 725 nm when coupled to PSI (state 2). PBS that are decoupled from the photosystems and phycocyanin that is not incorporated into PBS result in fluorescence emission from phycocyanin and allophycocyanin at 650-665 nm. Spectra show the averages of three biological replicates per time point (n = 3), and are normalized to PSI fluorescence at 725 nm.

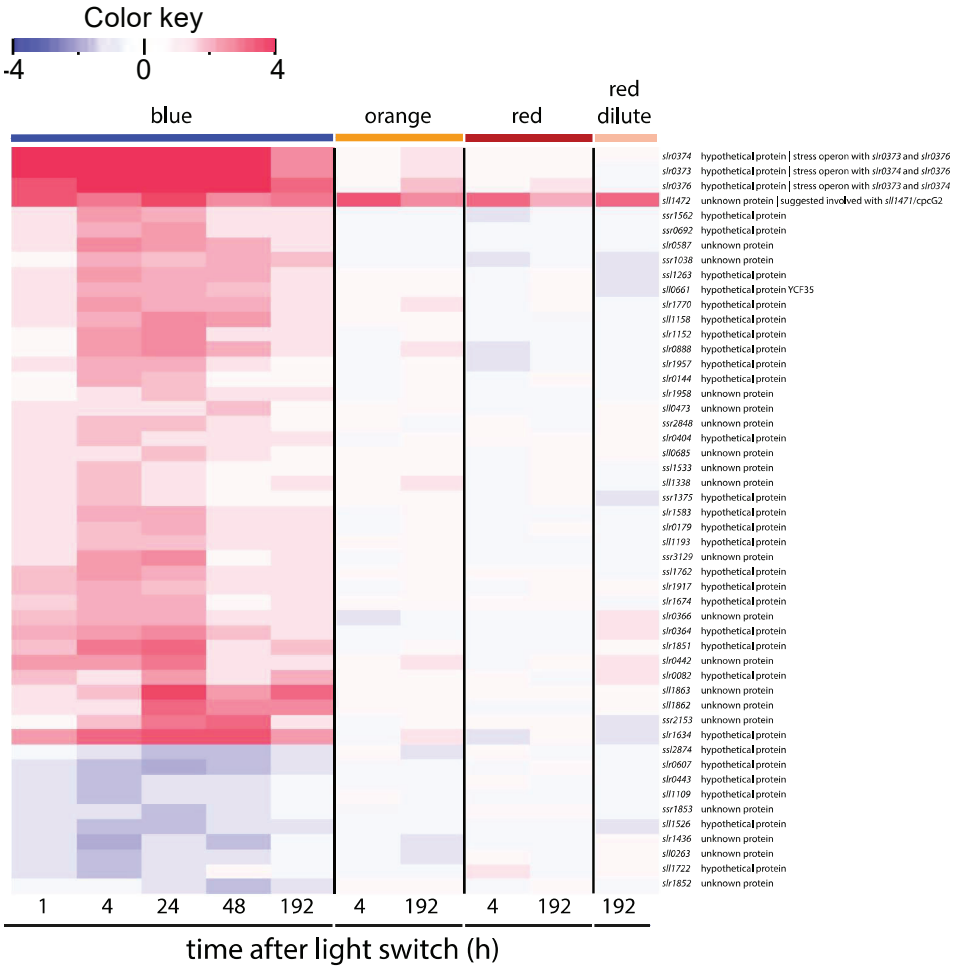

Supplementary Fig. S2 | Expression of 'hypothetical' and 'unknown' genes of *Synechocystis* sp. PCC 6803, after a switch from artificial white light to monochromatic blue, orange and red light. The heatmap shows changes in expression for all genes classified as hypothetical and unknown genes that were regulated in response to the light switch. The layout and analyses are as in Figs. 4 and 5.

Supplementary Table S1 | Loop design used to hybridize samples to the microarray chips.

Color	Sample	Replicate	Array	Dye	Chip
'white'	t = 0 h	1	1	Cy3	1
'white'	t = 0 h	2	10	Cy5	1
'white'	t = 0 h	3	11	Cy3	1
'white'	t = 0 h	4	12	Cy5	1
'white'	t = 0 h	5	13	Cy3	1
blue	t = 1 h	1	1	Cy5	1
blue	t = 1 h	2	2	Cy3	1
blue	t = 1 h	3	15	Cy5	1
blue	t = 4 h	1	2	Cy5	1
blue	t = 4 h	2	3	Cy3	1
blue	t = 4 h	3	16	Cy5	1
blue	t = 8 h	1	3	Cy5	1
blue	t = 8 h	2	4	Cy3	1
blue	t = 8 h	3	14	Cy5	1
blue	t = 24 h	1	4	Cy5	1
blue	t = 24 h	2	5	Cy3	1
blue	t = 24 h	3	15	Cy3	1
blue	t = 192 h	1	5	Cy5	1
blue	t = 192 h	2	6	Cy3	1
blue	t = 192 h	3	11	Cy5	1
orange	t = 4 h	1	9	Cy5	1
orange	t = 4 h	2	10	Cy3	1
orange	t = 4 h	3	14	Cy3	1
orange	t = 192 h	1	6	Cy5	1
orange	t = 192 h	2	7	Cy3	1
orange	t = 192 h	3	13	Cy5	1
red	t = 4 h	1	8	Cy5	1
red	t = 4 h	2	9	Cy3	1
red	t = 4 h	3	16	Cy3	1
red	t = 192 h	1	7	Cy5	1
red	t = 192 h	2	8	Cy3	1
red	t = 192 h	3	12	Cy3	1
red	t = 192 h	1	3	Cy5	2
red	t = 192 h	2	4	Cy3	2
red	t = 192 h	3	6	Cy3	2
red	red dilute t = 192 h	1	4	Cy5	2
red	red dilute t = 192 h	2	5	Cy3	2
red	red dilute t = 192 h	3	7	Cy3	2
blue	t = 48 h	1	1	Cy5	2
blue	t = 48 h	2	2	Cy3	2
blue	t = 48 h	3	7	Cy5	2
blue	t = 192 h	1	2	Cy5	2
blue	t = 192 h	2	3	Cy3	2
blue	t = 192 h	3	8	Cy3	2
'white'	t = 0 h	4	8	Cy5	2
'white'	t = 0 h	1	1	Cy3	2
'white'	t = 0 h	2	5	Cy5	2
'white'	t = 0 h	3	6	Cy5	2

Supplementary Table S2 | Genes that were differentially expressed during the study. Genes expressed with a $\log_2$ fold change of <-1.4 or >1.4 and $p < 0.05$ were considered differentially expressed. We used Cyanobase (http://genome.kazusa.or.jp/cyanobase) as a guideline to distinguish between genes of different functional categories. We have also designated several genes that are listed as unknown or hypothetical in CyanoBase, but are annotated in the Kyoto Encyclopedia of Genes and Genomes (KEGG) (https://www.kegg.jp/) or in recent literature. In the latter case, references are added. References not included in the main text are listed as footnotes.

This Table is available online in the Supporting Information of this article at:
https://onlinelibrary.wiley.com/doi/full/10.1111/ppl.13086

Supplementary Table S3 | Genes that were differentially expressed during the study and their annotation.

ORF ID	Gene name	Time after light switch										Functional category and gene function (Cyanobase, KEGG, recent literature)	Reference (if not annotated in Cyanobase or KEGG)
		blue light		orange light			red light		red dilute				
		1h	4h	24h	48h	192h	4h	192h	4h	192h	192h		
Photosynthesis and respiration													
sll1326	*atpA*	-0.76	-1.54	-1.64	-0.64	-0.42	-0.11	-0.25	-0.14	-0.19	-0.20	ATP synthase alpha chain	
sll1327	*atpC*	-0.74	-1.45	-1.39	-0.72	-0.27	-0.03	-0.15	-0.07	-0.10	-0.04	ATP synthase gamma chain	
sll1325	*atpD*	-0.78	-1.64	-1.68	-0.69	-0.48	-0.09	-0.34	-0.05	-0.13	-0.12	ATP synthase delta chain of CF(1)	
slr1330	*atpE*	-1.03	-1.53	-1.50	-0.64	-0.35	0.00	-0.39	0.32	0.23	0.54	ATP synthase epsilon chain of CF(1)	
sll1324	*atpF*	-0.92	-1.81	-1.80	-0.74	-0.53	-0.04	-0.38	0.01	-0.14	-0.15	ATP synthase B chain (subunit I) of CF(0)	
sll1323	*atpG*	-1.00	-1.74	-1.89	-0.76	-0.61	-0.09	-0.38	-0.01	-0.12	-0.13	ATP synthase subunit b' of CF(0)	
ssl2615	*atpH*	-0.75	-1.34	-1.70	-0.77	-0.58	-0.06	-0.28	-0.01	-0.15	-0.26	ATP synthase C chain of CF(0)	
sll1031	*ccmM*	-1.15	-1.48	-1.75	-1.16	-0.59	0.15	-0.07	-0.02	0.02	0.16	Carbon dioxide concentrating mechanism protein CcmM, putative carboxysome structural protein	
sll1032	*ccmN*	-0.94	-1.41	-1.37	-1.02	-0.35	0.19	-0.17	0.08	-0.10	0.40	Carbon dioxide concentrating mechanism protein CcmN, putative carboxysome assembly protein	
sll1471	*cpcG2*	3.61	3.38	3.63	2.85	2.69	3.81	2.80	3.33	2.47	2.74	Phycobilisome rod-core linker polypeptide CpcG2	
ssl0452	*nblA1*	2.52	2.34	2.47	1.31	1.23	0.27	0.80	0.04	0.41	0.45	Phycobilisome degradation protein NblA	
ssl0453	*nblA2*	1.98	1.84	1.82	0.59	0.68	0.32	0.88	0.02	0.17	0.15	Phycobilisome degradation protein NblA	
slr1687	*nblB2*	1.80	1.66	1.41	1.74	1.60	-0.28	-0.08	0.01	0.01	-0.20	Phycobilisome degradation protein NblB	Li and Sherman 2002
slr1311	*psbA2*	1.43	2.36	2.12	2.40	2.47	-0.18	0.15	0.13	0.17	-0.21	Photosystem II D1 protein	
sll1867	*psbA3*	1.39	2.30	2.10	2.40	2.45	-0.22	0.12	0.16	0.17	-0.25	Photosystem II D1 protein	
slr0906	*psbB*	0.91	1.61	1.13	1.03	0.83	-0.11	0.30	-0.03	0.06	-0.26	Photosystem II core light harvesting protein	
sll0849	*psbD*	1.01	1.82	0.94	1.22	0.96	-0.37	0.06	-0.12	-0.06	-0.40	Photosystem II reaction center D2 protein	
slr0927	*psbD2*	1.14	2.07	1.45	1.75	1.44	-0.27	0.10	-0.03	-0.03	-0.32	Photosystem II reaction center D2 protein	
Other known categories and functions													
sll1473	*CcaS; hik32*	1.31	1.25	1.69	1.19	1.08	1.85	1.19	1.71	0.89	1.29	Hypothetical; two-component sensor histidine kinase Hik32	Hirose et al. 2008
sll1475	*CcaS; hik32*	0.77	0.81	0.95	0.92	0.87	1.91	0.98	1.51	0.96	1.22	Regulatory functions; two-component sensor histidine kinase Hik32	
slr0473	*cph1, hik35*	1.14	2.16	2.15	1.10	0.83	-0.20	0.78	-0.48	0.06	0.22	Regulatory functions; cyanobacterial phytochrome 1, two-component sensor histidine kinase Hik35	
slr1251	*cyp*	-1.12	-1.69	-1.31	-1.57	-0.63	-0.10	-0.59	0.08	-0.03	0.21	Translation; protein modification and translation factors; peptidyl-prolyl cis-trans isomerase	

slr0676	*cysC*	-1.28	-1.82	-1.55	-1.31	-0.82	0.07	-0.42	0.40	0.01	-0.12	Amino acid biosynthesis; serine family/sulfur assimilation; adenylylsulfate kinase	
sll1441	*desB*	-1.24	-1.27	-0.85	-1.57	-0.61	-0.32	-0.95	0.46	-0.24	-0.25	Fatty acid, phospholipid and sterol metabolism; acyl-lipid desaturase (omega-3)	
sll0662	*Fed7*	0.68	1.23	1.49	1.62	1.03	-0.08	0.12	-0.10	-0.10	-0.50	Hypothetical protein; 4Fe-4S type iron-sulfur protein ferredoxin 7	Marteyn et al. 2009[1]
sll1009	*FrpC*	1.28	2.20	2.72	2.07	1.32	0.12	1.16	-0.28	0.66	0.00	Unknown protein; iron-regulated protein	
sll0145	*frr, rrf*	-1.16	-1.30	-1.41	-0.91	-0.75	-0.08	-0.22	-0.29	-0.17	-0.51	Translation; protein modification and translation factors; ribosome releasing factor	
slr1604	*ftsH*	1.66	1.55	1.24	1.16	1.12	-0.26	-0.27	-0.15	0.13	-0.25	Cellular processes; cell division protein FtsH	
slr0228	*ftsH*	1.53	1.55	1.08	1.40	1.20	-0.11	-0.21	0.08	0.15	-0.05	Cellular processes; cell division protein FtsH	
ssl1911	*gifA*	1.56	2.23	3.06	2.21	2.54	-0.46	-0.15	-1.27	-0.58	0.17	Hypothetical protein; glutamine synthetase inactivating factor IF7	García-Domínguez et al. 1999[2]
sll1515	*gifB*	1.23	1.95	2.52	2.44	2.42	-0.26	-0.59	-1.15	-0.75	-0.11	Unknown protein; glutamine synthetase inactivating factor IF17	García-Domínguez et al. 1999[2]
slr1124	*gpmB*	-1.35	-1.62	-1.31	-0.60	-0.60	-0.05	-0.39	0.41	0.27	0.03	Energy metabolism; glycolysis; phosphoglycerate mutase	
slr1992	*gpx2*	1.42	0.72	0.21	0.60	0.66	-0.19	-0.66	0.08	-0.09	0.05	Biosynthesis of cofactors, prosthetic groups, and carriers; glutathione peroxidase-like NADPH peroxidase	
slr2076	*groEL1*	-1.99	-3.26	-2.99	-1.72	-1.01	-0.09	-0.44	0.13	-0.23	-0.06	Cellular processes; 60kD chaperonin	
sll0416	*groEL-2*	-1.67	-2.75	-2.70	-1.38	-0.76	-0.02	-0.22	0.33	-0.03	0.02	Cellular processes; 60 kDa chaperonin 2, GroEL2, molecular chaperone	
slr2075	*groES*	-1.87	-3.25	-2.94	-1.63	-0.95	-0.09	-0.47	0.03	-0.21	0.01	Cellular processes; 10kD chaperonin	
ssr2595	*hliB, scpD*	3.31	2.57	2.12	1.55	2.26	-0.01	0.25	0.41	0.11	0.10	Other categories; adaptations and atypical conditions; high light-inducible polypeptide HliB	Promnares et al. 2006; Yao et al. 2007
ssl1633	*hliC, scpB*	1.52	1.18	0.93	0.52	0.72	0.04	-0.16	0.27	-0.09	-0.09	Hypothetical; high light-inducible polypeptide HliC	Promnares et al. 2006; Yao et al. 2007
sll0576	*HrEpiB*	-1.22	-1.83	-1.84	-1.28	-0.73	-0.11	-0.28	-0.12	-0.34	-0.42	Other categories; putative sugar-nucleotide epimerase/dehydratease	
sll1514	*hspA*	0.84	1.40	2.13	1.41	0.99	-0.86	0.25	0.15	-0.13	-0.45	Cellular processes; 16.6 kDa small heat shock protein, molecular chaperone	
sll0430	*htpG*	-1.06	-1.59	-0.91	-1.02	-0.47	0.03	-0.19	0.02	-0.11	-0.02	Cellular processes; heat shock protein 90, molecular chaperone	
slr1544	*lilA*	3.08	2.56	1.95	1.48	2.00	0.18	0.11	0.55	0.20	0.10	Unknown protein; member of the extended light-harvesting-like (Lil) protein family	Kufryk et al. 2008
slr1165	*met3*	-1.35	-1.86	-1.73	-1.30	-0.67	-0.17	-0.59	0.21	-0.06	0.14	Amino acid biosynthesis; serine family/sulfur assimilation; sulfate adenylyltransferase	
sll0657	*mraY*	-1.30	-1.40	-1.42	-0.87	-0.81	-0.06	-0.42	-0.08	0.00	-0.42	Cell envelope; murein sacculus and peptidoglycan; phospho-N-acetylmuramoyl-pentapeptide-transferase	
sll1450	*nrtA*	-0.30	-0.69	-1.55	-1.06	-1.32	0.28	-0.03	0.39	0.25	-0.23	Transport and binding proteins; nitrate/nitrite transport system substrate-binding protein	
slr0743	*nusA*	-0.75	-1.16	-1.45	-1.22	-0.54	-0.05	-0.57	0.16	-0.10	0.34	Transcription; RNA synthesis, modification, and DNA transcription; similar to N utilization substance protein	

slr1734	*opcA*	1.01	1.43	0.75	0.36	0.12	0.11	0.42	0.00	0.46	-0.03	Energy metabolism; pentose phosphate pathway; glucose 6-phosphate dehydrogenase assembly protein	
sll1694	*pilA1*	2.66	2.74	2.85	1.60	1.13	0.44	1.28	-0.26	0.73	0.49	Cellular processes; pilin polypeptide PilA1	
sll1695	*pilA2*	2.28	1.95	2.56	0.67	0.85	0.51	1.01	0.03	0.50	0.87	Cellular processes; chemotaxis; pilin polypeptide PilA2	
sll1696		1.46	0.84	1.55	0.39	0.60	0.50	0.62	0.13	0.29	1.29	Hypothetical; part of *pilA1,2* operon	Bhaya et al. 2000
slr2015	*pilA9*	1.11	1.23	1.67	1.31	1.13	0.15	0.04	0.18	0.36	0.44	Unknown protein; type 4 pilin-like protein, essential for motility	Chandra et al. 2015
slr2016	*pilA10*	1.46	1.64	2.38	2.00	1.55	0.34	0.31	0.17	0.52	0.59	Unknown protein; type 4 pilin-like protein, essential for motility	Chandra et al. 2015
slr2017	*pilA11*	1.38	1.75	2.63	2.08	1.60	0.43	0.53	0.28	0.50	0.84	Unknown protein; type 4 pilin-like protein, essential for motility	Chandra et al. 2015
slr2018		1.22	1.53	2.09	1.88	1.38	0.29	0.36	0.26	0.53	0.47	Unknown protein; part of *pilA* operon *sll2015-2019*	Chandra et al. 2015
slr1622	*ppa*	-1.11	-1.68	-1.40	-0.86	-0.63	-0.19	-0.45	-0.10	-0.07	-0.28	Central intermediary metabolism; Phosphorus compounds; soluble inorganic pyrophosphatase	
sll0680	*pstS*	-0.98	-1.69	-1.62	-1.12	-0.79	-0.39	-0.31	-0.63	0.00	-0.23	Transport and binding proteins; phosphate-binding periplasmic protein precursor (PBP)	
slr2132	*pta*	0.61	1.18	1.43	0.48	0.62	-0.16	0.15	-0.30	-0.25	0.26	Energy metabolism; pyruvate and acetyl-CoA metabolism; phosphotransacetylase	
sll0144	*pyrH*	-0.96	-1.07	-1.42	-0.97	-0.76	-0.08	-0.38	-0.11	-0.17	-0.52	Purines, pyrimidines, nucleosides, and nucleotides; uridine monophosphate kinase	
sll1744	*rpl1*	-0.60	-1.64	-1.68	-1.74	-0.65	0.08	-0.36	0.12	-0.17	0.21	Translation; ribosomal proteins: synthesis and modification; 50S ribosomal protein L1	
sll1745	*rpl10*	-0.04	-1.52	-1.73	-1.59	-0.67	0.04	-0.19	0.01	-0.21	0.12	Translation; ribosomal proteins: synthesis and modification; 50S ribosomal protein L10	
sll1746	*rpl12*	-0.45	-1.61	-1.93	-1.78	-0.75	0.16	-0.18	0.09	-0.09	0.04	Translation; ribosomal proteins: synthesis and modification; 50S ribosomal protein L12	
sll1806	*rpl14*	-1.21	-2.53	-2.39	-1.76	-0.77	-0.09	-0.41	0.05	-0.18	0.30	Translation; ribosomal proteins: synthesis and modification; 50S ribosomal protein L14	
sll1813	*rpl15*	-0.86	-1.88	-1.87	-1.23	-0.72	-0.04	-0.28	0.22	-0.02	0.40	Translation; ribosomal proteins: synthesis and modification; 50S ribosomal protein L15	
sll1805	*rpl16*	-1.31	-2.45	-2.37	-1.74	-0.71	-0.08	-0.44	0.19	-0.14	0.41	Translation; ribosomal proteins: synthesis and modification; 50S ribosomal protein L16	
sll1811	*rpl18*	-0.89	-2.03	-1.89	-1.32	-0.68	-0.09	-0.30	0.08	-0.15	0.28	Translation; ribosomal proteins: synthesis and modification; 50S ribosomal protein L18	
sll1802	*rpl2*	-1.60	-2.52	-2.58	-1.81	-0.89	-0.04	-0.38	0.17	-0.06	0.42	Translation; ribosomal proteins: synthesis and modification; 50S ribosomal protein L2	
sll1803	*rpl22*	-1.34	-2.38	-2.40	-1.59	-0.72	-0.12	-0.41	0.12	-0.19	0.38	Translation; ribosomal proteins: synthesis and modification; 50S ribosomal protein L22	
sll1801	*rpl23*	-1.45	-2.42	-2.37	-1.78	-0.79	-0.02	-0.39	0.14	-0.07	0.38	Translation; ribosomal proteins: synthesis and modification; 50S ribosomal protein L23	
sll1807	*rpl24*	-1.16	-2.47	-2.30	-1.67	-0.65	-0.07	-0.43	0.09	-0.19	0.34	Translation; ribosomal proteins: synthesis and modification; 50S ribosomal protein L24	

ssl3436	*rpl29*	-1.22	-2.48	-2.25	-1.66	-0.67	-0.08	-0.41	0.10	-0.17	0.35	Translation; ribosomal proteins: synthesis and modification; 50S ribosomal protein L29
sll1799	*rpl3*	-1.49	-2.28	-2.34	-1.72	-0.71	0.08	-0.31	0.27	-0.01	0.40	Translation; ribosomal proteins: synthesis and modification; 50S ribosomal protein L3
sll1800	*rpl4*	-1.42	-2.31	-2.42	-1.66	-0.81	-0.03	-0.41	0.21	-0.12	0.28	Translation; ribosomal proteins: synthesis and modification; 50S ribosomal protein L4
sll1808	*rpl5*	-1.08	-2.38	-2.20	-1.74	-0.65	-0.04	-0.39	0.12	-0.18	0.37	Translation; ribosomal proteins: synthesis and modification; 50S ribosomal protein L5
sll1810	*rpl6*	-0.87	-2.07	-1.91	-1.33	-0.61	-0.08	-0.27	0.19	-0.17	0.34	Translation; ribosomal proteins: synthesis and modification; 50S ribosomal protein L6
sll1818	*rpoA*	-0.85	-1.59	-1.51	-1.14	-0.54	0.00	-0.35	0.23	-0.03	0.38	Transcription; RNA synthesis, modification, and DNA transcription; RNA polymerase alpha subunit
sll1101	*rps10*	-0.85	-1.44	-0.89	-1.26	-0.34	0.16	-0.31	0.29	-0.04	0.20	Translation; ribosomal proteins: synthesis and modification; 30S ribosomal protein S10
ssl3437	*rps17*	-1.18	-2.46	-2.30	-1.69	-0.67	-0.05	-0.43	0.12	-0.16	0.37	Translation; ribosomal proteins: synthesis and modification; 30S ribosomal protein S17
ssl3432	*rps19*	-1.45	-2.46	-2.56	-1.67	-0.83	-0.09	-0.38	0.11	-0.14	0.39	Translation; ribosomal proteins: synthesis and modification; 30S ribosomal protein S19
sll1260	*rps2*	-0.59	-1.78	-1.42	-1.17	-0.60	0.04	-0.30	0.19	-0.08	0.15	Translation; ribosomal proteins: synthesis and modification; 30S ribosomal protein S2
sll1804	*rps3*	-1.41	-2.48	-2.52	-1.69	-0.82	-0.11	-0.44	0.13	-0.17	0.40	Translation; ribosomal proteins: synthesis and modification; 30S ribosomal protein S3
sll1812	*rps5*	-0.86	-1.89	-1.72	-1.44	-0.70	-0.04	-0.19	0.12	-0.10	0.25	Translation; ribosomal proteins: synthesis and modification; 30S ribosomal protein S5
sll1767	*rps6*	-0.70	-1.44	-1.15	-1.02	-0.41	0.00	-0.09	-0.05	0.01	-0.16	Translation; ribosomal proteins: synthesis and modification; 30S ribosomal protein S6
sll1809	*rps8*	-0.97	-2.28	-2.04	-1.59	-0.63	-0.10	-0.32	0.11	-0.16	0.41	Translation; ribosomal proteins: synthesis and modification; 30S ribosomal protein S8
sll1688	*thrC*	0.65	1.41	1.59	0.63	0.26	0.28	-0.50	0.50	-0.13	-0.87	Amino acid biosynthesis; aspartate family; threonine synthase
sll1261	*tsf*	-0.72	-1.37	-1.51	-1.33	-0.71	0.29	-0.34	0.40	0.07	0.04	Translation; protein modification and translation factors; elongation factor TS
slr0798	*ziaA*	0.72	1.08	1.41	0.53	0.43	0.24	0.20	0.09	-0.02	-0.02	Transport and binding proteins; zinc-transporting P-type ATPase (zinc efflux pump) involved in zinc tolerance
slr0915		1.33	1.73	1.97	1.91	1.35	0.20	0.43	-0.25	0.08	-0.34	DNA replication, restriction, modification, recombination, and repair; putative endonuclease
slr1166		-1.19	-1.57	-1.34	-0.79	-0.31	-0.08	-0.45	0.09	-0.04	0.37	Energy metabolism; sugars; UDP-glucose:tetrahydrobiopterin glucosyltransferase
slr1853		-1.04	-1.33	-1.55	-1.57	-1.41	0.04	0.04	0.01	-0.01	-0.31	Other categories; carboxymuconolactone decarboxylase
sll1255		-0.04	0.68	1.52	-0.37	-0.45	0.42	0.61	0.59	0.16	0.12	Putative transposase [ISY203_c]
slr1635		-0.02	0.59	1.41	-0.38	-0.47	0.36	0.57	0.53	0.11	0.14	Putative transposase [ISY203_e]
slr0180		-0.04	0.65	1.48	-0.35	-0.48	0.35	0.60	0.56	0.08	0.10	Putative transposase [ISY203_f]

sll1474	-0.06	0.60	1.45	-0.39	-0.47	0.37	0.60	0.55	0.09	0.16	Putative transposase [ISY203_g]	
slr1682	0.11	0.78	1.83	-0.03	-0.42	0.49	0.55	0.56	-0.12	0.07	Putative transposase [ISY391_b1]	
slr1859	-1.09	-1.49	-1.18	-1.48	-0.96	-0.05	0.12	-0.49	-0.19	-0.12	Transcription; RNA synthesis, modification, and DNA transcription; anti-sigma f factor antagonist	
sll0224	-0.83	-1.44	-1.71	-1.27	-0.89	-0.01	-0.02	-0.10	-0.13	-0.43	Transport and binding proteins; amino-acid ABC transporter binding protein	
Hypothetical and unknown proteins												
sll0263	-1.04	-1.55	-0.83	-1.31	-0.28	0.00	-0.84	0.27	-0.02	0.27	Unknown protein	
sll0473	0.82	1.09	1.37	1.42	0.60	0.02	0.29	-0.39	-0.04	0.12	Unknown protein; NitT/TauT family transport system substrate-binding protein	
sll0661	1.08	1.90	1.73	1.66	1.04	0.10	0.37	-0.01	0.21	-0.80	Hypothetical protein; YCF35	
sll0685	1.06	1.12	1.46	0.79	0.57	0.02	0.01	-0.03	0.13	0.07	Hypothetical protein; thioredoxin-like protein	
sll1109	-0.85	-1.45	-1.26	-1.15	-0.66	0.09	-0.24	-0.09	-0.12	-0.12	Hypothetical protein	
sll1158	1.34	1.75	2.29	2.11	1.38	0.07	0.60	-0.06	-0.03	-0.53	Hypothetical protein	
sll1193	1.17	1.64	1.64	0.94	0.84	0.04	0.43	-0.12	-0.19	-0.04	Hypothetical protein	
sll1338	1.20	1.67	1.16	0.52	0.78	0.12	0.85	-0.13	0.10	-0.28	Unknown protein	
sll1472	3.31	2.78	3.54	2.53	2.57	3.29	2.36	2.87	1.80	2.93	Unknown protein; part of *ccaS* gene cluster	Hirose et al. 2008
sll1526	-1.17	-1.67	-1.50	-0.80	-0.74	-0.22	-0.48	-0.52	-0.47	-0.73	Hypothetical protein; methyltransferase	
sll1722	-1.35	-1.50	-0.74	0.01	-0.16	-0.49	-0.55	0.72	-0.22	0.29	Hypothetical protein	
sll1862	1.00	1.05	2.99	2.27	2.47	0.18	0.50	-0.13	-0.19	0.17	Unknown protein	
sll1863	1.31	1.68	3.64	2.17	2.90	0.53	0.47	0.14	0.25	0.06	Unknown protein	
slr0082	1.56	0.98	2.24	1.27	1.83	0.50	0.34	0.04	-0.24	1.08	Hypothetical protein; ribosomal protein S12; methylthiotransferase	
slr0144	0.55	1.79	1.67	0.68	0.50	-0.31	0.50	-0.61	0.08	-0.19	Hypothetical protein; L-myo -inositol 1-phosphate synthase	
slr0179	1.07	1.57	1.82	1.05	0.88	-0.26	0.34	-0.31	0.12	-0.25	Hypothetical protein	
slr0364	1.93	2.07	2.41	1.43	1.25	-0.63	-0.68	-0.44	-0.54	0.99	Hypothetical protein	
slr0366	1.66	1.96	1.95	1.21	1.01	-0.77	-0.66	-0.42	-0.63	1.08	Unknown protein	
slr0373	4.40	5.37	4.97	4.28	2.52	0.24	1.25	0.04	0.66	-0.21	Hypothetical protein; part of operon *slr0373-slr0374-slr0376*	Singh and Sherman 2002
slr0374	4.11	5.01	4.56	3.85	2.34	0.30	1.17	0.22	0.62	0.03	Hypothetical protein; cell division cycle protein; part of operon *slr0373-slr0364-slr0376*	Singh and Sherman 2002
slr0376	3.36	4.57	5.04	3.81	3.09	0.63	1.66	0.50	0.95	-0.03	Hypothetical protein; part of operon *slr0373-slr0374-slr0376*	Singh and Sherman 2002
slr0404	0.85	1.50	1.20	1.26	0.84	-0.04	0.15	0.12	0.21	0.27	Hypothetical protein	
slr0442	2.19	1.99	2.64	0.88	1.00	0.35	1.10	-0.23	0.43	0.88	Unknown protein	
slr0443	-1.09	-1.46	-1.09	-1.04	-0.35	-0.03	-0.43	0.10	-0.07	-0.65	Hypothetical protein	

slr0587	0.82	2.54	2.02	1.79	1.19	-0.49	-0.30	-0.43	-0.20	-0.04	Unknown protein
slr0607	-1.11	-1.58	-1.76	-1.47	-1.03	-0.12	-0.59	-0.09	0.07	-0.31	Hypothetical protein
slr0888	0.26	2.00	2.37	1.75	1.04	-0.62	0.83	-1.08	-0.26	-0.06	Hypothetical protein
slr1152	0.49	2.08	2.41	1.08	1.18	-0.54	0.32	-0.68	-0.28	-0.51	Hypothetical protein
slr1436	-1.29	-1.93	-1.19	-1.43	-0.56	-0.28	-0.70	-0.54	-0.22	0.39	Unknown protein
slr1583	0.96	1.89	1.73	0.77	0.93	-0.12	0.08	-0.43	0.00	-0.34	Hypothetical protein
slr1634	2.02	2.97	3.23	3.29	2.20	-0.10	1.11	-0.74	0.13	-0.77	Hypothetical protein
slr1674	1.40	1.81	1.90	0.53	1.11	0.18	0.38	0.54	0.39	-0.24	Hypothetical protein
slr1770	1.21	2.03	1.88	1.76	0.99	0.23	0.72	-0.04	0.18	-0.35	Hypothetical protein
slr1851	1.45	2.68	3.04	1.23	1.63	-0.18	0.15	-0.49	-0.05	0.03	Hypothetical protein
slr1852	-0.28	-0.33	-0.80	-1.46	-1.15	0.14	0.15	0.00	0.06	-0.28	Unknown protein
slr1917	1.41	1.96	1.52	0.96	0.78	-0.03	0.35	-0.18	0.25	0.36	Hypothetical protein
slr1957	0.77	1.73	1.85	1.04	0.64	-0.39	0.55	-0.99	-0.43	-0.32	Hypothetical protein
slr1958	0.41	0.88	1.58	0.89	0.76	-0.13	0.51	-0.32	-0.21	-0.07	Unknown protein
ssl1263	1.23	2.05	1.91	1.74	1.12	0.09	0.37	-0.05	0.25	-0.77	Unknown protein
ssl1533	1.05	1.44	0.84	0.25	0.35	0.02	0.44	-0.32	0.22	-0.08	Unknown protein
ssl1762	1.63	2.26	1.92	1.15	0.74	0.18	0.45	0.03	0.13	-0.31	Hypothetical protein
ssl2874	-0.68	-1.07	-1.45	-1.54	-0.94	0.11	-0.80	0.25	-0.23	-0.21	Hypothetical protein
ssr0692	1.18	1.71	2.02	1.25	1.30	-0.32	-0.35	-0.61	-0.15	-0.35	Hypothetical protein
ssr1038	0.65	1.83	1.66	1.94	1.41	-0.16	-0.30	-0.75	-0.63	-0.86	Unknown protein
ssr1375	0.70	1.58	1.03	0.01	0.20	0.09	0.18	-0.06	0.08	-0.90	Hypothetical protein
ssr1562	1.09	2.03	1.76	1.11	0.89	-0.29	-0.08	-0.71	-0.29	-0.54	Hypothetical protein
ssr1853	-0.79	-1.25	-1.51	-0.98	-0.63	-0.17	-0.48	0.46	0.11	-0.18	Unknown protein
ssr2153	0.58	1.43	2.64	2.88	1.23	-0.30	0.66	0.67	0.18	-1.22	Unknown protein
ssr2848	1.12	1.50	1.46	1.22	0.60	0.25	-0.01	0.09	0.00	0.16	Unknown protein
ssr3129	1.20	2.08	2.38	0.63	0.89	-0.17	0.21	-0.32	-0.01	-0.04	Unknown protein

[1]Marteyn B, Domain F, Legrain P, Chauvat F, Cassier-Chauvat C (2009) The thioredoxin reductase-glutaredoxins-ferredoxin crossroad pathway for selenate tolerance in *Synechocystis* PCC6803. Mol Microbiol 71:520-532

[2]García-Domínguez M, Reyes JC, Florencio FJ (1999) Glutamine synthetase inactivation by protein-protein interaction. Proc Natl Acad Sci USA 96:7161-7166

Chapter 5

Changes in water color shift competition between phytoplankton species with contrasting light-harvesting strategies

Veerle M. Luimstra[1,2], Jolanda M. H. Verspagen[1], Tianshuo Xu[1], J. Merijn Schuurmans[1], Jef Huisman[1*]

[1]Department of Freshwater and Marine Ecology, Institute for Biodiversity and Ecosystem Dynamics, University of Amsterdam, Amsterdam, The Netherlands
[2]Wetsus, European Centre of Excellence for Sustainable Water Technology, Leeuwarden, The Netherlands

This chapter is published in:
Ecology 101:e02951 (2020)

Abstract

The color of many lakes and seas is changing, which is likely to affect the species composition of freshwater and marine phytoplankton communities. For example, cyanobacteria with phycobilisomes as light-harvesting antennae can effectively utilize green or orange-red light. However, recent studies show that they use blue light much less efficiently than phytoplankton species with chlorophyll-based light-harvesting complexes, even though both phytoplankton groups may absorb blue light to a similar extent. Can we advance ecological theory to predict how these differences in light-harvesting strategy affect competition between phytoplankton species? Here, we develop a new resource competition model in which the absorption and utilization efficiency of different colors of light are varied independently. The model was parameterized using monoculture experiments with a freshwater cyanobacterium and green alga, as representatives of phytoplankton with phycobilisome-based versus chlorophyll-based light-harvesting antennae. The parameterized model was subsequently tested in a series of competition experiments. In agreement with the model predictions, the green alga won the competition in blue light whereas the cyanobacterium won in red light, irrespective of the initial relative abundances of the species. These results are in line with observed changes in phytoplankton community structure in response to lake brownification. Similarly, in marine waters, the model predicts dominance of *Prochlorococcus* with chlorophyll-based light-harvesting complexes in blue light but dominance of *Synechococcus* with phycobilisomes in green light, with a broad range of coexistence in between. These predictions agree well with the known biogeographical distributions of these two highly abundant marine taxa. Our results offer a novel trait-based approach to understand and predict competition between phytoplankton species with different photosynthetic pigments and light-harvesting strategies.

Introduction

Phytoplankton provide the base of the food web in freshwater and marine ecosystems (Sterner and Elser 2002; Falkowski 2012), and their photosynthetic activity is responsible for almost 50% of the global primary production (Field et al. 1998). The color of lakes and seas is changing, however (Roulet and Moore 2006; Kritzberg 2017; Dutkiewicz et al. 2019). In temperate and boreal regions, for instance, many clear blue lakes have changed into turbid waters due to both increasing eutrophication and an

enhanced influx of organic matter (i.e., the "greening" and "browning" of lakes; Leech et al. 2018). It is likely that phytoplankton communities will be affected by these changes in the underwater light spectrum, as they consist of a taxonomically diverse set of species that deploy different photosynthetic pigments and light-harvesting strategies (Ting et al. 2002; Kirk 2011; Croce and van Amerongen 2014). Can we use ecological theory to predict which light-harvesting strategies will be favored in which environments?

All phytoplankton species use the ubiquitous pigment chlorophyll *a*, which absorbs both blue and red light (Kirk 2011). In addition, most cyanobacteria and red algae possess large light-harvesting antennae known as phycobilisomes (PBS) (Fig. 1a). PBS contain phycobili-pigments absorbing cyan, green or orange-red light, and transfer the absorbed light energy to the photosystems (Tandeau de Marsac 2003; Six et al. 2007; Watanabe and Ikeuchi 2013). Cyanobacteria allocate most of their chlorophyll *a* to photosystem I (PSI), whereas PBS are mostly coupled to photosystem II (PSII) (e.g., Myers et al. 1980; Luimstra et al. 2018). It has been hypothesized that PBS can dynamically move back and forth between PSII and PSI by state transitions (Mullineaux et al. 1997; van Thor et al. 1998), but recent research does not fully support this hypothesis (Chukhutsina et al. 2015; Ranjbar Choubeh et al. 2018; Calzadilla et al. 2019). By contrast, the cyanobacterium *Prochlorococcus*, green algae and many other eukaryotic phytoplankton (e.g., diatoms, coccolithophores, dinoflagellates) lack PBS, but contain light-harvesting complexes consisting of chlorophylls and carotenoids that can effectively transfer light energy to both photosystems (Chisholm et al. 1992; Natali and Croce 2015; Nawrocki et al. 2016) (Fig. 1b). Hence, we can distinguish between PBS-based and chlorophyll-based light harvesting antennae, each with their own distinct photosynthetic pigments and light absorption spectra (Fig. 1c).

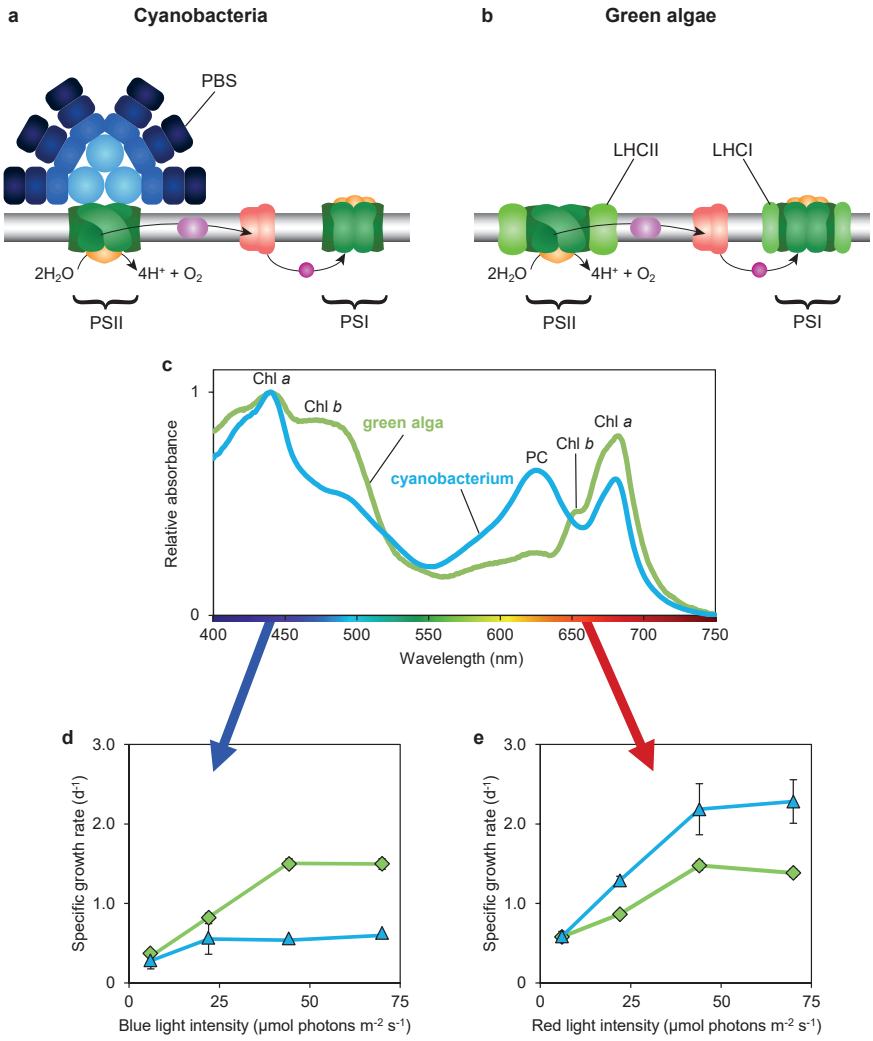

Fig. 1 | Light-harvesting strategies of cyanobacteria and green algae. Cyanobacteria and green algae both contain two photosystems (PSI and PSII). (a) Most cyanobacteria use phycobilisomes (PBS) as light-harvesting antennae, which transfer their absorbed light energy mostly to PSII. (b) Green algae and higher plants use chlorophyll-based light-harvesting complexes (LHCI and LHCII), which serve as light-harvesting antennae for both photosystems. (c) Absorption spectra of a green alga (*Chlorella sorokiniana* 211-8K) and a cyanobacterium (*Synechocystis* sp. PCC 6803). The spectrum of the green alga shows absorption peaks of Chl *a* (440 and 678 nm) and Chl *b* (480 and 650 nm), whereas the cyanobacterium shows absorption peaks of Chl *a* and of the phycobili-pigment phycocyanobilin (PC, at 625 nm). Both species also contain carotenoids, which absorb photons in the 400–500 nm range.(d) The green alga *Chlorella* (green diamonds) has higher specific growth rates in blue light, whereas (e) the cyanobacterium *Synechocystis* (blue triangles) has higher specific growth rates in red light. Data in panels d and e are averages of three biological replicates ± SD, from experiments of Luimstra et al. (2018).

Interestingly, the two contrasting light-harvesting strategies lead to different photosynthetic efficiencies in blue light. In essence, PBS pigments do not absorb blue light < 450 nm (Tandeau de Marsac 2003; Six et al. 2007), and therefore cannot transfer the energy of blue light to PSII. Chlorophylls and carotenoids do absorb blue light. However, PBS-containing cyanobacteria invest most of their chlorophyll *a* in PSI. Moreover, in cyanobacteria, only carotenoids of PSI appear to be involved in light harvesting, whereas carotenoids of PSII are involved in heat dissipation (Stamatakis et al. 2014). This yields an imbalance between the two photosystems, with a shortage of excitation energy at PSII and hence a low photosynthetic efficiency of PBS-containing cyanobacteria in blue light (Pulich and van Baalen 1974; Solhaug et al. 2014; Luimstra et al. 2018, 2019) (Fig. 1d). By contrast, chlorophyll-based light-harvesting complexes do absorb blue light and can distribute the absorbed light energy over both photosystems, which gives green algae and *Prochlorococcus* a higher photosynthetic efficiency in blue light than PBS-containing cyanobacteria (Nawrocki et al. 2016; Luimstra et al. 2018) (Fig. 1d). These differences in photosynthetic efficiency suggest that species with chlorophyll-based light-harvesting antennae will have a competitive advantage in blue light.

Resource competition theory can predict the outcome of competition for nutrients and light between photosynthetic organisms (Tilman 1977; Grover 1997; Passarge et al. 2006; Jäger and Diehl 2014; Burson et al. 2018). At first, competition models treated light as a single resource (Huisman and Weissing 1994, 1995). In this case, theory predicts that the species with lowest critical light intensity is the superior competitor for light, and will competitively displace all other species (Huisman et al. 1999; Passarge et al. 2006). In reality, however, light is not a single resource but offers a spectrum of resources. Phytoplankton species exploit this environmental variation by employing different photosynthetic pigments that absorb different colors of light. Therefore, the earlier competition models were extended by incorporation of the full spectrum of light (Stomp et al. 2004, 2007b). These spectral models predict stable coexistence of species if they absorb different parts of the light spectrum, a theoretical prediction that has been verified by both laboratory competition experiments and field data (Stomp et al. 2004, 2007b; Burson et al. 2019).

The observation that PBS-containing cyanobacteria absorb blue light but use it less efficiently than other colors of light (Solhaug et al. 2014; Luimstra et al. 2018, 2019) adds a new layer of physiological complexity that has not yet been considered in previous models of competition for light. It can be interpreted as a kind of luxury consumption, in which species

make resources unavailable for other species even though they do not use these resources themselves (de Mazancourt and Schwartz 2012). In principle, luxury consumption can destabilize species coexistence through preemption of limiting resources, which may lead to rapid competitive exclusion and might even promote priority effects where the species that arrives first monopolizes the available resources. These considerations undermine the key assumption of earlier spectral competition models (Stomp et al. 2004, 2007b) that species utilize all absorbed photons with the same photosynthetic efficiency.

Here, we develop a new resource competition model to investigate competition for light between species with different light-harvesting strategies. In this model, contrary to the previous spectral competition models of Stomp et al. (2004, 2007b), resource acquisition (light absorption) and resource use efficiency (photosynthetic efficiency) of different light colors can be varied independently. Model parameters of a freshwater cyanobacterium and a green alga, as representatives of phytoplankton with either PBS-based or chlorophyll-based light-harvesting antennae, were estimated from monoculture experiments in blue and red light. The model predictions were tested in competition experiments between the two species exposed to different combinations of blue and red light. The competition experiments started from different initial conditions to examine possible priority effects resulting from luxury consumption of blue light by the cyanobacterium. To investigate the suitability of this approach for marine ecosystems, we subsequently applied the competition model to the two most abundant marine phytoplankton taxa, *Synechococcus* and *Prochlorococcus*, which also deploy PBS-based versus chlorophyll-based light-harvesting strategies.

The model

Our model considers a well-mixed vertical water column, with a depth that runs from $z = 0$ at the surface to $z = z_m$ at the bottom of the water column. The water column is illuminated from above, with an incident light spectrum $I_{in}(\lambda)$, where λ is wavelength. The underwater light spectrum changes with depth as a result of selective absorption of different wavelengths by phytoplankton, water, dissolved organic matter (gilvin) and suspended particles (tripton).

Let $I(\lambda,z)$ denote light intensity of wavelength λ at depth z. According to Lambert-Beer's law, light intensity decreases exponentially with depth:

$$I(\lambda, z) = I_{\mathrm{in}}(\lambda) \exp\left(-\sum_{i=1}^{n} k_i(\lambda) C_i\, z - K_{\mathrm{bg}}(\lambda) z\right) \quad (1)$$

where $k_i(\lambda)$ is the specific light absorption coefficient of species i as function of wavelength λ (i.e., the *absorption spectrum*) and C_i is the population density of species i. The summation term indicates that light is absorbed by n phytoplankton species in total, each with its own light absorption spectrum, and $K_{bg}(\lambda)$ is the wavelength-dependent background turbidity caused by water, gilvin and tripton. We define $I_{out}(\lambda)$ as the light intensity of wavelength λ that reaches the bottom of the water column, i.e., $I_{out}(\lambda) = I(\lambda,z_m)$.

The model assumes that dynamic changes in the population densities of phytoplankton species are determined by their growth and loss rates. We consider eutrophic waters in which nutrients are available in excess. The growth rates of the species can then be described as the production rates integrated over the light spectrum and averaged over depth:

$$\frac{dC_i}{dt} = \left(\frac{1}{z_{\mathrm{m}}} \iint_{z,\lambda} p_i(\lambda, z)\, d\lambda dz - m_i\right) C_i \quad (2)$$

where $i = 1,\ldots,n$, $p_i(\lambda,z)$ is the specific production rate of species i as function of wavelength λ and depth z, and m_i is the specific mortality rate of species i.

The productivity of a species depends on the number of photons it absorbs and the efficiency at which it uses these absorbed photons for growth. For simplicity, we assume that the specific production rate $p_i(\lambda,z)$ is a linear function of light intensity. This simplification applies to relatively low light intensities, where light does not yet saturate photosynthesis. That is,

$$p_i(\lambda, z) = \phi_i(\lambda) k_i(\lambda) I(\lambda, z) \quad (3)$$

where the product $k_i(\lambda)I(\lambda,z)$ describes the number of photons of wavelength λ at depth z absorbed by species i, and $\phi_i(\lambda)$ is the efficiency at which absorbed photons of wavelength λ are converted into biomass production (i.e., the *photosynthetic efficiency*). The product $\phi_i(\lambda)k_i(\lambda)$ of the photosynthetic efficiency and absorption spectrum of a species

is known as the *action spectrum* of that species. Cyanobacteria and eukaryotic phytoplankton all absorb both blue and red light. In contrast to most eukaryotic phytoplankton, however, PBS-containing cyanobacteria have a much lower photosynthetic efficiency in blue than in red light.

Inserting Eq.1 and Eq. 3 into Eq. 2, and solving the depth integral, yields

$$\frac{dC_i}{dt} = \left(\int_{400}^{700} \phi_i(\lambda) k_i(\lambda) I_{\text{avg}}(\lambda) d\lambda - m_i \right) C_i \tag{4}$$

where the depth-averaged light intensity of wavelength λ, $I_{\text{avg}}(\lambda)$, is given by

$$I_{\text{avg}}(\lambda) = \frac{1}{z_m} \int_0^{z_m} I(\lambda, z) dz$$

$$= \frac{I_{\text{in}}(\lambda) - I_{\text{out}}(\lambda)}{\ln\left(I_{\text{in}}(\lambda)\right) - \ln\left(I_{\text{out}}(\lambda)\right)} \tag{5}$$

We note that $I_{\text{avg}}(\lambda)$ is monotonically related to $I_{\text{out}}(\lambda)$, i.e., turbid waters with a low depth-averaged light intensity also have a low light transmission through the water column.

In our experiments the underwater light field consisted of a series of distinct colors instead of the full light spectrum. In this case, Eq. 4 simplifies to

$$\frac{dC_i}{dt} = \left(\sum_{j=1}^{k} \phi_{ij} k_{ij} I_{\text{avg},j} - m_i \right) C_i \tag{6}$$

where the production rate is summed over colors $j = 1,\ldots,k$ to obtain the total production of species i.

Materials and Methods

Strains and culture conditions

The PBS-containing cyanobacterium *Synechocystis* sp. PCC 6803, which absorbs orange-red light with the pigment phycocyanobilin, was provided by D. Bhaya (University of Stanford, USA). The green alga *Chlorella sorokiniana* 211-8K, which employs chlorophyll-containing light-harvesting complexes, was obtained from the SAG culture collection (Göttingen, Germany). All cultures were grown at 30°C in 1.8 L flat-panel chemostats

under light-limited conditions (Huisman et al. 2002), with an optical path length of z_m = 5 cm and dilution rate of D = 0.015 h^{-1}.

The chemostats were provided with a nutrient-rich mineral medium (BG-11 medium; Merck, Darmstadt, Germany) supplemented with 5 mM Na_2CO_3 and mixed by bubbling with CO_2-enriched air (2% v/v) flowing at a rate of 30 L h^{-1}. CO_2 concentration of the gas mixture was monitored with an Environmental Gas Monitor (EGM-4; PP Systems, Amesbury, MA, USA). Light was provided by LED panels (custom made by Philips Lighting BV, Eindhoven, The Netherlands) at a total incident light intensity (I_{in}) of 45 µmol photons m^{-2} s^{-1}.

Experimental design

The population dynamics of *Synechocystis* and *Chlorella* were studied in twelve chemostat experiments, including 4 monoculture experiments and 8 competition experiments. First, we ran monoculture experiments with *Synechocystis* and *Chlorella* in blue LED light (450 nm) and in red LED light (660 nm). Both LED colors had a full width at half maximum of ~20 nm. After the monoculture experiments had reached steady-state, they served as inoculum for the competition experiments. We applied four light treatments in the competition experiments, with only blue light (100% blue), only red light (100% red), and two mixtures of blue and red LEDs (33% blue/67% red and 67% blue/33% red). For each light treatment we ran two competition experiments, one with an initial dominance of *Chlorella* (90% *Chlorella*/10% *Synechocystis*, based on biovolume) and the other with an initial dominance of *Synechocystis* (10% *Chlorella*/90% *Synechocystis*) to test for alternative stable states.

Sampling and measurements

Light intensities transmitted through the chemostats (I_{out}), light absorption spectra and population densities were measured almost daily during the first two weeks and subsequently 2-3 times per week until the end of the experiment. Total I_{out} integrated over 400-700 nm was measured with a LI-250 light meter (LI-COR Biosciences, Lincoln, NE, USA) and I_{out} spectra were recorded using a RAMSES ACC-VIS spectroradiometer (TriOS, Oldenburg, Germany). Light absorption spectra of phytoplankton were measured from 400-750 nm using an updated Aminco DW2000 photospectrometer (OLIS, Bogart, GA, USA), and normalized to maximum absorbance at the chlorophyll *a* peak at 440 nm after subtraction of the minimum absorbance at 750 nm.

A CASY1 TTC cell counter with 60 µm capillary (Schärfe Systems GmbH, Reutlingen, Germany) was used to count cells of the monoculture

experiments and measure their biovolume. To distinguish between cyanobacteria and green alga, cells in the competition experiments were counted using an Accuri C6 flow cytometer (BD Biosciences, San Jose, California, USA) equipped with a blue laser (488 nm) and red laser (640 nm). To obtain biovolumes of the two species in competition, cell counts obtained by flow cytometry were multiplied by cell volumes measured in the monocultures. Because the species differed in size, we expressed their population densities as total biovolume per liter ($mm^3\ L^{-1}$).

Parameter estimation

Model parameters consisted of system parameters and species parameters (Supplementary Table S1). System parameters (incident light intensity I_{in}, optical path length of the chemostat z_m, and dilution rate D) were set experimentally. We assumed that specific mortality rates (m_i) of the species were dominated by the dilution rate (i.e., $m_i = D$). Background turbidities in blue and red light were estimated from light transmission through chemostats filled with mineral medium but without phytoplankton using Lambert-Beer's law. Light absorption coefficients of the species in blue light ($k_{i,blue}$, at 450 nm) and red light ($k_{i,red}$, at 660 nm) were estimated from absorption spectra of the species (Fig. 1c). Photosynthetic efficiencies of the species in blue light ($\Phi_{i,blue}$) and red light ($\Phi_{i,red}$) were estimated by fitting the dynamic model predictions to observed trajectories of population density and blue and red light transmitted through the chemostats during the monoculture experiments, using a least-squares method (Huisman et al. 1999; Passarge et al. 2006).

We also used the model to investigate competition between marine *Synechococcus* and *Prochlorococcus* in blue and green light. For this purpose, system parameters were the same as in the chemostat experiments, light absorption coefficients in blue light ($k_{i,blue}$, at 450 nm) and green light ($k_{i,green}$, at 550 nm) were estimated from measured absorption spectra of *Synechococcus* and *Prochlorococcus*. The absorption spectrum of *Prochlorococcus* was obtained from a field sample of the deep chlorophyll maximum at station ALOHA, north of the island of Oahu, Hawaii (collected by M. Stomp, L.J. Stal and J. Huisman). The *Synechococcus* spectrum was of *Synechococcus* strain WH7803 (kindly provided by dr. L. Garczarek). Photosynthetic efficiencies in blue and green light of *Synechococcus* and *Prochlorococcus* were assumed to be similar to those in blue and red light of *Synechocystis* and *Chlorella*, respectively (Supplementary Table S1).

Results

Model analysis

Competition for a single color - If species compete for a single color of light, the competitive dynamics predicted by the model are straightforward. For each species *i* and color *j*, we can calculate the depth-averaged critical light intensity $I^*_{\mathrm{avg},ij}$ at which this species remains stationary (i.e., at which $dC_i/dt = 0$). According to Eq. 6, this gives:

$$I^*_{\mathrm{avg},ij} = \frac{m_i}{\phi_{ij} k_{ij}} \tag{7}$$

Similar to previous derivations (Huisman and Weissing 1994; Weissing and Huisman 1994), it can be shown that the species with lowest depth-averaged critical light intensity is the superior competitor for this color and will competitively displace all other species.

Competition for two colors of light - Now consider competition between two species, a cyanobacterium and a green alga, competing for blue and red light. The outcome of competition can be represented graphically, in style with previous resource competition models (Tilman 1982). For this purpose, we draw a resource plane with (the depth-average of) blue light along the x-axis and red light along the y-axis (Fig. 2a,b).

The zero isocline of a species is obtained by solving the equilibrium condition $dC_i/dt = 0$ for two colors of light. According to Eq. 6, the zero isocline of the green alga is:

$$I_{\mathrm{avg,red}} = \frac{m_{\mathrm{g}}}{\phi_{\mathrm{g,red}} k_{\mathrm{g,red}}} - \frac{\phi_{\mathrm{g,blue}} k_{\mathrm{g,blue}}}{\phi_{\mathrm{g,red}} k_{\mathrm{g,red}}} I_{\mathrm{avg,blue}} \tag{8a}$$

and that of the cyanobacterium is

$$I_{\mathrm{avg,red}} = \frac{m_{\mathrm{c}}}{\phi_{\mathrm{c,red}} k_{\mathrm{c,red}}} - \frac{\phi_{\mathrm{c,blue}} k_{\mathrm{c,blue}}}{\phi_{\mathrm{c,red}} k_{\mathrm{c,red}}} I_{\mathrm{avg,blue}} \tag{8b}$$

where subscripts *g* and *c* refer to the green alga and cyanobacterium, and subscripts *red* and *blue* refer to red and blue light. The zero isoclines of the two species can be plotted as lines in the resource plane. The slope of the zero isocline of a species corresponds to the ratio $\phi_{i,\mathrm{blue}} k_{i,\mathrm{blue}} / \phi_{i,red} k_{i,red}$. The intercepts of the zero isocline with the x-axis and y-axis correspond to its critical light intensities for blue and red light, respectively (the I^* values in Fig. 2a).

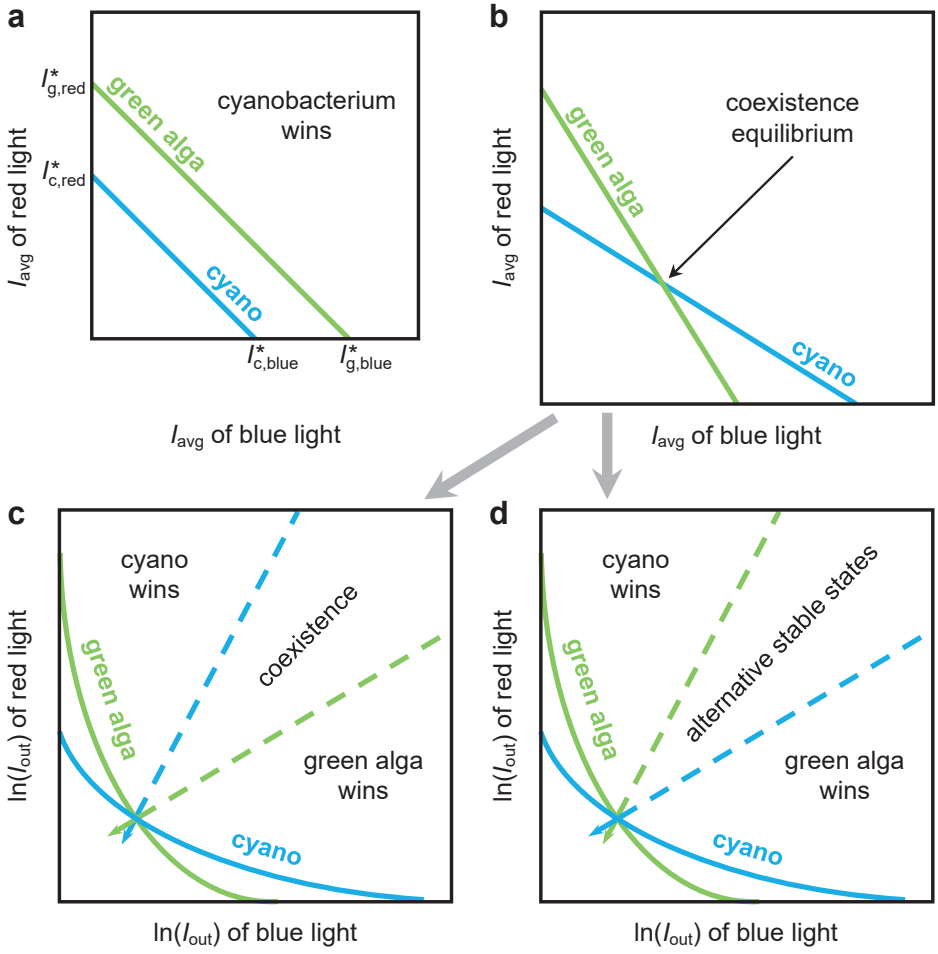

Fig. 2 | Graphical representation of competition for blue and red light between a green alga (green lines) and a cyanobacterium (blue lines). (a) The cyanobacterium is a stronger competitor for both blue and red light than the green alga (i.e., the critical light intensities I^*_{blue} and I^*_{red} are both lower for the cyanobacterium). In this case, the zero isoclines (solid lines) of the species do not intersect and the cyanobacterium always wins. (b) The cyanobacterium is a stronger competitor for red light, whereas the green alga is a stronger competitor for blue light. Intersection of the two zero isoclines indicates a coexistence equilibrium, which may be either stable or unstable. In (c) and (d), the coordinates are transformed to light transmission I_{out} on a logarithmic scale. Coexistence is feasible for all supply points located in the conical region bounded by the two absorption vectors (dashed lines). (c) The coexistence equilibrium is stable if the cyanobacterium has a steeper absorption vector than the green alga. (d) The coexistence equilibrium is unstable if the green alga has a steeper absorption vector than the cyanobacterium; in this case, the system displays alternative stable states where the winner depends on the initial abundances of the species.

Suppose that the cyanobacterium is a better competitor (i.e., has lower critical light intensities) for both blue and red light than the green alga. In this case, the zero isocline of the cyanobacterium is located completely below the zero isocline of the green alga, and the cyanobacterium will win the competition irrespective of the prevailing light color (Fig. 2a).

Now consider a scenario in which the green alga is a better competitor for blue light, whereas the cyanobacterium is a better competitor for red light. The zero isoclines are therefore arranged as in Fig. 2b, where the slope of the zero isocline of the green alga is steeper downwards than that of the cyanobacterium and the two zero isoclines intersect. The intersection point represents a coexistence equilibrium (Fig. 2b). The cyanobacterium and green alga will coexist if this coexistence equilibrium is both feasible and stable.

Feasibility of the coexistence equilibrium - The coexistence equilibrium is feasible if the green alga and cyanobacterium can both sustain a positive population at equilibrium (i.e., if both $C_g > 0$ and $C_c > 0$). According to Lambert-Beer's law, in Eq. 1, light absorption is a linear function of the population densities of the species if light intensities are expressed on a logarithmic scale:

$$\ln\left(I_{\mathrm{out,red}}\right) = \ln\left(I_{\mathrm{in,red}}\right) - K_{\mathrm{bg,red}} z_{\mathrm{m}} - k_{\mathrm{g,red}} z_{\mathrm{m}} C_{\mathrm{g}} - k_{\mathrm{c,red}} z_{\mathrm{m}} C_{\mathrm{c}} \qquad (9a)$$

$$\ln\left(I_{\mathrm{out,blue}}\right) = \ln\left(I_{\mathrm{in,blue}}\right) - K_{\mathrm{bg,blue}} z_{\mathrm{m}} - k_{\mathrm{g,blue}} z_{\mathrm{m}} C_{\mathrm{g}} - k_{\mathrm{c,blue}} z_{\mathrm{m}} C_{\mathrm{c}} \qquad (9b)$$

After some algebra, it follows from Eqs. 9a,b that the coexistence equilibrium is feasible if

$$\frac{k_{\mathrm{c,red}}}{k_{\mathrm{c,blue}}} > \frac{\ln\left(I_{\mathrm{in,red}}\right) - K_{\mathrm{bg,red}} z_{\mathrm{m}} - \ln\left(I^{*}_{\mathrm{out,red}}\right)}{\ln\left(I_{\mathrm{in,blue}}\right) - K_{\mathrm{bg,blue}} z_{\mathrm{m}} - \ln\left(I^{*}_{\mathrm{out,blue}}\right)} > \frac{k_{\mathrm{g,red}}}{k_{\mathrm{g,blue}}} \qquad (10)$$

or if both inequality signs in this equation are reversed. Here, the superscript * indicates that $I_{\mathrm{out,red}}$ and $I_{\mathrm{out,blue}}$ are evaluated at the coexistence equilibrium.

The condition in Eq. 10 can be visualized graphically if the coordinates of the resource plane are transformed logarithmically, from ($I_{\mathrm{avg,blue}}$,$I_{\mathrm{avg,red}}$) to ($\ln(I_{\mathrm{out,blue}})$,$\ln(I_{\mathrm{out,red}})$) (Fig. 2c,d). We note that order is preserved when the coordinates are transformed, since $I_{\mathrm{avg},j}$ is a monotonic function of $\ln(I_{\mathrm{out},j})$. Hence, if zero isoclines intersect in the linear resource plane, then they intersect in the logarithmic resource plane as well. Analogous to Tilman's (1982) consumption vectors, we can draw absorption vectors in this resource plane to describe the relative amounts of blue and red light absorbed by a species (Fig. 2c,d). According to Eqs. 9a,b, the

absorption vector of the green alga has a slope $k_{g,red}/k_{g,blue}$ and that of the cyanobacterium has a slope $k_{c,red}/k_{c,blue}$ Furthermore, we can plot a supply point in the resource plane, with coordinates $\ln(I_{out,blue}) = \ln(I_{in,blue}) - K_{bg,blue} z_m$ and $\ln(I_{out,red}) = \ln(I_{in,red}) - K_{bg,red} z_m$. The supply point describes transmission of blue and red light through the water column prior to phytoplankton growth.

In Fig. 2c and 2d, we have drawn two dashed lines spreading out from the coexistence equilibrium, with slopes given by the absorption vectors of the green alga ($k_{g,red}/k_{g,blue}$) and cyanobacterium ($k_{c,red}/k_{c,blue}$), respectively. According to Eq. 10, the coexistence equilibrium is feasible for all supply points that fall in the conical region bounded by these two dashed lines. The cyanobacterium (the best competitor for red light) wins for all supply points above this region, whereas the green alga (the best competitor for blue light) wins for all supply points below this region (Fig. 2c,d).

Stability of the coexistence equilibrium - Whether species will coexist for supply points within the conical region of Fig. 2c and 2d depends on the stability of the coexistence equilibrium. Previous models assumed that the photosynthetic efficiency of a species is independent of wavelength (Stomp et al. 2004, 2007b). In this case, the coexistence equilibrium is always stable (Appendix S1: Section 1).

If photosynthetic efficiency varies with wavelength, stability of the coexistence equilibrium is not guaranteed. Recall that we assume that chlorophyll-based green algae are better competitors for blue light and PBS-based cyanobacteria for red light. In this case, the coexistence equilibrium is locally stable if the cyanobacterium absorbs relatively more red than blue light in comparison to the green alga (Appendix S1: Eq. S12):

$$\frac{k_{c,red}}{k_{c,blue}} > \frac{k_{g,red}}{k_{g,blue}} \qquad (11)$$

whereas the coexistence equilibrium is unstable if this inequality is reversed.

Graphically, this implies that stability depends on the slopes of the absorption vectors of the cyanobacterium ($k_{c,red}/k_{c,blue}$) and green alga ($k_{g,red}/k_{g,blue}$). If the absorption vector of the cyanobacterium is steeper than that of the green alga, the coexistence equilibrium is stable. In this case, the model predicts that the cyanobacterium and green algae will stably coexist (Fig. 2c). Conversely, if the absorption vector of the cyanobacterium is less steep than that of the green alga, the coexistence equilibrium is unstable. In this case, the model predicts two alternative

stable states, where either the green alga or the cyanobacterium wins depending on the initial abundances of the species (Fig. 2d).

Monoculture experiments

In blue light, the monoculture of the green alga *Chlorella* increased its biomass and reached steady state after ~9 days (Fig. 3a). The green alga absorbed all incident blue light, such that light transmission I_{out} through the monoculture was depleted to < 0.5 µmol photons m^{-2} s^{-1} (Fig. 3a). In red light, the *Chlorella* monoculture reached a slightly higher biomass at steady state, and also depleted light transmission I_{out} through the monoculture to < 0.5 µmol photons m^{-2} s^{-1} (Fig. 3b).

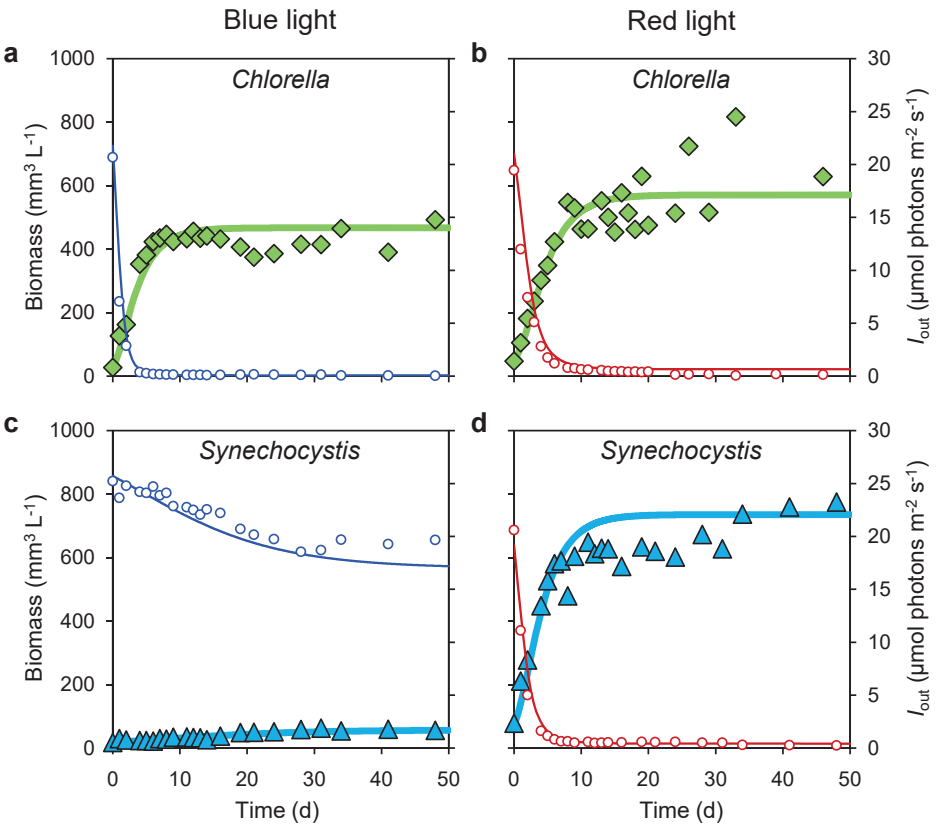

Fig. 3 | Monoculture experiments. The monocultures are of the green alga *Chlorella* (green diamonds) in blue light (a) and red light (b), and of the cyanobacterium *Synechocystis* (blue triangles) in blue light (c) and red light (d). Small open circles represent light transmission (I_{out}) of blue and red light, respectively, through the monocultures. Solid lines represent model fits. Parameter values of the model are listed in Supplementary Table S1.

In blue light, the monoculture of the PBS-containing cyanobacterium *Synechocystis* increased slowly and approached steady-state only towards the end of the experiment (after 30 days) (Fig. 3c). At steady state, the biomass of *Synechocystis* was almost 10 times lower than that of the green alga *Chlorella* in blue light, and light transmission I_{out} through the monoculture remained high at ~20 µmol photons m^{-2} s^{-1} (Fig. 3c). By contrast, in red light, the cyanobacterium *Synechocystis* increased to steady state in 10 days, produced a higher biomass in monoculture than the green alga *Chlorella*, and depleted light transmission I_{out} to < 0.5 µmol photons m^{-2} s^{-1} (Fig. 3d).

Comparison of the data and model results shows that the model generally fitted well to the monoculture experiments. Parameter estimates obtained from the monoculture experiments (Supplementary Table S1) were used to predict the dynamics and outcome of the competition experiments.

According to our model, the species with the lowest critical light intensity for a particular color is predicted to be the best competitor for that color. The depth-averaged critical light intensities were calculated from Eq. 7, using the parameter estimates obtained from the monocultures. In blue light, the critical light intensity was much lower for *Chlorella* than for *Synechocystis* (7.0 versus 28.8 µmol photons m^{-2} s^{-1}; see Supplementary Table S2). Conversely, in red light, the critical light intensity was lower for *Synechocystis* than for *Chlorella* (9.5 versus 10.4 µmol photons m^{-2} s^{-1}; see Supplementary Table S2). *Chlorella* is therefore predicted to win the competition in blue light, whereas *Synechocystis* is predicted to win in red light.

Competition experiments

Competition between the green alga *Chlorella* and cyanobacterium *Synechocystis* was studied at four combinations of blue and red light (Fig. 4). For each combination, we ran two experiments that differed in initial relative abundances of the two species. In blue light, *Chlorella* competitively displaced *Synechocystis* regardless of their initial relative abundances (Fig. 4a,b).

Chlorella was also the final winner in the experiments with 67% blue and 33% red light (Fig. 4c,d) and 33% blue and 67% red light (Fig. 4e,f). Interestingly, when *Synechocystis* represented 90% of the initial biomass, *Synechocystis* increased in biomass during the first week before it was competitively excluded by *Chlorella* (Fig. 4d,f). Furthermore, *Synechocystis* persisted longer in the experiments with 33% blue and 67% red light than in the experiments with 67% blue and 33% red light (compare Fig. 4d and Fig. 4f).

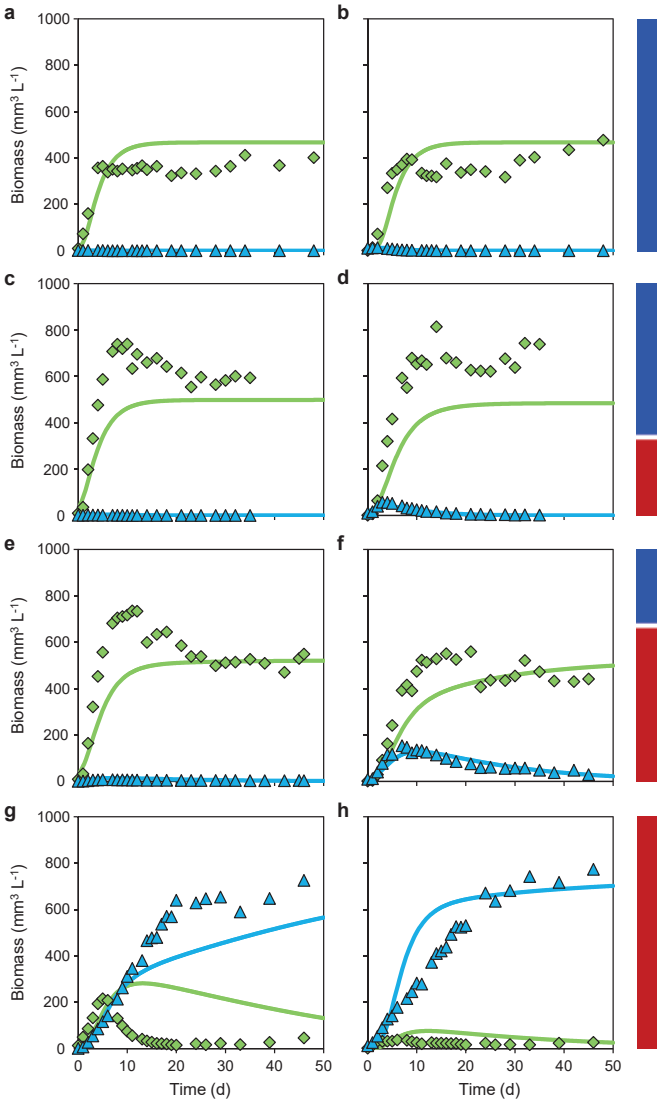

Fig. 4 | Competition experiments between the cyanobacterium *Synechocystis* (blue triangles) and the green alga *Chlorella* (green diamonds). The experiments were exposed to four different mixtures of red and blue light, as indicated by bars at the right-hand side, with the same total light intensity. 100% blue light (a,b), 67% blue light and 33% red light (c,d), 33% blue light and 67% red light (e,f), and 100% red light (g,h). The experiments were inoculated with two different initial relative abundances of the species, as indicated by bars at the top. Panels a, c, e and g were inoculated with 90% *Chlorella* and 10% *Synechocystis* (based on biovolume); panels b, d, f and h were inoculated with 10% *Chlorella* and 90% *Synechocystis*. Solid lines represent model predictions based on parameters estimated from the monoculture experiments (see Supplementary Table S1 for parameter values). Light transmission (I_{out}) data are presented in Supplementary Fig. S1.

In red light, *Synechocystis* was the final winner regardless of the initial conditions (Fig. 4g,h). However, when *Chlorella* dominated the initial biomass, it increased substantially during the first week before it was competitively excluded by *Synechocystis* (Fig. 4g).

The model predictions correctly predicted the winner of competition in all experiments, and also captured the competitive dynamics (Fig. 4a-h) and light transmission (Supplementary Fig. S1) quite well. Only in the red light experiment with 90% *Chlorella*/10% *Synechocystis*, competitive exclusion of *Chlorella* clearly occurred faster than predicted by the model (Fig. 4g). In all competition experiments, the incident light was fully absorbed by the cultures, i.e., light transmission I_{out} was depleted to < 1 µmol photons m^{-2} s^{-1} for both blue and red light (Supplementary Fig. S1).

Summarizing, we find a color-dependent reversal in species dominance (Fig. 5). In line with the experimental data, the model predicts dominance of the green alga when blue light represents a substantial portion of the underwater light spectrum, a narrow region of species coexistence, and dominance of the cyanobacterium if red light prevails while blue light constitutes less than 10% of the underwater light spectrum (Fig. 5).

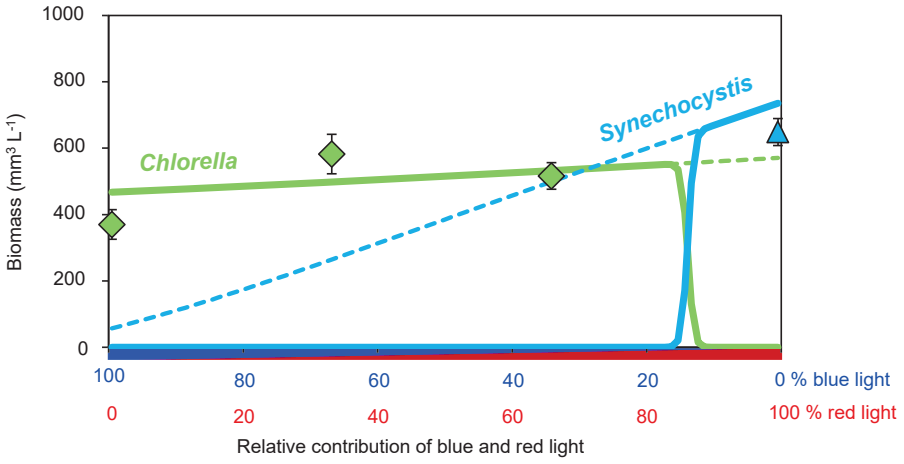

Fig. 5 | Steady-state outcomes of the competition experiments. Solid lines show the outcome of the competition experiments between the cyanobacterium *Synechocystis* (blue line) and the green alga *Chlorella* (green line) predicted by the model, as function of the relative contribution of red and blue light. Dashed lines indicate the steady-state biomass predicted in monoculture. Symbols show the observed steady-state biomass of *Synechocystis* (blue triangle) and *Chlorella* (green diamonds) in the competition experiments. This steady-state biomass was calculated as the average biomass ± SD of the last six datapoints in each pair of experiments (i.e., n = 12) in Fig. 4. Parameter values of the model are listed in Supplementary Table S1.

Application to marine *Prochlorococcus* and *Synechococcus*

Our resource competition model can be used to predict competition for light between the marine cyanobacteria *Synechococcus* and *Prochlorococcus* (Fig. 6). Blue and green wavelengths are the dominant light colors in most marine waters. *Prochlorococcus* is the numerically most abundant phytoplankton genus on our planet, and the ubiquitous *Synechococcus* is likely to rank second (Flombaum et al. 2013). Similar to freshwater *Synechocystis*, marine *Synechococcus* use PBS and, hence, have a low photosynthetic efficiency in blue light ≤ 450 nm (Luimstra et al. 2018). However, instead of the pigment phycocyanobilin, marine *Synechococcus* mostly use phycourobilin (PUB) and phycoerythrobilin (PEB) which absorb cyan (495 nm) and green light (545 nm), respectively (Six et al. 2007; Fig. 6a). *Prochlorococcus* lacks PBS but uses light-harvesting antennae composed of divinyl Chl *a* and *b*, which absorb blue and red wavelengths quite similar to green algae (Chisholm et al. 1992, Ting et al. 2002) (Fig. 6a).

We assessed competitive interactions between *Prochlorococcus* and *Synechococcus* using mixtures of blue (450 nm) and green (550 nm) light. The model predicts that *Prochlorococcus* wins in blue light whereas *Synechococcus* wins in green light, with an intermediate region of stable species coexistence when both blue and green light are available (Fig. 6b).

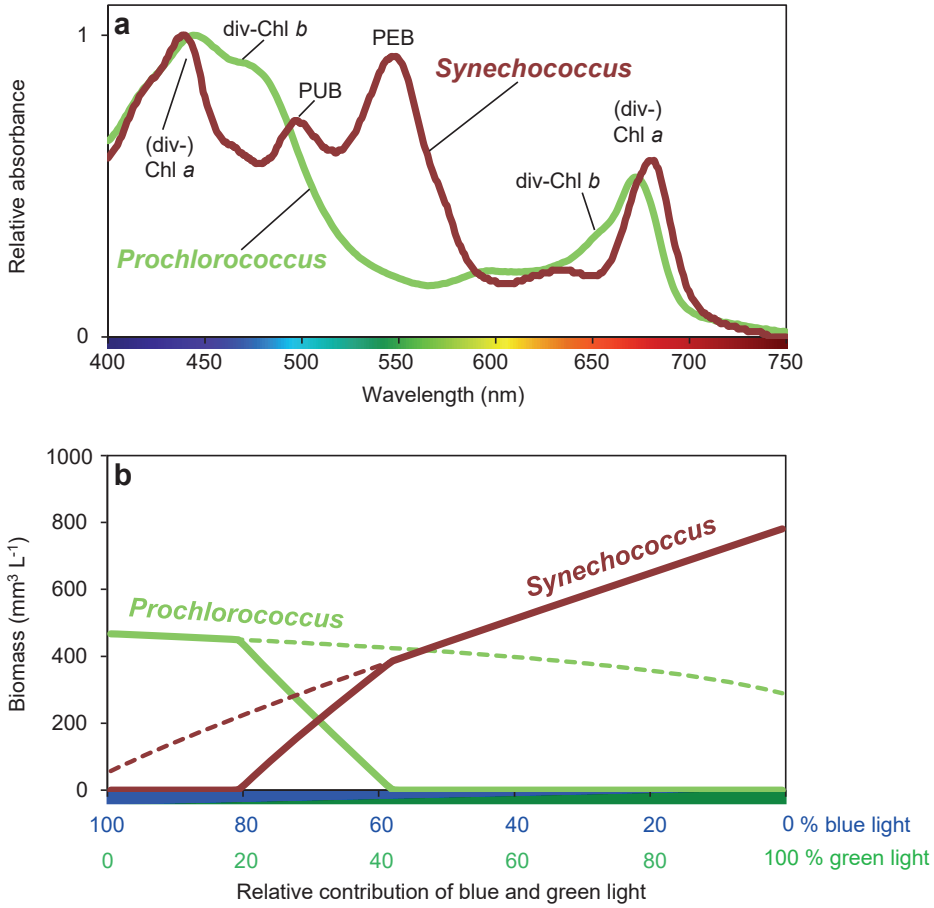

Fig. 6 | Competition between the marine cyanobacteria *Prochlorococcus* and *Synechococcus*. (a) Absorption spectra of *Prochlorococcus* and *Synechococcus*. The spectrum of *Prochlorococcus* shows absorption peaks of divinyl-Chl *a* (440 and 675 nm) and divinyl-Chl *b* (470 and 650 nm), whereas *Synechococcus* shows absorption peaks of Chl *a*, phycourobilin (PUB, at 495 nm) and phycoerythrobilin (PEB, at 545 nm). (b) Model predictions of competition between *Synechococcus* (red line) and *Prochlorococcus* (green line), as function of the relative contribution of blue (450 nm) and green (550 nm) light. Solid lines show the outcome of competition; dashed lines indicate the steady-state biomass in monoculture. The spectrum of *Prochlorococcus* was obtained from a field sample of the deep chlorophyll maximum at station ALOHA, north of the island of Oahu, Hawaii, collected by M. Stomp, L.J. Stal and J. Huisman. The spectrum of *Synechococcus* WH7803 was kindly provided by dr. L. Garczarek.

Discussion

Comparison of theoretical and experimental results

Our results show that light color has a major effect on the outcome of competition between phytoplankton species. According to the monoculture experiments, the PBS-containing cyanobacterium *Synechocystis* sp. PCC 6803 had a lower critical light intensity in red light, whereas the green alga *Chlorella* deploying a chlorophyll-based light-harvesting strategy had a lower critical light intensity in blue light. Hence, the zero isoclines of the two species will intersect (as in Fig. 2b-d). The green alga is therefore predicted to be a superior competitor for blue light, whereas the PBS-containing cyanobacterium is predicted to be a superior competitor for red light. This prediction is confirmed by our competition experiments, where *Chlorella* won in 100% blue light (Fig. 4a,b) and *Synechocystis* won in 100% red light (Fig. 4g,h).

The model predicts that, if the zero isoclines intersect, competition for mixtures of red and blue light may lead to either stable coexistence (Fig. 2c) or alternative stable states (Fig. 2d) depending on the absorption coefficients of the species. In our study, the better competitor for red light (*Synechocystis*) absorbed relatively more red than blue light (i.e., it had a high k_{red}/k_{blue} ratio; see Supplementary Table S1) than the better competitor for blue light (*Chlorella*). Hence, the stability criterion in Eq. 11 is met and the model predicts stable coexistence rather than alternative stable states. To verify this prediction, each competition experiment was performed with two different initial conditions (90% *Chlorella*/10% *Synechocystis* or 10% *Chlorella*/90% *Synechocystis*). In each set of experiments, the final winner was the same regardless of the initial abundances of the species (Fig. 4). Hence, in agreement with the model predictions, luxury consumption of blue light by the PBS-containing cyanobacterium did not lead to alternative stable states in our experiments.

Yet, stable coexistence of the two species was not observed in any of our competition experiments (Fig. 4). Why not? Previous competition studies showed that species with different photosynthetic pigments can coexist in white light (Stomp et al. 2004, 2007b; Burson et al. 2019). One might therefore expect ample opportunities for species coexistence when cyanobacteria and green algae compete for different colors of light. However, our model predictions indicate that coexistence between *Chlorella* and *Synechocystis* is possible only in a very narrow range of blue and red light (Fig. 5). The underlying reason is that *Chlorella* and *Synechocystis* absorb both blue light of 450 nm and red light of 660 nm to a similar extent (Fig. 1c; Supplementary Table S1). As a consequence,

the slopes of their absorption vectors are very similar (k_{red}/k_{blue} = 0.51 and 0.55, respectively) and, therefore, the parameter region with stable coexistence of *Chlorella* and *Synechocystis* is very narrow (Fig. 5).

The model predicts a broader range of coexistence if the absorption coefficients of the competing species are more divergent. This is nicely illustrated by the model predictions for marine *Prochlorococcus* and *Synechococcus* competing for blue and green light (Fig. 6). According to their absorption spectra, *Synechococcus* absorbs more strongly in the green and hence has a much steeper absorption vector (k_{green}/k_{blue} = 0.96) than *Prochlorococcus* (k_{green}/k_{blue} = 0.20) (Supplementary Table S1). This divergence in absorption properties enables stable coexistence of the two species in a relatively broad intermediate region where both blue and green light are available (Fig. 6b).

Underlying physiological traits

The experiments showed that the PBS-containing cyanobacterium *Synechocystis* was the superior competitor in red light. According to the model, the competitive ability of a species for a specific light color depends on the product of its photosynthetic efficiency and light absorption coefficient for that color (see Eq. 7). In this case, the green alga *Chlorella* had a slightly higher absorption coefficient in red light than *Synechocystis*, yet the cyanobacterium *Synechocystis* was a stronger competitor because it used the absorbed red light with a distinctly higher photosynthetic efficiency (Supplementary Table S1). The difference in photosynthetic efficiency might be size related, as *Synechocystis* is markedly smaller than *Chlorella* (Supplementary Table S2). Small cells are often considered to be strong competitors for nutrients and light (Grover 1989; Litchman et al. 2010; Marañón 2015; Burson et al. 2018). For instance, small cells are less affected by the 'package effect', i.e., the self-shading of photosynthetic pigments packaged within a cell (e.g., Kirk 2011), which results in a higher light use efficiency for smaller cells (Finkel 2001; Fujiki and Taguchi 2002; Key et al. 2010; Schwaderer et al. 2011). The higher photosynthetic efficiency of *Synechocystis* might also be related to structural differences in cellular organization between prokaryotic cyanobacteria and eukaryotic algae. In cyanobacteria the thylakoid membrane, in which the photosynthetic pigments are embedded, stretches out along the cell membrane and hence can readily absorb photons transmitted through the cell membrane (Nierzwicki-Bauer et al. 1983; Rast et al. 2015). By contrast, in eukaryotic algae the thylakoid membrane is contained in separate organelles, the chloroplasts. The eukaryotic cell wall and extra membrane layers of the chloroplast

may provide additional light-attenuating barriers before photons reach the photosynthetic pigments (Schwaderer et al. 2011). Furthermore, eukaryotic algae will have additional costs to produce and maintain their chloroplasts and other organelles, while cyanobacteria tend to have lower maintenance requirements (van Liere and Mur 1979).

Conversely, the green alga *Chlorella* was the superior competitor in blue light. Our model results show that this reversal in competitive dominance is a consequence of the much lower photosynthetic efficiency in blue light of *Synechocystis* (Supplementary Table S1). If, in our model, we assumed that *Synechocystis* had the same high photosynthetic efficiency in blue light as in red light, then application of Eq. 7 shows that the critical light intensities would have been lower for *Synechocystis* than for *Chlorella* in both blue and red light. In graphical terms, the zero isocline of *Synechocystis* would be located below the zero isocline of the green alga (Fig. 2a), and hence the cyanobacterium *Synechocystis* would have won the competition from *Chlorella* in both light colors. That was not the case, however, because PBS-containing cyanobacteria use blue light very inefficiently. This is commonly attributed to the low absorbance of blue light ≤ 450 nm by the PBS, which leads to an excitation imbalance between the photosystems PSI and PSII (Solhaug et al. 2014; Luimstra et al. 2018, 2019) (Fig. 1).

Implications for natural phytoplankton communities

5

Our model predicts that phytoplankton species that use chlorophyll-based light-harvesting antennae (e.g., green algae, diatoms, the cyanobacterium *Prochlorococcus*) are superior competitors in blue waters. Conversely, phytoplankton species that use PBS as light-harvesting antennae (many cyanobacteria, and also red algae and glaucophytes) will be favored in green and orange-red light environments. To what extent can these new insights aid in understanding and predicting the taxonomic composition of natural phytoplankton communities?

In recent years, dissolved organic carbon (DOC) concentrations have increased in temperate, boreal and arctic lakes across the northern hemisphere, which has been attributed to changes in land use, acid deposition and climate change (Monteith et al. 2007; Larsen et al. 2011; Weyhenmeyer et al. 2016; Kritzberg 2017). Light absorption by DOC decays exponentially with wavelength, with strong absorption in the blue and minor absorption in the red part of the spectrum (e.g., Kirk 2011). As a consequence, increasing DOC concentrations shift the underwater light color towards longer wavelengths, a phenomenon known as 'browning' or 'brownification' of lakes (Roulet and Moore 2006). Lake browning may

cause major changes in phytoplankton community structure that are consistent with our model predictions. For instance, a recent study of 1000+ lakes sampled across the continental USA showed a substantial decrease in the number of blue lakes and an increase in the number of murky lakes, caused by the simultaneous eutrophication ('greening') and browning of lake waters (Leech et al. 2018). In agreement with our model predictions, cyanobacterial abundance was lowest in blue lakes and highest in green and murky lakes. Other studies have also shown that lake browning may result in the loss of diatoms and green algae (Urrutia-Cordero et al. 2017), while it tends to favor cyanobacteria (Ekvall et al. 2013; Lebret et al. 2018; Feuchtmayr et al. 2019) and cryptophytes (Deininger et al. 2017; Urrutia-Cordero et al. 2017; Wilken et al. 2018). These patterns are supported by recent competition experiments that, similar to our results, revealed that the common bloom-forming cyanobacterium *Microcystis aeruginosa* lost the competition from a green alga in blue light, but won in orange-red light (Tan et al. 2019). Hence, while eutrophication and global warming are often considered to be the main drivers of the increased intensity, frequency and duration of cyanobacterial blooms across the globe (O'Neil et al. 2012; Huisman et al. 2018), lake browning may play a key role as well.

The proliferation of cryptophytes in waters with high DOC concentrations is usually attributed to their mixotrophic feeding behavior (Urrutia-Cordero et al. 2017; Wilken et al. 2018). Interestingly, however, their pigmentation is also well suited for photosynthesis in waters with high DOC concentrations. Similar to PBS-containing cyanobacteria, cryptophytes also contain a diverse set of phycobili-pigments (Cunningham et al. 2018; Greenwold et al. 2019), although their phycobili-pigments are not organized into PBS-like structures but are contained in the thylakoid lumen (van der Weij-de Wit et al. 2006). Hence, similar to PBS-containing cyanobacteria, cryptophytes can effectively exploit the green and orange-red part of the light spectrum generated by relatively high DOC concentrations.

Our findings are also consistent with the biogeographical distributions of the marine cyanobacteria *Prochlorococcus* and *Synechococcus*. As predicted, these two genera coexist in many regions across the global ocean but their distributions do not completely overlap (Ting et al. 2002; Flombaum et al. 2013). In agreement with the model predictions, *Prochlorococcus* uses chlorophyll-based light-harvesting antennae and is particularly abundant in blue waters of the oligotrophic subtropical gyres (Partensky et al. 1999; Biller et al. 2015), whereas the PBS-containing *Synechococcus* prevails in slightly more turbid oceanic and

coastal waters dominated by greenish blue and green light (Scanlan and West 2002; Ting et al. 2002; Grébert et al. 2018). Moreover, the highly diverse *Synechococcus* genus comprises several pigment types, that have branched out over a wide range of aquatic ecosystems in accordance with the underwater light colors that can be captured by their phycobili-pigments (Stomp et al. 2007b; Grébert et al. 2018). Hence, the predominance of *Prochlorococcus* in blue ocean waters and marine *Synechococcus* in more greenish waters, with a broad intermediate region where both genera coexist, can be readily explained by their contrasting light-harvesting strategies.

Implementation in resource competition theory and trait-based approaches

This work shows how the study of photosynthetic pigments and their role in light harvesting can be integrated into resource competition models and may contribute to the advancement of trait-based approaches in freshwater and marine ecology. Trait-based approaches provide a unifying framework to study biodiversity and community dynamics on the basis of the functional traits of species (McGill et al. 2006; Litchman and Klausmeier 2008). However, trait-based studies in phytoplankton ecology have mostly focused on traits related to cell size and nutrient uptake (Merico et al. 2009; Kruk et al. 2010; Edwards et al. 2011). As a consequence, even though photosynthetic properties are long recognized as important traits of phytoplankton (e.g., Engelmann 1883; Edwards et al. 2015), the role of the underwater light spectrum as a major selective factor in phytoplankton communities has received surprisingly little attention (but see Stomp et al. 2004, 2007b). Our results show that changes in the underwater light color of lakes and oceans may have a major and predictable impact on the photosynthetic pigments favored by natural selection and hence on the species composition of phytoplankton communities. These findings may offer a powerful trait-based approach to study the biogeographical distribution of some of the most abundant photosynthetic organisms on our planet.

Acknowledgments

This publication is dedicated to the memory of our late colleagues dr. Maayke Stomp and dr. Hans Matthijs, who provided a source of inspiration for this work. *Synechocystis* sp. PCC 6803 was kindly provided by professor D. Bhaya (University of Stanford, USA) and the absorption spectrum of *Synechococcus* sp. WH7803 was kindly provided by dr. L. Garczarek (CNRS). We thank participants of the Wetsus research theme "Algae" and the FAME department of the University of Amsterdam for valuable discussions, and two anonymous reviewers for excellent comments on the manuscript. This work was performed in the cooperation framework of Wetsus, European Centre of Excellence for Sustainable Water Technology (www.wetsus.eu). Wetsus is co-funded by the Dutch Ministry of Economic Affairs and Ministry of Infrastructure and Environment, the Province of Fryslân and the Northern Netherlands Provinces.

Supplementary information

Appendix S1. Stability analysis

The model

We consider two species competing for two colors of light, blue (b) and red (r). In this case, the competition model of Eq. 6 can be written as:

$$\begin{aligned}\frac{dC_1}{dt} &= \left(f_{1\mathrm{b}}\left(I_{\mathrm{out,b}}\right) + f_{1\mathrm{r}}\left(I_{\mathrm{out,r}}\right) - m_1\right)C_1 \\ \frac{dC_2}{dt} &= \left(f_{2\mathrm{b}}\left(I_{\mathrm{out,b}}\right) + f_{2\mathrm{r}}\left(I_{\mathrm{out,r}}\right) - m_2\right)C_2\end{aligned} \tag{S1}$$

where the growth rates of species *i* on blue and red light are given by

$$f_{i\mathrm{b}}(I_{\mathrm{out,b}}) = \phi_{i\mathrm{b}} k_{i\mathrm{b}} \left(\frac{I_{\mathrm{in,b}} - I_{\mathrm{out,b}}}{\ln\left(I_{\mathrm{in,b}}\right) - \ln\left(I_{\mathrm{out,b}}\right)}\right)$$

and

$$f_{i\mathrm{r}}(I_{\mathrm{out,r}}) = \phi_{i\mathrm{r}} k_{i\mathrm{r}} \left(\frac{I_{\mathrm{in,r}} - I_{\mathrm{out,r}}}{\ln\left(I_{\mathrm{in,r}}\right) - \ln\left(I_{\mathrm{out,r}}\right)}\right) \tag{S2}$$

Stability analysis

The local stability of the coexistence equilibrium is investigated by analyzing the Jacobian matrix of the system (e.g., Edelstein-Keshet 1988, Otto and Day 2007). The Jacobian matrix is given by

$$\boldsymbol{J} = \begin{pmatrix} A_{11} & A_{12} \\ A_{21} & A_{22} \end{pmatrix} = \begin{pmatrix} \dfrac{\partial (dC_1/dt)^*}{\partial C_1} & \dfrac{\partial (dC_1/dt)^*}{\partial C_2} \\ \dfrac{\partial (dC_2/dt)^*}{\partial C_1} & \dfrac{\partial (dC_2/dt)^*}{\partial C_2} \end{pmatrix} \tag{S3}$$

where the superscript * indicates that the matrix is to be evaluated at the coexistence equilibrium.

The coexistence equilibrium is stable if and only if:

$$\begin{aligned} trace(\boldsymbol{J}) &= A_{11} + A_{22} < 0 \\ det(\boldsymbol{J}) &= A_{11}A_{22} - A_{12}A_{21} > 0 \end{aligned} \tag{S4}$$

We note that, at the coexistence equilibrium, $f_{ib}(I_{out,b}) + f_{ir}(I_{out,r}) - m_i = 0$ for both species. Hence, the elements of the Jacobian matrix can be written as

$$A_{ij} = \frac{\partial f_{ib}}{\partial I_{out,b}} \frac{\partial I_{out,b}}{\partial C_j} + \frac{\partial f_{ir}}{\partial I_{out,r}} \frac{\partial I_{out,r}}{\partial C_j} \quad \text{(S5)}$$

It is straightforward to derive that both $\partial f_{ib}/\partial I_{out,b} > 0$ and $\partial f_{ir}/\partial I_{out,r} > 0$, whereas both $\partial I_{out,b}/\partial C_j < 0$ and $\partial I_{out,r}/\partial C_j < 0$. It follows that all $A_{ij} < 0$ and therefore $trace(\boldsymbol{J}) < 0$.

After some algebra, the determinant of the Jacobian matrix can be written as

$$det(\boldsymbol{J}) = \left(\frac{\partial f_{1b}}{\partial I_{out,b}} \frac{\partial f_{2r}}{\partial I_{out,r}} - \frac{\partial f_{2b}}{\partial I_{out,b}} \frac{\partial f_{1r}}{\partial I_{out,r}}\right) \left(\frac{\partial I_{out,b}}{\partial C_1} \frac{\partial I_{out,r}}{\partial C_2} - \frac{\partial I_{out,b}}{\partial C_2} \frac{\partial I_{out,r}}{\partial C_1}\right) \quad \text{(S6)}$$

From Lambert-Beer's law, we note that

$$\frac{\partial I_{out,b}}{\partial C_i} = -k_{ib} I_{out,b} \quad \text{and} \quad \frac{\partial I_{out,r}}{\partial C_i} = -k_{ir} I_{out,r} \quad \text{(S7)}$$

Furthermore,

$$\frac{\partial f_{ib}}{\partial I_{out,b}} = \phi_{ib} k_{ib} \frac{\partial I_{avg,b}}{\partial I_{out,b}} \quad \text{and} \quad \frac{\partial f_{ir}}{\partial I_{out,r}} = \phi_{ir} k_{ir} \frac{\partial I_{avg,r}}{\partial I_{out,r}} \quad \text{(S8)}$$

Hence, we obtain

$$det(\boldsymbol{J}) = (\phi_{1b}\phi_{2r}k_{1b}k_{2r} - \phi_{2b}\phi_{1r}k_{2b}k_{1r})(k_{1b}k_{2r} - k_{2b}k_{1r}) \frac{\partial I_{avg,b}}{\partial I_{out,b}} \frac{\partial I_{avg,r}}{\partial I_{out,r}} I_{out,b} I_{out,r} \quad \text{(S9)}$$

Since $\partial I_{avg,b}/\partial I_{out,b} > 0$ and $\partial I_{avg,r}/\partial I_{out,r} > 0$, the signs of the two bracketed terms in this equation determine whether the coexistence equilibrium is stable or unstable.

Case 1: Quantum yield independent of light color

Suppose that the quantum yield is independent of light color, i.e., a species utilizes all its absorbed photons with the same efficiency irrespective of wavelength, as assumed by Stomp et al. (2004, 2007b). Hence, $\phi_{1b} = \phi_{1r} = \phi_1$ and $\phi_{2b} = \phi_{2r} = \phi_2$, and the determinant simplifies to

$$det(\boldsymbol{J}) = \phi_1\phi_2(k_{1b}k_{2r} - k_{2b}k_{1r})^2 \frac{\partial I_{avg,1}}{\partial I_{out,1}} \frac{\partial I_{avg,2}}{\partial I_{out,2}} I_{out,1} I_{out,2} \quad \text{(S10)}$$

In this case, it follows that $det(\boldsymbol{J}) > 0$ and therefore the coexistence equilibrium is locally stable whenever it exists.

Case 2: Quantum yield depends on light color

More generally, the quantum yield varies with light color. Let us arbitrarily assume that species 1 is a better competitor for blue light and species 2 a better competitor for red light. Graphically, this implies that species 1 has a steeper zero isocline than species 2 (as in Fig. 2b, where the green alga would be species 1 and the cyanobacterium species 2). According to Eqs. 8a,b, this difference in slope of the zero isoclines implies

$$\frac{\phi_{1b}k_{1b}}{\phi_{1r}k_{1r}} > \frac{\phi_{2b}k_{2b}}{\phi_{2r}k_{2r}} \tag{S11}$$

Hence, the first bracketed term in Eq. S9 is positive, and therefore the sign of $det(\boldsymbol{J})$ depends only on the second bracketed term. This implies that $det(\boldsymbol{J}) > 0$ and, hence, the coexistence equilibrium is locally stable if

$$\frac{k_{2r}}{k_{2b}} > \frac{k_{1r}}{k_{1b}} \tag{S12}$$

whereas it is locally unstable if this inequality is reversed. In other words, if species 2 (the better competitor for red light) absorbs relatively more red than blue light in comparison to species 1, then coexistence of the two species is stable. Conversely, if species 2 absorbs relatively more blue than red light in comparison to species 1, then the coexistence equilibrium is unstable and the winner will depend on the initial abundances of the species.

Supplementary Table S1 | Model parameters estimated from the monoculture experiments.

Symbol	Definition	Value		Units
Variables				
C_i	Biomass of phytoplankton species *i*	-		$mm^3\ L^{-1}$
$I_{\text{out,blue}}$	Blue light transmitted through the chemostats	-		$\mu mol\ photons\ m^{-2}\ s^{-1}$
$I_{\text{out,red}}$	Red light transmitted through the chemostats	-		$\mu mol\ photons\ m^{-2}\ s^{-1}$
System parameters				
$I_{\text{in},j}$	Incident blue or red light intensity	45		$\mu mol\ photons\ m^{-2}\ s^{-1}$
$K_{\text{bg,blue}}$	Background turbidity of blue light	7.5		m^{-1}
$K_{\text{bg,red}}$	Background turbidity of red light	9		m^{-1}
$K_{\text{bg,green}}$	Background turbidity of green light	8		m^{-1}
$z_{\max}$	Maximum depth of water column	0.05		m
D	Dilution rate*	0.015		h^{-1}
Species parameters		*Chlorella*	*Synechocystis*	
$\phi_{i,\text{blue}}$	Photosynthetic efficiency in blue light	2.30×10^{-3}	0.69×10^{-3}	$mm^3\ \mu mol^{-1}$
$\phi_{i,\text{red}}$	Photosynthetic efficiency in red light	3.00×10^{-3}	3.80×10^{-3}	$mm^3\ \mu mol^{-1}$
$k_{i,\text{blue}}$	Specific light absorption coefficient in blue light	2.60×10^{-4}	2.10×10^{-4}	$m^2\ mm^{-3}$
$k_{i,\text{red}}$	Specific light absorption coefficient in red light	1.33×10^{-4}	1.16×10^{-4}	$m^2\ mm^{-3}$
		Prochlorococcus	*Synechococcus*	
$\phi_{i,\text{blue}}$	Photosynthetic efficiency in blue light	2.30×10^{-3}	0.69×10^{-3}	$mm^3\ \mu mol^{-1}$
$\phi_{i,\text{green}}$	Photosynthetic efficiency in green light	3.30×10^{-3}	3.80×10^{-3}	$mm^3\ \mu mol^{-1}$
$k_{i,\text{blue}}$	Specific light absorption coefficient in blue light	2.60×10^{-4}	2.10×10^{-4}	$m^2\ mm^{-3}$
$k_{i,\text{green}}$	Specific light absorption coefficient in green light	5.20×10^{-5}	2.02×10^{-4}	$m^2\ mm^{-3}$

*We assume that specific loss rates of the species are dominated by the dilution rate of the chemostat (i.e., $m_i = D$)

Supplementary Table S2 | Steady-state characteristics of monoculture experiments with the cyanobacterium *Synechocystis* and green alga *Chlorella* in blue and red light.

	Synechocystis		*Chlorella*	
	blue light	red light	blue light	red light
Population density (million cells mL^{-1})	7.5 ± 0.6	123.4 ± 12.6	25.4 ± 1.9	31.5 ± 5.5
Total biovolume (mm^3 L^{-1})	57 ± 4	696 ± 66	427 ± 39	640 ± 118
Cell volume (fL $cell^{-1}$)	7.7 ± 0.3	5.6 ± 0.2	16.8± 0.7	19.2 ± 1.9
Light transmission I_{out} (µmol photons m^{-2} s^{-1})	19.3 ± 0.5	< 0.5	< 0.5	< 0.5
Critical light intensity $I^*_{avg,ij}$ (µmol photons m^{-2} s^{-1})	28.8	9.5	7.0	10.4

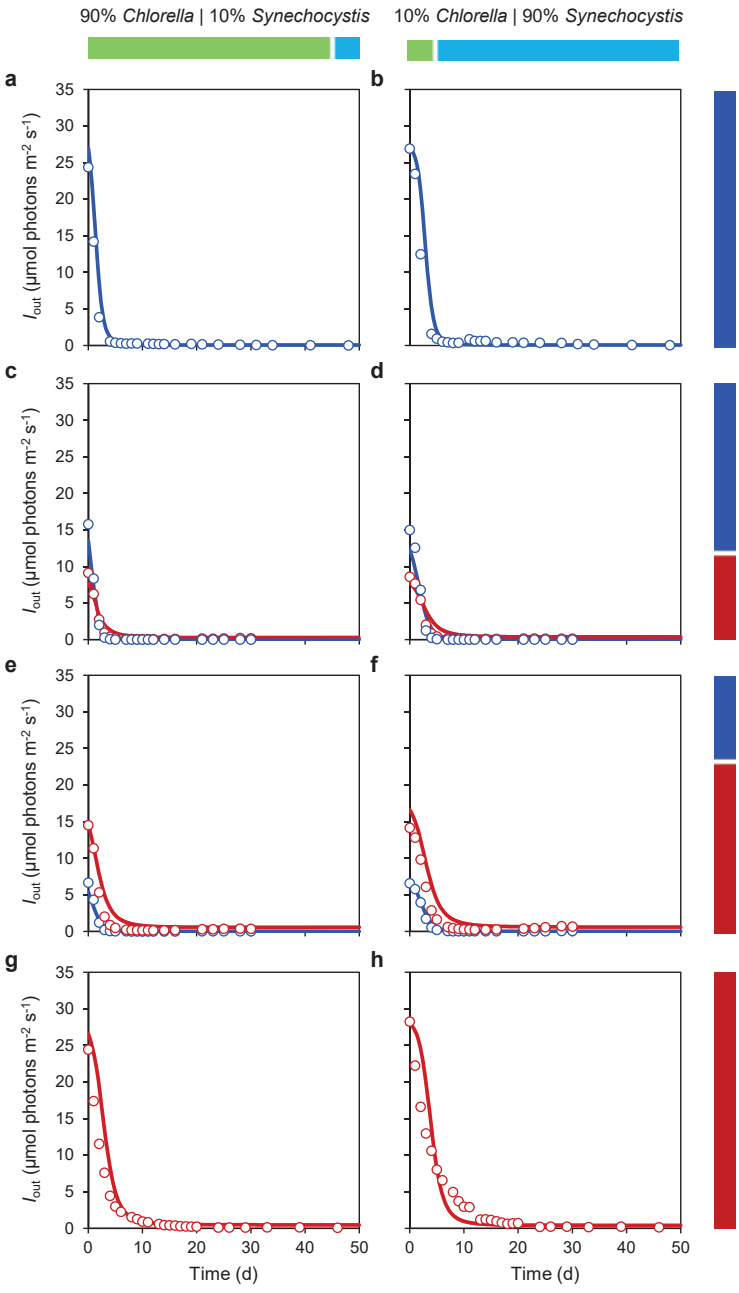

Supplementary Fig. S1 | Light transmission (I_{out}) through the competition experiments between the cyanobacterium *Synechocystis* and the green alga *Chlorella*. Blue circles represent blue light, red circled represent red light, and solid lines represent the model predictions. The graph has the same layout as Fig. 4 in the main text.

Chapter 6

General discussion

Introduction

The aim of this thesis was to study why many cyanobacteria display a low photosynthetic efficiency in blue light (as described in **chapters 1** and **2** and references therein), while this light color is absorbed by several of their photosynthetic pigments. Although this phenomenon has already been described by other studies, it is not widely known, and comprehensive studies of photosynthesis and growth of cyanobacteria in blue light were lacking.

We have investigated the hypothesis that the lack of blue-light absorption by the phycobilisomes (PBS) leads to an imbalance between the rate of excitation of photosystem I (PSI) and photosystem II (PSII), which results in a low photosynthetic efficiency of cyanobacteria in blue light. However, other explanations also exist. In this chapter, we will compare results obtained in our work with other studies, to assess which of these possible explanations fit the observations best. Next, we will discuss the implications of our research findings and outline recommendations for further research.

We note that light intensities can be expressed both as a flux of energy (in W m^{-2} or J m^{-2} s^{-1}) and as a flux of a large but discrete number of photons (in mol photons m^{-2} s^{-1}), because of the quantum nature of light. Our experimental comparison of the photosynthetic efficiencies in different light colors is based on the number of photons absorbed (e.g., in mol O_2 per mol photons) rather than the amount of light energy absorbed (in mol O_2 per J), because photosynthesis is governed by electron excitation by absorbed photons. In terms of light energy, however, our results would be even more pronounced, because blue photons have a higher energy content than red photons. Therefore, a low photosynthetic efficiency in blue light expressed per number of photons absorbed would imply an even lower photosynthetic efficiency in blue light when expressed per amount of light energy absorbed.

Possible explanations

Why do cyanobacteria have a low photosynthetic efficiency in blue light?
Explanation 1: In this thesis, we hypothesize that PBS-containing phytoplankton species have a lower photosynthetic efficiency in blue light than in red, orange or white light due to an excitation imbalance between PSI and PSII (**chapters 2-5**). This imbalance is attributed to the structural organization of the photosynthetic apparatus of PBS-containing cyanobacteria, where PBS transfer most of the absorbed light energy to PSII, but do not absorb blue light.

Explanation 2: Toyoshima et al. (2020) attribute the low light use efficiency in blue light to wasteful dissipation of absorbed light energy by carotenoids. Carotenoids absorb mainly blue and green light and can dissipate excess absorbed light energy, also from excited chlorophylls in the reaction centers, as heat (Braslavsky and Holzwarth 2012; Stamatakis 2014). If light absorbed by carotenoids is not efficiently transferred to the reaction centers of photosynthesis but instead dissipated, this would result in a low photosynthetic efficiency in blue light.

Explanation 3: Many phototrophs have higher rates of photoinhibition in blue light than in red light, resulting primarily in inactivation of the oxygen-evolving complex of PSII (Hakala et al. 2005; Campbell and Tyystjärvi 2012; Murphy et al. 2017), although photoinhibition of PSI can also occur (Shimakawa et al. 2016). Higher rates of photoinhibition in blue light could explain the lower growth rates in blue than in red light.

Explanation 4: Photoprotective mechanisms of PBS-containing cyanobacteria may dissipate blue light energy that is transferred to the PSII reaction center. Three important examples of photoprotective mechanisms involve the orange carotenoid protein (OCP; Kirilovsky and Kerfeld 2016), the flavodiiron proteins 2 and 4 (Flv2/4; Bersanini et al. 2014) and the iron-stress inducible protein A (IsiA; Havaux et al. 2005).

Explanation 1: An excitation imbalance between PSI and PSII in blue light

In this thesis, we have explored the hypothesis that in blue light, insufficient light energy arrives at PSII of PBS-containing cyanobacteria to sustain high rates of linear photosynthetic electron flow. Essentially, phycobili-pigments in the PBS cannot absorb blue light ≤ 450 nm very effectively (Tandeau de Marsac 2003; Six et al. 2007), and therefore are unable to transfer the energy of blue light to PSII. PBS are composed of an allophycocyanin (APC) core and protein rods that contain (combinations of) phycocyanobilin (PCB), phycoerythrobilin (PEB) and phycourobilin (PUB) (Six et al. 2007). Of these phycobili-pigments, PUB absorbs closest to the blue region of the light spectrum with an absorption maximum at 495 nm. However, absorption spectra (Six et al. 2007, Küpper et al. 2009) as well as fluorescence excitation spectra (Sanfilippo et al. 2019) of isolated PBS and phycobili-pigments show that absorption and transfer of blue light at wavelengths ≤ 450 nm by PUB and other phycobilins are negligibly low.

Chlorophyll *a* (Chl *a*) and carotenoids do absorb blue light. However, PBS-containing cyanobacteria usually have 2–5 times more PSI than PSII (Singh et al. 2009; Allahverdiyeva et al. 2014; Kirilovsky 2015). Furthermore, PSI of cyanobacteria contains ~100 molecules of Chl *a* (Jordan et al. 2001; Kennis et al. 2001), whereas PSII of cyanobacteria contains ~35 Chl *a* molecules (Guskov et al. 2009; Umena et al. 2011). As a consequence, in PBS-containing cyanobacteria most Chl *a* (around 80 to 90% of total chlorophyll) is invested in PSI (Myers et al. 1980; Fujita 1997). Moreover, in cyanobacteria, PSI contains higher amounts of carotenoids than PSII, and only the carotenoids in PSI seem to be involved in light harvesting (Ritz et al. 2000; Stamatakis et al. 2014). Taken together, this implies that most blue light available for photosynthesis is absorbed by PSI. The consequential excitation imbalance between the two photosystems causes a deficiency of light energy at PSII, which results in a low photosynthetic efficiency of PBS-containing cyanobacteria in blue light (Solhaug et al. 2014; Kirilovsky 2015).

To explore this hypothesis, we performed a range of experiments using the model cyanobacterium *Synechocystis* sp. PCC 6803 (hereafter *Synechocystis*) and the model green alga *Chlorella sorokiniana* 211-8K (hereafter *Chlorella*) in **chapter 2**. Our results show that the PBS-containing cyanobacterium *Synechocystis* indeed displayed lower growth rates in blue light than in red light, accompanied by low rates of oxygen evolution. We attribute the lower rate of oxygen evolution to a lower photosynthetic activity of PSII in blue light, which is in line with our hypothesis that a lower number of photons are absorbed at PSII. Our hypothesis was further supported by the observed low PSI:PSII ratio in blue light, indicative of increased investment in PSII and/or decreased investment in PSI, possibly in an attempt of the cells to rebalance excitation energy between the two photosystems.

In contrast to this PBS-containing cyanobacterium, the green alga *Chlorella* displayed similar growth rates in blue and red light, which further underlines that blue light affects the photosynthetic efficiency of PBS-containing cyanobacteria specifically. Green algae and plants deploy chlorophyll-based light-harvesting complex II (LHCII) as their light-harvesting antenna (Kühlbrandt et al. 1994) which, like PBS, generally associates with PSII but can move to PSI in the process of 'state transitions' (Nawrocki et al. 2016). Importantly, green algae and plants have a more balanced PSI:PSII ratio, i.e. close to 1:1, in comparison to PBS-containing cyanobacteria (Shen et al. 1993; Singh et al. 2009; Kirilovsky 2015). Furthermore, unlike the PBS, LHCII absorbs both blue and red light as it contains Chl *a*, Chl *b* and carotenoids (Kühlbrandt et al. 1994; Takaichi

2011). In other words, in these organisms both blue and red light are absorbed in a more balanced way by PSI and PSII, and LHCII is able to redistribute light energy of both colors between the photosystems to alleviate imbalances that may arise (i.e., via state transitions; see above). Hence, the experimental results described in **chapter 2** strongly support the hypothesis that blue light causes an excitation imbalance between the two photosystems in PBS-containing phytoplankton species, but not in species that use chlorophyll-based light-harvesting antennae.

We further strengthen this hypothesis in **chapter 3**, by showing that a *Synechocystis* mutant that lacks PBS displays a low photosynthetic efficiency in both blue and red light, similar to the wildtype grown in blue light. Due to its lack of phycobili-pigments, less light is harvested by PSII and this mutant is unable to redistribute light between PSI and PSII. The major light-harvesting pigment harnessed by this *Synechocystis* mutant is Chl *a*, which absorbs both blue and red light but is mostly located in PSI. Therefore, consistent with our results, the PBS-less mutant is expected to display the same excitation imbalance between PSI and PSII in both blue and red light as the wildtype in blue light only. In other words, growth of PBS-containing cyanobacteria in blue light is similar to growth of cyanobacteria not containing light-harvesting antennae at all. This further demonstrates that light absorption and subsequent redistribution by the light-harvesting antennae plays a major role in the photosynthetic efficiency of phototrophs, and that the low photosynthetic efficiency in blue light of PBS-containing cyanobacteria seems a direct consequence of the lack of light absorption by the PBS.

In further support of our hypothesis, the observed changes in the transcriptome of *Synechocystis* described in **chapter 4** demonstrate that its transcriptome was significantly impacted by blue light. A switch from a mixture of light colors to blue light induced major changes in the transcriptome, while only a few genes were differentially expressed after a switch to red or orange light. Moreover, one of the most striking changes in gene expression in blue light was the up-regulation of several PSII genes, including the D1 and D2 proteins that form the core of the PSII reaction center and the PSII-core antenna protein CP47. Furthermore, we observed up-regulation of several genes involved in the PSII repair cycle. In contrast, none of the genes involved in PSI production were differentially regulated in blue light. These gene expression results are consistent with the observed decrease of the PSI:PSII ratio in blue light, indicative of an attempt of the cells to manage the adverse growth conditions imposed by blue light in order to restore photosynthetic electron flow.

Explanation 2: Higher rates of energy dissipation by carotenoids in blue light

Recently, Toyoshima et al. (2020) analyzed growth, oxygen evolution and light absorption by *Synechocystis* in several light colors. In agreement with our results in **chapter 2**, they also observed lower rates of growth and oxygen evolution by *Synechocystis* in blue light than in red and orange light. Furthermore, they described similar results for the PBS-containing cyanobacterium *Arthrospira platensis* (Toyoshima et al. 2020), in line with our hypothesis that light absorption by the PBS plays a key role in light-use efficiency. However, this study attributed the low light-use efficiency in blue light to wasteful energy dissipation by carotenoids. Carotenoids are able to dissipate energy from excited chlorophylls as heat, and absorb strongly in the blue-green regions of the light spectrum (400–525 nm) (Braslavsky and Holzwarth 2012; Stamatakis 2014). Toyoshima et al. (2020) predicted that 85% of the blue photons were absorbed by carotenoids (versus 2% of red and orange photons), and they assumed that the energy of these absorbed photons was completely dissipated as heat.

The results described in **chapter 3** may aid to distinguish between our hypothesis and the hypothesis of Toyoshima et al. (2020). In **chapter 3**, we compare the growth and photophysiology of *Synechocystis* wildtype and a mutant strain that lacks PBS (the PAL mutant; Ajlani et al. 1995). Essentially, the poor photosynthetic performance of *Synechocystis* in blue light, which is not absorbed by PBS, was comparable to the performance of the PBS-less PAL mutant in both blue and red light. If the hypothesis of Toyoshima et al. (2020) would be correct, then approximately 85% of the blue photons but only 2% of the red photons would be dissipated by carotenoids, before reaching the reaction centers. In this case, the number of photons arriving at the reaction centers of PSI and PSII would be much higher in red light than in blue light, and therefore the PAL mutant would display much higher oxygen evolution rates and growth rates in red light than in blue light. This was not what we observed, however. In our experiments, the PAL mutant had similar low rates of photosynthesis and growth in both blue and red light (**chapter 3**). Thus, the results of **chapter 3** contradict the hypothesis of Toyoshima et al. (2020).

Moreover, other phytoplankton species that use chlorophyll-based light-harvesting antennae contain carotenoids as well (Kühlbrandt et al. 1994; Takaichi 2011). Green algae and plants have an even larger repertoire of carotenoids than cyanobacteria, of which many are located in the photosystems and indeed serve a role in photoprotection (Braslavsky and Holzwarth 2012), but others are present in the light-harvesting

antennae as accessory pigments absorbing blue and green light for photosynthesis (Ritz et al. 2000; Takaichi 2011). Green algae have a similar photosynthetic efficiency in blue and red light (**chapter 2**; see also Teo et al. 2014; Yan and Zheng 2014; Zhao et al. 2015; de Mooij et al. 2016; Tan et al. 2020). Hence, the presence of carotenoids does not necessarily lead to the excessive dissipation of blue light energy.

Yet, the hypothesis of Toyoshima et al. (2020) may contribute to some extent to the low photosynthetic efficiency in blue light. Carotenoids do absorb blue light, and their contribution to the absorption of blue light becomes more prominent when the PSI content decreases and hence less blue-light absorbing Chl *a* is present in the cell. However, it is important to take into account the location and function of the carotenoids. In cyanobacteria, carotenoids are more abundant in PSI than in PSII (Takaichi 2011), and only the carotenoids in PSI are involved in photosynthetic light-harvesting while those in PSII dissipate light energy (Kennis et al. 2001; Braslavsky and Holzwarth 2012; Stamatakis et al. 2014). Therefore, we propose that carotenoids indeed play a role in the low photosynthetic efficiency of PBS-containing cyanobacteria in blue light, by amplifying the excitation imbalance between PSI and PSII. However, the dissipation of blue light by carotenoids does not seem to be the main reason for the low photosynthetic efficiency of PBS-containing cyanobacteria in blue light.

Explanation 3: Higher rates of photoinhibition in blue light

Within the visible spectrum, the photons in blue light are the most energetic. At high light intensities these photons cause photodamage more efficiently than photons of longer wavelengths (Tyystjärvi et al. 2002; Muramatsu and Hihara 2012). Therefore, the low photosynthetic efficiency in blue light might also be explained by higher rates of photoinhibition in blue light than in red light. It has been shown that in plants and phytoplankton, UV light and visible blue light can cause photoinhibition by damaging the D1 protein of PSII and inactivating the oxygen-evolving complex of PSII, sometimes already at low light intensities (Hakala et al. 2005; Campbell and Tyystjärvi 2012). Murphy et al. (2017) show that blue light of ~450 nm also induces much higher rates of photoinhibition than red light of ~650 nm in *Synechococcus* sp. WH8102. This marine cyanobacterium employs PBS that contain phycourobilin (PUB) and phycoerythrobilin (PEB), absorbing blue-green light (495 nm) and green light (545 nm), respectively (Six et al. 2007). The finding of Murphy et al. (2017) is in agreement with our results from

chapters 2 and 5, where we describe that *Synechococcus* species using PEB and PUB also have lower growth rates in blue light ≤ 450 nm than in light colors absorbed by their PBS.

However, if higher rates of photoinhibition in blue light are the underlying cause for the low blue-light use efficiency, then the PBS-less PAL mutant of *Synechocystis* PCC 6803, and species with chlorophyll-based light-harvesting antennae such as *Prochlorococcus* and green algae would also display a lower photosynthetic efficiency in blue than in red light, similar to the *Synechocystis* wildtype. Yet, our experiments in **chapter 3** clearly show that the PAL mutant has similar low rates of oxygen production and growth in both blue and red light. Furthermore, growth rates are also similar in blue and red light for the green alga *Chlorella* (**chapter 2**). Hence, it is unlikely that enhanced photoinhibition in blue light occurs on a large enough scale to fully explain the described differences in photosynthetic performance of PBS-containing cyanobacteria in blue and red light.

Explanation 4: More strongly activated photoprotective mechanisms in blue light

Cyanobacteria employ several photoprotective mechanisms that dissipate energy to prevent damage to the photosynthetic apparatus (Fig. 1, see also Latifi et al. 2009; Kirilovsky 2015). High rates of energy dissipation at PSII may limit the rate of linear electron transport and decrease photosynthetic activity and growth. Three important photoprotective mechanisms of PBS-containing cyanobacteria involve OCP (Kirilovsky and Kerfeld 2016), Flv2/4 (Bersanini et al. 2014) and IsiA (Havaux et al. 2005). OCP, Flv2/4 and IsiA are highly conserved in PBS-containing cyanobacteria (Boulay et al. 2008; Allahverdiyeva et al. 2015; Li et al. 2019).

OCP is a carotenoid-containing protein complex that can be activated by blue light and binds to the PBS (Fig. 1), where it can dissipate up to 80% of the excitation energy before this energy is transferred to PSII (Rakhimberdieva et al. 2007; Gorbunov et al. 2011; Tian et al. 2012). As red light does not activate OCP, less dissipation will occur and a larger number of photons will arrive at PSII in red than in blue light. Therefore, activation of OCP may explain why PBS-containing cyanobacteria have a higher photosynthetic efficiency in red light than in blue light.

However, OCP functions through binding to the PBS (Fig. 1; see also Kirilovsky 2015), and hence is unable to perform its photoprotective role in the PBS-less PAL mutant. Therefore, if energy dissipation by OCP would cause the low photosynthetic efficiency of PBS-containing cyanobacteria in

blue light, then one would expect that the PAL mutant had higher oxygen evolution rates in blue light than the wildtype. However, this is not what we found. Instead of an improved photosynthetic efficiency of the PAL mutant in blue light, we observed a similarly low photosynthetic efficiency of the PAL mutant in both blue and red light as the wildtype in blue light (**chapter 3**). In addition, OCP is strongly upregulated and activated by high intensities of blue light (Kirilovsky 2007), whereas our experiments in **chapter 2 and 3** were performed at relatively low light intensities (maximally 70 µmol photons m^{-2} s^{-1}). Therefore, we expect that any effect of OCP-mediated energy dissipation is absent or too small to explain the observed large differences between blue and red light in our experiments.

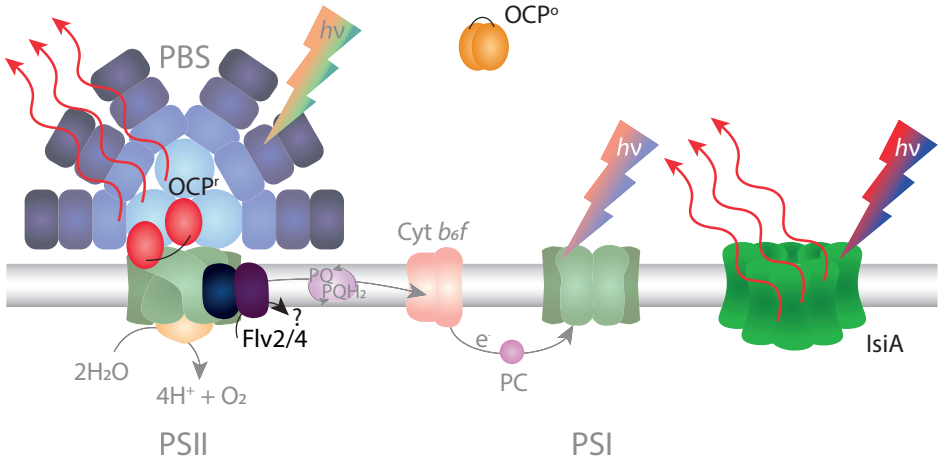

Figure 1 | Localization of the photoprotective proteins OCP, Flv2/4 and IsiA within the thylakoid of a PBS-containing cyanobacterium. OCP is always present in the cells in its inactive, orange form (OCP^o; see Kirilovsky and Kerfeld 2016). Strong blue-green light transforms OCP into its red, active form (OCP^r), which interacts with the PBS core and dissipates absorbed light energy as heat. The heterodimer Flv2/4 functions in photoprotection of PSII by acting as an electron sink; however, thus far the exact electron donor and acceptor of Flv2/4 have not been identified (Santana-Sanchez et al. 2019). Chl-binding aggregates or 'rings' of IsiA are suggested to absorb and dissipate excess light energy (Ihalainen et al. 2005). Arrows indicate electron (e^-) transfer. Flv2/4: heterodimer of flavodiiron protein 2 and 4; IsiA: iron stress inducible protein A; OCP: orange carotenoid protein; PBS: phycobilisome; PSI: photosystem I; PSII: photosystem II; PQ: plastoquinone; PQH_2: plastoquinol; Cyt b_6f: cytochrome b_6f; PC: plastocyanin; *hv*: photon.

The photoprotective heterodimer of Flv 2/4 can dissipate excitation energy at PSII before it is passed on to plastoquinone (Fig. 1; see also Bersanini et al. 2014; Chukhutsina et al. 2015). Previous research revealed that up to 30% of the excited electrons originating from PSII can be dissipated by Flv 2/4 (Zhang et al. 2012; Bersanini et al. 2014). Because blue light is more energetic than orange and red light, Flv 2/4 might be more active or upregulated, causing stronger dissipation in blue light than in orange or red light. However, while some studies have shown that Flv2/4 can be present under high CO_2 conditions, this is only in low quantities (Zhang et al. 2009) and it seems that Flv2/4 is mostly active under carbon-limited conditions (Shimakawa et al. 2015; Santana-Sanchez et al. 2019). In our experiments, carbon was not limiting, as CO_2 was supplied at 2% v/v and cultures were supplemented with Na_2CO_3. Furthermore, no significant changes in expression of *flv2* and *flv4* were observed in the microarray experiments described in **chapter 4**. Therefore, excessive energy dissipation by Flv2/4 is not likely to cause the lower photosynthetic efficiency in blue light.

Lastly, cyanobacteria possess the iron-stress inducible protein IsiA that contributes to the storage of chlorophylls under iron-limited conditions and can also aid in the dissipation of excess excitation energy absorbed by Chl *a* (Fig. 1; see also Bibby et al. 2001; Boekema et al. 2001; Yeremenko et al. 2004; Havaux et al. 2005; Ihalainen et al. 2005; Berera et al. 2009; Chen et al. 2018). IsiA binds chlorophylls and carotenoids, and is shown to be upregulated when the PSI:PSII ratio decreases (Sandström et al. 2002). This suggests that IsiA might play a role in blue light. However, up-regulation of the *isiA* gene is observed in particular under iron limitation and also under several other environmental stress conditions favoring energy dissipation by IsiA (Vinnemeier et al. 1998; Yeremenko et al. 2004; Havaux et al. 2005; Berera et al. 2009). In contrast, iron and other nutrients were supplied in sufficient amounts in all our experiments, and hence many of the stress conditions that usually induce IsiA production were not present in our study. Furthermore, our transcriptome data show that the *isiA* gene was not significantly upregulated in blue light (**chapter 4**). Thus, we have no indications for enhanced energy dissipation by an increased IsiA content in blue light.

Which of these explanations are most plausible?

In conclusion, our results show that an excitation imbalance between PSI and PSII is the most plausible explanation for the low photosynthetic efficiency of PBS-containing cyanobacteria in blue light. This is supported by the growth rates in blue and red light (**chapters 2-5**), the oxygen production rates (**chapters 2 and 3**), the changes in PSI:PSII ratio (**chapters 2-4**), the gene expression patterns (**chapter 4**) and the low photosynthetic efficiency of a PBS-less mutant in both blue and red light (**chapter 3**).

The four explanations discussed above are not mutually exclusive, however. In fact, carotenoids do absorb blue light, and photoprotective mechanisms mediated by OCP, Flv 2/4 and IsiA do play a key role to protect cyanobacteria and other oxygenic phototrophs against excess light energy. Hence, the processes underlying these four explanations are all intertwined and the excitation imbalance may be influenced by combinations of the abovementioned explanations. In particular, energy dissipation by carotenoids and photoprotective mechanisms may be of major importance to protect cyanobacterial cells against high rates of photoinhibition in blue light. Many photoprotective mechanisms, including IsiA and OCP, but also mechanisms of green algae and higher plants, make use of the efficient dissipating capacities of different carotenoids (Takaichi 2011). The evolution of these energy-dissipating mechanisms may thus have been influenced by the dispersal of cyanobacterial populations to environments in which blue light is an important component, but these energy-dissipating mechanisms do not seem to be the underlying cause of the low photosynthetic efficiency of PBS-containing cyanobacteria in blue light.

Implications for biotechnological applications

Choosing the right colors

Effects of light color on photosynthetic efficiency of cyanobacteria and green algae may have major implications for their use in biotechnology. Not only do they form the base of aquatic ecosystems, phototrophic phytoplankton have also received increasing interest in the search for sustainable production of food, renewable energy sources, and even biodegradable polymers (for recent reviews see, e.g., Wijffels and Barbosa 2010; Gerardo et al. 2015; van Alphen and Hellingwerf 2018). Amongst the oxygenic phototrophs, cyanobacteria are considered particularly promising in biotechnology, as they are relatively easy to genetically transform in comparison to eukaryotic algae (Branco dos Santos et al.

2014) and have lower cellular maintenance costs (van Liere and Mur 1979). However, due to their larger cell size and corresponding cytosolic storage capacity, eukaryotic algae may prove to be more suitable for 'biorefinery' approaches, aiming to produce e.g., proteins, lipids and starch (Wijffels et al. 2013; Gerardo et al. 2015), while cyanobacteria appear to be most promising for direct, extracellular production of e.g., fatty acids, cellulose, ethanol and butanol (Hellingwerf and Teixeira de Mattos 2009; Lips et al. 2018). Using a combination of technologies that make optimal use of the photosynthetic characteristics of cyanobacteria and algae may play an important role in the bio-based economy that is foreseen in the near future.

One of the major limiting factors for growth of oxygenic phototrophs is often light availability. Hence, an advanced understanding of photosynthesis and the process of light harvesting and conversion is of considerable importance for optimization of culture conditions. In particular, the spectral differences in photosynthetic efficiency of cyanobacteria described in this thesis may affect the choice of suitable light colors for biotechnological applications. Almost 50% of the solar energy is not used by oxygenic phototrophs, such as cyanobacteria and eukaryotic algae, as it exceeds the 400-700 nm range (i.e., the range of photosynthetically active radiation), the only range that can effectively be absorbed and used by their photosynthetic pigments (Zhu et al. 2008). In fact, for any given phototrophic species an even larger percentage of the solar energy is not available for photosynthesis, because each species has its own distinct pigment composition which it can use to absorb some colors more effectively than others. Therefore, algal cultures illuminated with light of one or more distinct colors, specifically targeting the photosynthetic pigments of the species concerned, may improve the yield per photon significantly.

Longer-wavelength red photons are energetically less expensive to produce than shorter-wavelength blue photons, and LED lights provide a relatively inexpensive source of lighting. Hence, providing a culture with red LED light without compromising photosynthetic efficiency might greatly improve cost-effectiveness of cyanobacterial and algal mass culture, relative to illumination with white or blue light. For example, our results in **chapter 2-5** suggest that red light of 660 nm is effectively used by both green algae and cyanobacteria (Fig. 2b). Even though both taxa can use the same light color effectively, our results from **chapter 5** indicate that stable coexistence is not likely when species are cultured together in a single light color, but rather that one species always seems to outcompete the other (see also Stomp et al. 2007b).

It has been shown that a mix of blue (~450-465 nm) and red (~650-670 nm) light is beneficial for plant growth in agriculture and horticulture (see, e.g., Yorio et al. 2001; Heo et al. 2002; Son and Oh 2013; Liu et al. 2014; Wang et al. 2016; Pennisi et al. 2019). This is illustrated by an increasing number of greenhouses, in the Netherlands as well as other countries, that emit a purplish glow from the combination of red and blue LEDs (Fig. 2c,d). Of course, vascular plants are much more complex than unicellular algae, and differences in light color also play a role in, e.g., leaf size, morphology and shoot formation (Pennisi et al. 2019). Yet, blue and red light are absorbed by both Chl *a* and Chl *b* utilized by green algae and terrestrial plants. Hence, this color combination provides light energy to the light-harvesting antennae and photosystems, which

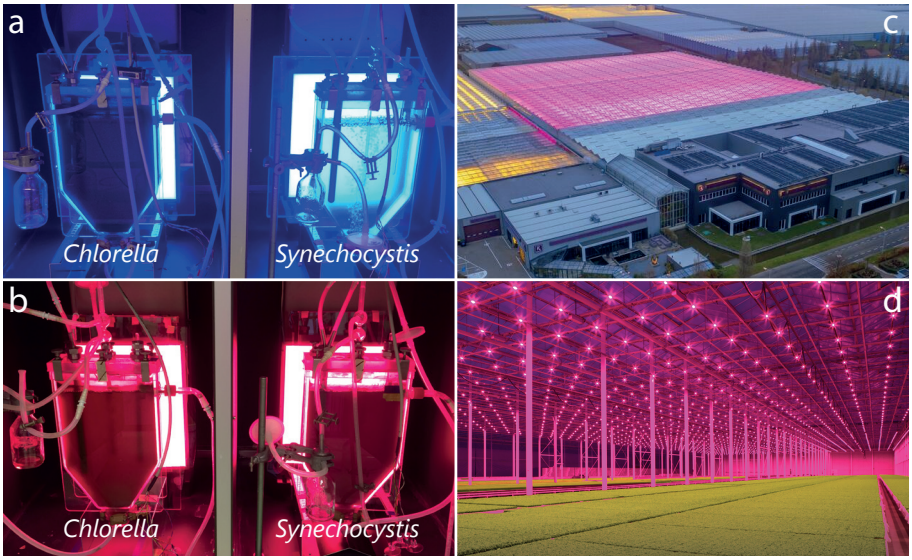

Figure 2 | When choosing the light colors for phototrophic growth, it is essential to take into account a species' absorption properties as well as photosynthetic efficiency at different wavelengths. Steady-state chemostats (photobioreactors) of the green alga *Chlorella sorokiniana*, and the PBS-containing cyanobacterium *Synechocystis* sp. PCC 6803 in 45 µmol photons m^{-2} s^{-1} of (a) blue light of 440 nm and (b) red light of 660 nm reveal these differences in photosynthetic efficiency. Blue light is absorbed by both species, but allows the green alga to reach high cell densities whereas the cyanobacterial culture remains very dilute. In contrast, both species reach high cell densities in red light. A combination of these two light colors has proven beneficial for higher plants. Aerial (c) and inside (d) views of a greenhouse located in Monster, The Netherlands, show how a combination of blue and red LED light is used to optimize growth of cress by Koppert Cress, resulting in a purplish light color. Pictures in panel (a) and (b) were taken by Veerle M. Luimstra during the experiments described in **chapter 5** and pictures in panels (c) and (d) were kindly provided by Koppert Cress.

allows a balanced energy distribution between PSI and PSII and optimal rates of photosynthesis (**chapter 2**). At first thought, one might therefore presume that a similar combination of light colors will be beneficial for unicellular phototrophs as well.

In PBS-containing cyanobacteria, however, a combination of red and blue light will be counterproductive, because cyanobacteria have a low photosynthetic efficiency in blue light (**chapter 2**). Instead, it is likely that a mix of two light colors that are efficiently used by PBS and PSI may prove beneficial for cyanobacteria. Examples would be the application of red light (680 nm) absorbed by Chl *a* in combination with orange light (620 nm), green light (545 nm) or blue-green light (495 nm) absorbed by phycocyanobilin, phycoerythrobilin or phycourobilin, respectively. Table 1 lists some suggestions that may optimize growth of cyanobacteria and green algae by using directed (combinations of) light colors, based on the absorption spectra (e.g., Fig. 2 in **chapter 2**) and expected photosynthetic efficiency of both taxa.

Table 1 | Examples of light colors that may favor growth of cyanobacteria and/or green algae. Chl: chlorophyll; PCB: phycocyanobilin; APC: allophycocyanin.

Single color		
Light color (wavelength)	*Absorbed by*	*Favored species*
Blue (440 nm)	Chl *a*	Green algae
Blue-green (480 nm)	Chl *b*	Green algae
Orange (620 nm)	PCB	Cyanobacteria
Red (660 nm)	Chl *a*, Chl *b*, APC	Green algae or cyanobacteria
Dark red (680 nm)	Chl *a*	Green algae
Dual color		
Blue (440 nm) and dark red (680 nm)	Chl *a*	Green algae
Blue (440 nm) and orange (620 nm)	Chl *a*, PCB	Coexistence of green algae and cyanobacteria
Blue-green (480 nm) and orange (620 nm)	Chl *b*, PCB	Coexistence of green algae and cyanobacteria
Orange (620 nm) and red (660 nm)	PCB, APC, Chl *a*	Cyanobacteria

Furthermore, our competition experiments in **chapter 5** suggest that choosing the right light colors can even help to control the species composition in biotechnological applications. Cultures of PBS-containing cyanobacteria will be favored in orange light, whereas blue light will favor green algae (Table 1). These results imply that infections by undesirable phototrophic species may be prevented or at least hampered by applying specific colors of light while omitting other colors. For example, invasive growth of toxic cyanobacteria in green algal cultures can be drastically suppressed by the use of blue light (but note the extra costs of these higher-energy photons).

Using a combination of light colors that favor coexistence of different species may provide a valuable strategy to optimize co-cultures. Co-cultures can have higher resistance to contamination and can use a wider range of resources compared to monocultures (Magdouli et al. 2016; Jones and Wang 2018). Our model predicts a broad range of species coexistence if the competing species absorb distinctly different colors of light (**chapter 5**). That is, if one species absorbs (and uses) mainly color A whereas the other species absorbs mainly color B. For example, combinations of blue-green light targeting Chl *b* and orange light targeting phycocyanobilin may allow for stable coexistence of green algae and cyanobacteria with phycocyanobilin-rich PBS, where the relative abundances of these two taxa can be adjusted by the ratios of the two applied light colors. Coexistence of different phytoplankton species does not necessarily increase total biomass (Stomp et al. 2004; Zhao et al. 2014; Gonçalves et al. 2016), but combinations of cyanobacteria and green algae have been shown to enhance, e.g., nutrient removal from wastewater and the production of exopolysaccharides and lipids from CO_2 (Angelis et al. 2012; Silva-Benavides and Torzillo 2012; Silaban et al. 2014; Zhao et al. 2014; Gonçalves et al. 2016).

Truncation of light-harvesting antennae

Truncation of light-harvesting antennae to increase biomass production has been investigated extensively in the past years (see, e.g., Ort and Melis 2011; Work et al. 2012; de Mooij et al. 2015; Kirst et al. 2017; Hu et al. 2019). This concept is based on decreasing light attenuation through algal cultures with high biomass densities. In dense algal cultures, cells closer to the surface are exposed to high light intensities, which will be largely dissipated as heat by means of their photoprotective mechanisms, while cells in deeper water layers will absorb insufficient light for high rates of photosynthesis (Melis 2009; Blankenship and Chen 2013). Truncation of the light-harvesting antennae may decrease this wasteful dissipation of light energy in cells near the surface, while allowing more light to reach cells deeper down in the water column. This principle has proven beneficial in green algal cultures aimed at biomass production (Polle et al. 2002; Perrine et al. 2012; de Mooij et al. 2015; Shin et al. 2016).

Our results in **chapter 3**, however, indicate that truncation of the PBS of cyanobacteria may have a different effect than truncation of the chlorophyll-based antennae of green algae. Green algae have a more even ratio of PSI and PSII (close to 1:1), light-harvesting antennae that absorb the same light colors as their photosystems (Shen et al. 1993; Singh et al. 2009; Kirilovsky 2015), and more extensive possibilities for state

transitions than cyanobacteria (Nawrocki et al. 2016; Wobbe et al. 2016). Therefore, absorption of blue light is more balanced in these organisms than in cyanobacteria. In cyanobacteria, truncation of the PBS, that mainly transfer light energy to PSII, would likely increase the imbalance between PSI and PSII. Indeed, our experiments with the fully truncated PAL mutant, as well as results from other studies, showed that the PAL mutant has a lower PSI:PSII ratio than the wildtype (see **chapter 3** and references therein). Yet, the decrease in PSI:PSII ratio was apparently not enough to restore the balance between the two photosystems, as the growth rate of the PAL mutant was much lower than that of the wildtype in red light. As a consequence, complete removal of the PBS alone will not stimulate biomass production by cyanobacteria (**chapter 3**).

Partial truncation might prove more beneficial, as it reduces overall absorbance but still allows the PBS to distribute absorbed light energy between PSI and PSII (Lea-Smith et al. 2014). However, other studies have shown that in partially truncated *Synechocystis* strains the PSI:PSII ratio decreases proportionally with antenna size (Ajlani et al. 1995; Olive et al. 1997; Bernát et al. 2009; Stadnichuk et al. 2009; Collins et al. 2012; Kwon et al. 2013; Liberton et al. 2017), possibly aiming to restore the excitation balance between PSI and PSII. Of these studies, only one study reports a slightly higher productivity due to partial antenna truncation (Kwon et al. 2013). They investigated the Olive mutant, which lacks the orange-light absorbing phycocyanobilin rods but still contains the allophycocyanin core (Rögner et al. 1990). Yet, because these studies were performed in white light, a large proportion of the light spectrum will not have been absorbed by the truncated PBS, which indicates that excitation energy still cannot be effectively balanced between PSI and PSII. Possibly, culturing the Olive mutant in orange-red light, matching the absorption of allophycocyanin, will result in a more productive culture in comparison to the wildtype. Combining partial PBS truncation with truncation of the internal chlorophyll antenna of PSI might also prove beneficial, as overall light absorption is decreased while the smaller PBS can still harvest light for PSII and rebalance excitation energy.

Evolution of photosynthetic pigments

Early oxygenic phototrophs

At present, oxygenic photosynthesis is the dominant type of photosynthesis, but the first phototrophs in the early history of our planet performed anoxygenic photosynthesis. Like oxygenic photosynthesis, anoxygenic photosynthesis often involves (bacterio)chlorophyll-based reaction

centers. However, some prokaryotes use retinal-based proteorhodopsins as proton pumps to convert light energy into chemical energy, which can thus be viewed as another type of photosynthesis although no carbon is fixed in this process (Béjà et al. 2000; Bryant and Frigaard 2006). Although anoxygenic and oxygenic photosynthesis using chlorophylls probably account for more than 90% of the global photosynthesis, retinal-based phototrophs are widely distributed in aquatic environments (Béjà et al. 2000; McCarren and DeLong 2007; Atamna-Ismaeel et al. 2008).

Tracking the evolution of photosynthesis is obscured by the widespread occurrence of lateral gene transfer, which seems to have contributed significantly to the distribution of chlorophylls, phycobili-pigments and proteorhodopsins amongst Archaea and Bacteria (Ochman et al. 2000; Raymond et al. 2002; Gogarten and Townsend 2005). This increases the complexity of tracing genes back to their origin and seems to undermine the original proposition of a simple 'Tree of Life' (Darwin 1859). Consequently, no consensus has yet been reached on the exact evolutionary path of life on Earth, and several alternative hypotheses have been presented, including the 'Ring(s) of Life' and 'Web of Life' (see e.g., Iwabe et al. 1989; Rivera and Lake 2004; Bapteste and Walsh 2005; McInerney et al. 2015; Soucy et al. 2015). Here, we will only discuss the evolution of oxygenic phototrophs and their major pigments.

The earliest oxygenic phototrophs used only a primitive form of the blue and red light absorbing Chl *a* (Larkum 2006), while present-day phytoplankton consist of many different species that deploy a wide range of photosynthetic pigments (Ting et al. 2002; Kirk 2011; Croce and van Amerongen 2014; see also Table 1 in **chapter 1**). Nowadays, five chlorophylls are known to exist: Chl *a*, *b*, *c*, *d* and *f* (Larkum 2006) and many phytoplankton species harvest additional light colors using phycobili-pigments that absorb orange, green and/or blue-green light (Grossman et al. 1993; Tandeau de Marsac 2003; Six et al. 2007) and carotenoids that absorb violet and blue-green light (Ritz et al. 2000; Croce and van Amerongen 2014). The evolution of these pigments will have been strongly influenced by the light colors that were available in the environments in which these ancient phototrophs lived.

Current evidence suggests that the first oxygenic phototrophs, primitive cyanobacteria, evolved around 3 billion years ago from anoxygenic phototrophs that used Mg-3,8-pheoporphyrin a_5 monomethyl ester (Mg-DVP) (Larkum 2006; Larkum et al. 2007). Chlorophylls later replaced Mg-DVP, and Chl *a* is now present in the reaction centers of PSI and PSII of almost all oxygenic phototrophs (Larkum 2006) while some species also use Chl *d* in their reaction center (Chen 2014).

The ancestral cyanobacteria likely evolved in a freshwater environment, with enough red light to be absorbed by their Chl *a* (Ponce-Toledo et al. 2017; Sanchez-Baracaldo et al. 2017; see also Fig. 4 in **chapter 1**). These first oxygen-producing cyanobacteria are widely held responsible for the great oxygenation event 2.3 billion years ago (Schirrmeister et al. 2015), increasing the atmospheric oxygen concentration to 1-2% (Holland 2006). After this event, oxygen levels remained rather stable until around 850 million years ago, when atmospheric levels rose to the ~20% that we have today (Holland 2006). This second increase is suggested to be related to the primary endosymbiosis event 1.5 billion years ago and the subsequent evolution of different algal species that started colonizing terrestrial and marine environments (Berner 1999; Palmer 2003; Holland 2006; Hohmann-Marriott and Blankenship 2011). Primary endosymbiosis gave rise to three eukaryotic algal lineages: glaucophytes, red algae and green algae (Fig. 3; see also Keeling 2004). Several secondary and tertiary endosymbiosis events, involving mostly the red algae, caused the emergence of new algal phyla such as cryptophytes and dinoflagellates (Keeling 2010). All green algae and higher plants have evolved from the green algal lineage, but land plants did not appear until ~0.5 billion years ago (Bhattacharya and Medlin 1998). Interestingly, there are also species such as the apicomplexans that still have remnants of chloroplasts, but lost the capacity for photosynthesis completely (Köhler et al. 1997).

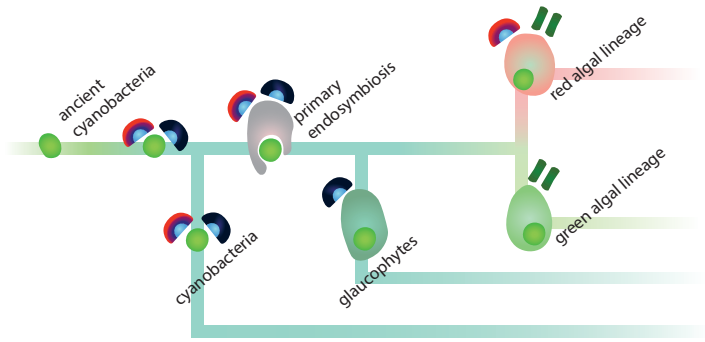

Figure 3 | Schematic overview of the emergence of major groups of eukaryotic algae following primary endosymbiosis. An ancient, primitive cyanobacterium that likely contained Chl *a*, Chl *b*, PBS and carotenoids was endocytosed by a eukaryotic cell and integrated into this host cell as the first chloroplast. Most cyanobacteria and glaucophytes lost Chl *b* but retained the phycobili-pigments (and). After divergence of the glaucophytes, the precursor of red and green algae developed Chl *a*/*b*-containing LHC antennae ( ), which are present in both lineages. While the red algae retained PBS, the green algae lost them.

Age estimates based on fossil records and genomic data indicate that dispersal of cyanobacteria towards the open ocean, and the following diversification of marine cyanobacteria including the currently most abundant taxa *Synechococcus* and *Prochlorococcus*, occurred much later than primary endosymbiosis, between 1 and 0.5 billion years ago (Sanchez-Baracaldo et al. 2017). Green and red algae also began to colonize marine environments around 850–650 million years ago, i.e. early in their evolutionary history (Moreira et al. 2000; Parfrey et al. 2011). The ancient oxygenic phototrophs have had to compete amongst themselves and with the growing variety of other phototrophic species for the past 1.5–2 billion years, and matching light absorption to the available spectrum and niche differentiation likely played an important role in the survival and evolution of phototrophs.

Diversification of pigments

In the past millions to billions of years, the early oxygenic phototrophs and their descendants spread over many different aquatic and terrestrial environments, each with specific light spectra, thus urging the evolution of new photosynthetic pigments. Since light offers a spectrum of resources, species may coexist if they absorb different light colors (**chapter 5**; see also Stomp et al. 2004; Stomp et al. 2007a; Burson et al. 2018). Chl *b* and Chl *c* likely evolved from Chl *a*, as part of the light-harvesting antennae of species spreading to habitats with a lower light availability, dominated by blue and green light (Larkum 2006). Absorption by Chl *b* and Chl *c* is shifted towards the blue-green part and the orange-red part of the visible spectrum, relative to Chl *a* (see Table 1 in **chapter 1** and Fig. 2 in **chapter 2**). The former two types of Chl are suggested to have evolved in chloroxybacteria, and Chl *b* was passed on to cyanobacteria very early in evolution, as one of the earliest accessory pigments (Larkum 2006). Chl *b* later became the characteristic chlorophyll of green algae and all descending higher plants including land plants (Katz et al. 2004).

Although it is unclear when exactly, it has been suggested that phycobili-pigments evolved much later than Chl *a* and *b*, when the urgency to harvest light of other colors in the visible light spectrum increased (Apt et al. 1995; Larkum 2006). The evolution of PBS containing phycobili-pigments, absorbing additional light colors, will have allowed new branches of cyanobacteria to occupy available spectral niches. All phycobili-pigments are suggested to share one common ancestral protein (Apt et al. 1995; Kirilovsky and Büchel 2019), which eventually evolved into the allophycocyanin (APC) core and the rod phycobilins phycocyanobilin

(PCB), phycoviolobilin (PVB), phycoerythrobilin (PEB) and phycourobilin (PUB) (Zhao and Qin 2006; Kirilovsky and Büchel 2019).

The ancestral cyanobacterium that became the chloroplast of present-day algae and their descendants most likely already possessed Chl *a*, Chl *b*, phycobili-pigments and carotenoids, which explains why these pigments are found in prokaryotic cyanobacteria as well as eukaryotes (Tomitani et al. 1999; Moreira et al. 2000; Kirilovsky and Büchel 2019). After primary endosymbiosis, red algae (rhodophytes) and glaucophytes retained (parts of) the PBS, whereas green algae and their descendants (including all land plants) have lost the PBS (Hohmann-Marriott and Blankenship 2011). By contrast, Chl *b* was lost in most cyanobacterial species that are present today, but is present in the light-harvesting complex (LHC) of the superfamily of red algae and green algae. The precursor LHC likely evolved prior to the divergence of the green and red algae, and presumably after the divergence of the glaucophytes, which do not appear to have the classic LHC proteins (Wolfe et al. 1994; Koziol et al. 2007). In addition, green algae greatly diversified in carotenoids which allowed them to absorb more light of 400 to 520 nm, both in their photosystems and their LHCs (Katz et al. 2004; Takaichi 2011). Synthesis of carotenoids and chlorophylls is metabolically cheaper than synthesis of nitrogen-rich phycobilins (Green 2019), and hence the switch from PBS to LHC likely provided an advantage for eukaryotic algae that were already at a disadvantage due to their higher maintenance requirements.

Pcb antennae of prochlorophytes

Although Chl *b* is most abundant in the LHC of eukaryotic algae, amongst the cyanobacteria these chlorophylls (or their divinyl derivatives) can be found in the Chl *a*/*b*-binding (Pcb) antennae of the prochlorophyte *Prochlorococcus* and the two other known prochlorophytes *Prochloron didemni* and *Prochlorothrix hollandica* (Burger-Wiersma et al. 1985; Chisholm et al. 1988; Bullerjahn et al. 1990; La Roche et al. 1996; van der Staay et al. 1998; Bibby et al. 2003). Because Chl *b* is found in the antennae of these cyanobacteria as well as in green algae and plants, it was originally suggested that the ancestor of chloroplast-containing algae was a unicellular prochlorophyte-like cyanobacterium (Morden and Golden 1989). However, the genetic distance between prochlorophytes and chloroplasts and the molecular differences between their light-harvesting antennae seem too large to justify this hypothesis (Turner et al. 1989; Hess et al. 2001). The Pcb antennae of prochlorophytes are homologous to the CP43 antenna protein of cyanobacteria, rather than to the light-

harvesting Chl *a/b*–binding (LHC) proteins of plants (La Roche et al. 1996). Hence, most likely, the light-harvesting antennae of prochlorophytes and chloroplasts have evolved independently (La Roche et al. 1996; Koziol et al. 2007).

Our results suggest that the loss of PBS in cyanobacteria does not seem to inflict additional negative effects on biological fitness in blue-light dominated environments, as the PBS-less PAL mutant displayed similar (low) growth rates in blue light as the wildtype (**chapter 3**). *Prochlorococcus* is one of the two most abundant cyanobacterial species in the world, is found in the blue-light dominated waters of the subtropical open ocean and indeed does not contain PBS but instead uses Pcb antennae (Partensky et al. 1999; Scanlan and West 2002). While some argue that the ancient Pcb antennae evolved before the evolution of PBS (Chen and Bibby 2005), others suggest that *Prochlorococcus* evolved from a PBS-containing cyanobacterium (Scanlan and West 2002; Kettler et al. 2007) because some *Prochlorococcus* strains still have genes for the synthesis of phycoerythrin (Hess et al. 1996; Hess et al. 2001). Our results in **chapter 3** suggest that the transition of an expensive PBS that does not absorb blue light ≤ 450 nm, to a CP43-like chlorophyll-based light-harvesting antenna that allowed *Prochlorococcus* to efficiently utilize blue light, will have provided a major evolutionary advantage that allowed these cyanobacteria to thrive in the blue oceans.

Ecological niche distributions

Underwater light colors

Microalgae have dispersed over almost every imaginable habitat and estimates of the number of algal species reach into several tens of thousands (Guiry 2012). Many ecological studies have been dedicated to the investigation of this incredibly large diversity, but mostly focused on traits such as nutrient uptake and cell size (Merico et al. 2009, Kruk et al. 2010, Edwards et al. 2011). However, our results in **chapter 5** show that available light colors may be a strong predictor of the species found in specific environments. Differences in underwater light spectra seem to have been a major factor in the evolutionary diversification of phytoplankton, and may still play a large role in the present-day ecological distribution of many different species. We argue that including pigment composition, light absorption and light use efficiency in ecological studies will lead to improved understanding of the ecological distributions of phytoplankton species.

Phytoplankton species with different pigments are able to coexist if they can utilize different parts of the light spectrum and thereby avoid heavy competition (Stomp et al. 2004; 2007b). The underwater light spectrum may therefore influence competition between species (**chapter 5**; see also Stomp et al. 2007a; Kirk 2011). Because water molecules absorb strongly in the red part of the light spectrum, blue is the dominant light color in clear waters, such as the oligotrophic ocean (Stomp et al. 2007a; Kirk 2011). In more turbid waters, dissolved organic matter absorbs strongly in the blue part of the light spectrum, which may shift the available underwater light color towards green, or even red wavelengths at high concentrations (see Fig. 4 in **chapter 1**). Phytoplankton species have adapted to these different habitats by tuning their photosynthetic pigments to the available underwater light colors.

It seems counterintuitive that the two most abundant marine phytoplankton species are cyanobacteria, which generally have a low photosynthetic efficiency in blue light. Yet, the marine cyanobacteria *Prochlorococcus* and *Synechococcus* flourish in the open ocean (Flombaum et al. 2013), where blue light dominates the underwater light spectrum. *Prochlorococcus* is the most dominant phytoplankton species in the clear blue waters of the oligotrophic subtropical oceans. It has exchanged its PBS for divinyl-Chl *a*/*b* binding Pcb antennae. Hence, similar to the chlorophyll-based light-harvesting antennae of green algae, its antennae effectively absorb blue light (**chapter 5**; see also Partensky et al. 1999; Ting et al. 2002).

Synechococcus strains are also widespread in marine environments, including the open ocean where *Synechococcus* strains with high contents of the phycobili-pigment PUB coexist with *Prochlorococcus* (Six et al. 2007; Grébert et al. 2018). The absorption maximum of PUB is at ~495 nm, which touches the blue part of the visible spectrum (Fig. 4). If blue photons would be absorbed by the PBS of these PUB-rich strains, they would be able to redistribute excitation energy between PSI and PSII, thereby avoiding the excitation imbalance observed in PBS-containing cyanobacteria rich in PCB. However, absorption spectra (Fig. 4; see also Six et al. 2007, Küpper et al. 2009) and fluorescence excitation spectra (Sanfilippo et al. 2019) show that blue-green wavelengths in the range 470-520 are absorbed and transferred by PUB, but absorption and transfer of wavelengths ≤ 450 nm by PUB is negligibly low. *Synechococcus* strains with a high PUB content are therefore specialized on the blue-green (cyan) part of the light spectrum, but are unlikely to efficiently use blue light ≤ 450 nm (Fig. 4).

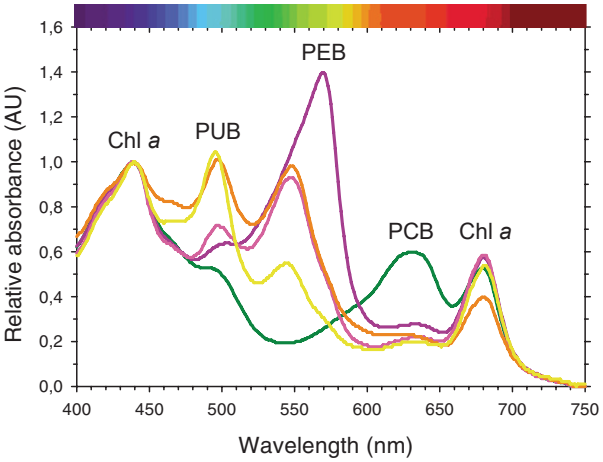

Figure 4 | Whole-cell absorption spectra of *Synechococcus* strains using different phycobili-pigments. Absorption peaks of photosynthetic pigments are indicated: Chl *a*: chlorophyll *a*; PUB: phycourobilin; PEB: phycoerythrobilin; PCB: phycocyanobilin. Adapted from Six et al. (2007), reprinted with permission of Springer Nature.

Our model results predict that *Prochlorococcus* will outcompete *Synechococcus* containing PUB and PEB in the clearest open ocean waters where blue light of ≤ 450 nm dominates the underwater light spectrum (Fig. 6 in **chapter 5**). Future research with laboratory competition experiments between *Prochlorococcus* and *Synechococcus* are recommended to confirm these model predictions. Furthermore, our expectation is that PUB-rich *Synechococcus* strains may coexist with *Prochlorococcus* in slightly more productive open ocean waters, where blue-green wavelengths prevail. Therefore, additional competition experiments and model exercises performed at slightly longer wavelengths (between 450 and 490 nm) can aid in determining until which wavelength PUB still contributes substantially to cyanobacterial photosynthesis. The results of these models and experiments may further increase our understanding of the gradual shift in the competitive balance between *Prochlorococcus* and *Synechococcus*, and the biogeographical distributions of these major phytoplankton species.

Ecological niches of *Prochlorothrix* and *Acaryochloris*

Like *Prochlorococcus*, *Prochlorothrix hollandica* uses Pcb antennae; but instead of the oligotrophic blue ocean, this freshwater prochlorophyte is found in the eutrophic lake Loosdrecht in The Netherlands (Burger-Wiersma et al. 1989; Matthijs et al. 1989). The underwater light

spectrum of this turbid peat lake is dominated by red light because high amounts of dissolved organic carbon absorb most of the light in the blue and green ranges of the visible light spectrum (Stomp et al. 2007a; Kirk 2011; see also Fig. 4 in **chapter 1**). Hence, in this case, the loss of PBS and evolution of chlorophyll-based Pcb antennae cannot be attributed to the predominance of blue light, but may be associated with the poor performance of PBS-containing cyanobacteria in red light ≥680 nm. In **chapter 2**, we hypothesized that red light ≥680 nm may result in a low light-use efficiency of PBS-containing cyanobacteria, comparable to blue light ≤ 450 nm. PBS do not absorb red light ≥680 nm effectively (Lemasson et al. 1973; Tandeau de Marsac 2003; MacColl 2004). However, wavelengths ≥680 nm are strongly absorbed by Chl *a*, like blue light, and hence we expect a similar excitation imbalance between PSI and PSII in red light ≥680 nm as in blue light ≤ 450 nm.

In agreement with this expectation, other studies have found low PSI:PSII ratios (Murakami 1997) and growth rates (Hübschmann et al. 2005; Bland and Angenent 2016) in PBS-containing cyanobacteria in red light ≥680 nm, comparable to our findings in blue light. In addition, our results from **chapter 4** and the results of Hübschmann et al. (2005) show that many genes involved in photosynthesis and growth are similarly regulated in blue and in far-red light. These findings support our hypothesis that both blue light ≤ 450 nm and red light ≥680 nm, both specifically targeting Chl *a*, result in an excitation imbalance between the two photosystems of PBS-containing cyanobacteria. Hence, in the red-light dominated environments where *P. hollandica* is found, the PBS would be as inefficient as it is in blue light. Accordingly, the use of chlorophyll-based light harvesting antennae will have allowed this unique species to dominate in the red-light dominated waters of lake Loosdrecht.

Interestingly, the recently discovered cyanobacterium *Acaryochloris marina* also uses Pcb-like light-harvesting antennae, rather than PBS (Miyashita et al. 1996; Chen et al. 2005). However, in contrast to the Pcb antennae of prochlorophytes, the Pcb antennae of *A. marina* contain Chl *d* which facilitates absorption in the near-infrared (~715 nm) and has thus far only been found in this cyanobacterial clade (Chen 2014). The clade of *A. marina* is found in a wide range of aquatic and terrestrial environments where far-red light dominates, such as biofilms, sediments and stromatolites (Loughlin et al. 2013). The acquisition of Chl *d* by *A. marina* can thus be viewed as a more extreme case of adaptation to red and near-infrared wavelengths than the acquisition of Chl *b* by *P. hollandica*.

Changes in the underwater light spectrum

The underwater light spectrum is not a static characteristic; in particular, coastal areas and lakes are strongly influenced by the inflow of organic matter and sediments from terrestrial sources. If the inflow of dissolved organic carbon (DOC) changes, the underwater light color changes towards longer wavelengths in the orange and red regions of the visible spectrum, a process also known as "lake browning" (Roulet and Moore 2006). Recently, many lakes across northern Europe, Canada and the USA have been shown to shift from clear blue and green waters to brown and murky waters (Monteith et al. 2007; Larsen et al. 2011; Leech et al. 2018).

Concurrently, many lakes have recently seen a strong increase in the frequency and intensity of (potentially toxic) cyanobacterial blooms (Paerl and Huisman 2009; Carmichael and Boyer 2016; Huisman et al. 2018). The increased incidence of cyanobacterial blooms has often been attributed to increased temperatures and nutrient availability as a consequence of global warming and eutrophication. However, DOC concentrations have also been shown to increase in many lakes (Monteith et al. 2007; Larsen et al. 2011; Weyhenmeyer et al. 2016; Kritzberg 2017), which shifts the underwater light color towards orange and red wavelengths. This may have strong effects on species composition, as our results indicate that a shift in underwater light color from blue and green towards orange and red will favor phytoplankton species using PCB, such as cyanobacteria and cryptophytes, at the expense of cyanobacteria using PUB and PEB, green algae and diatoms (**chapter 5**; see also Stomp et al. 2007b). Indeed, lake browning often leads to increasing relative abundances of cyanobacteria (Ekvall et al. 2013; Leech et al. 2018; Feuchtmayr et al. 2019) and cryptophytes (Deininger et al. 2017; Urrutia-Cordero et al. 2017; Wilken et al. 2018). Similar to cyanobacteria, cryptophytes can also utilize PCB to absorb orange light (Cunningham et al. 2019; Greenwold et al. 2019). Hence, although other aspects may contribute to the competitive success of these species in browning lakes, such as the mixotrophic feeding behavior of cryptophytes (Urrutia-Cordero et al. 2017; Wilken et al. 2018), changes in light color may play a key role as well.

In agreement with this prediction, Tan et al. (2020) showed that the toxic cyanobacterium *Microcystis aeruginosa*, which uses orange-light absorbing PCB in its PBS, outcompeted green algae in orange-red light but lost this competition in blue light, similar to our competition experiments in **chapter 5**. In addition, Tan et al. (2017) showed two years earlier that orange-red light is the dominant underwater light color in a harmful bloom of *M. aeruginosa* in lake Taihu. Hence, while blooms

of toxic cyanobacteria are often attributed to eutrophication and global change (O'Neil et al. 2012; Huisman et al. 2018), our results show that the change in underwater light colors may play an equally important role. This hypothesis could be verified by more extensive monitoring of the underwater light spectra of lakes and by extending our model described in **chapter 5** to other phytoplankton species that use phycobili-pigments, such as red algae and cryptophytes.

Concluding remarks

While the important role of phytoplankton pigments is widely recognized, many (ecological) studies have focused mostly on other functional traits such as nutrient uptake and cell size (Merico et al. 2009; Kruk et al. 2010; Edwards et al. 2013). However, the results described in this thesis show that light color is of pivotal importance in ecological studies and thus deserves more attention. In particular, our results demonstrate the importance of light absorption by the light-harvesting antennae, which allows oxygenic phototrophs to adapt to environments dominated by different underwater light colors. The wide diversity of phytoplankton pigments and light-harvesting strategies has strong implications for their use in biotechnological applications, but also explains the evolutionary divergence of phytoplankton taxa and helps in predicting present and future ecological distributions of different phytoplankton species. The resource competition model we have developed may aid in further investigation of competitive interactions and global distributions of phytoplankton species, which may prove particularly important since the underwater light spectrum of many lakes and coastal waters is changing.

References

Agostoni M, Waters CM, Montgomery BL (2016) Regulation of biofilm formation and cellular buoyancy through modulating intracellular cyclic di-GMP levels in engineered cyanobacteria. Biotechnol Bioeng 113: 311-319

Aguirre von Wobeser E, Ibelings BW, Bok J, Krasikov V, Huisman J, Matthijs HCP (2011) Concerted changes in gene expression and cell physiology of the cyanobacterium *Synechocystis* sp. strain PCC 6803 during transitions between nitrogen and light-limited growth. Plant Physiol 155: 1445-1457

Ajlani G, Vernotte C, DiMagno L, Haselkorn R (1995) Phycobilisome core mutants of *Synechocystis* PCC 6803. Biochim Biophys Acta Bioen 1231: 189-196

Ajlani G, Vernotte C (1998) Construction and characterization of a phycobiliprotein-less mutant of *Synechocystis* sp. PCC 6803. Plant Mol Biol 37: 577-580

Allahverdiyeva Y, Mustila H, Ermakova M, Bersanini L, Richaud P, Ajlani G, Battchikova N, Cournac L, Aro EM (2013) Flavodiiron proteins Flv1 and Flv3 enable cyanobacterial growth and photosynthesis under fluctuating light. Proc Natl Acad Sci USA. 110: 4111-4116

Allahverdiyeva Y, Suorsa M, Tikkanen M, Aro EM (2014) Photoprotection of photosystems in fluctuating light intensities. J Exp Bot 66: 2427-2436

Allahverdiyeva Y, Isojärvi J, Zhang P, Aro EM (2015) Cyanobacterial oxygenic photosynthesis is protected by flavodiiron proteins. Life 5: 716-743

Allen JF (2003) Cyclic, pseudocyclic and noncyclic photophosphorylation: new links in the chain. Trends Plant Sci 8: 15-19

Allen JF (2003) State transitions--a question of balance. Science 299:1530-1532

Ananyev G, Dismukes GC (2005) How fast can photosystem II split water? Kinetic performance at high and low frequencies. Photosynth Res 84: 355-365

Andrizhiyevskaya EG, Chojnicka A, Bautista JA, Diner BA, van Grondelle R, Dekker JP (2005) Origin of the F685 and F695 fluorescence in photosystem II. Photosynth Res 84: 173-180

Angelis S, Novak AC, Sydney EB, Soccol VT, Carvalho JC, Pandey A, Noseda MD, Tholozan JL, Lorquin J, Soccol CR (2012) Co-culture of microalgae, cyanobacteria, and macromycetes for exopolysaccharides production: process preliminary optimization and partial characterization. Appl Biochem Biotechnol 167: 1092-1106

Appleby JL, Parkinson JS, Bourret RB (1996) Signal transduction via the multi-step phosphorelay: not necessarily a road less traveled. Cell 86: 845-848

Apt KE, Collier JL, Grossman AR (1995) Evolution of the phycobiliproteins. J Mol Biol 248: 79-96

Arnold W, Oppenheimer JR (1950) Internal conversion in the photosynthetic mechanism of blue-green algae. J Gen Physiol 33: 423-435

Atamna-Ismaeel N, Sabehi G, Sharon I, Witzel KP, Labrenz M, Jürgens K, Barkay T, Stomp M, Huisman J, Béjà O (2008) Widespread distribution of proteorhodopsins in freshwater and brackish ecosystems. ISME J 2: 656-662

Baier K, Nicklisch S, Grundner C, Reinecke J, Lockau W (2001) Expression of two *nblA*-homologous genes is required for phycobilisome degradation in nitrogen-starved *Synechocystis* sp. PCC6803. FEMS Microbiol Lett 195: 35-39

Bañares-España E, Kromkamp JC, López-Rodas V, Costas E, Flores-Moya A (2013) Photoacclimation of cultured strains of the cyanobacterium *Microcystis aeruginosa* to high-light and low-light conditions. FEMS Microbiol Ecol 83: 700-710

Bapteste E, Walsh DA (2005) Does the 'Ring of Life' ring true? Trends Microbiol 13: 256-261

Beer LL, Boyd ES, Peters JW, Posewitz MC (2009) Engineering algae for biohydrogen and

biofuel production. Curr Opin Biotechnol 20: 264-271
Béjà O, Aravind L, Koonin EV, Suzuki MT, Hadd A, Nguyen LP, Jovanovich SB, Gates CM, Feldman RA, Spudich JL, Spudich EN, DeLong EF (2002) Bacterial rhodopsin: evidence for a new type of phototrophy in the sea. Science 289: 1902-1906
Berera R, van Stokkum IHM, d'Haene S, Kennis JTM, van Grondelle R, Dekker JP (2009) A mechanism of energy dissipation in cyanobacteria. Biophys J 96: 2261-2267
Bernát G, Waschewski N, Rögner M (2009) Towards efficient hydrogen production: the impact of antenna size and external factors on electron transport dynamics in *Synechocystis* PCC 6803. Photosynth Res 99: 205-216
Berner RA (1999) Atmospheric oxygen over Phanerozoic time. Proc Natl Acad Sci USA 96: 10955-10957
Bersanini L, Battchikova N, Jokel M, Rehman A, Vass I, Allahverdiyeva Y, Aro EM (2014) Flavodiiron protein Flv2/Flv4-related photoprotective mechanism dissipates excitation pressure of PSII in cooperation with phycobilisomes in cyanobacteria. Plant Physiol 164: 805-818
Bhattacharya D, Medlin L (1998) Algal phylogeny and the origin of land plants. Plant Physiol 116: 9-15
Bhaya D, Bianco NR, Bryant D, Grossman A (2000) Type IV pilus biogenesis and motility in the cyanobacterium *Synechocystis* sp. PCC6803. Mol Microbiol 37: 941-951
Bhaya D, Takahashi A, Grossman AR (2001) Light regulation of type IV pilus-dependent motility by chemosensor-like elements in *Synechocystis* PCC6803. Proc Natl Acad Sci USA 98: 7540-7545
Bibby TS, Nield J, Barber J (2001) Iron deficiency induces the formation of an antenna ring around trimeric photosystem I in cyanobacteria. Nature 412: 743-745
Bibby TS, Nield J, Chen M, Larkum AW, Barber J (2003) Structure of a photosystem II supercomplex isolated from *Prochloron didemni* retaining its chlorophyll *a*/*b* light-harvesting system. Proc Natl Acad Sci USA 100: 9050-9054
Biller SJ, Berube PM, Lindell D, Chisholm SW (2015) *Prochlorococcus*: the structure and function of collective diversity. Nature Rev Microbiol 13: 13-27
Billis K, Billini M, Tripp HJ, Kyrpides NC, Mavromatis K (2014) Comparative transcriptomics between *Synechococcus* PCC 7942 and *Synechocystis* PCC 6803 provide insights into mechanisms of stress acclimation. PLoS One 9: e109738
Bland E, Angenent LT (2016) Pigment-targeted light wavelength and intensity promotes efficient photoautotrophic growth of cyanobacteria. Biores Technol 216: 579-586
Blankenship RE, Chen M (2013) Spectral expansion and antenna reduction can enhance photosynthesis for energy production. Curr Opin Chem Biol 17: 457-461
Blankenship RE (2014) Molecular mechanisms of photosynthesis, Second Edition. John Wiley & Sons, West Sussex, UK
Boekema EJ, Hifney A, Yakushevska AE, Piotrowski M, Keegstra W, Berry S, Michel K-P, Pistorius EK, Kruip J (2001) A giant chlorophyll-protein complex induced by iron deficiency in cyanobacteria. Nature 412: 745-748
Boulay C, Abasova L, Six C, Vass I, Kirilovsky D (2008) Occurrence and function of the orange carotenoid protein in photoprotective mechanisms in various cyanobacteria. Biochim Biophys Acta Bioen 1777: 1344-1354
Branco dos Santos F, Du W, Hellingwerf KJ (2014) *Synechocystis*: not just a plug-bug for CO_2, but a green *E. coli*. Front Bioeng Biotech 2: 36
Braslavsky SE, Holzwarth AR (2012) Role of carotenoids in photosystem II (PSII) reaction centers. Int J Thermophys 33: 2021-2025
Brecht M, Skandary S, Hellmich J, Glöckner C, Konrad A, Hussels M, Meixner AJ, Zouni A, Schlodder E (2014). Spectroscopic properties of photosystem II core complexes from *Thermosynechococcus elongatus* revealed by single-molecule experiments. Biochim Biophys Acta 1837: 773-781
Bryant DA (1994) The molecular biology of cyanobacteria. Dordrecht: Kluwer Academic

Press, Dordrecht, The Netherlands
Bryant DA, Frigaard NU (2006) Prokaryotic photosynthesis and phototrophy illuminated. Trends Microbiol 11: 488-496
Bullerjahn GS, Jensen TC, Sherman DM, Sherman LA (1990) Immunological characterization of the *Prochlorothrix hollandica* and *Prochloron* sp. chlorophyll *a*/*b* antenna proteins. FEMS Microbiol Lett 67: 99-105
Burger-Wiersma T, Veenhuis M, Korthals H, van de Wiel CCM, Mur LR (1986) A new prokaryote containing chlorophylls *a* and *b*. Nature 320: 262-264
Burger-Wiersma T, Stal LJ, Mur LR (1989) *Prochlorothrix hollandica* gen. nov. sp. nov., a filamentous oxygenic photoautotrophic procaryote containing chlorophylls *a* and *b*: assignment to *Prochlorotrichaceae* fam. nov. and order *Prochlorales* Florenzano, Balloni, and Materassi 1986, with omendation of the ordinal description. Int J Syst Evol Microbiol 39: 250-257
Burson A, Stomp M, Greenwell E, Grosse J, Huisman J (2018) Competition for nutrients and light: testing advances in resource competition with a natural phytoplankton community. Ecology 99: 1108-1118
Burson A, Stomp M, Mekkes L, Huisman J (2019) Stable coexistence of equivalent nutrient competitors through niche differentiation in the light spectrum. Ecology 100: e02873
Calzadilla PI, Zhan J, Sétif P, Lemaire C, Solymosi D, Battchikova N, Wang Q, Kirilovsky D (2019) The cytochrome b_6f complex is not involved in cyanobacterial state transitions. Plant Cell 31: 911-931
Campbell D (1996) Complementary chromatic adaptation alters photosynthetic strategies in the cyanobacterium *Calothrix*. Microbiology 142: 1255-1263
Campbell D, Hurry V, Clarke AK, Gustafsson P, Öquist G (1998) Chlorophyll fluorescence analysis of cyanobacterial photosynthesis and acclimation. Microbiol Mol Biol Rev 62: 667-683
Campbell DA, Tyystjärvi E (2012) Parameterization of photosystem II photoinactivation and repair. Biochim Biophys Acta Bioen 1817: 258-265
Capra EJ, Laub MT (2012) Evolution of two-component signal transduction systems. Annu Rev Microbiol 66: 325-347
Carmichael WW, Boyer GL (2016) Health impacts from cyanobacteria harmful algae blooms: Implications for the North American Great Lakes. Harmful Algae 54: 194-212
Chen M, Bibby TS (2005) Photosynthetic apparatus of antenna-reaction centres supercomplexes in oxyphotobacteria: insight through significance of Pcb/IsiA proteins. Photosynth Res 86: 165-173
Chen M, Hiller RG, Howe CJ, Larkum AWD (2005) Unique origin and lateral transfer of prokaryotic chlorophyll-*b* and chlorophyll-*d* light-harvesting systems. Mol Biol Evol 22: 21-28
Chen HB, Wu JY, Wang CF, Fu CC, Shieh CJ, Chen CI, Wang CY, Liu YC (2010) Modeling on chlorophyll *a* and phycocyanin production by *Spirulina platensis* under various light-emitting diodes. Biochem Eng J 53: 52-56
Chen M, Schliep M, Willows RD, Cai ZL, Neilan BA, Scheer H (2010) A red-shifted chlorophyll. Science 329:1318-1319
Chen M (2014) Chlorophyll modifications and their spectral extension in oxygenic photosynthesis. Annu Rev Biochem 83: 317-340
Chen HYS, Bandyopadhyay APHB, Pakrasi HB (2018) Function, regulation and distribution of IsiA, a membrane-bound chlorophyll a-antenna protein in cyanobacteria. Photosynthetica 56: 322-333
Cheregi O, Sicora C, Kós PB, Barker M, Nixon PJ, Vass I (2007) The role of the FtsH and Deg proteases in the repair of UV-B radiation-damaged photosystem II in the cyanobacterium *Synechocystis* PCC 6803. Biochimica et Biophysica Acta 1767:

820-828
Chisholm SW, Olson RJ, Zettler ER, Goericke R, Waterbury JB, Welschmeyer NA (1988) A novel free-living prochlorophyte abundant in the oceanic euphotic zone. Nature 334: 340-343
Chisholm SW, Frankel SL, Goericke R, Olson RJ, Palenik B, Waterbury JB, West-Johnsrud L, Zettler ER (1992) *Prochlorococcus marinus* nov. gen. nov. sp.: an oxyphototrophic marine prokaryote containing divinyl chlorophyll *a* and *b*. Arch Microbiol 157:297-300
Choi CY, Kim NN, Shin HS, Park HG, Cheon S, Kil G (2013) The effect of various wavelengths of light from light-emitting diodes on the antioxidant system of marine cyanobacteria, *Synechococcus* sp. Mol Cell Toxicol 9: 295-302
Chukhutsina V, Bersanini L, Aro EM, van Amerongen H (2015) Cyanobacterial *flv4-2* operon-encoded proteins optimize light harvesting and charge separation in photosystem II. Plant Physiol 8: 747-761
Chukhutsina V, Bersanini L, Aro EM, van Amerongen H (2015) Cyanobacterial light-harvesting phycobilisomes uncouple from photosystem I during dark-to-light transitions. Sci Rep 5: 14193
Collins AM, Liberton M, Jones HD, Garcia OF, Pakrasi HB, Timlin JA (2012) Photosynthetic pigment localization and thylakoid membrane morphology are altered in *Synechocystis* 6803 phycobilisome mutants. Plant Physiol 158: 1600-1609
Conradi FD, Zhou RQ, Oeser S, Schuergers N, Wilde A, Mullineaux CW (2019) Factors controlling floc formation and structure in the cyanobacterium *Synechocystis* sp. strain PCC 6803. J Bacteriol 201:e00344-19. 10.1128/JB.00344-19
Croce R, van Amerongen H (2014) Natural strategies for photosynthetic light harvesting. Nature Chem Biol 10:492-501
Cunningham BR, Greenwold MJ, Lachenmyer EM, Heidenreich KM, Davis AC Dudycha JL, Richardson TL (2018) Light capture and pigment diversity in marine and freshwater cryptophytes. J Phycol 55:552-564
Darwin C (1859) On the origin of species by means of natural selection, or the preservation of favoured races in the struggle for life. John Murray, London
de Mazancourt C, Schwartz MW (2012) Starve a competitor: evolution of luxury consumption as a competitive strategy. Theor Ecol 5: 37-49
de Mooij T, Janssen M, Cerezo-Chinarro O, Mussgnug JH, Kruse O, Ballottari M, Bassi R, Bujaldon S, Wollman F, Wijffels RH (2015) Antenna size reduction as a strategy to increase biomass productivity: a great potential not yet realized. J Appl Phycol 27: 1063-1077
de Mooij T, de Vries G, Latsos C, Wijffels RH, Janssen M (2016) Impact of light color on photobioreactor productivity. Algal Res 15: 32-42
Deininger A, Faithfull CL, Bergström A-K (2017) Phytoplankton response to whole lake inorganic N fertilization along a gradient in dissolved organic carbon. Ecology 98: 982-994
Demmig-Adams B (1990) Carotenoids and photoprotection in plants: a role for the xanthophyll zeaxanthin. Biochim Biophys Act Bioeng 1020:1-24
Du W, Jongbloets JA, Hernández HP, Bruggeman FJ, Hellingwerf KJ, Branco dos Santos F (2016) Photonfluxostat: a method for light-limited batch cultivation of cyanobacteria at different, yet constant, growth rates. Algal Res 20: 118-125
Dutkiewicz S, Hickman AE, Jahn O, Henson S, Beaulieu C, Monier E (2019) Ocean colour signature of climate change. Nature Comm 10: 578
Duysens LNM (1951) Transfer of light energy within the pigment systems present in photosynthesizing cells. Nature 168: 548-550
Eberhard S, Finazzi G, Wollman FA (2008) The dynamics of photosynthesis. Annu Rev Gen 42:463-515
Edelstein-Keshet L (1988) Mathematical models in biology. Random House, New York

Edwards KF, Klausmeier CA, Litchman E (2011) Evidence for a three-way trade-off between nitrogen and phosphorus competitive abilities and cell size in phytoplankton. Ecology 92: 2085-2095

Edwards KF, Litchman E, Klausmeier CA (2013) Functional traits explain phytoplankton community structure and seasonal dynamics in a marine ecosystem. Ecol Lett 16: 56-63

Edwards KF, Thomas MK, Klausmeier CA, Litchman E (2015) Light and growth in marine phytoplankton: allometric, taxonomic, and environmental variation. Limnol Oceanography 60: 540-552

Eisenhut M, Von Wobeser EA, Jonas L, Schubert H, Ibelings BW, Bauwe H, Matthijs HCP, Hagemann M (2007) Long-term response toward inorganic carbon limitation in wild type and glycolate turnover mutants of the cyanobacterium *Synechocystis* sp. strain PCC 6803. Plant Physiol 144: 1946-1959

Ekvall MK, de la Calle Martin, J., Faassen EJ, Gustafsson S, Lürling M, Hansson L (2013) Synergistic and species-specific effects of climate change and water colour on cyanobacterial toxicity and bloom formation. Freshwat Biol 58: 2414-2422

El Bissati K, Kirilovsky D (2001) Regulation of *psbA* and *psaE* expression by light quality in *Synechocystis* species PCC 6803: a redox control mechanism. Plant Physiol 125: 1988-2000

Emerson R, Lewis CM (1942) The photosynthetic efficiency of phycocyanin in *Chroococcus*, and the problem of carotenoid participation in photosynthesis. J Gen Physiol 25: 579-595

Engelmann TW (1882) Über Sauerstoffausscheidung von Pflanzenzellen im Mikrospektrum. Pflug Arch Eur J Phy 27: 485-489

Engelmann TW (1883) Farbe und Assimilation. I. Assimilation findet nur in den farbstoffhaltigen Plasmatheilchen statt. II. Näherer Zusammenhang zwischen Lichtabsorption und Assimilation. III. Weitere Folgerungen. Bot Zeit 41: 1-29

Engelmann TW (1884) Untersuchungen über die quantitativen Beziehungen zwischen Absorption des Lichtes und Assimilation in Pflanzenzellen. Bot Zeit 44: 43-52

Enomoto G, Ni-Ni-Win, Narikawa R, Ikeuchi M (2015) Three cyanobacteriochromes work together to form a light color-sensitive input system for c-di-GMP signaling of cell aggregation. Proc Natl Acad Sci USA 112: 8082-8087

Everroad C, Six C, Partensky F, Thomas JC, Holtzendorff J, Wood AM (2006) Biochemical bases of type IV chromatic adaptation in marine *Synechococcus* spp. J Bacteriol 188: 3345-3356

Falkowski PG (2006) Tracing oxygen's imprint on Earth's metabolic evolution. Science 311: 172-1725

Falkowski PG (2012) The power of plankton. Nature 483: S17-S20

Feuchtmayr H, Pottinger TG, Moore A, De Ville MM, Caillouet L, Carter HT, Pereira MG, Maberly SC (2019) Effects of brownification and warming on algal blooms, metabolism and higher trophic levels in productive shallow lake mesocosms. Sci Total Environ 678: 227-238

Fiedler B, Börner T, Wilde A (2005) Phototaxis in the cyanobacterium *Synechocystis* sp. PCC 6803: role of different photoreceptors. Photochem Photobiol 81: 1481-1488

Field CB, Behrenfeld MJ, Randerson JT, Falkowski P (1998) Primary production of the biosphere: integrating terrestrial and oceanic components. Science 281:237-240

Figueroa FL, Aguilera J, Niell FX (1995) Red and blue light regulation of growth and photosynthetic metabolism in *Porphyra umbilicalis* (Bangiales, Rhodophyta). Eur J Phycol 30: 11-18

Finkel ZV (2001) Light absorption and size scaling of light-limited metabolism in marine diatoms. Limnol Oceanography 46: 86-94

Flombaum P, Gallegos JL, Gordillo RA, Rincon J, Zabala LL, Jiao N, Karl DM, Li WKW, Lomas MW, Veneziano D, Vera CS, Vrugt JA, Martiny AC (2013) Present and future global

distributions of the marine cyanobacteria *Prochlorococcus* and *Synechococcus*. Proc Natl Acad Sci USA 110: 9824-9829

Fujiki T, Taguchi S (2002) Variability in chlorophyll *a* specific absorption coefficient in marine phytoplankton as a function of cell size and irradiance. J Plankton Res 24: 859-874

Fujita Y (1997) A study on the dynamic features of photosystem stoichiometry: accomplishments and problems for future studies. Photosynth Res 53: 83-93

Gerardo ML, van den Hende S, Vervaeren H, Coward T, Skill SC (2015) Harvesting of microalgae within a biorefinery approach: A review of the developments and case studies from pilot-plants. Algal Res 11: 248-262

Gill RT, Katsoulakis E, Schmitt W, Taroncher-Oldenburg G, Misra J, Stephanopoulos G (2002) Genome-wide dynamic transcriptional profiling of the light-to-dark transition in *Synechocystis* sp. strain PCC 6803. J Bacteriol 184: 3671-3681

Glazer AN, Bryant DA (1975) Allophycocyanin B (λ_{max} 671, 618 nm). Arch Microbiol 104: 15-22

Goedheer JC (1969) Energy transfer from carotenoids to chlorophyll in blue-green, red and green algae and greening bean leaves. Biochim Biophys Acta Bioeng 172: 252-265

Gogarten JP, Townsend JP (2005) Horizontal gene transfer, genome innovation and evolution. Nature Rev Microbiol 3: 679-687

Gonçalves AL, Pires JCM, Simões M (2016) Biotechnological potential of *Synechocystis salina* co-cultures with selected microalgae and cyanobacteria: Nutrients removal, biomass and lipid production. Biores Technol 200: 279-286

Gorbunov MY, Kuzminov FI, Fadeev VV, Kim JD, Falkowski PG (2011) A kinetic model of non-photochemical quenching in cyanobacteria. Biochim Biophys Acta 1807: 1591-1599

Grébert T, Doré H, Partensky F, Farrant GK, Boss ES, Picheral M, Guidi L, Pesant S, Scanlan DJ, Wincker P, Acinas SG, Kehoe DM, Garczarek L (2018) Light color acclimation is a key process in the global ocean distribution of *Synechococcus* cyanobacteria. Proc Natl Acad Sci USA 115: E2010–E2019

Green BR (2019) What happened to the phycobilisome? Biomolecules 9: 748

Greenwold MJ, Cunningham BR, Lachenmyer EM, Pullman JM, Richardson TL, Dudycha JL (2019) Diversification of light capture ability was accompanied by the evolution of phycobiliproteins in cryptophyte algae. Proc R Soc B 286: 20190655

Grossman AR, Schaefer MR, Chiang GG, Collier JL (1993) The phycobilisome, a light-harvesting complex responsive to environmental conditions. Microbiol Rev 57: 725-749

Grover JP (1989) Influence of cell shape and size on algal competitive ability. J Phycol 25: 402-405

Grover JP (1997) Resource competition. Chapman & Hall, London, UK

Guiry MD (2012) How many species of algae are there? J Phycol 48: 1057-1063

Guskov A, Kern J, Gabdulkhakov A, Broser M, Zouni A, Saenger W (2009) Cyanobacterial photosystem II at 2.9-Å resolution and the role of quinones, lipids, channels and chloride. Nat Struct Mol Biol 16: 334-342

Gust D, Kramer D, Moore A, Moore TA, Vermaas W (2008) Engineered and artificial photosynthesis: human ingenuity enters the game. MRS bulletin 33: 383-387

Hakala M, Tuominen I, Keränen M, Tyystjärvi T, Tyystjärvi E (2005) Evidence for the role of the oxygen-evolving manganese complex in photoinhibition of photosystem II. Biochim Biophys Acta Bioen 1706: 68-80

Havaux M, Guedeney G, Hagemann M, Yeremenko N, Matthijs HCP, Jeanjean R (2005) The chlorophyll-binding protein IsiA is inducible by high light and protects the cyanobacterium *Synechocystis* PCC6803 from photooxidative stress. FEBS Lett 579: 2289-2293

Haverkamp THA, Schouten D, Doeleman M, Wollenzien U, Huisman J, Stal LJ (2009) Colorful microdiversity of *Synechococcus* strains (picocyanobacteria) isolated from the Baltic Sea. ISME J 3: 397-408

Hellingwerf KJ, Teixeira de Mattos MJ (2009) Alternative routes to biofuels: light-driven biofuel formation from CO_2 and water based on the 'photanol' approach. J Biotechnol 142: 87-90

Heo J, Lee C, Chakrabarty D, Paek K (2002) Growth responses of marigold and salvia bedding plants as affected by monochromic or mixture radiation provided by a light-emitting diode (LED). J Plant Growth Regul 38: 225-230

Herrero A, Flores E (2008) The Cyanobacteria: molecular biology, genomics and evolution. Caister Academic Press, Sevilla, Spain

Hess WR, Partensky F, Van der Staay GWM, Garcia-Fernandez JM, Börner T, Vaulot D (1996) Coexistence of phycoerythrin and a chlorophyll *a/b* antenna in a marine prokaryote. Proc Natl Acad Sci USA 93: 11126-11130

Hess WR, Rocap G, Ting CS, Larimer F, Stilwagen S, Lamerdin J, Chisholm SW (2001) The photosynthetic apparatus of *Prochlorococcus*: insights through comparative genomics. Photosynth Res 70: 53-71

Hihara Y, Kamei A, Kanehisa M, Kaplan A, Ikeuchi M (2001) DNA microarray analysis of cyanobacterial gene expression during acclimation to high light. Plant Cell 13: 793-806

Hirose Y, Shimada T, Narikawa R, Katayama M, Ikeuchi M (2008) Cyanobacteriochrome CcaS is the green light receptor that induces the expression of phycobilisome linker protein. Proc Natl Acad Sci USA 105: 9528-9533

Hohmann-Marriott MF, Blankenship RE (2011) Evolution of photosynthesis. Annu Rev Plant Biol 62: 515-548

Holland HD (2002) Volcanic gases, black smokers, and the Great Oxidation Event. Geochim Cosmochim Acta 66: 3811-3826

Holland HD (2006) The oxygenation of the atmosphere and oceans. Phil Trans R Soc B 361: 903-915

Hu G, Fan Y, Zheng Y, Xu F, Zhang L, Li F (2019) Photoprotection capacity of microalgae improved by regulating the antenna size of light-harvesting complexes. J Appl Phycol https://doi.org/10.1007/s10811-019-01969-5

Huang L, McCluskey MP, Ni H, LaRossa RA (2002) Global gene expression profiles of the cyanobacterium *Synechocystis* sp. strain PCC 6803 in response to irradiation with UV-B and white light. J Bacteriol 184: 6845-6858

Hübschmann T, Yamamoto H, Gieler T, Murata N, Börner T (2005) Red and far-red light alter the transcript profile in the cyanobacterium *Synechocystis* sp. PCC 6803: impact of cyanobacterial phytochromes. FEBS Lett 579: 1613-1618

Hughes J, Lamparter T, Mittmann F, Hartmann E, Gärtner W, Wilde A, Börner T (1997) A prokaryotic phytochrome. Nature 386: 663

Huisman J, Weissing FJ (1994) Light-limited growth and competition for light in well-mixed aquatic environments: an elementary model. Ecology 75: 507-520

Huisman J, Weissing FJ (1995) Competition for nutrients and light in a mixed water column: a theoretical analysis. Am Nat 146: 536-564

Huisman J, Jonker RR, Zonneveld C, Weissing FJ (1999) Competition for light between phytoplankton species: experimental tests of mechanistic theory. Ecology 80: 211-222

Huisman J, Matthijs HCP, Visser PM, Balke H, Sigon CAM, Passarge J, Weissing FJ, Mur LR (2002) Principles of the light-limited chemostat: theory and ecological applications. Antonie Leeuwenhoek 81: 117-133

Huisman J, Codd GA, Paerl HW, Ibelings BW, Verspagen JMH, Visser PM (2018) Cyanobacterial blooms. Nature Rev Microbiol 16: 471-483

Ihalainen JA, D'Haene S, Yeremenko N, van Roon H, Arteni AA, Boekema EJ, van

Grondelle R, Matthijs HCP, Dekker JP (2005) Aggregates of the chlorophyll-binding protein IsiA (CP43') dissipate energy in cyanobacteria. Biochem 44: 10846-10853
Iwabe N, Kuma KI, Hasegawa M, Osawa S, Miyata T (1989) Evolutionary relationship of archaebacteria, eubacteria, and eukaryotes inferred from phylogenetic trees of duplicated genes. Proc Natl Acad Sci USA 86: 9355-9359
Jäger CG, Diehl S (2014) Resource competition across habitat boundaries: asymmetric interactions between benthic and pelagic producers. Ecol Monograph 84: 287-302
Jiang H, Song W, Cheng H, Qiu B (2015) The hypothetical protein Ycf46 is involved in regulation of CO_2 utilization in the cyanobacterium *Synechocystis* sp. PCC 6803. Planta 241: 145-155
Jones CS, Mayfield SP (2012) Algae biofuels: versatility for the future of bioenergy. Curr Opin Biotechnol 23: 346-351
Jones JA, Wang X (2018) Use of bacterial co-cultures for the efficient production of chemicals. Curr Opin Chem Biol 52: 33-38
Jordan P, Fromme P, Witt HT, Klukas O, Saenger W, Krauß N (2001) Three-dimensional structure of cyanobacterial photosystem I at 2.5 Å resolution. Nature 411: 909-917
Jørgensen BB, Cohen Y, Des Marais DJ (1987) Photosynthetic action spectra and adaptation to spectral light distribution in a benthic cyanobacterial mat. Appl Environ Microbiol 53: 879-886
Joshua S, Bailey S, Mann NH, Mullineaux CW (2005) Involvement of phycobilisome diffusion in energy quenching in cyanobacteria. Plant Physiol 138: 1577-1585
Kana TM, Darkangelo C, Hunt MD, Oldham JB, Bennett GE, Cornwell JC (1994) Membrane inlet mass spectrometer for rapid high-precision determination of N_2, O_2, and Ar in environmental water samples. Anal Chem 66: 4166-4170
Katz ME, Finkel ZV, Grzebyk D, Knoll AH, Falkowski PG (2004) Evolutionary trajectories and biogeochemical impacts of marine eukaryotic phytoplankton. Annu Rev Ecol Evol Syst 35: 523-556
Keeling PJ (2004) Diversity and evolutionary history of plastids and their hosts. Am J Bot 91: 1481-1493
Keeling PJ (2010) The endosymbiotic origin, diversification and fate of plastids. Phil Trans R Soc B 365: 729–748
Kennis JTM, Gobets B, van Stokkum IHM, Dekker JP, van Grondelle R, Fleming GR (2001) Light harvesting by chlorophylls and carotenoids in the photosystem I core complex of *Synechococcus elongatus*: a fluorescence upconversion study. J Phys Chem 105: 4485-4494
Kettler GC, Martiny AC, Huang K, Zucker J, Coleman ML, Rodrigue S, Chen F, Lapidus A, Ferriera S, Johnson J, Steglich C, Church GM, Richardson P, Chisholm SW (2007) Patterns and implications of gene gain and loss in the evolution of *Prochlorococcus*. PLoS Genetics 3: e231
Key T, McCarthy A, Campbell DA, Six C, Roy S, Finkel ZV (2010) Cell size trade-offs govern light exploitation strategies in marine phytoplankton. Environ Microbiol 12: 95-104
Kirilovsky D (2007) Photoprotection in cyanobacteria: the orange carotenoid protein (OCP)-related non-photochemical-quenching mechanism. Photosynth Res 93: 7
Kirilovsky D (2015) Modulating energy arriving at photochemical reaction centers: orange carotenoid protein-related photoprotection and state transitions. Photosynth Res 126: 3-17
Kirilovsky D, Kerfeld CA (2016) Cyanobacterial photoprotection by the orange carotenoid protein. Nature Plants 2: 16180
Kirilovsky D, Büchel C (2019) Evolution and function of light-harvesting antenna in oxygenic photosynthesis. Adv Bot Res 91: 247-293
Kirk JTO (2011) Light and Photosynthesis in Aquatic Ecosystems, Third Edition. Cambridge University Press, Cambridge, UK

Kirst H, Gabilly ST, Niyogi KK, Lemaux PG, Melis A (2017) Photosynthetic antenna engineering to improve crop yields. Planta 245: 1009-1020

Köhler S, Delwiche CF, Denny PW, Tilney LG, Webster P, Wilson RJM, Palmer JD, Roos DS (1997) A plastid of probable green algal origin in Apicomplexan parasites. Science 275: 1485-1489

Komenda J, Barker M, Kuvikova S, de Vries R, Mullineaux CW, Tichy M, Nixon PJ (2006) The FtsH protease slr0228 is important for quality control of photosystem II in the thylakoid membrane of *Synechocystis* sp. PCC 6803. J Biol Chem 281: 1145-1151

Kondo K, Geng XX, Katayama M, Ikeuchi M (2005) Distinct roles of CpcG1 and CpcG2 in phycobilisome assembly in the cyanobacterium *Synechocystis* sp. PCC 6803. Photosynth Res 84: 269-273

Kondo K, Ochiai Y, Katayama M, Ikeuchi M (2007) The membrane-associated CpcG2-phycobilisome in *Synechocystis*: a new photosystem I antenna. Plant Physiol 144: 1200-1210

Koziol AG, Borza T, Ishida K, Keeling P, Lee RW, Durnford DG (2007) Tracing the evolution of the light-harvesting antennae in chlorophyll *a*/*b*-containing organisms. Plant Physiol 143: 1802-1816

Krasikov V, Aguirre von Wobeser E, Dekker HL, Huisman J, Matthijs HCP (2012) Time-series resolution of gradual nitrogen starvation and its impact on photosynthesis in the cyanobacterium *Synechocystis* PCC 6803. Physiol Plant 145: 426-439

Kritzberg ES (2017) Centennial-long trends of lake browning show major effect of afforestation. L&O Lett 2: 105-112

Kruk C, Huszar VLM, Peeters ETHM, Bonilla S, Costa L, Lürling M, Reynolds CS, Scheffer M (2010) A morphological classification capturing functional variation in phytoplankton. Freshwat Biol 55: 614-627

Kufryk G, Hernández-Prieto MA, Kieselbach T, Miranda H, Vermaas W, Funk C (2008) Association of small CAB-like proteins (SCPs) of *Synechocystis* sp. PCC 6803 with Photosystem II. Photosynth Res 95: 135-145

Kühlbrandt W, Wang DAN, Fujiyoshi Y (1994) Atomic model of plant light-harvesting complex by electron crystallography. Nature 367: 614

Küpper H, Andresen E, Wiegert S, Šimek M, Leitenmayer B, Šetlík I (2009) Reversible coupling of individual phycobiliprotein isoforms during state transitions in the cyanobacterium *Trichodesmium* analysed by single-cell fluorescence kinetic measurements. Biochim Biophys Acta 1787: 155-167

Kwon J, Bernát G, Wagner H, Rögner M, Rexroth S (2013) Reduced light-harvesting antenna: consequences on cyanobacterial metabolism and photosynthetic productivity. Algal Res 2: 188-195

La Roche J, van der Staay GWM, Partensky F, Ducret A, Aebersold R, Li R, Golden SS, Hiller RG, Wrench PM, Larkum AWD, Green BR (1996) Independent evolution of the prochlorophyte and green plant chlorophyll *a*/*b* light-harvesting proteins. Proc Natl Acad Sci USA 93: 15244-15248

Larkum AWD (2006) The evolution of chlorophylls and photosynthesis. Chlorophylls and bacteriochlorophylls. Springer, Dordrecht, pp 261-282

Larkum AWD, Lockhart PJ, Howe CJ (2007) Shopping for plastids. Trends Plant Sci 12: 189-195

Larsen S, Andersen T, Hessen DO (2011) Climate change predicted to cause severe increase of organic carbon in lakes. Global Change Biol 17: 1186-1192

Latifi A, Ruiz M, Zhang C (2009) Oxidative stress in cyanobacteria. FEMS Microbiol Rev 33: 258-278

Lea-Smith DJ, Bombelli P, Dennis JS, Scott SA, Smith AG, Howe CJ (2014) Phycobilisome-deficient strains of *Synechocystis* sp. PCC 6803 have reduced size and require carbon-limiting conditions to exhibit enhanced productivity. Plant Physiol 165: 705-714

Lebret K, Langenheder S, Colinas N, Östman Ö, Lindström ES (2018) Increased water colour affects freshwater plankton communities in a mesocosm study. Aquat Microb Ecol 81: 1-17

Leech DM, Pollard AI, Labou SG, Hampton SE (2018) Fewer blue lakes and more murky lakes across the continental US: Implications for planktonic food webs. Limnol Oceanogr 63: 2661-2680

Lemasson C, Tandeau de Marsac N, Cohen-Bazire G (1973) Role of allophycocyanin as light-harvesting pigment in cyanobacteria. Proc Natl Acad Sci USA 70: 3130-3133

Ley AC, Butler WL (1980) Effects of chromatic adaptation on the photochemical apparatus of photosynthesis in *Porphyridium cruentum*. Plant Physiol 65: 714-722

Li H, Sherman LA (2002) Characterization of *Synechocystis* sp. strain PCC 6803 and Δ*nbl* mutants under nitrogen-deficient conditions. Arch Microbiol 178: 256-266

Li Q, Huisman J, Bibby TS, Jiao N (2019) Biogeography of cyanobacterial *isiA* genes and their link to iron availability in the ocean. Front Microbiol 10: 650

Liberton M, Chrisler WB, Nicora CD, Moore RJ, Smith RD, Koppenaal DW, Pakrasi HB, Jacobs JM (2017) Phycobilisome truncation causes widespread proteome changes in *Synechocystis* sp. PCC 6803. PLoS One 12: e0173251

Lips D, Schuurmans JM, Branco dos Santos F, Hellingwerf KJ (2018) Many ways towards 'solar fuel': quantitative analysis of the most promising strategies and the main challenges during scale-up. Energy Environ Sci 11: 10-22

Litchman E, Klausmeier CA (2008) Trait-based community ecology of phytoplankton. Annu Rev Ecol Evol and System 39: 615-639

Litchman E, de Tezanos Pinto P, Klausmeier CA, Thomas MK, Yoshiyama K (2010) Linking traits to species diversity and community structure in phytoplankton. Hydrobiologia 653: 15–28

Liu M, Xu Z, Guo S, Tang C, Liu X, Jao X (2014) Evaluation of leaf morphology, structure and biochemical substance of balloon flower (*Platycodon grandiflorum* (Jacq.) A. DC.) plantlets in vitro under different light spectra. Sci Hort 174: 112-118

Loughlin P, Lin Y, Chen M (2013) Chlorophyll *d* and *Acaryochloris marina*: current status. Photosynth Res 116: 277-293

Luimstra VM, Schuurmans JM, Verschoor AM, Hellingwerf KJ, Huisman J, Matthijs HCP (2018) Blue light reduces photosynthetic efficiency of cyanobacteria through an imbalance between photosystems I and II. Photosynth Res 138: 177-189

Luimstra VM, Schuurmans JM, de Carvalho CFM, Matthijs HCP, Hellingwerf KJ, Huisman J (2019) Exploring the low photosynthetic efficiency of cyanobacteria in blue light using a mutant lacking phycobilisomes. Photosynth Res 141: 291-301

Luimstra VM, Verspagen JMH, Xu T, Schuurmans JM, Huisman J (2020) Changes in water color shift competition between phytoplankton species with contrasting light-harvesting strategies. Ecology 101: e02951

MacColl R (2004) Allophycocyanin and energy transfer. Biochim Biophys Acta Bioeng 1657: 73-81

MacKenzie TDB, Burns RA, Campbell DA (2004) Carbon status constrains light acclimation in the cyanobacterium *Synechococcus elongatus*. Plant Physiol 136:3301-3312

Magdouli S, Brar SK, Blais JF (2016) Co-culture for lipid production: Advances and challenges. Biomass Bioenergy 92: 20-30

Mao HB, Li GF, Li DH, Wu QY, Gong YD, Zhang XF, Zhao NM (2003) Effects of glycerol and high temperatures on structure and function of phycobilisomes in *Synechocystis* sp. PCC 6803. FEBS Lett 553: 68-72

Marañón E (2015) Cell size as a key determinant of phytoplankton metabolism and community structure. Annu Rev Mar Sci 7: 241-264

Margulis L (1993) Symbiosis in cell evolution: Microbial communities in the Archean and Proterozoic eons. W. H. Freeman, San Francisco, USA

Matthijs HCP, van der Staay GWM, van Amerongen H, van Grondelle R, Garab G (1989)

Structural organization of chlorophyll *b* in the Prochlorophyte *Prochlorothrix hollandica*. Biochim Biophys Acta 975: 185-187
McCarren J, DeLong EF (2007) Proteorhodopsin photosystem gene clusters exhibit co-evolutionary trends and shared ancestry among diverse marine microbial phyla. Environ Microbiol 9: 846–858
McGill BJ, Enquist BJ, Weiher E, Westoby M (2006) Rebuilding community ecology from functional traits. Trends Ecol Evol 21: 178-185
McInerney J, Pisani D, O'Connell MJ (2015) The ring of life hypothesis for eukaryote origins is supported by multiple kinds of data. Phil Trans R Soc Lond B Biol Sci 370: 20140323
Melis A (2009) Solar energy conversion efficiencies in photosynthesis: Minimizing the chlorophyll antennae to maximize efficiency. Plant Sci 177: 272-280
Merico A, Bruggeman J, Wirtz K (2009) A trait-based approach for downscaling complexity in plankton ecosystem models. Ecol Model 220: 3001-3010
Minagawa J (2011) State transitions—the molecular remodeling of photosynthetic supercomplexes that controls energy flow in the chloroplast. Biochim Biophys Acta Bioen 1807:897-905
Miyashita H, Ikemoto H, Kurano N, Adachi K, Chihara M, Miyachi S (1996) Chlorophyll *d* as a major pigment. Nature 383: 402
Miyashita H, Adachi K, Kurano N, Ikemot H, Chihara M, Miyachi S (1997) Pigment composition of a novel oxygenic photosynthetic prokaryote containing chlorophyll *d* as the major chlorophyll. Plant Cell Physiol 38: 274-281
Mizuno T, Kaneko T, Tabata S (1996) Compilation of all genes encoding bacterial two-component signal transducers in the genome of the cyanobacterium, *Synechocystis* sp. strain PCC 6803. DNA Res 3: 407-414
Monteith DT, Stoddard JL, Evans CD, de Wit HA, Forsius M, Høgåsen T, Wilander A, Skjelkvåle BL, Jeffries DS, Vuorenmaa J, Keller B, Kopácek J, Vesely J (2007) Dissolved organic carbon trends resulting from changes in atmospheric deposition chemistry. Nature 450: 537-540
Moon Y, Lee E, Park YM, Park YS, Chung W, Chung Y (2010) The role of cyanopterin in UV/blue light signal transduction of cyanobacterium *Synechocystis* sp. PCC 6803 phototaxis. Plant Cell Physiol 51: 969-980
Morden CW, Golden SS (1989) *psbA* genes indicate common ancestry of prochlorophytes and chloroplasts. Nature 337: 382-385
Moreira D, Le Guyader H, Philippe H (2000) The origin of red algae and the evolution of chloroplasts. Nature 405: 69-72
Mullineaux CW, Tobin MJ, Jones GR (1997) Mobility of photosynthetic complexes in thylakoid membranes. Nature 390: 421-424
Mullineaux CW, Emlyn-Jones D (2004) State transitions: an example of acclimation to low-light stress. J Exp Bot 56:389-393
Mullineaux CW (2008) Phycobilisome-reaction centre interaction in cyanobacteria. Photosynth Res 95: 175-182
Mullineaux CW (2014) Co-existence of photosynthetic and respiratory activities in cyanobacterial thylakoid membranes. Biochim Biophys Acta 1837: 503-511
Mullineaux CW (2014) Electron transport and light-harvesting switches in cyanobacteria. Front Plant Sci 5: 7
Munekage Y, Hashimoto M, Miyake C, Tomizawa K, Endo T, Tasaka M, Shikanai T (2004) Cyclic electron flow around photosystem I is essential for photosynthesis. Nature 429: 579-582
Murakami A (1997) Quantitative analysis of 77K fluorescence emission spectra in *Synechocystis* sp. PCC 6714 and *Chlamydomonas reinhardtii* with variable PS I/PS II stoichiometries. Photosynth Res 53: 141-148
Murakami A, Kim SJ, Fujita Y (1997) Changes in photosystem stoichiometry in response

to environmental conditions for cell growth observed with the cyanophyte *Synechocystis* PCC 6714. Plant Cell Physiol 38: 392-397
Muramatsu M, Hihara Y (2012) Acclimation to high-light conditions in cyanobacteria: from gene expression to physiological responses. J Plant Res 125: 11-39
Murphy CD, Roodvoets MS, Austen EJ, Dolan A, Barnett A, Campbell DA (2017) Photoinactivation of Photosystem II in *Prochlorococcus* and *Synechococcus*. PLoS One 12: e0168991
Myers J, Graham JR, Wang RT (1980) Light harvesting in *Anacystis nidulans* studied in pigment mutants. Plant Physiol 66: 1144-1149
Natali A, Croce R (2015) Characterization of the major light-harvesting complexes (LHCBM) of the green alga *Chlamydomonas reinhardtii*. PLoS ONE 10: e0119211
Nawrocki WJ, Santabarbara S, Mosebach L, Wollman FA, Rappaport F (2016) State transitions redistribute rather than dissipate energy between the two photosystems in *Chlamydomonas*. Nature Plants 2: 16031
Nelson N, Yocum CF (2006) Structure and function of photosystems I and II. Annu Rev Plant Biology 57: 521-565
Nevo R, Charuvi D, Shimoni E, Schwarz R, Kaplan A, Ohad I, Reich Z (2007) Thylakoid membrane perforations and connectivity enable intracellular traffic in cyanobacteria. EMBO J 26:1467-1473
Ng WO, Grossman AR, Bhaya D (2003) Multiple light inputs control phototaxis in *Synechocystis* sp. strain PCC6803. J Bacteriol 185: 1599-1607
Nierzwicki-Bauer SA, Balkwill DL, Stevens SE (1983) Three-dimensional ultrastructure of a unicellular cyanobacterium. J Cell Biol 97: 713-722
Nitta K, Suzuki N, Honma D, Kaneko Y, Nakamoto H (2005) Ultrastructural stability under high temperature or intensive light stress conferred by a small heat shock protein in cyanobacteria. FEBS Lett 579: 1235-1242
Nogales J, Gudmundsson S, Knight EM, Palsson BO, Thiele I (2012) Detailing the optimality of photosynthesis in cyanobacteria through systems biology analysis. Proc Natl Acad Sci USA 109: 2678-2683
Nutman AP, Bennett VC, Friend CRL, van Kranendonk MJ, Chivas AR (2016) Rapid emergence of life shown by discovery of 3,700-million-year-old microbial structures. Nature 537: 535–538
O'Neil JM, Davis TW, Burford MA, Gobler CJ (2012) The rise of harmful cyanobacteria blooms: the potential roles of eutrophication and climate change. Harmful Alg 14: 313-334
Ochman H, Lawrence JG, Groisman EA (2000) Lateral gene transfer and the nature of bacterial innovation. Nature 405: 299–304
Ogawa T, Misumi M, Sonoike K (2017) Estimation of photosynthesis in cyanobacteria by pulse-amplitude modulation chlorophyll fluorescence: problems and solutions. Photosynth Res 133: 63-73
Ogawa K, Yoshikawa K, Matsuda F, Toya Y, Shimizu H (2018) Transcriptome analysis of the cyanobacterium *Synechocystis* sp. PCC 6803 and mechanisms of photoinhibition tolerance under extreme high light conditions. J Biosci Bioeng 126: 596-602
Okamoto S, Ikeuchi M, Ohmori M (1999) Experimental analysis of recently transposed insertion sequences in the cyanobacterium *Synechocystis* sp. PCC 6803. DNA Res 6: 265-273
Olive J, Ajlani G, Astier C, Recouvreur M, Vernotte C (1997) Ultrastructure and light adaptation of phycobilisome mutants of *Synechocystis* PCC 6803. Biochim Biophys Acta 1319: 275-282
Ort DR, Melis A (2011) Optimizing antenna size to maximize photosynthetic efficiency. Plant Physiol 155: 79-85
Otto SP, Day T (2007) A biologist's guide to mathematical modeling in ecology and evolution. Princeton University Press, NJ, USA

Paerl HW, Huisman J (2009) Climate change: a catalyst for global expansion of harmful cyanobacterial blooms. Environ Microbiol Rep 1: 27-37

Page LE, Liberton M, Pakrasi HB (2012) Reduction of photoautotrophic productivity in the cyanobacterium *Synechocystis* sp. strain PCC 6803 by phycobilisome antenna truncation. Appl Environ Microbiol 78: 6349-6351

Palenik B (2001) Chromatic adaptation in marine *Synechococcus* strains. Appl Environ Microbiol 67: 991-994

Palmer JD (2003) The symbiotic birth and spread of plastids: how many times and whodunit? J Phycol 39: 4-11

Panichkin VB, Arakawa-Kobayashi S, Kanaseki T, Suzuki I, Los DA, Shestakov SV, Murata N (2006) Serine/threonine protein kinase SpkA in *Synechocystis* sp. strain PCC 6803 is a regulator of expression of three putative *pilA* operons, formation of thick pili, and cell motility. J Bacteriol 188: 7696-7699

Parfrey LW, Lahr DJG, Knoll AH, Katz LA (2011) Estimating the timing of early eukaryotic diversification with multigene molecular clocks. Proc Natl Acad Sci USA 108: 13624-13629

Partensky F, Hess WR, Vaulot D (1999) *Prochlorococcus*, a marine photosynthetic prokaryote of global significance. Microbiol Mol Biol Rev 63: 106-127

Passarge J, Hol S, Escher M, Huisman J (2006) Competition for nutrients and light: stable coexistence, alternative stable states, or competitive exclusion? Ecol Monograph 76: 57-72

Pennisi G, Orsini F, Blasioli S, Cellini A, Crepaldi A, Braschi I, Spinelli F, Nicola S, Fernandez JA, Stanghellini C, Gianquinto G, Marcelis LFM (2019) Resource use efficiency of indoor lettuce (*Lactuca sativa L.*) cultivation as affected by red:blue ratio provided by LED lighting. Sci Rep 9: 14127

Perrine Z, Negi S, Sayre RT (2012) Optimization of photosynthetic light energy utilization by microalgae. Algal Res 1: 134-142

Planavsky NJ, Asael D, Hofmann A, Reinhard CT, Lalonde SV, Knudsen A, Wang X, Ossa Ossa F, Pecoits E, Smith AJB, Beukes NJ, Bekker A, Johnson TM, Konhauser KO, Lyons TW, Rouxel OJ (2014) Evidence for oxygenic photosynthesis half a billion years before the Great Oxidation Event. Nat Geosci 7:283–286

Platt T, Jassby AD (1976) The relationship between photosynthesis and light for natural assemblages of coastal marine phytoplankton. J Phycol 12: 421-430

Polle JEW, Kanakagiri S, Jin ES, Masuda T, Melis A (2002) Truncated chlorophyll antenna size of the photosystems: a practical method to improve microalgal productivity and hydrogen production in mass culture. Int J Hydrogen Energy 27: 1257-1264

Ponce-Toledo RI, Deschamps P, López-García P, Zivanovic Y, Benzerara K, Moreira D (2017) An early-branching freshwater cyanobacterium at the origin of plastids. Curr Biol 27: 386-391

Porra RJ, Thompson WA, Kriedemann PE (1989) Determination of accurate extinction coefficients and simultaneous equations for assaying chlorophylls a and b extracted with four different solvents: verification of the concentration of chlorophyll standards by atomic absorption spectroscopy. Biochim Biophys Acta Bioeng 975: 384-394

Promnares K, Komenda J, Bumba L, Nebesarova J, Vacha F, Tichy M (2006) Cyanobacterial small chlorophyll-binding protein ScpD (HliB) is located on the periphery of photosystem II in the vicinity of PsbH and CP47 subunits. J Biol Chem 281: 32705-32713

Pulich WM, van Baalen C (1974) Growth requirements of blue-green algae under blue light conditions. Arch Microbiol 97: 303-312

R Development Core Team (2017) R: A Language and Environment for Statistical Computing. R Foundation for Statistical Computing: Vienna, Austria

Rakhimberdieva MG, Boichenko VA, Karapetyan NV, Stadnichuk IN (2001) Interaction of phycobilisomes with photosystem II dimers and photosystem I monomers and

trimers in the cyanobacterium *Spirulina platensis*. Biochem 40: 15780-15788
Rakhimberdieva MG, Bolychevtseva YV, Elanskaya IV, Karapetyan NV (2007) Protein–protein interactions in carotenoid triggered quenching of phycobilisome fluorescence in *Synechocystis* sp. PCC 6803. FEBS Lett 581: 2429-2433
Ranjbar Choubeh R, Wientjes E, Struik PC, Kirilovsky D, van Amerongen H (2018) State transitions in the cyanobacterium *Synechococcus elongatus* 7942 involve reversible quenching of the photosystem II core. Biochim Biophys Acta Bioen 1859: 1059-1066
Rast A, Heinz S, Nickelsen J (2015) Biogenesis of thylakoid membranes. Biochim Biophys Acta Bioen 1847: 821-830
Raymond J, Zhaxybayeva O, Gogarten JP, Gerdes SY, Blankenship RE (2002) Whole-genome analysis of photosynthetic prokaryotes. Science 298: 1616-1620
Ritchie ME, Silver J, Oshlack A, Holmes M, Diyagama D, Holloway A, Smyth GK (2007) A comparison of background correction methods for two-colour microarrays. Bioinformatics 23: 2700-2707
Ritchie ME, Phipson B, Wu D, Hu Y, Law CW, Shi W, Smyth GK (2015) *limma* powers differential expression analyses for RNA-sequencing and microarray studies. Nucleic Acids Res 43: e47
Ritz T, Damjanović A, Schulten K, Zhang JP, Koyama Y (2000) Efficient light harvesting through carotenoids. Photosynth Res 66: 125-144
Rivera MC, Lake JA (2004) The ring of life provides evidence for a genome fusion origin of eukaryotes. Nature 431: 152–155
Rocap G, Larimer FW, Lamerdin J, Malfatti S, Chain P, Ahlgren NA, Arellano A, Coleman M, Hauser L, Hess WR (2003) Genome divergence in two *Prochlorococcus* ecotypes reflects oceanic niche differentiation. Nature 424: 1042-1047
Rögner M, Nixon PJ, Diner BA (1990) Purification and characterization of photosystem I and photosystem II core complexes from wild-type and phycocyanin-deficient strains of the cyanobacterium *Synechocystis* PCC 6803. J Biol Chem 265: 6189-6196
Rosenberg JN, Oyler GA, Wilkinson L, Betenbaugh MJ (2008) A green light for engineered algae: redirecting metabolism to fuel a biotechnology revolution. Curr Opin Biotechnol 19:430-436
Roulet N, Moore TR (2006) Browning the waters. Nature 444: 283-284
Sakthivel K, Watanabe T, Nakamoto H (2009) A small heat-shock protein confers stress tolerance and stabilizes thylakoid membrane proteins in cyanobacteria under oxidative stress. Arch Microbiol 191: 319-328
Sanchez-Baracaldo P, Raven JA, Pisani D, Knoll AH (2017) Early photosynthetic eukaryotes inhabited low-salinity habitats. Proc Natl Acad Sci USA 114: E7737-7745
Sandström S, Ivanov AG, Park Y-I, Öquist G, Gustafsson P (2002) Iron stress responses in the cyanobacterium *Synechococcus* sp. PCC7942. Phys Plant 116: 255-263
Sanfilippo JE, Nguyen AA, Garczarek L, Karty JA, Pokhrel S, Strnat JA, Partensky F, Schluchter WM, Kehoe DM (2019) Interplay between differentially expressed enzymes contributes to light color acclimation in marine *Synechococcus*. Proc Natl Acad Sci USA 116: 6457-6462
Santana-Sanchez A, Solymosi D, Mustila H, Bersanini L, Aro EM, Allahverdiyeva Y (2019) Flavodiiron proteins 1-to-4 function in versatile combinations in O_2 photoreduction in cyanobacteria. eLife 8: e45766
Sato T, Minagawa S, Kojima E, Okamoto N, Nakamoto H (2010) HtpG, the prokaryotic homologue of Hsp90, stabilizes a phycobilisome protein in the cyanobacterium *Synechococcus elongatus* PCC 7942. Mol Microbiol 76: 576-589
Savakis P, de Causmaecker S, Angerer V, Ruppert U, Anders K, Essen L, Wilde A (2012) Light-induced alteration of c-di-GMP level controls motility of *Synechocystis* sp. PCC 6803. Mol Microbiol 85: 239-251

Scanlan DJ, West NJ (2002) Molecular ecology of the marine cyanobacterial genera *Prochlorococcus* and *Synechococcus*. FEMS Microbiol Ecol 40: 1-12

Scanlan DJ, Ostrowski M, Mazard S, Dufresne A, Garczarek L, Hess WR, Post AF, Hagemann M, Paulsen I, Partensky F (2009) Ecological genomics of marine picocyanobacteria. Microbiol Mol Biol Rev 73: 249-299

Schirrmeister BE, Gugger M, Donoghue PC (2015) Cyanobacteria and the Great Oxidation Event: evidence from genes and fossils. Palaeontology 58: 769-785

Schuurmans RM, Matthijs HCP, Hellingwerf KJ (2017) Transition from exponential to linear photoautotrophic growth changes the physiology of *Synechocystis* sp. PCC 6803. Photosynth Res 132: 69-82

Schuurmans JM, Brinkmann BW, Makower AK, Dittmann E, Huisman J, Matthijs HCP (2018) Microcystin interferes with defense against high oxidative stress in harmful cyanobacteria. Harmful Algae 78: 47-55

Schwaderer A S, Yoshiyama K, de Tezanos Pinto P, Swenson NG, Klausmeier CA, Litchman E (2011) Eco-evolutionary differences in light utilization traits and distributions of freshwater phytoplankton. Limnol Oceanography 56: 589-598

Scott M, Klumpp S, Mateescu EM, Hwa T (2014) Emergence of robust growth laws from optimal regulation of ribosome synthesis. Mol Syst Biol 10: 747

Shen G, Boussiba S, Vermaas WF (1993) *Synechocystis* sp PCC 6803 strains lacking photosystem I and phycobilisome function. Plant Cell 5: 1853-1863

Shimakawa G, Shaku K, Nishi A, Hayashi R, Yamamoto H, Sakamoto K, Makino A, Miyake C (2015) Flavodiiron2 and flavodiiron4 proteins mediate an oxygen-dependent alternative electron flow in *Synechocystis* sp. PCC 6803 under CO_2-limited conditions. Plant Physiol 167: 472-480

Shimakawa G, Shaku K, Miyake C (2016) Oxidation of P700 in photosystem I is essential for the growth of cyanobacteria. Plant Physiol 172: 1443-1450

Shin W, Lee B, Jeong B, Chang YK, Kwon J (2016) Truncated light-harvesting chlorophyll antenna size in *Chlorella vulgaris* improves biomass productivity. J Appl Phycol 28: 3193-3202

Silaban A, Bai R, Gutierrez-Wing MT, Negulescu II, Rusch KA (2014) Effect of organic carbon, C:N ratio and light on the growth and lipid productivity of microalgae/cyanobacteria coculture. Eng Life Sci 14: 47-56

Silva-Benavides AM, Torzillo G (2012) Nitrogen and phosphorus removal through laboratory batch cultures of microalga *Chlorella vulgaris* and cyanobacterium *Planktothrix isothrix* grown as monoalgal and as co-cultures. J Appl Phycol 24: 267-276

Singh AK, Sherman LA (2002) Characterization of a stress-responsive operon in the cyanobacterium *Synechocystis* sp. strain PCC 6803. Gene 297: 11-19

Singh AK, Li H, Sherman LA (2004) Microarray analysis and redox control of gene expression in the cyanobacterium *Synechocystis* sp. PCC 6803. Physiol Plant 120: 27-35

Singh AK, Elvitigala T, Bhattacharyya-Pakrasi M, Aurora R, Ghosh B, Pakrasi HB (2008) Integration of carbon and nitrogen metabolism with energy production is crucial to light acclimation in the cyanobacterium *Synechocystis*. Plant Physiol 148: 467-478

Singh AK, Bhattacharyya-Pakrasi M, Elvitigala T, Ghosh B, Aurora R, Pakrasi HB (2009) A systems-level analysis of the effects of light quality on the metabolism of a cyanobacterium. Plant Physiol 151: 1596-1608

Six C, Thomas J, Garczarek L, Ostrowski M, Dufresne A, Blot N, Scanlan DJ, Partensky F (2007) Diversity and evolution of phycobilisomes in marine *Synechococcus* spp.: a comparative genomics study. Genome Biol 8: R259

Smyth GK, Speed T (2003) Normalization of cDNA microarray data. Methods 31: 265-273

Smyth GK (2004) Linear models and empirical Bayes methods for assessing differential

expression in microarray experiments. Stat Appl Gen Mol Biol 3: 3
Smyth GK, Michaud J, Scott HS (2005) Use of within-array replicate spots for assessing differential expression in microarray experiments. Bioinformatic 21: 2067-2075
Solhaug KA, Xie L, Gauslaa Y (2014) Unequal allocation of excitation energy between photosystem II and I reduces cyanolichen photosynthesis in blue light. Plant Cell Physiol 55: 1404-1414
Son K, Oh M (2013) Leaf shape, growth, and antioxidant phenolic compounds of two lettuce cultivars grown under various combinations of blue and red light-emitting diodes. HortScience 48: 988-995
Soucy SM, Huang J, Gogarten JP (2015) Horizontal gene transfer: building the web of life. Nature Rev Genet 16: 472-482
Stadnichuk IN, Lukashev EP, Elanskaya IV (2009) Fluorescence changes accompanying short-term light adaptations in photosystem I and photosystem II of the cyanobacterium *Synechocystis* sp. PCC 6803 and phycobiliprotein-impaired mutants: State 1/State 2 transitions and carotenoid-induced quenching of phycobilisomes. Photosynth Res 99: 227-241
Stadnichuk IN, Tropin IV (2017) Phycobiliproteins: structure, functions and biotechnological applications. Appl Biochem Microbiol 53: 1-10
Stamatakis K, Tsimilli-Michael M, Papageorgiou GC (2014) On the question of the light-harvesting role of *β*-carotene in photosystem II and photosystem I core complexes. Plant Physiol Biochem 81: 121-127
Steglich C, Mullineaux CW, Teuchner K, HessWR, Lokstein H (2003). Photophysical properties of *Prochlorococcus marinus* SS120 divinyl chlorophylls and phycoerythrin in vitro and in vivo. FEBS Lett 553:79-84
Sterner RW, Elser JJ (2002) Ecological stoichiometry: the biology of elements from molecules to the biosphere. Princeton University Press, Princeton, NJ, USA
Stomp M, Huisman J, de Jongh F, Veraart AJ, Gerla D, Rijkeboer M, Ibelings BW, Wollenzien UI, Stal LJ (2004) Adaptive divergence in pigment composition promotes phytoplankton biodiversity. Nature 432: 104-107
Stomp M, Huisman J, Stal LJ, Matthijs HCP (2007a) Colorful niches of phototrophic microorganisms shaped by vibrations of the water molecule. ISME J 1: 271-282
Stomp M, Huisman J, Vörös L, Pick FR, Laamanen M, Haverkamp T, Stal LJ (2007b) Colourful coexistence of red and green picocyanobacteria in lakes and seas. Ecol Lett 10: 290-298
Stomp M (2008) Colourful coexistence: a new solution to the plankton paradox. PhD thesis. University of Amsterdam, The Netherlands
Takaichi S (2011) Carotenoids in algae: distributions, biosyntheses and functions. Mar Drugs 9: 1101-1118
Tamary E, Kiss V, Nevo R, Adam Z, Bernát G, Rexroth S, Rögner M, Reich Z (2012) Structural and functional alterations of cyanobacterial phycobilisomes induced by high-light stress. Biochim Biophys Acta 1817: 319-327
Tan X, Liu QQ, Duan Z, Li NG (2017) Underwater spectra of Lake Taihu in summer and influences of chromatic light on *Microcystis* colonies. China Environ Sci 37: 4277-4283
Tan X, Zhang D, Duan Z, Parajuli K, Hu J (2020) Effects of light color on interspecific competition between *Microcystis aeruginosa* and *Chlorella pyrenoidosa* in batch experiment. Environ Sci Pollut Res 27: 344-352
Tandeau de Marsac N (2003) Phycobiliproteins and phycobilisomes: the early observations. Photosynth Res 76: 193-205
Teo CL, Atta M, Bukhari A, Taisir M, Yusuf AM, Idris A (2014) Enhancing growth and lipid production of marine microalgae for biodiesel production via the use of different LED wavelengths. Biores Tech 162: 38-44
Terauchi K, Ohmori M (2004) Blue light stimulates cyanobacterial motility via a cAMP

signal transduction system. Mol Microbiol 52: 303-309
Tian L, Gwizdala M, van Stokkum IH, Koehorst RB, Kirilovsky D, van Amerongen H (2012) Picosecond kinetics of light harvesting and photoprotective quenching in wild-type and mutant phycobilisomes isolated from the cyanobacterium *Synechocystis* PCC 6803. Biophys J 102: 1692-1700
Tilman D (1977) Resource competition between planktonic algae: an experimental and theoretical approach. Ecology 58: 338-348
Tilman D (1982) Resource competition and community structure. Princeton University Press, NJ, USA
Ting CS, Rocap G, King J, Chisholm SW (2002) Cyanobacterial photosynthesis in the oceans: the origins and significance of divergent light-harvesting strategies. Trends Microbiol 10: 134-142
Tomitani A, Okada K, Miyashita H, Matthijs HCP, Ohno T, Tanaka A (1999) Chlorophyll *b* and phycobilins in the common ancestor of cyanobacteria and chloroplasts. Nature 400: 159-162
Toyoshima M, Toya Y, Shimizu H (2020) Flux balance analysis of cyanobacteria reveals selective use of photosynthetic electron transport components under different spectral light conditions. Photosynth Res 143: 31-43
Tsinoremas NF, Schaefer MR, Golden SS (1994) Blue and red light reversibly control *psbA* expression in the cyanobacterium *Synechococcus* sp. strain PCC 7942. J Biol Chem 269: 16143-16147
Turner S, Burger-Wiersma T, Giovannoni SJ, Mur LR, Pace NR (1989) The relationship of a prochlorophyte *Prochlorothrix hollandica* to green chloroplasts. Nature 337: 380-382
Tyystjärvi T, Tuominen I, Herranen M, Aro EM, Tyystjärvi E (2002) Action spectrum of *psbA* gene transcription is similar to that of photoinhibition in *Synechocystis* sp. PCC 6803. FEBS Lett 516: 167-171
Umena Y, Kawakami K, Shen J, Kamiya N (2011) Crystal structure of oxygen-evolving photosystem II at a resolution of 1.9 Å. Nature 473: 55
Urrutia-Cordero P, Ekvall MK, Ratcovich J, Soares M, Wilken S, Zhang H, Hansson L (2017) Phytoplankton diversity loss along a gradient of future warming and brownification in freshwater mesocosms. Freshwat Biol 62: 1869-1878
van Alphen P, Hellingwerf KJ (2018) Harvesting sunlight with cyanobacteria and algae for sustainable production in a bio-based economy. In: Light harvesting in photosynthesis. Croce R, van Grondelle R, van Amerongen H, van Stokkum I, pp 565-578
van der Staay GWM, Yurkova N, Green BR (1998) The 38 kDa chlorophyll *a*/*b* protein of the prokaryote *Prochlorothrix hollandica* is encoded by a divergent *pcb* gene. Plant Mol Biol 36: 709-716
van der Weij-de Wit CD, Doust AB, van Stokkum IHM, Dekker JP, Wilk KE, Curmi PMG, Scholes GD, van Grondelle R (2006) How energy funnels from the phycoerythrin antenna complex to photosystem I and photosystem II in cryptophyte *Rhodomonas* CS24 cells. J Phys Chem B 110: 25066-25073
van Liere L, Mur LR (1979) Growth kinetics of *Oscillatoria agardhii* Gomont in continuous culture, limited in its growth by the light energy supply. J Gen Microbiol 115: 153-160
van Thor JJ, Mullineaux CW, Matthijs HCP, Hellingwerf KJ (1998) Light harvesting and state transitions in cyanobacteria. Plant Biol 111: 430-443
Vinnemeier J, Kunert A, Hagemann M (1998) Transcriptional analysis of the *isiAB* operon in salt-stressed cells of the cyanobacterium *Synechocystis* sp. PCC 6803. FEMS Microbiol Lett 169: 323-330
Wahadoszamen M, D'Haene S, Ara AM, Romero E, Dekker JP, van Grondelle R, Berera R (2015) Identification of common motifs in the regulation of light harvesting: the

case of cyanobacteria IsiA. Biochim Biophys Acta 1847: 486-492
Wang CY, Fu CC, Liu YC (2007) Effects of using light-emitting diodes on the cultivation of *Spirulina platensis*. Biochem Eng J 37: 21-25
Wang J, Lu W, Tong Y, Yang Q (2016) Leaf morphology, photosynthetic performance, chlorophyll fluorescence, stomatal development of lettuce (*Lactuca sativa L.*) exposed to different ratios of red light to blue light. Front Plant Sci 7: 250
Watanabe M, Ikeuchi M (2013) Phycobilisome: architecture of a light-harvesting supercomplex. Photosynth Res 116: 265-276
Weissing FJ, Huisman J (1994) Growth and competition in a light gradient. J Theor Biol 168: 323-336
Weyhenmeyer GA, Müller RA, Norman M, Tranvik LJ (2016) Sensitivity of freshwaters to browning in response to future climate change. Clim Change 134: 225-239
Wientjes E, van Amerongen H, Croce R (2013) LHCII is an antenna of both photosystems after long-term acclimation. Biochim Biophys Acta 1827:420–426
Wijffels RH, Barbosa MJ (2010) An outlook on microalgal biofuels. Science 329: 796-799
Wijffels RH, Kruse O, Hellingwerf KJ (2013) Potential of industrial biotechnology with cyanobacteria and eukaryotic microalgae. Curr Opin Biotechnol 24:405-413
Wilde A, Churin Y, Schubert H, Börner T (1997) Disruption of a *Synechocystis* sp. PCC 6803 gene with partial similarity to phytochrome genes alters growth under changing light qualities. FEBS Lett 406: 89-92
Wilken S, Soares M, Urrutia-Cordero P, Ratcovich J, Ekvall MK, van Donk E, Hansson L-A (2018) Primary producers or consumers? Increasing phytoplankton bacterivory along a gradient of lake warming and browning. Limnol Oceanogr 63: S142-S155
Wilson A, Boulay C, Wilde A, Kerfeld CA, Kirilovsky D (2007) Light-induced energy dissipation in iron-starved cyanobacteria: roles of OCP and IsiA proteins. Plant Cell 19: 656-672
Wobbe L, Bassi R, Kruse O (2016) Multi-level light capture control in plants and green algae. Trends Plant Sci 21: 55-68
Wolfe GR, Cunningham FX, Durnfordt D, Green BR, Gantt E (1994) Evidence for a common origin of chloroplasts with light-harvesting complexes of different pigmentation. Nature 367: 566-568
Work VH, D'Adamo S, Radakovits R, Jinkerson RE, Posewitz MC (2012) Improving photosynthesis and metabolic networks for the competitive production of phototroph-derived biofuels. Curr Opin Biotechnol 23: 290-297
Wyman M, Fay P (1986) Underwater light climate and the growth and pigmentation of planktonic blue-green algae (Cyanobacteria) II. The influence of light quality. Proc R Soc London, Ser B 227: 381-393
Xiong Q, Feng J, Li ST, Zhang GY, Qiao ZX, Chen Z, Wu Y, Lin Y, Li T, Ge F, Zhao JD (2015) Integrated transcriptomic and proteomic analysis of the global response of *Synechococcus* to high light stress. Mol Cell Proteomics 14: 1038-1053
Xu W, Wang Y (2019) Sequences, domain architectures, and biological functions of the serine/threonine and histidine kinases in *Synechocystis* sp. PCC 6803. Appl Biochem Biotechnol 188: 1022-1065
Yan C, Zheng Z (2014) Performance of mixed LED light wavelengths on biogas upgrade and biogas fluid removal by microalga *Chlorella* sp. Appl Energy 113: 1008-1014
Yao D, Kieselbach T, Komenda J, Promnares K, Hernández-Prieto MA, Tichy M, Vermaas W, Funk C (2007) Localization of the small CAB-like proteins in photosystem II. J Biol Chem 282: 267-276
Yeremenko N, Kouřil R, Ihalainen JA, D'Haene S, van Oosterwijk N, Andrizhiyevskaya EG, Keegstra W, Dekker HL, Hagemann M, Boekema EJ, Matthijs HCP, Dekker JP (2004) Supramolecular organization and dual function of the IsiA chlorophyll-binding protein in cyanobacteria. Biochem 43: 10308-10313
Yeremenko N, Jeanjean R, Prommeenate P, Krasikov V, Nixon PJ, Vermaas WFJ, Havaux

M, Matthijs HCP (2005) Open reading frame *ssr2016* is required for antimycin A-sensitive photosystem I-driven cyclic electron flow in the cyanobacterium *Synechocystis* sp. PCC 6803. Plant Cell Physiol 46: 1433-1436

Yorio NC, Goins GD, Kagie HR, Wheeler RM, Sager JC (2001) Improving spinach, radish, and lettuce growth under red light-emitting diodes (LEDs) with blue light supplementation. HortScience 36: 380-383

Yoshihara S, Geng X, Okamoto S, Yura K, Murata T, Go M, Ohmori M, Ikeuchi M (2001) Mutational analysis of genes involved in pilus structure, motility and transformation competency in the unicellular motile cyanobacterium *Synechocystis* sp. PCC6803. Plant Cell Physiol 42: 63-73

Yoshihara S, Ikeuchi M (2004) Phototactic motility in the unicellular cyanobacterium *Synechocystis* sp. PCC 6803. Photochem Photobiol Sci 3: 512-518

Zavřel T, Očenášová P, Červený J (2017) Phenotypic characterization of Synechocystis sp. PCC 6803 substrains reveals differences in sensitivity to abiotic stress. PLoS ONE 12: 1-21

Zavřel T, Faizi M, Loureiro C, Poschmann G, Stühler K, Sinetova M, Zorina A, Steuer R, Červený J (2019) Quantitative insights into the cyanobacterial cell economy. eLife 8: e42508

Zhang P, Allahverdiyeva Y, Eisenhut M, Aro EM (2009) Flavodiiron proteins in oxygenic photosynthetic organisms: photoprotection of photosystem II by Flv2 and Flv4 in *Synechocystis* sp. PCC 6803. PLoS One 4: e5331

Zhang P, Eisenhut M, Brandt AM, Carmel D, Silen HM, Vass I, Allahverdiyeva Y, Salminen TA, Aro EM (2012) Operon *flv4-flv2* provides cyanobacterial photosystem II with flexibility of electron transfer. Plant Cell 24: 1952-1971

Zhao F, Qin S (2006) Evolutionary analysis of phycobiliproteins: implications for their structural and functional relationships. J Mol Evol 63: 330-340

Zhao P, Yu X, Li J, Tang X, Huang Z (2014) Enhancing lipid productivity by co-cultivation of *Chlorella* sp. U4341 and *Monoraphidium* sp. FXY-10. J Biosci Bioeng 118: 72-77

Zhao Y, Sun S, Hu C, Zhang H, Xu J, Ping L (2015) Performance of three microalgal strains in biogas slurry purification and biogas upgrade in response to various mixed light-emitting diode light wavelengths. Biores Tech 187: 338-345

Zhu XG, Long SP, Ort DR (2008) What is the maximum efficiency with which photosynthesis can convert solar energy into biomass? Curr Opin Biotechnol 19: 153-159

Zhu XG, Long SP, Ort DR (2010) Improving photosynthetic efficiency for greater yield. Annu Rev Plant Biol 61: 235-261

Summary

Cyanobacteria represent the most abundant phytoplankton species in marine environments and can form dense blooms in eutrophic lakes. They play a key role in aquatic ecosystems and in the global carbon cycle. Their photosynthetic activity is commonly held responsible for the early oxygenation of the Earth's atmosphere and they capture large quantities of CO_2. Cyanobacteria are therefore of great interest in the pursuit of renewable energy sources, sustainable food production, and the production of biobased chemicals. Hence, a thorough understanding of their photosynthetic activity is important for both ecological and biotechnological applications.

Similar to green algae and terrestrial plants, cyanobacteria use the photosynthetic pigment chlorophyll *a* (Chl *a*) to absorb blue and red light. Therefore, one would expect that cyanobacteria use blue and red light for photosynthesis at similar efficiencies. However, in contrast to green algae and plants, the photosynthetic efficiency of many cyanobacteria is much lower in blue light than in other light colors that are absorbed by their photosynthetic pigments. Although the low efficiency of cyanobacteria in blue light has been described in earlier studies, this intriguing phenomenon is not widely known and thus far a comprehensive investigation of the underlying mechanisms is lacking. The work described in this thesis aims to address this knowledge gap.

To explore the effect of different light colors on the photosynthetic efficiency of cyanobacteria, we first conducted an extensive study of the cyanobacterium *Synechocystis* sp. PCC 6803 (**chapter 2**). This model cyanobacterium accommodates Chl *a* in its photosystems, absorbing blue and red light, and in addition employs phycobilisomes (PBS) that contain the orange light-absorbing phycobili-pigment phycocyanobilin. We investigated the photosynthetic activity, relative composition of the photosynthetic apparatus, and growth rate of *Synechocystis* in blue, orange and red light, to elucidate how its photophysiology and growth are affected by these light colors.

In blue light, the rates of photosynthesis and growth of *Synechocystis* were much lower than in orange and red light. This was accompanied by a strong decrease in the ratio of photosystem I (PSI) to photosystem II (PSII), indicative of an attempt of the organism to increase the amount of excitation energy arriving at PSII, relative to PSI. We compared the growth of *Synechocystis* with other PBS-containing cyanobacteria that use phycocyanobilin (absorbing orange light) or phycoerythrobilin (absorbing

green light), and with the green alga *Chlorella sorokiniana*, which uses light-harvesting antennae containing chlorophyll (absorbing blue and red light) and carotenoids (absorbing blue and green light), instead of PBS. Our experiments showed that green algae have similarly high growth rates in blue and red light, whereas all investigated PBS-containing cyanobacteria had a low growth rate in blue light, regardless of the phycobili-pigments contained in their PBS. Based on these results, we hypothesized that in cyanobacteria that use PBS as light-harvesting antennae, blue light causes an excitation imbalance between PSI and PSII.

This hypothesis is based on the fact that cyanobacteria invest most of their Chl *a* in PSI. Because PSI contains about three times more Chl *a* than PSII and cyanobacteria contain about 2-5 times more PSI than PSII, the contribution of PSI in the absorption of blue light is much higher than that of PSII. To compensate for this imbalance, the PBS of cyanobacteria transfer most of their absorbed light energy to PSII. However, the phycobili-pigments of PBS cannot effectively absorb and redistribute photons of wavelengths ≤ 450 nm, which we propose underlies the failure to rebalance the excitation pressure between the two photosystems in blue light. Unlike cyanobacteria, green algae and plants have a more balanced PSI:PSII ratio. In addition, they use light-harvesting antennae composed of chlorophylls and carotenoids instead of PBS, allowing them to absorb and redistribute both blue and red light energy between the two photosystems. As a consequence, green algae can achieve similarly high growth rates in both light colors.

To confirm the proposed role of the PBS, we compared growth and photosynthesis of *Synechocystis* wildtype and a mutant strain that lacks PBS, and is therefore unable to transfer additional light energy to PSII (**chapter 3**). The expectation derived from our hypothesis is that the photosynthetic efficiency of this mutant strain will be low in both blue and red light. Measurements of photosynthetic oxygen evolution and growth confirmed the low photosynthetic efficiency of the PBS-less mutant in both blue and red light, similar to that of the PBS-containing wildtype *Synechocystis* in blue light only. In addition, the mutant's PSI:PSII ratio was low in both light colors, even lower than that of the wildtype in blue light. These findings further support our hypothesis that the inability of the PBS to absorb blue light leads to an uneven distribution of excitation energy between PSI and PSII.

In view of the strong photophysiological response of PBS-containing cyanobacteria, we expected that gene expression will also be strongly affected by blue light. Therefore, we compared the transcriptional response

of *Synechocystis* after a switch from artificial white light to monochromatic blue, orange and red light (**chapter 4**). Our results revealed differential expression of almost 150 genes in blue light, whereas expression of only a handful of genes was altered in orange and red light. In particular, genes encoding structural PSII proteins and proteins related to the PSII repair cycle were strongly upregulated in blue light, in line with the observed decrease in the PSI:PSII ratio. Furthermore, the strong decrease in growth rate in blue light coincided with downregulation of genes encoding ATP synthase and ribosomal proteins, as well as other genes related to protein synthesis. Hence, as expected, blue light induced major changes in the transcriptome of this PBS-containing cyanobacterium, in line with its attempt to restore linear electron flow via PSII and PSI.

The low photosynthetic efficiency of PBS-containing cyanobacteria in blue light may have considerable consequences for their ecological distribution and competitive interactions with other species. In aquatic environments, light colors vary greatly; e.g., blue light dominates the oligotrophic oceans whereas turbid lakes are dominated by orange to red light. The prevailing light color might thus provide a strong selective pressure favoring different pigments, and hence different species, in different underwater light environments. Previous competition models did not consider the low photosynthetic efficiency of cyanobacteria in blue light. Therefore, we have developed a new resource competition model, in which both light absorption and photosynthetic efficiency vary with wavelength (**chapter 5**).

The model predicts a strong competitive advantage for phytoplankton species with chlorophyll-based light-harvesting antennae (e.g., green algae) in blue light, whereas PBS-containing cyanobacteria will have an advantage in those light colors that can be absorbed by their PBS. These model predictions were confirmed using competition experiments. The freshwater cyanobacterium *Synechocystis* competitively displaced the green alga *Chlorella* in red light, whereas the green alga prevailed in blue light. The model also provides an explanation for a subtle niche differentiation between the two most abundant marine phytoplankton taxa, *Prochlorococcus* and *Synechococcus*. *Prochlorococcus* uses chlorophyll-based light-harvesting antennae, quite similar to green algae, whereas marine *Synechococcus* strains use PBS that often contain the blue-green and green light-absorbing phycobili-pigments phycourobilin and phycoerythrobilin. As predicted by the new model, *Prochlorococcus* is highly abundant in the blue waters of oligotrophic subtropical gyres, whereas *Synechococcus* is relatively more abundant in coastal waters

and more turbid oceanic regions where blue-green and green light are available. These results confirm that the available light colors indeed play a prominent role in the biogeographical distributions of phytoplankton species.

The fundamental research described in this thesis is likely to be of significance for several research fields (**chapter 6**). For example, it may guide the selection of suitable light colors to culture cyanobacteria in biotechnological applications. Furthermore, our findings complement current knowledge of the evolution of phytoplankton species and their photosynthetic pigments. Finally, our results may lead to improved prediction of how human-induced changes in underwater light color, as evident from the brownification of many lakes, will affect the species composition of natural phytoplankton communities.

Nederlandse samenvatting

Cyanobacteriën vormen de meest abundante fytoplanktonsoorten in mariene ecosystemen, en kunnen 'blauwalgenbloei' veroorzaken in eutrofe meren. Ze spelen een sleutelrol in aquatische ecosystemen en in de wereldwijde koolstof kringloop. Hun fotosynthetische activiteit heeft gezorgd voor de accumulatie van zuurstof in de atmosfeer van de Aarde en faciliteert de opname van grote hoeveelheden CO_2. Om deze redenen is er grote interesse in cyanobacteriën, ook vanwege de zoektocht naar hernieuwbare energiebronnen, duurzame voedselproductie en de productie van 'groene' chemicaliën. Diepgaande kennis van de fotosynthetische activiteit van deze organismen is daarom belangrijk voor zowel ecologische als biotechnologische toepassingen.

Net als groenalgen en (land)planten gebruiken cyanobacteriën het fotosynthetische pigment chlorofyl a (Chl *a*) voor het absorberen van blauw en rood licht. Je zou daarom verwachten dat cyanobacteriën rood en blauw licht dan ook even efficiënt kunnen gebruiken voor fotosynthese. Het tegendeel is waar: in tegenstelling tot groenalgen en planten is de fotosynthetische efficiëntie van cyanobacteriën vaak lager in blauw licht dan in andere lichtkleuren die geabsorbeerd worden door hun fotosynthetische pigmenten. Hoewel deze lage efficiëntie in blauw licht eerder is beschreven, is dit niet algemeen bekend en ontbreekt een uitgebreid onderzoek naar de onderliggende mechanismen daarvan. Het doel van dit proefschrift is om het mechanisme achter dit intrigerende fenomeen op te helderen.

Om de fotosynthetische efficiëntie van cyanobacteriën in verschillende kleuren licht te onderzoeken hebben we allereerst de fotosynthese van de cyanobacterie *Synechocystis* sp. PCC 6803 uitgebreid bestudeerd (**hoofdstuk 2**). Deze model-cyanobacterie bevat Chl *a* in haar fotosystemen, wat blauw en rood licht absorbeert, en gebruikt daarnaast fycobilisomen (PBS) om oranje licht te absorberen met het fycobili-pigment fycocyanobiline. We hebben de fotosynthetische activiteit, de relatieve samenstelling van het fotosynthese apparaat, en de groeisnelheid van *Synechocystis* onderzocht in blauw, oranje en rood licht, om te achterhalen hoe de fotofysiologie en groei van deze cyanobacterie beïnvloed worden door selectief gebruik van deze lichtkleuren.

In blauw licht waren de fotosynthese- en groeisnelheid veel lager dan in oranje en rood licht. Dit ging gepaard met een sterke afname in de verhouding tussen de hoeveelheden fotosysteem I (PSI) en

fotosysteem II (PSII) die worden aangemaakt, wat wijst op een poging van het organisme de excitatie-energie te herverdelen van PSI naar PSII. We hebben de groei van *Synechocystis* vergeleken met andere PBS-bevattende cyanobacteriën die fycocyanobiline (absorbeert oranje licht) of fycoërytrobiline (absorbeert groen licht) bevatten, en met de groenalg *Chlorella sorokiniana*, die gebruik maakt van chlorophyll-bevattende fotosynthese antennes (absorberen blauw en rood licht) en carotenen (absorberen blauw en groen licht), in plaats van PBS. Onze experimenten laten zien dat groenalgen vergelijkbare hoge groeisnelheden hebben in blauw en rood licht, terwijl alle door ons onderzochte PBS-bevattende cyanobacteriën een lagere groeisnelheid hadden in blauw licht, ongeacht het type fycobili-pigment in hun PBS. Onze hypothese, op basis van deze resultaten, is dat in cyanobacteriën die PBS gebruiken, exclusief gebruik van blauw licht de verdeling van excitatie energie tussen PSI en PSII uit balans brengt.

Deze hypothese is gebaseerd op het feit dat cyanobacteriën het overgrote deel van hun Chl *a* inbouwen in PSI. Omdat PSI ongeveer drie keer meer Chl *a* bevat dan PSII en cyanobacteriën 2-5 keer meer PSI dan PSII bevatten, is de bijdrage van PSI aan de absorptie van blauw licht vele malen hoger dan die van PSII. Om dit verschil te compenseren, dragen PBS in cyanobacteriën het meeste van hun geabsorbeerde lichtenergie over aan PSII. Fycobili-pigmenten kunnen echter geen fotonen van een golflengte ≤ 450 nm absorberen en herverdelen, wat volgens ons ten grondslag ligt aan het onvermogen van deze organismen om in blauw licht het verstoorde evenwicht tussen de twee fotosystemen te herstellen. In tegenstelling tot cyanobacteriën, hebben groenalgen en planten een meer gebalanceerde PSI:PSII ratio. Daarnaast gebruiken zij fotosynthese antennes bestaande uit chlorofyl en carotenen in plaats van PBS, waardoor zij in staat zijn energie van zowel blauw als rood licht te absorberen en te verdelen over beide fotosystemen, om zo vergelijkbare hoge groeisnelheden te bereiken in beide lichtkleuren.

Om de veronderstelde rol van PBS te bevestigen, hebben we de groei en fotosynthese van wildtype *Synechocystis* vergeleken met een mutant die geen PBS bevat (**hoofdstuk 3**). De verwachting gebaseerd op onze hypothese is dat de fotosynthetische efficiëntie van deze mutant laag zou zijn in zowel blauw als rood licht. Metingen van fotosynthetische zuurstofontwikkeling en groei bevestigen de lage fotosynthetische efficiëntie van de PBS-loze mutant in zowel blauw als rood licht, vergelijkbaar met die van het PBS-bevattende wildtype *Synechocystis* in monochromatisch blauw licht. Verder was de PSI:PSII ratio van de mutant laag in beide lichtkleuren, zelfs lager dan in het wildtype in blauw licht.

Deze resultaten ondersteunen onze hypothese dat het onvermogen van het PBS om blauw licht te absorberen leidt tot een ongelijke verdeling van excitatie-energie tussen PSI en PSII.

Met het oog op de sterke fotofysiologische respons van PBS-bevattende cyanobacteriën was onze verwachting dat genexpressie ook aanzienlijk beïnvloed zou worden door blauw licht. Om deze reden hebben wij de respons van het volledige transcriptoom van *Synechocystis* onderzocht, na omschakeling van kunstmatig wit licht naar blauw, oranje of rood licht (**hoofdstuk 4**). Onze resultaten lieten in blauw licht een veranderde expressie van bijna 150 genen zien, terwijl in oranje en rood licht de expressie van slechts een handjevol genen veranderde. Vooral de expressie van genen die coderen voor structurele PSII eiwitten en eiwitten gerelateerd aan de PSII reparatiecyclus was sterk verhoogd in blauw licht, in lijn met de geobserveerde afname van de PSI:PSII ratio. Bovendien ging de sterke afname van de groeisnelheid in blauw licht gepaard met verminderde expressie van genen die coderen voor ATP synthase en ribosomale eiwitten, en andere eiwitsynthese-gerelateerde genen. Dit wijst erop dat, zoals verwacht, blauw licht grote veranderingen teweegbrengt in het transcriptoom van deze PBS-bevattende cyanobacterie, die overeenkomen met een poging tot herstel van het lineaire elektronentransport via PSI en PSII.

De lage fotosynthetische efficiëntie van PBS-bevattende cyanobacteriën in blauw licht kan belangrijke gevolgen hebben voor hun ecologische verspreiding en concurrentie met andere soorten. In aquatische ecosystemen kan de lichtkleur aanzienlijk varieren. In de voedselarme oceanen domineert bijvoorbeeld blauw licht, terwijl in troebele meren oranje tot rood licht de boventoon voert. De heersende lichtkleur kan dus een sterke selectiedruk opleggen die leidt tot een voordeel van het gebruik van specifieke pigmenten, en dus verschillende soorten, in verschillende onderwater lichtkleuren. Eerdere competitiemodellen hielden geen rekening met de lage fotosynthetische efficiëntie van cyanobacteriën in blauw licht. Daarom hebben wij een nieuw competitiemodel ontwikkeld, waarin zowel lichtabsorptie als fotosynthetische efficiëntie kunnen variëren per golflengte (**hoofdstuk 5**).

Dit model voorspelt een sterk concurrentievoordeel in blauw licht voor fytoplanktonsoorten met fotosynthese antennes gebaseerd op chlorofyl (zoals groenalgen), terwijl PBS-bevattende cyanobacteriën een voordeel hebben in die kleuren licht die geabsorbeerd worden door hun PBS. Deze modelvoorspellingen zijn bevestigd met competitie experimenten. De zoetwater cyanobacterie *Synechocystis* verdringt de groenalg *Chlorella* in rood licht, terwijl de groenalg de competitie wint in blauw licht. Het

nieuwe model geeft ook een verklaring voor de subtiele niche differentiatie tussen de twee meest voorkomende mariene fytoplankton taxa, *Prochlorococcus* en *Synechococcus*. *Prochlorococcus* gebruikt chlorofyl-gebaseerde fotosynthese antennes vergelijkbaar met die van groenalgen, terwijl de mariene *Synechococcus* stammen gebruik maken van PBS met daarin vaak de blauwgroen- en groen licht-absorberende fycobili-pigmenten fycourobiline en fycoërytrobiline. Zoals het model voorspelt, komt *Prochlorococcus* in grote aantallen voor in de blauwe wateren van de nutriëntarme subtropische oceanen, terwijl *Synechococcus* relatief veel voorkomt in kustwateren en meer troebele delen van de oceanen waar blauw-groen en groen licht beschikbaar zijn. Deze resultaten bevestigen dat de beschikbare lichtkleur inderdaad een prominente rol speelt in de biogeografische verspreiding van fytoplanktonsoorten.

Het fundamentele onderzoek beschreven in dit proefschrift is naar verwachting van betekenis voor verschillende onderzoeksvelden (**hoofdstuk 6**). Het kan bijvoorbeeld een leidraad zijn in de selectie van geschikte lichtkleuren voor het kweken van cyanobacteriën in biotechnologische toepassingen. Bovendien dragen onze bevindingen bij aan de huidige kennis van de evolutie van fytoplanktonsoorten en hun fotosynthetische pigmenten. Tenslotte kunnen onze resultaten leiden tot verbeterde voorspellingen over de effecten van door de mens veroorzaakte veranderingen in onderwater lichtkleur, zoals het steeds bruiner worden van veel meren, op de samenstelling van natuurlijke fytoplankton gemeenschappen.

A

Author contributions

Chapter 2 | VML, HCPM and AMV conceived the original research plan; HCPM, JMS and VML designed the experiments; VML performed the experiments and analyzed the data, with technical assistance from JMS and scientific supervision by HCPM, KJH and JH; VML, JMS and JH wrote the manuscript, and all authors except our late co-author HCPM commented on the final version.

Chapter 3 | VML, JMS, and HCPM conceived the original research plan and designed the experiments; VML and CFMC performed the experiments and analyzed the data, with technical assistance from JMS and scientific supervision by KJH and JH; all authors except HCPM contributed to the writing of the manuscript, and VML and JH wrote the final version.

Chapter 4 | All authors were involved in designing the experiments. VML performed the experiments with technical support from JMS. JMS and VML analyzed the microarray data. VML and JH wrote the manuscript and all authors except our late colleague HCPM commented on the final version.

Chapter 5 | VML, JMHV, JMS and JH designed the study. VML performed the experiments with technical assistance from JMS. JH and JMHV developed the model, JH performed the mathematical analysis, and JMHV and TX the model simulations. VML and JH wrote the manuscript and all authors commented on the final version.

A

Acknowledgments

Here it is, after many years: the end of my PhD. A project like this is never a one-(wo)man effort, and I could almost write a second book about everyone who helped me to get here. Because of the nature (and length) of my PhD I have had the privilege to share this turbulent journey with many fantastic people. The highs and the lows were all worth it and I feel grateful for having you all to accompany me along the road.

Hans, wij hadden al meteen een klik toen je 10 jaar geleden mijn begeleider op afstand werd tijdens mijn masteronderzoek in Nieuw Zeeland. We hadden veel gemeen; je enthousiasme was aanstekelijk en je wakkerde in no-time mijn interesse voor fotosynthese en algjes aan. Ik schreef daarna ook mijn masterscriptie onder jouw hoede, en na een jaartje weg van de academische wereld haalde je me weer terug voor een promotieplek. Daar hoefde ik niet lang over na te denken, en wat hebben we een mooie tijd gehad. Naast theoretische discussies over experimenten en manuscripten hebben we ook enorm veel plezier gehad in het lab, en wat heb ik in die tijd veel van je mogen leren. Ook buiten academische vaardigheden: dat je als academicus warm en sociaal kunt zijn was voor mij een groot voorbeeld, en ik denk met liefde terug aan hoe begaan jij was met alle PhD's en studenten. Hans, wat had ik graag gewild dat je nog kon zien wat het resultaat is geworden. Je hebt een grote rol gespeeld in mijn ontwikkeling tot de persoon die ik nu ben. Bedankt voor alles!

Merijn, vanaf dag 1 mijn 'opperhelpdesk'. Ik heb zo veel van je geleerd in het lab, bovenal hoe alles soms (vaak (bijna altijd)) anders gaat dan verwacht. Jouw flexibiliteit en probleemoplossend vermogen zijn ongeëvenaard en iedereen kan altijd bij jou terecht in grote en kleine crisissituaties. Ook als er geen paniek is ben je er, om gezellig een biertje te pakken in de Oerknal of de Polder, en om te vieren wat er wel goed gaat. Het was voor jou niet makkelijk om dit project met mij door te zetten, en ik denk dat ik je geduld best op de proef heb gesteld. Ik denk ook dat je weet dat ik het zonder jou misschien niet had afgemaakt. Dank je wel voor je positiviteit en begeleiding de afgelopen jaren!

Jef, ook jij was als promotor betrokken vanaf het begin, maar pas later werd je gedwongen hier een actievere rol in te spelen. We moesten allebei onze draai opnieuw vinden in een moeilijke en rare tijd, maar wat hebben we een fijne samenwerking voor elkaar gekregen. Ik heb genoten van onze inhoudelijke discussies en gezamenlijke schrijfsessies (soms uren aan één stuk!), waar ik enorm veel van heb geleerd. Als ik dacht dat ik een experiment of stuk tekst tot in de puntjes had uitgewerkt wist jij het

nog tien keer sterker te maken. Toch heeft een groot deel van wat jij me geleerd hebt niets met wetenschap te maken, maar met karakter. Dank je wel voor je geduld en je vertrouwen dat ik het kon.

Klaas, eigenlijk was jouw pensioen voor mij de tijd dat ik juist meer met jou te maken kreeg. Ik prijs me gelukkig met een team van begeleiders en promotores uit zulke uiteenlopende disciplines, waardoor ik ondersteuning had bij de belichting van verschillende kanten. Ook tijdens het schrijven had je fantastische feedback en wist je elk stuk nóg een beetje helderder te maken en te verdiepen. Het maakte niet uit waar op deze aardbol je was, elk stuk tekst waar ik advies over vroeg kreeg ik binnen een paar dagen terug. Dank je wel!

Anthony, ook jij bedankt voor je begeleiding! Zeker toen ik wel/niet/wel/niet/wel/toch niet naar Leeuwarden verhuisde was het enorm fijn een vriendelijk gezicht en een helpende hand te hebben aan de 'andere kant', iemand die me hielp mijn draai te vinden in een nieuw lab. En ook toen alles anders liep was je er met je eindeloze geduld en behulpzaamheid. Ons algenteam is niet meer, maar wij delen een verleden met NIOO, UvA, Wetsus en nu zelfs W+B, en ik weet zeker dat onze paden nog een keer kruisen. Ik kijk er naar uit!

Ik begon mijn onderzoek in de groep Aquatische Microbiologie in Amsterdam (nu Freshwater and Marine Ecology) en alleen daar lopen al zo veel mensen rond om dankbaar voor de zijn. Allereerst de harde kern, de technicians. **Pieter**, wat heb ik vaak verwilderd bij je bureau gestaan dat alles nú mis ging. Dank je wel dat je altijd bereid was mee te denken. **Bas**, jouw hulp kwam vaak in de vorm van een schop onder mijn kont... Dank je wel voor je zachte hardheid en je fantastische luchtige humor. **Corrien**, mede algenkweker en luisterend oor, dank je wel voor je oprechte interesse in wat er speelde en hoe het ging. **Maria**, we hebben niet lang samen gewerkt, maar met jou als mede-fytoplanktonanalist klikte het direct. Bij de vaste kern horen ook **Pascale**, **Mary**, **Tanya** en **Saskia**: de 'backbone' van het IBED. Dank jullie wel voor jullie grenzeloos geduld en ondersteuning in alles wat maar geregeld moest worden.

Jolanda, jij werd bijna begeleider nummer 6: op papier nooit gebeurd, maar dat voelde anders. Dank je wel voor een knuffel in nood en je hulp bij misschien wel mijn mooiste paper, waarin we het gedachtegoed van Hans en Maayke combineerden. **Maayke**, je was al een inspiratie tijdens mijn master L&O. Je vrolijkheid en kracht, wat er ook op je pad kwam, waren voor mij een inspiratie en ik ben dankbaar dat ik je nog heb mogen kennen. **Petra**, bij jou denk ik nog steeds eerst aan Curaçao, waar ik nog als student mee naar toe ging. Het was ontzettend gezellig en die lijn heeft zich alleen maar doorgezet tijdens mijn PhD. **Gerard**, altijd

geïnteresseerd hoe het gaat en vol begrip over de lastige kanten van het promoveren bij zowel de UvA als Wetsus. **Susanne**, ook jij bedankt voor een korte, maar gezellige overlap!

Of course I also owe big thanks to my students! **Tania**, je legde de lat hoog voor de rest. Je was ook mijn eerste stagiaire, en ik weet niet wie er meer van geleerd heeft: jij of ik! **Joris**, ik ben nog steeds apetrots op hoe positief en vol energie jij je project hebt volbracht terwijl je al vroeg wist dat je een andere kant op wilde. Bedankt voor de lol in het lab! **Carolina**, no matter how much bad luck you had, you always handled your chemostats smiling. **Tianshuo**, thank you for helping me with the model for our Ecology paper!

And then there are my closest co-workers: my office mates of C4.225 and those from the corner office (I still don't know the room number). Guys, you've been there through my bluest blues and my highest highs. The blues are almost forgotten (who knew!), covered under a layer of fond memories. I have enjoyed our lunches, borrels, parties, half marathons across Europe and GoT nights, and I miss you all so much. I hope Covid-19 will allow us to celebrate together! **Amanda**, sitting a desk across from you made my start in a new job feel like a warm bath and that feeling never stopped. You possess a unique combination of strength, humor and warmth that still amazes me. (And on behalf of the whole group; THANK YOU for all the baking!) **Anca**, you played such a big role in keeping the group together! I can't imagine you ever walking away from any challenge: you and your optimism can move mountains and encouraged me to try the same. **Jason**, the hours I spent in the dark studying light would have been so boring without you there, too. Thank you so much for sharing the burden of chemostats and MIMS measurements (and renovating homes), for dragging me to the USC to punch away my frustration, and for our shared final sprint! **Catarina**, the driving force of the shared (sports) activities and a true friend when things get hard. You and **Tim** played a vital role in keeping our group a group, thanks for all the runs and funs! **Muhe**, right next to me for how many years? I couldn't have wished for a better neighbor, thank you! **Gio**, there for any social activity, the silent force of the hard core. **Tom**, you have proven yourself an inexhaustible source of knowledge and useless trivia, and you always manage to lighten up (almost) any situation with your dry humor. **Lisette**, as a student you already impressed everyone and as a PhD you proved that your strength and willpower have no limits, nor does your good mood! **Natasha**, suddenly you were there in our office, in our hearts, in my home, and I'm still thankful that initially there was no space in 'your' office! **Erik**, thank you for being there. Always smiling, still interested in how others were

doing no matter how bad you felt yourself. **Cherel**, thanks for the fun and the shared enthusiasm for travelling and for new homes! **Ruben**, always in for fun activities and a good talk. **Estelle**, when you moved into our office you brightened the air!

Also many thanks to all others that have been part of the group over the past years: **Amber**, **Arie**, **Baptiste**, **Ben**, **Bregje**, **Charlotte**, **Ciska**, **Emily**, **Ernesto**, **Gea**, **Harm**, **Jip**, **Judith**, **Lex**, **Maria M**, **Martijn**, **Meggie**, **Michiel**, **Milo**, **Naomi**, **Nicoletta**, **Nienke**, **Niklas**, **Paula**, **Rachid**, **Rick**, **Rob**, **Sam A**, **Sara**, **Sebastiaan**, **Tadzio**, **Tiedo**, **Tom T**, **Qian**, and everyone I may have forgotten to mention here!

Mijn dank gaat ook uit naar het SILS: **Dennis**, I lost count of how many chemostats and bottles of medium you sterilized for me… **Milou**, another Schuurmans who was there through some of my bluest days. Thank you! **Que**, we had so much fun at the conference in Arizona; thank you for standing next to me in a weird and sad time. **Pascal** and **Wei**, fellow *Synechocystis* growers; thank you for a shared passion for this green bug.

De mannen van de technologie: **Johan**, **Mattijs**, **Theo**, **Gerrit**, zonder jullie (en zonder de Bee Gees) was het niks geworden met de multicultivator. **Bernadette**, dank je wel voor je eyeopeners en duw in de rug toen ik die nodig had.

Also at Wetsus, I was welcomed warmly every time I arrived. My office mates were always happy to see me and the technicians have helped me so often setting everything up. Special thanks to **Bert**, master in peptalks! **Sam**, jij gaf mij een home away from home! Later met **Casper** erbij; ik had altijd een plek om naar toe te komen in Ljouwert. Dank jullie wel voor nachtelijke discussies met wijn en eeuwige welkom. **Sebastián**, my last fellow Algae theme member. I hope we'll get to work together again someday. Zelfs na de 'ontmanteling' van het Algae team bleef er interesse vanuit de partners; in het bijzonder wil ik **Marcel Geers** en **Arthur Kroon** bedanken. **Hardy** en **Marcel**, vanuit de WUR nog een extra supportteam om te steunen met de laatste loodjes.

And then, amidst my 'now what?'-crisis, **Sjaak** and **Huib** gave me the opportunity to join the Chemical Immunology group at the LUMC as research technician (and show-off clone), to help Jolien complete the experimental work of her PhD. I know Huib will be missed greatly and I will never forget the example he set on how to take care of each other. Thank you, to all the **Ovaas** and **Neefjes** for welcoming (co-adopting) me in your group, for all the skills you taught me and for the fun times. Special thanks to my office mates that all squeezed in to create an extra workspace for me, and to the MHC chickies for making me one of them.

Het blijkt dat ik nooit uitgeleerd ben, en zo ben ik ineens technoloog

bij Witteveen+Bos. Een nieuwe richting vol uitdagingen, waar ik mijn achtergrond in aquatische ecologie kan inzetten in de praktijk. Dank jullie wel voor deze kans om mijzelf te ontwikkelen en mijn kennis om te zetten in toepassingen, en voor jullie begrip en ruimte om mijn proefschrift ernaast af te maken. Het zou niet gelukt zijn zonder mijn fijne collega's. In het bijzonder **Arjan**, **Arjen**, **Casper**, **Coen**, **Freek**, **Heleen**, **Jaïr**, **Wesley** en **Yannick**, bedankt voor jullie support, dat jullie me alles leren en vooral bedankt voor de gezelligheid!

Nu lijkt dit al een hele lijst, maar buiten al die collega's om zijn er nog zo veel mensen geweest die me vanaf de andere kant hebben ondersteund. **Am**, tweederde van mijn leven ken ik je al, en je bent er no matter what. Al jaren veel te ver weg maar nooit uit het hart. **Floortje**, dank je wel voor je begrip voor alles en je steun door dik en dun. Hoeveel pech (en pijn) je zelf ook had de afgelopen twee jaar, je bleef altijd vragen hoe het met mij en mijn proefschrift ging. 'Is je hoofdstuk nog afgekomen?', 'Wat vond Jef van je nieuwe stuk?', 'Is je paper geaccepteerd?', 'Heb je al wat gehoord?', 'Ben je klaar?'... Ja, ik ben eindelijk klaar. **Evelien**, **Jarno**, **Yvonne**, **Tim**, **Marc**, **Justien**, **Yvette**, **Kostas**, **Marije**, **Richard**, **Jaap**, **Wimpie**, **Petra** en **Sander**: eindeloos hebben jullie mijn geblaat over algjes en planktonnetjes aangehoord, en hoe vaak heb ik jullie niet afgewimpeld met 'te druk!'. Gelukkig bleven jullie aanhouden, steunen en wachten tot het eindelijk klaar was. Dank jullie wel, het is zo ver.

Lieve familie! Twee **oma's**, **Aafke, Anne-Rose**, **Eva**, **Job**, **Lizette**, **Madi**, **Manon**, **Marcel**, **Mieke**, **Ole**, **Tom** en **Willem**. Jullie hebben zo meegeleefd en keer op keer de lab-frustraties van twee meiden tegelijk aangehoord. Dank jullie wel voor jullie interesse en blijdschap als er weer een artikel af was. Ik weet dat jullie ze allemaal woord voor woord hebben gelezen. **Aafke**, samen met **Heleen** heb je flink wat moeite gedaan om er wat relativeringsvermogen in te pompen. Dat heeft gewerkt, en ik betrap mezelf erop dat ik jullie tips met succes extrapoleer naar nieuwe situaties.

Carla en **Wim**, **Fred** en **Madelon**, **Tim** en **Angelique**, wat een voorrecht zo'n fijne schoonfamilie te hebben. Jullie steun en hulp bij alles wat er maar mag spelen (denk aan spoedverhuizingen, huizen slopen, huizen opbouwen…) is echt fantastisch. Ook **Frieda** en **Wilco** ben ik intens dankbaar, en natuurlijk alle Tamelingen en Valkenhoven! En niet te vergeten de Van de Brinkies: **Henk**, **Wil** en **Linda**. Mike en ik grappen altijd dat we een derde set schoonfamilie hebben. Jullie oprechte interesse en opname in de familie zijn hartverwarmend en we vinden het ontzettend gezellig jullie er bij te hebben. En dank jullie wel voor Robert.

Daph, niemand snapt het zoals jij. Met jou deelde ik de afgelopen jaren tranen van het huilen maar ook van het lachen. Met zijn drietjes naar

Texel, Curaçao, New York, de Malediven, het wordt weer tijd voor ergens heen! Dank je wel voor een fijne tijd op de Roomtuintjes, je steun vanaf de andere vleugel op de UvA en dat je na al die jaren ook straks naast me staat. **Ro**, wat een zegen dat ik ineens een broer heb. En eentje met een ongekend optimisme en doorzettingsvermogen (zeker als die turbo-knop om gaat!), die altijd klaar staat voor de mensen om hem heen. Dank je wel voor je relativeringsvermogen en je talent om rust te brengen, te zorgen dat we allemaal wat meer genieten in plaats van maar door rennen. Hoewel we dat rennen samen ook wel erg goed kunnen; of dat nou is naar een finishlijn of heen en weer achter een klein stuiterballetje aan. Het wordt tijd dat jullie weer dichtbij komen wonen!

Lieve **pap** en **mam**, door de wetenschap dat jullie altijd achter me staan heb ik me in zoveel nieuwe dingen durven storten. Altijd staan jullie klaar met raad, daad, dak, luisterend oor of sloophamer. Wat ik ook besluit me op de hals te halen, jullie steunen me en zorgen dat ik het beste uit mezelf haal. Of ik nou besluit om meermaals van studie/werkrichting te veranderen, maandenlang aan de andere kant van de wereld stage te gaan lopen, een racemotor te gaan rijden, vulkanen te beklimmen in de Andes of een bouwval te kopen en op te knappen, door jullie opvoeding heb ik het vertrouwen dat ik het kon, en kan, en dat het goed komt. **Myrt**, wat ben ik dankbaar voor jou als zus(je). Jij laat me inzien dat je niet alles hoeft te begrijpen om het te snappen, om achter iemand te staan. Dank je wel voor een luisterend oor, lieve post als ik er doorheen zit en enorme hulp bij het slopen. En laten we de lol niet vergeten! Lekker samen door Australië reizen, jaarlijkse zussenweekendjes en lekker gek doen. Dank je wel dat je van klein zusje naar grote vriendin bent gegaan. **Lien**, wat een rare tijd voor ons allebei, met gedeelde frustratie (en soms irritatie), gedeelde liefde voor biologie en chemie, veel te gedetailleerde gesprekken, bizar verdriet, extreme blijdschap en voor ons beiden een herontdekking van wat we nou echt willen doen 'als we later groot zijn'. Ik ben intens dankbaar dat we dit hebben kunnen delen.

Tot slot! Iedereen in de wetenschap weet dat de laatste persoon in een rijtje namen een bijzonder plekje heeft. **Mike**, ik heb geen woorden om te omschrijven hoe gelukkig ik ben met jou. Dank je wel voor een liefdevolle schop onder mijn kont als ik dacht dat ik het niet kon, perfect gecombineerd met terugfluiten als ik te veel wilde doen. Je hebt van begin tot eind, de hele achtbaan, naast me gestaan om mijn successen te vieren en (met engelengeduld) mijn hand vast te houden toen ik het moeilijk had (en soms vooruit te sleuren). En naast dat alles vonden we de tijd om samen het avontuur op te zoeken, zowel dichtbij als ver weg. Met jou is alles genieten. Op naar de rest!

C

Curriculum vitae

Veerle Luimstra was born on September 18th, 1987, in Amsterdam. She has always had a fascination for biology and so after finishing her VWO with 'Nature & Health' profile in 2005, she began her Bachelor studies in Biomedical Sciences. In this time she also had her first experiences with the underwater world through scuba diving, diverting her view to marine biology.

After her graduation in 2008 Veerle took a gap year, working as a teaching assistant at her former high school. She then continued her studies with the Master's program Biological Sciences, shifting her focus from medical biology to water biology. In the Oceanography and Limnology track she could literally immerse herself in marine biology during the various field trips, such as research excursions to the Dutch island Texel and a slightly more tropical and further away Dutch island: Curaçao. As part of a short research project at the Netherlands Institute for Ecology in Nieuwersluis (now in Wageningen) she was involved in the plankton section of Artis Zoo's Micropia, an exhibition dedicated to microorganisms. Her love for nature and interest in microorganisms led Veerle to the Cawthron Institute in Nelson, New Zealand, where she conducted a 9-month research project developing a photosynthetic microbial fuel cell 'powered by' cyanobacteria.

Back in The Netherlands, Veerle obtained her Master's degree in 2012. Her experience with cyanobacteria was a great asset for Aquon, a well-known institute for water research and consultancy. As analyst hydrobiology and phytoplankton Veerle carried out microscopic analyses of phytoplankton, as well as risk assessments of Dutch swimming waters in relation to (potentially) toxic cyanobacteria. After a few months, she took the opportunity to further research phytoplankton in a joint PhD position at the Institute for Biodiversity and Ecosystem Dynamics of the University of Amsterdam, and Wetsus, European centre of excellence for sustainable water technology. She started the PhD program at the end of 2013, supervised by dr. Hans Matthijs, dr. Merijn Schuurmans, dr. Anthony Verschoor, prof. dr. Klaas Hellingwerf and prof. dr. Jef Huisman. During her PhD, Veerle studied the effect of light quality on photosynthesis and growth efficiency of cyanobacteria and green algae.

In the first half of 2019 Veerle spent a short 6-month biomolecular intermezzo as a research technician at the Department of Cell and Chemical Biology at the Leiden University Medical Center, where she provided experimental support in the development of tools to monitor adaptive immune cells. Since September 2019 Veerle is employed at Witteveen+Bos, an engineering and consultancy firm focusing on sustainable solutions to societal challenges. As process engineer she is involved in various projects related to water quality and waste water treatment technology.

Figure 1 | Featured on the UvA building: *Freshwater and marine laboratories*
Behind one of the doors in the Institute for Biodiversity and Ecosystem Dynamics you can find this laboratory equipped with photo bioreactors. The reactors have been developed in house and are used to study phytoplankton: tiny organisms at the basis of both freshwater and marine food webs that use sunlight to convert CO_2 into biomass. The different phytoplankton species are sampled from lakes and oceans. After being cultivated in Erlenmeyer flasks, their growth and species composition are studied in the bioreactors under controlled experimental conditions.

Here, Veerle Luimstra is selecting some species for her experiments, in which she investigates how cyanobacteria (‘blauwalg’ in Dutch) adapt their photosynthetic systems to different colors of light. Other studies focus on toxin production by harmful algal species, or the consumption of bacteria by predatory phytoplankton. Furthermore, these lab facilities are used to assess how phytoplankton responds to ocean acidification and climate change.

Photo: Jorn van Eck, for 'Een nieuw fundament: beeld van de bètasector' (NWO 2019)

List of publications

Luimstra VM, Schuurmans JM, Hellingwerf KJ, Matthijs HCP, Huisman J (2020) Blue light induces major changes in the gene expression profile of the cyanobacterium *Synechocystis* sp. PCC 6803. *Physiologia Plantarum* 170:10-26

Luimstra VM, Verspagen JMH, Xu T, Schuurmans JM, Huisman J (2020) Changes in water color shift competition between phytoplankton species with contrasting light-harvesting strategies. *Ecology* 101:e02951

Luimstra VM, Schuurmans JM, de Carvalho CFM, Matthijs HCP, Hellingwerf KJ, Huisman J (2019) Exploring the low photosynthetic efficiency of cyanobacteria in blue light using a mutant lacking phycobilisomes. *Photosynthesis Research* 141:291-301

Luimstra VM, Schuurmans JM, Verschoor AM, Hellingwerf KJ, Huisman J, Matthijs HCP (2018) Blue light reduces photosynthetic efficiency of cyanobacteria through an imbalance between photosystems I and II. *Photosynthesis Research* 138:177–189

Sandrini G, Ji X, Verspagen JMH, Tann RP, Slot PC, **Luimstra VM**, Schuurmans JM, Matthijs HCP, Huisman J (2016) Rapid adaptation of harmful cyanobacteria to rising CO_2. *Proceedings of the National Academy of Sciences of the USA* 113:9315-9320

Weenink FJ, **Luimstra VM**, Schuurmans JM, van Herk MJ, Visser PM, Matthijs HCP (2015) Combatting cyanobacteria with hydrogen peroxide: A laboratory study on the consequences for phytoplankton community and diversity. *Frontiers in Microbiology* 6:714

Luimstra VM, Kennedy SJ, Güttler J, Wood SA, Williams DE, Packer MA (2014) A cost-effective microbial fuel cell to detect and select for photosynthetic electrogenic activity in algae and cyanobacteria. *Journal of Applied Phycology* 26:15-23